NASA TECHNICAL
TRANSLATION

NASA TT F-542
c. 1

NASA TT F-542

TECH LIBRARY KAFB, NM
0069008

LOAN COPY: RETURN TO
AFWL (WLOL-2)
KIRTLAND AFB, N MEX

AERODYNAMICS AND FLIGHT DYNAMICS OF TURBOJET AIRCRAFT

by T. I. Ligum

Transport Press, Moscow, 1967

NATIONAL AERONAUTICS AND SPACE ADMINISTRATION • WASHINGTON, D. C. • SEPTEMBER 1969

TECH LIBRARY KAFB, NM
0069008

AERODYNAMICS AND FLIGHT DYNAMICS OF TURBOJET AIRCRAFT

By T. I. Ligum

Translation of "Aerodinamika i Dinamika Poleta
Turboreaktivnykh Samoletov"
Transport Press, Moscow, 1967

NATIONAL AERONAUTICS AND SPACE ADMINISTRATION

For sale by the Clearinghouse for Federal Scientific and Technical Information
Springfield, Virginia 22151 – CFSTI price $3.00

Table of Contents

INTRODUCTION

Jet-powered passenger aircraft have been adopted and introduced into general use in civil aviation. /3*

The first turbojet passenger aircraft built in the Soviet Union was the Tu-104, and the first foreign turbojets were the De Havilland Comet, the Sud Aviation Caravelle, the Boeing-707, the Douglas DC-8, the Convair 880 and others. These aircraft have been given the name first-generation turbojet aircraft.

In building the first turbojet passenger aircraft, the designers attempted to achieve long flight range and to perfect the high-speed properties of the aircraft, thereby compensating for the heavy fuel consumption required by the jet engines. The desire to create new aircraft capable of competing with the old passenger aircraft which were equipped with highly economic piston engines led to a maximum increase in the lifting capacity, and flight distance and speed. The realization of these qualities became possible only because of the appearance of jet engines.

Experience in using aircraft has shown that turbojet passenger aircraft may be economic not only in terms of long-range flight, but for medium- and even short-range flight as well. As a result, second-generation turbojet passenger aircraft have appeared: in the Soviet Union there are the Tu-124, the Tu-134 and the Yak-40, while abroad there are the De Havilland-121 "Trident", the Bak-1-11, the Boeing-727, the DC-9 and others. These aircraft are substantially smaller in dimensions and intended for use on short-range nets. The high power and low unit load on the wing permit flights from airfields having relatively short take-off and landing runways.

Turbojet engines surpass piston engines in reliability. With their short time in series production and use, service periods of 2,000 - 3,000 hours between maintenance checks have been established. This is an important fact in increasing the economy of using turbojet aircraft, because the cost of these engines substantially exceeds that of piston engines. In the Five Year Plan for the development of the Russian economy from 1966 to 1970, the further development of civil aviation is anticipated and the volume of air travel should increase by a factor of 1.8. New passenger aircraft are going into service in the airlines. /4

Turbojet passenger aircraft have flight characteristics which differ from those of aircraft with piston and turboprop engines in several respects. These flight features result from the unique high-speed and high-altitude characteristics of the engines, as well as the flight conditions at these high speeds and altitudes.

---

* Numbers in the margin indicate pagination in the foreign text.

With the appearance of jet aviation, there has been a resultant increase in the importance of high-velocity aerodynamics, i.e., the motion of bodies in air viewed in terms of the effect of its compressibility, i.e., the properties to change density with a change in pressure. The first to indicate the necessity of estimating the effect of air compressibility was the Russian scientist S.A. Chaplygin, in his work "On Gas Flows" published in 1902. It was he who developed a method for the theoretical solution of problems of the motion of gas with allowance made for its compressibility.

The Soviet scientists Academicians S.A. Khristianovich, M.V. Keldysh, A.A. Dorodnitsyn, Professors V.S. Pyshnov, F.I. Frankl', I.V. Ostoslavskiy, B.T. Goroshchenko, Ya.M. Serebriyskiy, A.P. Mel'nikov and others, through their studies in the field of high-velocity aerodynamics, contributed much which was of great value in the design of high-speed aircraft.

The Soviet turbojet passenger aircraft created by aeronautical engineers A.N. Tupolev, S.V. Ilushin and A.S. Yakovlev, take their places in the ranks of the first-class aircraft.

The successful use of new aviation technology by flight and engineering personnel is unthinkable without a deep understanding of the laws of aerodynamics.

Aircraft aerodynamics, when thought of in terms of the flight crew, is usually called practical aerodynamics. The number of problems involved in aerodynamics is quite substantial. These include studying the laws of the motion of air and the interaction of air flows with bodies moving in them, the interaction of shock waves with various parts of the aircraft, aircraft flight dynamics as affected by the forces applied to the aircraft (including aerodynamic forces), and aircraft stability and handiness.

It is the object of this book to examine these questions in terms of turbojet passenger aircraft.

CHAPTER 1

THE PHYSICAL BASIS OF HIGH-SPEED AERODYNAMICS

ABSTRACT. This book presents the physical bases of high-speed aerodynamics, and the influence of air compressibility on the aerodynamic characteristics of wings and aircraft. Primary attention is turned to passenger jets. The following areas are covered: takeoff characteristics of jets and methods of improving them; best climbing modes; horizontal flight; the descent; the landing approach; turns and corners; controllability and stability; icing and its influence on flying characteristics; and the characteristics of modern jet engines.

§ 1. Variations in the Parameters of Air with Altitude. The Standard Atmosphere

The flight of aircraft, like that of other flight vehicles, is affected by the condition of the atmosphere -- the shell of air surrounding the earth. Therefore, it is quite vital to know the processes occurring in the atmosphere. /5

Only the atmosphere's lower boundary, the earth's surface itself, is clearly delineated. The upper atmosphere is more difficult to establish because the density of air decreases constantly with altitude and even at an altitude of 100 km it measures approximately one millionth that on the earth's surface. Normally, the upper limit of the atmosphere is considered the altitude at which the air density approaches that of the gases filling interplanetary space.

Data from direct and indirect observations show that the atmosphere has a layered structure. In 1951 the International Geodesic and Geophysical Union adopted the division of the atmosphere into five basic spheres or layers: the troposphere, the stratosphere, the mesosphere, the thermosphere and the exosphere.

The Troposphere is the lowest layer of the atmosphere, which in the middle latitudes extends to an altitude of 10-12 km, in the tropics -- to an altitude of 16-18 km, and in the polar regions -- to an altitude of 8-10 km. This layer is of tremendous practical interest in aviation, because all the most important phenomena encountered by the pilot occur basically in the troposphere. It is here that the formation of clouds and fogs, the fall of precipitation, and the development of storms occur.

The most significant feature of the troposphere is the decrease in temperature with a rise in altitude (averaging 6.5° per km of altitude). The troposphere is the area of thermal turbulence resulting from the unequal heating of layers of air at the earth's surface and at various altitudes, as well as the dynamic turbulence resulting from the friction of the air with the earth's surface and its intense vertical displacement at the boundaries between cold and warm air masses of atmospheric fronts. /5

The troposphere ends in the layer of the tropopause. The thickness of the tropopause fluctuates from a few hundred meters to several kilometers. It is usually a continuous layer which surrounds the earth's sphere itself, while its altitude and temperature are functions of the geographic latitude, the time of year and the atmospheric processes developing. Over the equator and its neighboring areas, the tropopause is located at an average altitude of 16-18 km (India), while in the middle latitudes it is located at an altitude of 10-12 km, and in the polar regions it has an altitude of 8-10 km, while over the pole it may drop to 5-6 km. Jet aircraft normally fly close to the limit of the tropopause, a characteristic feature of which is the existence of cyclic bumps beneath the tropopause itself.

The stratosphere is located above the tropopause and extends to approximately an altitude of 35-40 km. Constant temperature with altitude is characteristic of its lower layers. The insignificant content of water vapor in the stratosphere results in the lack of clouds from which precipitation would fall. According to data from pilots who have flown at altitudes of 12-16 km, in the lower stratosphere it is most frequently cloudless. The air is stable and vertical motion is slight. This aids in smooth flight. There is seldom bumpiness, and only then close to the tropopause.

The mesosphere runs from the upper boundary of the stratosphere to an altitude of 80 km.

The thermosphere is located above the mesosphere and extends to an altitude of 800 km.

The exosphere is the outer layer of the atmosphere, or the dissipative layer, and is located above the thermosphere. Gases here are so rarefied and at the high temperatures observed there have such high velocities that their particles (helium and hydrogen) break away from the earth's attractive force and move into interplanetary space.

Thus we have a brief description of a structure of the atmosphere.

Atmospheric conditions are characterized by the various meteorological elements -- atmosphere pressure, temperature, humidity, cloud cover, precipitation, wind, etc. The atmosphere may be characterized as a variable medium.

As a result of unequal heating of the air masses at the equator and poles, flows are formed which result in the passage of cold air toward the equator and warmer air toward the poles. The effect of the earth's rotation in the northern hemisphere causes the air flow to deviate to the right and move from

the south to the southwest, while approaching 30° N it moves to the west. Therefore, flights from west to east over the territory of the USSR are /7
accompanied by tail winds, while east-to-west flights encounter head winds. The shift from westerly winds to easterly occurs at altitudes around 20 km. Whereas piston aircraft fly only in the lower troposphere, jet aircraft, in contrast, fly in the upper and -- to a certain extent -- in the lower stratosphere.

The further development of high-speed aviation will in the near future permit us to fly at supersonic speeds corresponding to Mach = 2.5-3. At this point, flights will be in the stratosphere.

Before the perfectioning of jet aircraft, it was assumed that at high altitudes the flights would encounter favorable weather conditions. However, it was found that at altitudes of 10,000 - 12,000 m cloud cover and bumpiness were sometimes encountered. To these well-known phenomena, there were added the jet streams characteristic of altitudes of 9-12 km.

The jet streams are the broad expanses of zones of very strong winds observed in the upper layers of the troposphere, usually at altitudes of 9000 - 12,000 m. Post-war studies showed that the minimum velocity of the jet stream (along its axis) equalled approximately 100 km/hr, while the maximum was 750 km/hr (over the Pacific Ocean). Over the USSR, the wind speed in the jet stream reaches 100 - 200 and sometimes even 350 km/hr, while over the North Atlantic and Northern Europe it reaches 300 - 400, 500 over the USA, and 650 km/hr over Japan. The jet stream is comparable to a gigantic highly oblate channel with a height averaging 2-4 km and a width of 500 - 1000 km. These flows run basically west-east, but in certain sections they may vary significantly.

Flight speed may be increased by the selective use of jet stream tail winds, while flight against the head wind should be one or two km above or below the axis of this stream. As a rule, the jet streams are to be found in the region where the tropopause is situated.

In studying aircraft flight and determining the forces acting on aircraft, we may consider the air as a continuous medium.

At sea level, the air consists of a mixture of nitrogen (78.08% of the volume of dry air), oxygen (20.95%) and insignificant quantities of other gases (argon, carbon dioxide, hydrogen, neon, helium, etc.). The air also contains water vapors.

In the troposphere and stratosphere the temperature, pressure and density of the air vary within rather broad limits as a function of the geographic latitude of the locale, the time of year, the time of day and the weather.

In order to achieve a common concept of the characteristics of the atmosphere (pressure, temperature and density), the standard atmosphere was

arrived at -- the arbitrary distribution, in the atmosphere, of pressure, density and temperature for dry, clean air (containing neither moisture nor dust) of a constant composition applicable for engineering -- primarily aviation -- calculations with respect to their comparability (for example, in calculating the lift and drag and for graduating various aerial navigation instruments such as altimeters and others). /8

In the standard atmosphere, the altitude is computed from sea level. Normal conditions at sea level are: atmospheric pressure p_0 = 760 mm Hg, air density ρ = 0.125 kG · sec^2/m^4, temperature t_0 = 15°C (or T_0 = 288°K) and specific weight of the air γ_0 = 1.225 kG/m^3.

Variations in air pressure and density with altitude, which proceed in accordance with a specific law, are calculated per each altitude according to special formulas. The air temperature in the standard atmosphere up to an altitude of 11,000 m drops uniformly by 6.5°C per 1000 m. Above 11,000 m, the temperature is considered constant and equal to -56.5°C. In fact, however, at this altitude it may reach -80°C. Results of calculations are given in the table. Below we present an abbreviated table of the standard atmosphere.

TABLE 1. STANDARD ATMOSPHERE (SA)

Altitude (H), m	Temperature (t_H), °C	Pressure (p_H), mm Hg	Pressure, kG/m^2	Density per unit weight (γ_H) kG/m^3	Mass density (ρ_H), $\frac{kG/sec^2}{m^4}$	Relative density $\Delta = \frac{p_H}{p_0}$	$\Delta^{0.7}$	Speed of sound (a)	
								m/sec	km/hr
1 000	21,5	854,6	—	1,3476	1,1374	1,096	1,069	344,9	1242
0	15	760	10332,3	1,225	0,1250	1,00	1,00	340,4	1225
1 000	8,5	674	9164,2	1,11	0,1134	0,9074	0,934	336,6	1211
2 000	2,0	596	8105,4	1,006	0,1027	0,8215	0,871	332,7	1197
3 000	—4,5	526	7148,0	0,909	0,0927	0,742	0,812	328,7	1183
4 000	—11	462	6284,2	0,819	0,0636	0,6685	0,754	324,7	1168
5 000	—17,5	405	5507,0	0,7362	0,0751	0,6007	0,70	320,7	1154
6 000	—24,0	354	4809,5	0,659	0,0673	0,5383	0,648	316,6	1139
7 000	—30,5	308	4185,3	0,589	0,0601	0,4810	0,599	312,4	1125
8 000	—37,0	267	3628,4	0,525	0,0536	0,4285	0,553	308,2	1110
9 000	—43,5	230	3133,1	0,466	0,0476	0,3805	0,509	303,9	1094
10 000	—50,5	188	2694,0	0,412	0,0421	0,337	0,467	299,6	1078
11 000	—56,5	169,6	2306,1	0,363	0,0371	0,297	0,427	295,2	1063
12 000	—56,5	144,6	1969,5	0,310	0,0317	0,253	—	295,2	1063
13 000	—56,5	123,7	1682,0	0,265	0,0270	0,216	—	295,2	1063
14 000	—56,5	105,6	1436,5	0,226	0,0231	0,185	—	295,2	1063
15 000	—56,5	90,1	1226,9	0,193	0,0197	0,158	—	295,2	1063
16 000	—56,5	77,1	1047,8	0,165	0,0166	0,135	—	295,2	1063
17 000	—56,5	65,8	894,8	0,141	0,0144	0,115	—	295,2	1063
18 000	—56,5	56,2	764,2	0,120	0,123	0,0984	—	295,2	1063
19 000	—56,5	48,0	652,7	0,103	0,0105	0,084	—	295,2	1063
20 000	—56,5	40,9	557,4	0,088	0,009	0,0717	—	295,2	1063

Tr. Note: Commas indicate decimal points.

§ 2. Compressibility of Air /9

Compressibility is the property of gases (and fluids) to change their initial volume (and, consequently, density) under the effect of pressure or a change in temperature.

In solving technical problems, compressibility is taken into account in those cases when changes in volume (density) are considerable by comparison to the initial volume (density).

If the volume of water with an increase in pressure of 1 at. with constant temperature changes an average of only 1/21,000 of its initial value, i.e., only 1/210 of a percent, air, which has a high compressibility, requires a change in pressure of only one one hundredth that of atmosphere (0.01 at.) to change its volume by 1% under normal atmospheric conditions.

Therefore, all gases are considerably more compressible than dropping liquid. For example, if the pressure in a given mass of gas increases in such a way that its temperature does not vary during this change, the volume of the gas decreases. When the initial pressure is doubled, the volume decreases by 50%. The change in volume for gas is equally high during heating.

Differences in compressibility of liquids and gases are explained by their molecular structure. In liquids, the inter-molecular distance is small, i.e., the molecules are rather dense, which determines the small capability liquids have of compressing. By comparison with liquids, gases have an extremely low density. For example, the density of water is 816 times that of air. The low density of air and other gases is explained by the fact that in gases the inter-molecular distance substantially exceeds the dimensions of the molecules themselves. Therefore, when there is an increase in the pressure, the volume of the gas decreases due to the decreasing distance between molecules. Thus arises the elasticity which gas possesses.

In aviation problems, the need to account for air compressibility results from the fact that at high flight speeds in air, substantial differences in pressure arise which are the cause of substantial changes in its density.

To evaluate the effect of compressibility, let us examine the speed of sound.

§ 3. The Propagation of Small Disturbances in Air. Sound and Sound Waves.

The property of compressibility is intimately related to the phenomenon of the propagation of sound in gases. The speed of the propagation of sound plays a vital role in high-speed aerodynamics. The effect of compressibility on the aerodynamic characteristics of aircraft is a function of the degree to which the flight speed of the aircraft approaches the speed of sound. When air flows at speeds greater than the speed of sound, qualitative changes occur /10 in the character of the flow.

The sensation which we perceive as sound is the result of the effect, on

our auditory apparatus, of the oscillatory motion of air caused, for example, by the motion of some body in it. The displacement of each particle of air during its vibration is insignificantly small. The particles vibrate around their equilibrium configuration, which corresponds to their initial state. However, the laboratory process is propagated a very long distance.

The human ear perceives as sound those disturbances which are transmitted with a frequency from 20 to 20,000 vibrations per second. Those with a frequency of less than 20 per second are called infrasound, and those above 20,000 per second are called ultrasound.

By small disturbances we mean slight changes in the pressure and density of the medium (gas or liquid). Disturbances being propagated in the medium, such as air, are called waves (due to the similarity of this phenomenon to waves on the surface of water).

The speed of the propagation of the disturbances in space (the wave velocity) is quite substantial. The speed of propagation of a sound wave, i.e., small changes in density and pressure, is called the speed of sound. It is a function of the medium in which the sound is being propagated and of its temperature.

In high-speed aerodynamics, sound is considered as waves of perturbations created in the air by a flying aircraft.

The speed of sound in gases is a function of temperature. The higher the gas temperature, the less compressed it is. Heated gas has a high elasticity and therefore is more difficult to compress. Cold air is easily compressed. For example, at a gas temperature $T = 0$ (or $t = -273°C$), the speed of sound equals zero because under these conditions the gas particles are immobile and exercise only slight disturbances, with the result that they can create no sound.

The dependence of the speed of sound in air on temperature may be determined according to the following approximate formula:

$$a = 20 \sqrt{T} \text{ m/sec.}$$

Within the limits of troposphere, the air temperature decreases with altitude. Consequently, in the troposphere the speed of sound also decreases with altitude. On the earth's surface under standard conditions ($p = 760$ mm Hg, $t = 15$ sec), $a = 340$ m/sec. With an increase in altitude for every 250 m, /11 the speed of sound decreases by 1 m/sec.

At altitudes above 11,000 m, the temperature is (according to the standard atmosphere) considered constant and equal to -56.5°C. Consequently, the speed of sound at these altitudes should also be considered constant and equal to $a = 20 \sqrt{273 - 56.5} = 296$ m/sec (Fig. 1).

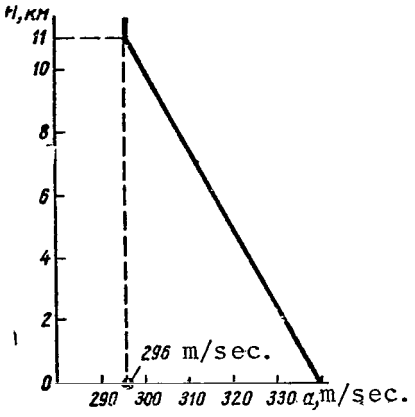

Figure 1. The Change in the Speed of Sound with Altitude.

§ 4. The Speed of Sound as a Criterion for the Compressibility of Gases

In gas dynamics, for the speed of sound there is the well-known formula:

$$a = \sqrt{\frac{\Delta p}{\Delta \rho}} \quad \text{m/sec},$$

where Δp is the change in pressure, $\Delta \rho$ is the change in gas density which it causes. The more compressed the gas is, the slower the speed of sound, so that one and the same change in density may be obtained through a slight change in pressure. And, in contrast, the less the compressibility of the medium and the greater its elasticity, the greater the speed of sound in the same medium. In this case, a slight change in density may be achieved only through a great change in pressure. The speed of sound is taken into consideration in any case in which there is an evaluation of the effect of compressibility in any aerodynamic phenomena, because the value of the speed of sound characterizes the compressibility of the medium. If the medium is elastic (compressible), compressions and expansions will vary substantially from layer to layer with the speed of sound. If the medium is absolutely incompressible, i.e., for any increase in pressure the volume or density remains unchanged, then as can be seen from the formula given above, the speed of sound will be quite high. In such a medium, any disturbances are propagated any distance instantaneously.

As was shown above, the value of the speed of sound varies in different gases and, in addition, it is a function of temperature. With an increase in altitude, temperature and the speed of sound decrease. Therefore, the effect of compressibility on the flight of aircraft at high altitudes should appear even greater. Let us introduce several values for the speed of sound at $t = 0°C$: for nitrogen it is 337.3, for hydrogen it is 1300, and for water it is 1450 m/sec.

For solid bodies, which are less compressible than gases, the speed of sound is still greater. Thus, in wood the speed of sound is 2800 m/sec, while in steel it is 5000 and in glass it is 5600.

An aircraft in flight, repelling air on all sides, partially compresses it as well. At low flight speeds, the air in front of the aircraft succeeds in being displaced and adapts itself to the flow around the aircraft so that compression is insignificant in this case. At higher flight speeds, however, the air compression begins to play a more important role. In this case, therefore, for a scale of flight speed we must use a characteristic speed which may /12 serve as a criterion for the compressibility of the medium. Such a speed is the speed of sound, inasmuch as it is a function of the temperature and

properties of the gas.

§ 5. The Mach Number and its Value in Flight Problems

The ratio of the flight (or flow) speed to the speed of sound is called the Mach number:

$$M = \frac{V}{a} .$$

Let us assume that the true flight speed (see § 6 of this Chapter) of an aircraft at an altitude of 10,000 m is 920 km/hr (255 m/sec). Then the Mach number $M = \frac{255}{300} = 0.85$, where a = 300 m/sec. In other words, the flight speed is 85% of the speed of sound at this given altitude.

Thus, in comparing the speed of the motion of the body in the air with the speed of sound under the same conditions, we may determine the effect of air compressibility on the character of the flow around the body. The Mach number is the index of the air compressibility. The greater the Mach number, the greater the air compressibility should be during flight.

To monitor the Mach number in flight, an instrument -- the Mach indicator (Machmeter) -- is usually set up on the pilot's instrument panel. In high-speed flight, especially when maneuvers are being performed which result in a loss of altitude, the reading on this instrument must be followed, and the pilot must not exceed the Mach number which the instructions permit for the given aircraft. If flight speed remains constant as altitude increases, the Mach number will increase due to the decrease in the speed of sound.

Failure to monitor the Mach number in jet aircraft would result in grave trouble because knowing the indicated speed (see § 6 of this Chapter) and even the true speed does not give the pilot a full understanding of the flight Mach number at any specific altitude. For example, if the aircraft is flying at an indicated speed of 500 km/hr at an altitude of 12,000 m, the true speed will be around 930 km/hr while the speed of sound is 1063 km/hr, so that under these given flight conditions the Mach number = 0.875. If, however, the aircraft is flying with an indicated speed of 500 km/hr at an altitude of 1000 m, the true speed is only 525 km/hr, while the Mach number = 0.43.

In turbojet aircraft, a change in the Mach number may be represented in the following way. After takeoff and retraction of the landing gear and wing flaps, the aircraft picks up speed until it achieves an indicated speed of 500 - 600 km/hr and starts climbing. Starting at an altitude of around 1000 m, the Machmeter shows a Mach number of M = 0.5 - 0.55. As the aircraft climbs, the true speed will increase, the speed of sound will decrease, and /13
the Mach number increase. When the aircraft reaches an altitude of 8-9 km, the Mach number reaches a value of 0.63 - 0.66 (depending on the actual temperature at that altitude). At altitudes of 10-12 km, during acceleration the Mach number increases to 0.80 - 0.85. At high altitudes the Mach number

will be greater when the same true speeds are maintained. Turbojet aircraft, like many other high-speed aircraft, have a limit to their Mach number because of conditions of stability and handiness (more will be said concerning the selection of the Mach number in Chapters 7 and 11). Therefore (especially at high altitudes), it is insufficient to monitor flight simply with respect to speed; the Mach indicator must also be observed.

§ 6. Flight Speed. Corrections to Instrument Readings Necessitated by Compressibility

Aircraft speed indicators measure directly not only the speeds, but the velocity head $q = \rho V^2/2$. The actual flight speed is not the same as this speed, which is indicated by the instrument, because the air-pressure sensor indicates the effect of perturbations created by the aircraft and the air compressibility. In addition, the value of the actual flight speed depends on instrumental corrections.

Therefore, to eliminate the above-mentioned errors in the instrument readings, the following corrections are introduced: aerodynamic, which accounts for the difference in the local pressures (at the point where the air-pressure sensor is located) from pressures in the undisturbed incident flow, corrections for compressibility, and instrument corrections*.

The speed which would be shown on an ideal (i.e., error-free) speed indicator is called the indicated speed V_i. The speed which is read from the instrument (read from the wide needle), does not as a rule equal the indicated speed. Therefore, a special name has been created for it -- instrument speed V_{inst}.

The true air speed is the speed of the aircraft's motion relative to the air (and is read from the thin arrow on the instrument).

The KUS-1200 combined speed indicator, which jet aircraft flying at Mach speeds up to 0.9 are equipped with, shows the instrument speed and the true air speed. During low-altitude flight (where the air density is close to that of the earth's surface, equal to 0.125 kG $\cdot$ sec^2/m^4), the instrument and true air speeds agree and both arrows on the instrument move together, being superimposed. With an increase in altitude, the true air speed surpasses the instrument speed and the arrows diverge, forming a "fork." /14
Knowing the true air speed and wind speed, it is possible to determine the ground speed, i.e., the speed of the aircraft's displacement relative to the earth. In flying and aerodynamic computations, both the indicated and instrument speeds are used. And what is the difference between them? To switch from instrument speed to indicated speed, we must introduce an aerodynamic correction and a correction for air compressibility:

---

* M.G. Kotik, et al., Flight Testing of Aircraft, Mashinostroyeniye, 1965 (Available in NASA translation).

$$V_{inst} = V_i + \delta V_a + \delta V_{comp} = V_{i_g} + \delta V_a,$$

where V_i = indicated speed,

δV_a = aerodynamic correction,

δV_{comp} = correction for compressibility, and

V_{i_g} = indicated ground speed.

For high-speed aircraft, an essential correction is the correction for air compressibility, whose value may range from 10 to 100 km/hr. The effect of air compressibility increases the speed indicator reading, so that δV_{comp} is always negative (Fig. 2).

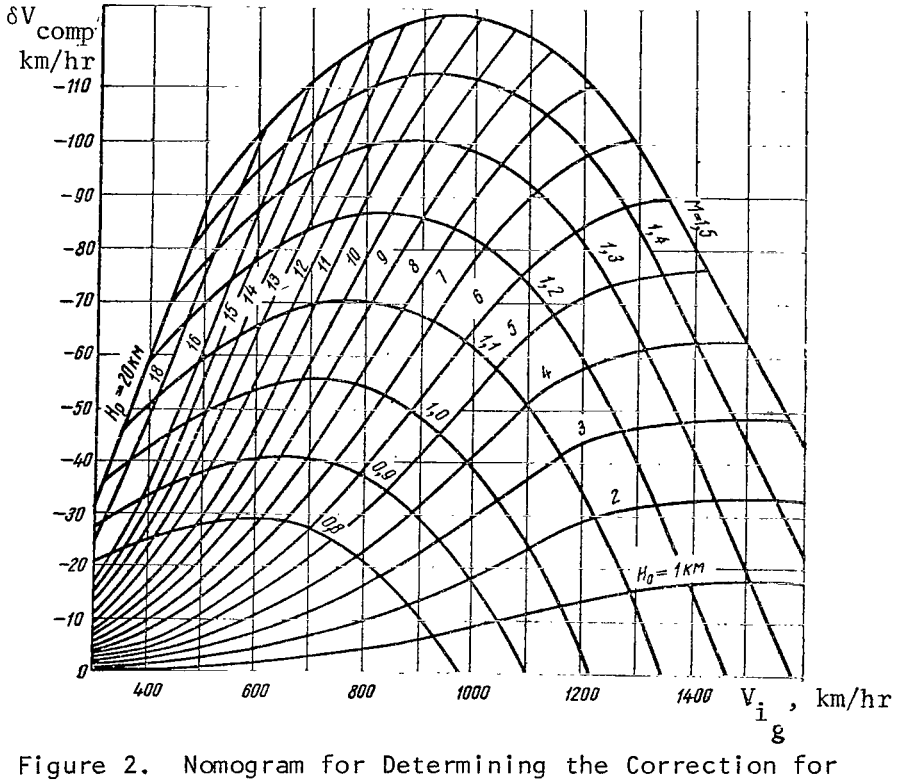

Figure 2. Nomogram for Determining the Correction for Air Compressibility

The aerodynamic correction may reach values from 5 to 25 km/hr and may be either positive or negative. Whereas the correction for compressibility is identical for all aircraft, the aerodynamic correction is basically a function of the type of aircraft or, more specifically, the position and features of /15

the engine. Therefore, each aircraft has its own graph of aerodynamic corrections.

The indicated speed with the correction for compressibility is called the indicated ground speed: $V_{i_g} = V_i + \delta V_{comp}$. At sea level, irrespective of air temperature, $V_{i_g} = V_i$. According to the nomogram in Figure 3, we may find the flight Mach number being given the value of V_{i_g}, and then determine the true flight speed: $V_t = aM$. For example, we must determine the true speed and flight Mach number for the aircraft if at an altitude of 10,000 m, V_{inst} = = 500 km/hr. Taking the aerodynamic correction $\delta V_a = -10$ km/hr, we find: $V_{i_g} = 490$ km/hr. For this speed, according to the nomogram (Figure 2), we obtain $\delta V_{comp} = -23$ km/hr. Then let us determine the indicated speed $V_i = V_{inst} - 10 - 23 = 500 - 33 = 467$ km/hr. The true flight speed may be found from the following expression:

$$V_t = \frac{V_i}{\sqrt{\Delta}} = \frac{467}{0.58} = 810 \text{ km/hr},$$

where for H = 10,000 m, $\Delta = 0.337$, a $\sqrt{\Delta} = 0.58$ (see the table for the standard atmosphere). Or, for speed $V_{i_g} = 490$ km/hr, according to the nomogram (Fig. 3), we obtain a Mach number of 0.75. Knowing the speed of sound at H = 10,000 m and the flight Mach number, it is easy to determine the true speed: $V_t = aM = 300 \cdot 0.75 \cdot 3.6 = 810$ km/hr. /16

The accepted value $\delta V_a = -10$ km/hr is characteristic of modern high-speed aircraft within the range of their indicated speeds of 220 - 600 km/hr. Later we will determine the correction for air compressibility in each concrete case according to the nomogram in Figure 2, while we will assume that the aerodynamic correction is $\delta V_a = -10$ km/hr.

§ 7. The Character of the Propagation of Minor Perturbations in Flight at Various Altitudes

In an example of aircraft flight, let us examine the manner in which slight fluctuations in density and pressure, i.e., minor perturbations, will be propagated in the air flow. The aircraft, being the source of the perturbations, has an effect on the air particles located in front of it and perturbations are sent forward from one particle to the next at the speed of sound.

Let us first take an aircraft flying at below the speed of sound (Fig. 4a).

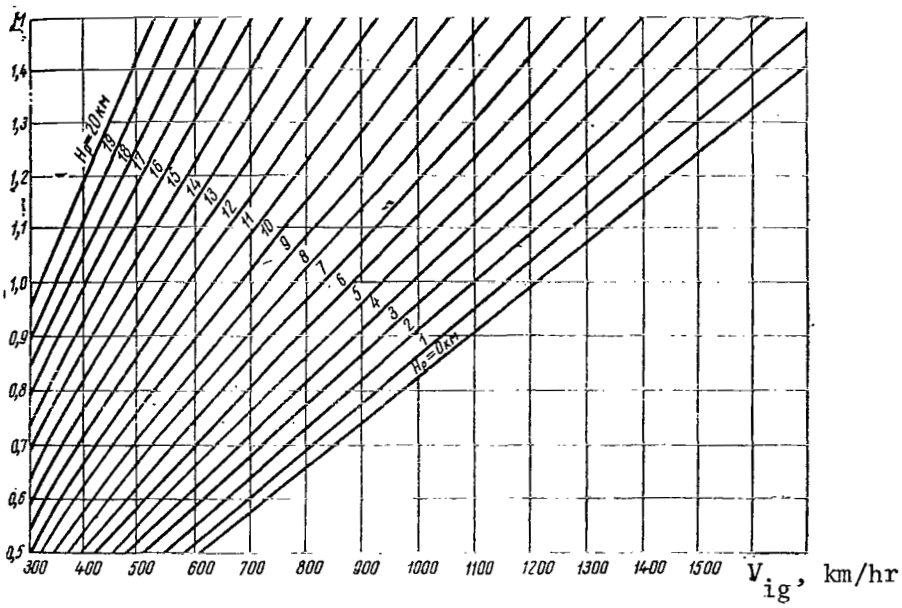

Figure 3. Nomogram for Determining the Mach Number

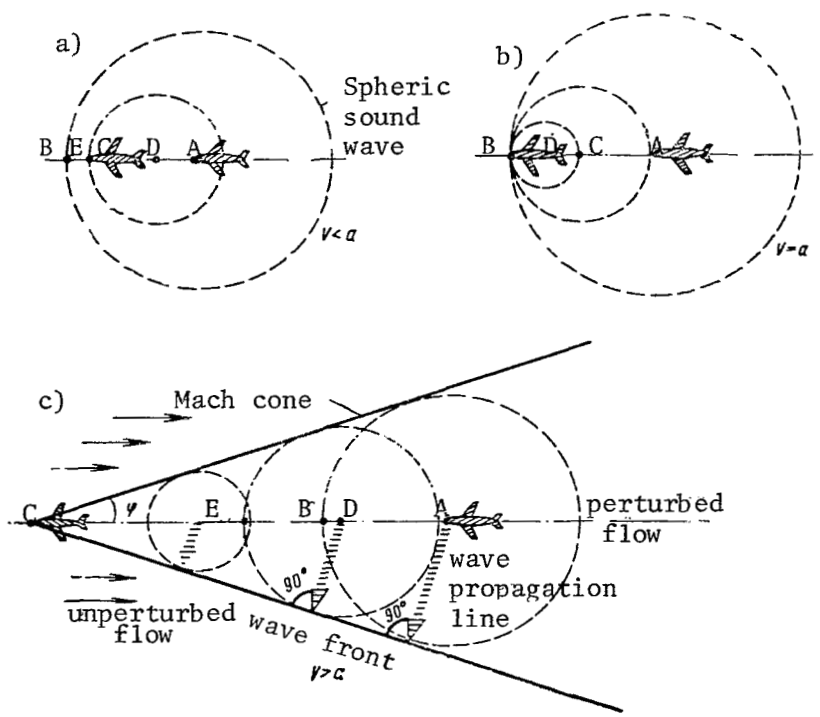

Figure 4. Propagation Characteristics for Sound Waves

When the aircraft passes through point A the perturbations created by it at that given moment, propagating along a sphere at the speed of sound, over take the aircraft. After a short time, the Mach wave reaches point B, while during this time the aircraft has succeeded only in progressing to point C; thus, its flight speed is below the speed of sound. Passing through point D, it again creates perturbations which will be propagated with the speed of sound and in a short while reach point E. The aircraft, however, during this time will not have reached point E but will be located between points C and E. Thus, the aircraft remains constantly within the sphere created by its sound wave. If, however, the aircraft flies at the speed of sound (Fig. 4b), then point B is reached simultaneously by both the aircraft and the sound waves, i.e., the perturbations created by it at points A, C and D.

Thus, in front of the aircraft there are always Mach waves which, becoming superimposed upon each other, form a dense section of air called the compression shock or shock wave.

If the aircraft flies above the speed of sound, it moves ahead of the spherical waves it has created (Fig. 4c). The aircraft will reach point C at the moment when the perturbation it created at point A has reached only point B, while the perturbation created at point D has reached point E. Thus, behind an aircraft flying at supersonic speed a Mach cone is formed which consists of an infinite number of Mach waves propagated along the sphere at the speed of sound. However, the air mass within the Mach cone is displaced /17
relative to the earth at the aircraft's speed. The greater the aircraft's speed, the sharper the angle at the tip of the Mach cone. This angle is determined according to the formula (Fig. 4c):

$$\sin \phi = \frac{1}{M} .$$

If the Mach number is 1, then $\phi = 90°$, while the full angle is 180° (normal shock); for $M = 2$, $\sin \phi = 0.5$ and the angle $\phi = 30°$ (full angle 60°).

Compression shocks are both normal and oblique. A normal compression shock is one whose surface is perpendicular to the direction of the incident flow, i.e., which forms an angle $\beta = 90°$ with it (Fig. 5a). Oblique shocks are those whose surface forms an acute angle of $\beta < 90°$ with the direction of the incident flow (Fig. 5b).

The greatest speed losses and increases in pressure are observed when the flow passes through a normal compression shock. The braking of the flow on this shock is so substantial that behind the shock the flow velocity must /18
be below the speed of sound (by as much as it was above the speed of sound in front of the shock).

In an oblique shock the losses are less than with a normal shock, specifically, proportionately little the more the shock was inclined in the direction of the flow, i.e., the less the angle β. The intensity of an oblique shock is also substantially less than a normal shock. If the angle β

is close to 90°, then behind the oblique shock the speed of the flow is subsonic, while somewhat greater than that which would be obtained if the shock were normal.

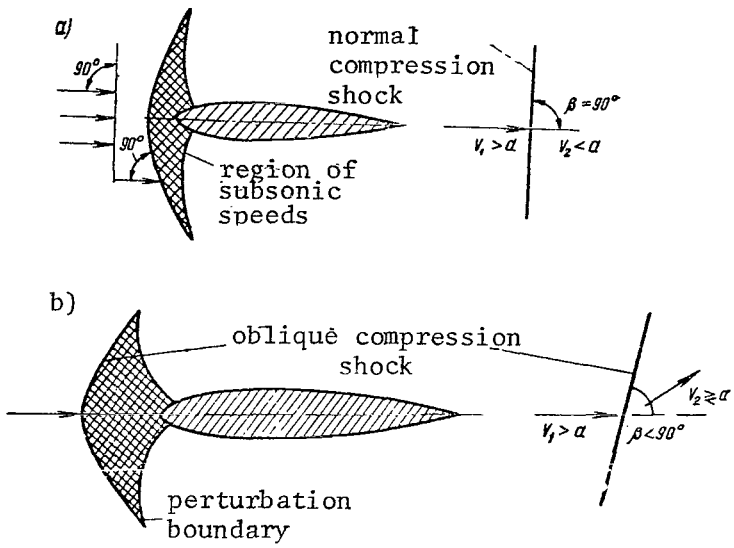

Figure 5. Formation of Normal (a) and Oblique (b) Compression Shocks.

Streams passing through an oblique shock change the direction of their motion, deviating from their initial direction. During flow around a wing or fuselage with a speed exceeding the speed of sound, an oblique shock developes in front of the wing or fuselage.

Aircraft intended for trans- and supersonic speeds must have aerodynamic shapes which do not generate normal compression shocks. The forward edge of the wing on supersonic aircraft must be knife-like, and the wing itself must be quite thin.

§ 8. Trans- or Supersonic Flow of Air Around Bodies

In the case of low-velocity flow around bodies, the flow is deformed at a substantial distance from the body and air particles, in breaking away, flow smoothly around it (Fig. 6a). When this occurs, the pressure close to the body varies insignificantly, which permits us to consider air density as constant. As a result of the difference in pressures under and over the wing, left is created. /19

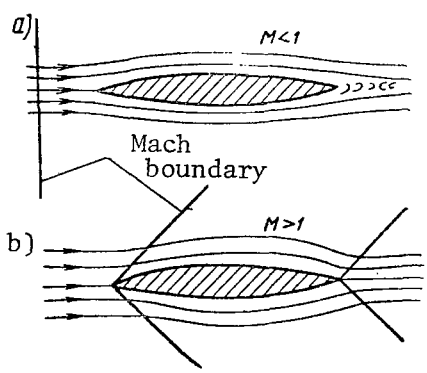

Figure 6. Subsonic (a) and Supersonic (b) Flow Around a Wing Profile.

In the case of sonic or supersonic flow around a body, local air pressure and density variations arise which, propagating at the speed of sound, form a sonic or supersonic shock wave in front of the body.

This occurs because the speed of the air particles close to the body suddenly varies in both amount and direction. When this occurs, the flow in a sense "encounters" an obstacle which, depending on the situation, may be the body itself or an "air cushion" in front of it and form a compression shock

(shock wave). At this compression shock there is an uneven change in the basic parameters characterizing the conditions of the air, i.e., speed V, pressure p, density ρ and temperature T. Shock waves may be formed either in front of the profile or close to its trailing portion. Precise calculations and measurements have shown that the thickness of the shock waves or compression shocks is negligibly small and has an order of length of the free path of the molecules, i.e., 10^{-4} - 10^{-5} mm (0.0001 - 0.00001 mm).

§ 9. Sonic "boom"

Supersonic flight is accompanied by the characteristic sonic "boom."

This phenomenon is the result of the formation of a system of compression shocks and expansion waves in front of the nose of a fuselage, the cabin, or where the wing and tail assembly join the fuselage.* The most powerful shock waves are formed by the aircraft's nose and wing, which during flight are the first to encounter the air particles, and the tail assembly. These shock waves are labeled bow and tail shock waves, respectively (Fig. 7a). Intermediate shock waves either catch up with the bow shock and merge with it or fall behind and merge with the tail shock. /20

Behind the bow shock, the air pressure increases unevenly, becoming greater than atmospheric pressure, and then decreases smoothly and becomes even less than atmospheric, after which it again increases unevenly until it is practically atmospheric again at the tail wave.

The sudden pressure drop is transmitted to the air around it in a direction perpendicular to the wave surface. Persons on the ground feel this drop as a strong "boom." Sometimes a second "boom" is heard -- this is the result of the successive effects of both the bow and tail shock waves.

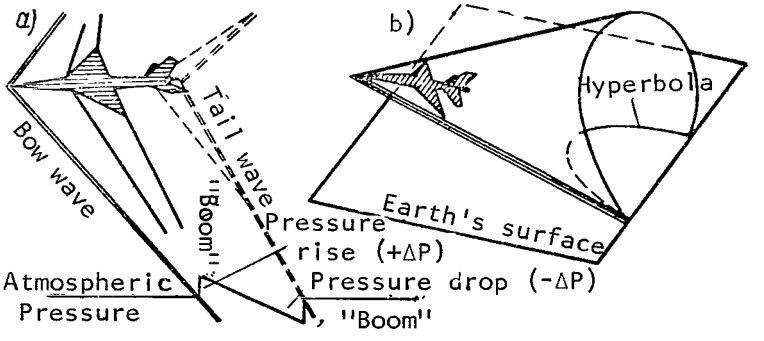

Figure 7. Air Pressure Changes during a "boom" in the Vertical Plane below the Aircraft (a), and the Interception of the Conic Shock Wave with the Earth's Surface (b).

* A.D. Mironov, Supersonic "Floc" in Aircraft. Voyenizdat, 1964.

Repeated observations have established that the two successive sonic booms are distinctly heard only when there is more than 1/8th of a second between them.

The longer the aircraft, the longer the time interval between the occurrence of the bow wave and the tail wave. Therefore, two "booms" are distinctly heard in the case of an aircraft with a long fuselage. And, in contrast, an only vaguely separated "boom" indicates that the aircraft has small dimensions or is flying at a relatively low altitude.

If the aircraft flies at a constant supersonic speed, the "boom" is heard simultaneously at different points on the earth's surface. If these points were to be joined by a line, we would obtain a hyperbola forming as a result of the interception of the conic shock wave with the plane of the earth's surface (Fig. 7b). One hyperbola corresponds to the bow wave, and the other -- to the tail wave. The lines of simultaneous audibility of the "boom" are displaced along the earth's surface, following behind the aircraft and forming unusual trails. At the same time, directly below the aircraft there is a substantially louder "boom," which attenuates as a function /21
of distance and under certain circumstances it is completely inaudible. The ground observer who hears the "boom" from an aircraft flying, let us say, at an altitude of 15 km with a speed twice that of sound will not observe the aircraft above him; at an altitude of 15 km, it takes sound approximately 50 sec to reach the ground at an average speed of 320 m/sec, while during this time the aircraft will have covered approximately 30 km.

To get an idea of the effect of a pressure drop on building structures, let us point out that the overpressure $\Delta p = 10$ kG/m^2 creates a short-lift load of 20 kG on a door with an area of 2 m^2, for example. A fighter with a fuselage length of 15 m at Mach 1.5 and H = 6000 m creates $\Delta p = 11$ kG/m^2. A heavy, delta-winged supersonic aircraft weighing 70 tons will, flying at an altitude of 20 km and at Mach 2 create $\Delta p = 5$ kG/m^2, and at low altitudes (5-8 km) a drop may reach 12-18 kG/m^2. It is a known fact that in their design, buildings are planned for the so-called wind load, which corresponds to the force of the pressure of air moving at a speed of 40 m/sec, i.e., greater than 140 km/hr. This type wind will create an overpressure of 100 kg on 1 m^2 of wall surface. The pressure in the "boom" at permissible flight altitudes is 1/5th or 1/6th that of the design allowance for wind load.

The characteristics of the effect of pressure drops in shock waves during "booms" are given in Table 2. For example, on a wall with an area of 12 m^2 during an overpressure of 50-150 kG/m^2, there is a short-lived load of 600-1800 kG. Under the effect of such a load, wooden structures may collapse. Therefore, aircraft are forbidden to accelerate to supersonic velocities below 9-10 km over populated areas. In the opinion of foreign specialists, a sonic "boom" with an intensity of 5 kG/m^2 is the most which can be tolerated harmlessly. Therefore, future supersonic jet aircraft with heavy flight weights (140 - 170 tons) will have to fly at altitudes of 18-24 km in order to minimize the effect of pressure drops. In this case, they will have to climb to altitudes of 9-10 km at subsonic light regimes (Mach number = 0.9 - /22
0.92), while beyond that at up to scheduled flight altitude at Mach M = 1.0 -

1.2, and only at this altitude will they be able to accelerate to supersonic cruising speed.

TABLE 2

Pressure Drop, kG/m^2	Relative Loudness and Resultant Destruction
0.5 - 1.5	Distant blast
1.5 - 5	Close blast or thunder
5 - 15	Very close, loud thunder (window glass rattles and shatters)
15 - 50	Large window panes shatter
50 - 150	Light structures collapse

The sound of the sonic boom is a function of the flight altitude, Mach number, aircraft's angle of attack, flight trajectory, atmospheric pressure at sea level and at the flight altitude, and wind direction with respect to altitude. For example, the "boom" from an aircraft flying at an altitude of 15 km and at Mach 2 (V = 2120 km/hr) is heard to a distance of 40 km from the aircraft's path, while at an altitude of 11 km it is heard only to a distance of 33 km. During flight at an altitude of 1.5 km at Mach 1.25, the "boom" is heard only within a belt 8 km wide.

A tail wind may displace the shock wave, resulting in displace of the audibility zone. The climbing and descent speeds and the angle of inclination Θ of the trajectory have significant effects on the size of the audibility zone and the loudness of the "boom." For example, in gaining altitude at an angle of $\Theta = 15°$ at H = 5 km, the "boom" is heard on the ground at $M > 1.2$. In descending from an altitude of 10-11 km at an angle $\Theta = -10°$, the "boom" reaches the ground only at M = 1.03.

In conclusion, let us dwell on the effect of the shock wave created by a supersonic aircraft on a passenger aircraft in flight. As has already been said, the pressure drop during a compression shock is 5-18 kG/m^2. If for the mean value we select 10 kG/m^2, it amounts to less than 0.1% of the air pressure at ground level ($p = 10{,}332\ kG/m^2 = 1$ at.). The velocity head for a jet passenger aircraft flying at a speed of 850 km/hr and at an altitude of 10 km is approximately $1200 kG/m^2$, i. e., more than 100 times the pressure drop in the "boom." Consequently, such a drop has essentially no effect on an aircraft in flight. However, there may be a certain effect on the aircraft's behavior as created by the accompanying jet from the aircraft flying by; this effect is comparable to that of a slight gust (a single gust of "bumpy air"), directed along the propagating line of the shock wave. As a result, the aircraft will experience slight bumpiness.

§ 10. Features of the Formation of Compression Shock during Flow Around Various Shapes of Bodies

Let us now look at the features of the formation of compression shocks first with the example of flow around the air inlet of a jet engine during supersonic flight, and then let us consider flow around the profile.

The existence of a normal shock at the intake to the diffuser leads to substantial losses of total pressure (kinetic energy) of the air entering the compressor and the combustion chamber.

During deceleration in the diffuser, the supersonic flow is transformed as it passes through the normal compression shock. When this occurs, one part of the kinetic energy of the air is used for its compression, while the other is transformed into heat (lost energy). However, during flight of the Mach number $M < 1.5$, losses at the shock are small. As a rule, therefore, for such flight speeds intake devices are used on subsonic aircraft. /23

At flight greater than 1.5 Mach, however, losses at the normal shock become greater. To eliminate this, the process of air deceleration in the intake device is achieved through the creation of systems of oblique shocks which terminate in a weak normal shock. Because overall energy losses in a system of oblique shocks are less than in one normal shock, the pressure at the end of the deceleration will retain a high value. Thus, the normal shock is divided into a series of oblique shocks. Structurally, this is achieved through setting up in the diffuser a special spike in the shape of several cones whose tips are directed according to flight (Fig. 8a).

When flight speed is decreased, the angles of inclination of the oblique shocks increase (the angle β tends toward 90°; see Figure 5). As speed is increased, the reverse occurs, and these angles decrease. This hinders the operation of the input device inasmuch as the front for all the shocks will not pass through the input edge of the cone (Fig. 8b). Therefore, sometimes the spike is adjustable, so that in the event of changes in speed, its position can be varied axially, thereby helping the shock to pass through the leading edge of the air intake at all flight speeds.

On the wing profile, the formation of compression shocks occurs even substantially below the speed of sound. As soon as the flow speed of the convergent stream exceeds the speed of sound somewhere on the profile, Mach waves appear which, in accumulating, form a shock. It must be noted that this shock wave is formed first on the upper profile surface close to some point corresponding to the maximum of the local speed and the minimum pressure on the profile. As soon as the speed of the flow surpasses the speed of sound, a shock wave forms on the lower profile surface as well (Fig. 9). /24

1. At point C the point of least pressure on the profile, the speed of the motion of the air has attained the local speed of sound (Fig. 9a). The Mach waves move from the source of the perturbation toward point C and, running into each other, form a weak normal compression shock.

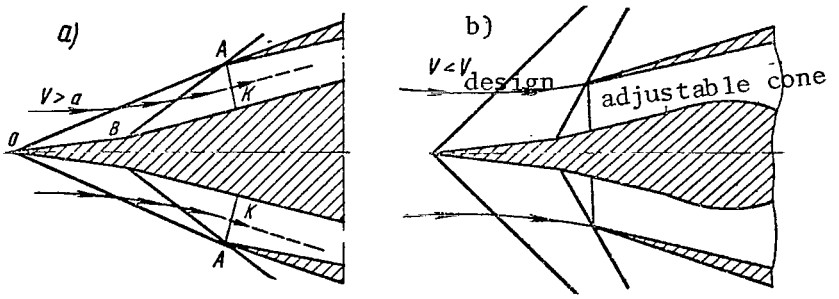

Figure 8. Formation of Compression Shocks at the Intake to the Diffuser of a Turbojet Engine at Supersonic Flight Speeds: a - line drawing of input device with cone: OA, BA -- oblique compression shocks, AK -- normal compression shock; b - operational configuration of supersonic diffuser during flight speed below its design speed.

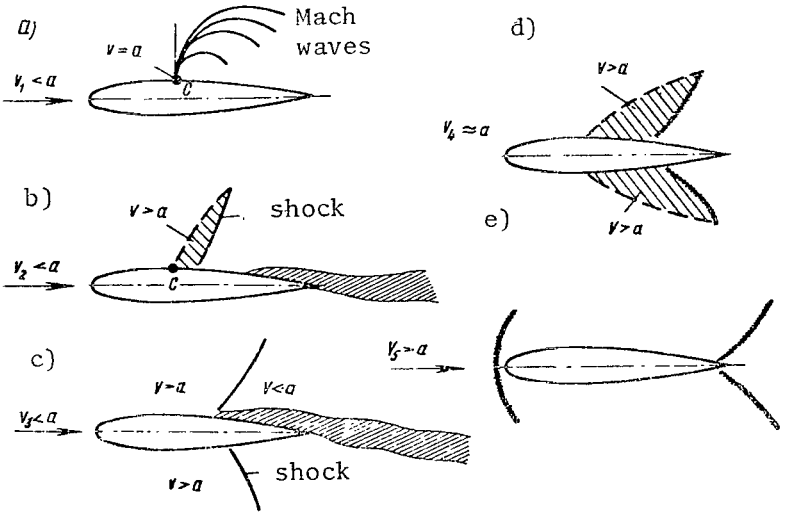

Figure 9. The Formation of Compression Shocks at Various Streamline Flows.

2. As the speed of sound increases somewhat (at $V_2 > V_1$), the speed of the flow around the profile increases (Fig. 9b). Behind point C, the speed of the flow becomes greater than the speed of sound. A section appears where the flow moves at supersonic velocity, resulting in the formation of an oblique shock.

3. At a speed of V_3 ($V_3 < a$), regions of sonic and supersonic flow also form on the bottom of the profile, resulting in the formation of compression shocks (Fig. 9c).

4. At a speed of V_4 close to the speed of sound, the compression shocks are displaced toward the trailing edge, thereby increasing the section of the profile which encounters supersonic flow past it (Fig. 9d).

5. When velocity V_5 becomes somewhat greater than the speed of sound, a bow wave forms in front of the profile and a tail wave forms behind it (Fig. 9e).

During flow around a blunted body, the compression shock forms at a slight distance from its forward section and assumes a curvilinear form (Fig. 10a). At its forward edge, the shock is normal -- here it is perpendicular to the incident flow. Depending on the distance from the body, the angles of inclination of the shock decrease. During supersonic flow around a knife-edged body such as a wedge with a large open angle (Fig. 10b), the shock is formed also at a slight distance from the bow point and also has a curvilinear form. If the open angle of the wedge is small enough, the compression shock "seats itself" on the sharp edges (Fig. 10c). /25

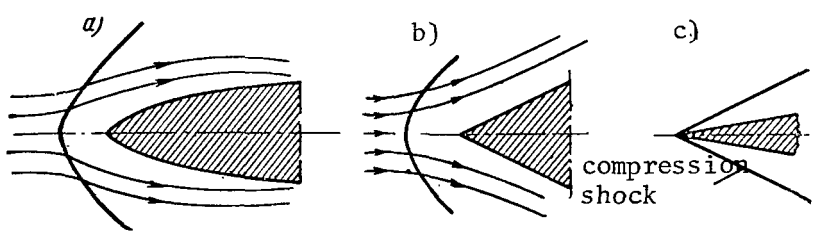

Figure 10. The Formation of Compression Shocks at Identical Flow Velocities: a - in front of a blunted body, b and c - in front of knife-edged bodies.

§ 11. Critical Mach Number. The Effect of Compressibility on the Motion of Air Flying Around a Wing

The compressibility of the air begins to manifest itself gradually as speed is increased. Up to a Mach number of 0.4, the effect of compressibility on the aerodynamic characteristics of the wing is only slight and may in practice be ignored. With a further increase in speed, this effect becomes more and more noticeable and can no longer be ignored. Starting at flight speeds of 600 - 700 km/hr and above, drag increases sharply because of compressibility. This occurs due to the fact that local speeds of the motion of the air over the wing and at points where the wing attaches to the fuselage substantially surpass the flight speed. In flowing around the convex surface of the wing, for example, the air streams are compressed and their

cross-section decreases. However, because the span across the stream must remain constant, the speed in it is increased. At any sufficiently high flight speed, the local air speed at any point on the wing or other point on the structure comes to equal the local speed of sound (Fig. 11).

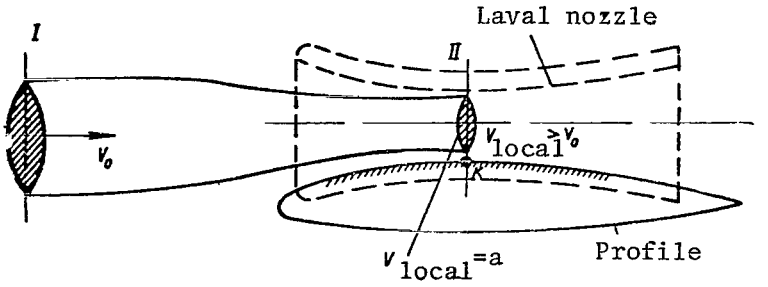

Figure 11. The Formation of the Local Speed of Sound in Flow around a Profile.

The flight speed at which the local speed of sound will appear anywhere on the wing is called the critical flight speed V_{cr}, while its corresponding Mach number is called the critical Mach number M_{cr}. Higher values for the /26 local speeds are observed on the upper air foil profile. As the speed of the incident flow or the flight speed increases, the local speed reaches the speed of sound fastest at this point.

Let us examine the air stream surrounding the profile (Fig. 11). Let us select two characteristic cross-sections of this stream: the large one I and the small one II. The local air speeds in section II will be greater than the local speeds in section I as a result of differences between the areas of these sections. If we increase the speed of the incident unperturbed flow, the local speeds increase in both sections, but in section II it is greater than in section I. This is explained by the fact that as a result of the increase in speed there is a drop in density which is more intense the faster the speed of the stream. To retain the steadiness of the mass flow weight rate of air along the stream, the speed in section II must increase additionally in order to compensate for the great density drop in this section. At the threshold, the local speed of the flow of air in section II may come to equal the local speed of sound.

From this it follows that during flight with speed V_{cr}, the local speed of sound is achieved at the narrowest point of the stream. It has been established theoretically that at this instant the critical pressure drop forms between section I and II which is equal to $p_{II} : p_I = 0.528$.

It is well known that if the speed of sound is achieved at the narrowest part of the stream, the speed increases and becomes supersonic if the stream continues broadening. Therefore, a fully supersonic zone of flow is formed down with portion of the profile surface during flight with $M > M_{cr}$.

The greater the flight speed, the greater the zone of supersonic speed will be. However, far behind the profile the speed must be the same as the flight speed. Therefore, at some point on the profile there must develop deceleration of the air from supersonic to subsonic speed. Such deceleration, as experience has shown, occurs only with the formation of a compression shock.

§ 12. The Dependence of the Speed of the Gas Flow on the Shape of the Channel. The Laval Nozzle /27

A means for obtaining supersonic speeds in the motion of the gas was developed by the engineer Laval (Switzerland) during his work in the 1880's on improving a steam turbine he had invented. Laval obtained a supersonic flow of vapor as it flowed from a special nozzle.

This nozzle, subsequently called the Laval Nozzle (Fig. 11), is a tube which is first compressed and then expanded. The narrowest section of the tube is called the critical section. If a vapor or gas is run through such a nozzle at a slight pressure drop in which the speed of the flow in the critical section becomes subsonic, in the expanded portion of the nozzle the speed will drop; in this case the Laval Nozzle operates as a typical Venturi tube. However, if the difference in pressures at the input to the nozzle and at its output are sufficiently great, in the critical section the speed of the flow becomes equal to the local speed of sound. In this case, beyond the critical section, i.e., in the broadened portion of the nozzle, the speed of the flow does not decrease but, on the contrary, increases. Thus, it was observed that in sub- and supersonic flows, the dependence of the speed of the flow of gases on the shape of the channel is directly opposite.

Subsonic flow accelerates in the compression channel and decelerates in the expansion portion. In contrast, however, supersonic flow loses its speed in the compression section, while it increases it in the expansion section.

Therefore, in Figure 11 we see the appearance of supersonic speed after the stream has passed through the narrow section (point K).

However, supersonic speed does not increase along the entire length of the nozzle; at some point it must decelerate to subsonic speed. And herein lies the cause for the formation of the compression shock.

§ 13. Laminar and Turbulent Flow of Air

Under the effect of internal friction due to the viscosity of air and the roughness of the surface of the body around which the flow moves, the speed of air at this surface becomes equal to zero. Depending on the distance from the surface, the speed of the flow increases and reaches the speed of free flow. The layer of air in which there is a change in speed from zero to the speed of free flow is called the boundary layer.

It is well known that the flow of air in the boundary layer may be laminar (stratified) when the gas flows without being mixed in the neighboring

layers and turbulent when there is random mixing of gas particles throughout the volume of the flow. The boundary layer also entails phenomena such as burbling (flow separation), the formation of surface friction drag, aerodynamic heating, etc. /28

The interaction of the boundary layer and the compression shocks results in the following. If the flow in the boundary layer is laminar (Fig. 12), an oblique compression shock developes directly on the airfoil profile. Behind the shock there is separation and turbulence of the boundary layer; in the turbulent region a normal shock developes. In general, the oblique and normal shocks are combined. When there is an oblique shock, the intensity of the normal shock will be substantially less because the flow approaches it, having already attenuated its speed somewhat in the oblique shock, with the result that the drag decreases. Therefore, laminarized airfoils, i.e., airfoils with very smooth surfaces, are suitable in that they offer the least surface friction drag and wave drag at supercritical flight Mach numbers.

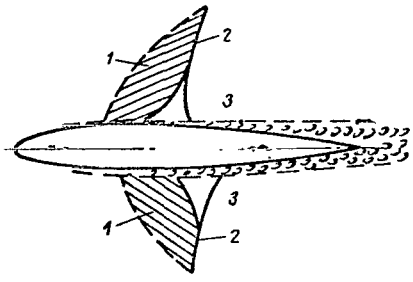

Figure 12. Compression Shocks on the Profile: 1 - Supersonic Zones; 2 - Compression Shocks; 3 - Subsonic Zones.

After the normal compression shock there begins the so-called wave flow separation, which is accompanied by a decrease in the local air speed. This in turn results in a sharp drop in the airfoil lift.

During turbulent flow around an airfoil there is no oblique shock and only one normal shock. The appearance of local shocks on the airfoil institutes the so-called shock stall. Part of the kinetic energy in the shock is transformed into heat which is then irreversibly propagated.

At high flight speeds, the characteristics of the compression shock are a function of the nature of the boundary layer. Experience has shown that flow in a boundary layer is usually laminar over a certain portion and then switches to turbulent.

The position of the transfer points of laminar boundary flow to turbulent depend on the shape of the profile, its thickness, roughness, etc. The surface of a body in laminar flow experiences less friction and less aerodynamic heating at high speeds than does one in a turbulent layer.

The state of the boundary layer is reflected not only in the wing drag, but in its lifting capacity as well. In the boundary layer a flow separation arises which determines the critical angle of attack and its corresponding maximum lift ratio.

§ 14. Pressure Distribution at Sub- and Supercritical Mach Numbers /29

Pressure distribution along a wing profile under flow conditions is shown in Figure 13. The arrows represent the values of the differences between the local and atmospheric pressures at each point on the profile. The positive overpressure (atmospheric pressure less than local) is indicated by arrows pointing toward the contour, whereas negative pressure or rarefaction (atmospheric pressure greater than local) is shown by arrows pointed away from the contour.

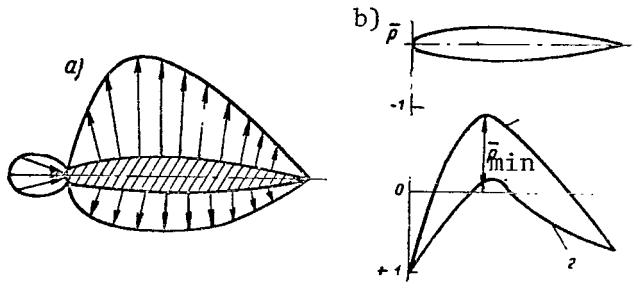

Figure 13. Diagram of the Pressure Distributions along the Airfoil Profile: a - vectoral; b - expressed by the pressure coefficient (1 - upper wing surface, 2 - lower surface).

To determine and compute the force of the evacuation on those points of the profile at which pressure measurements were taken, the profile chord for a line parallel to the chord is projected, then the measured values for the pressure are plotted at a selected scale from points specified along the perpendicular to the chord: positive overpressure is usually plotted below and evacuation is plotted above. The points thus obtained then merge in a smooth curve.

In diagrams used in aerodynamics, normally the pressure coefficients (Fig. 13b), which represent the ratio of the overpressure at any given point on the profile to the velocity head of the turbulent flow are plotted at points on the profile rather than the overpressure, as follows:

$$p = \frac{p_{over}}{q} = \frac{p_{local} - p_{at.}}{\rho \frac{V^2}{2}}$$

where p_{local} - is the absolute pressure at a given point;

$p_{at.}$ - is the static pressure in the unperturbed flow, i.e., the atmospheric pressure at flight altitudes;

q - is the velocity head in the unperturbed flow, determined by the flight speed and altitude.

From the above it follows that the pressure coefficient $\bar{p}$ characterizes /30 the degree of differentiation (in units of the velocity head) of the local pressure at any point on the upper and lower profile surfaces from the static pressure in the unperturbed flow. The coefficient $\bar{p}$ will be negative if the local pressure on the profile is below atmospheric pressure. Consequently, a negative value for $\bar{p}$ corresponds to the presence on the profile of rarefaction, where a positive value indicates an increased pressure.

At small Mach numbers, the diagram for the pressure distribution for each angle of attack has its own constant form because the air compressibility has no effect on the nature of the distribution of the pressure coefficients on the upper and lower surfaces. At high Mach numbers (0.6 and greater), there is an increase in the rarefaction in which greater rarefaction arises to a greater degree. This increase in the rarefaction is explained by the effect of compressibility -- density decreases as speed increases. Consequently, to maintain the constancy of the speed flow rate around the profile, it must increase further, which in turn causes a further increase in the rarefaction. At portions of the profile where the flow around it has its greatest speed, i.e., where rarefaction is greatest, the affect of compressibility will also be greater.

To further increase the speed of the incident flow (above M_{cr}), the rarefaction on the leading edge of the airfoil profile decreases while it increases sharply at the trailing edge, so that here the flow becomes supersonic and there is additional rarefaction.

The resultant zone of supersonic speed culminates in a compression shock behind which the local speeds become subsonic. Such a characteristic in the change of the local speeds for flow around an airfoil profile qualitatively changes the situation with respect to pressure rarefaction along the profile as compared to subcritical flow.

From Figure 14 it is clear that at that point on the profile where the compression shock formed there is a sharp and irregular pressure increase (i.e., decrease of rarefaction). At Mach numbers greater than critical, the increase in pressure in the leading portion of the profile and an increase in rarefaction in the trailing portion leads to a substantial increase in the drag coefficient. Shocks are normally manifested on the upper then lower surface in modern profiles at positive angles of attack.

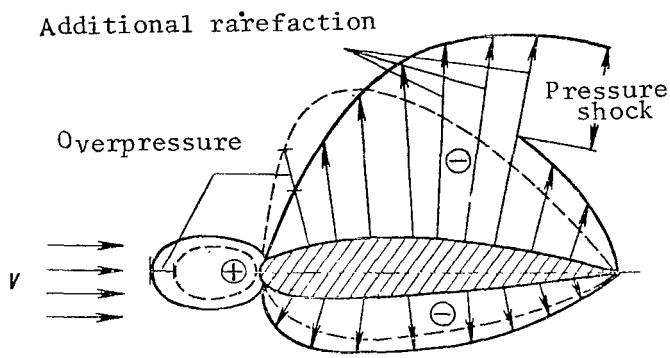

Figure 14. Pressure Distribution Along the Profile for Mach Numbers Below (broken line) and Above (solid line) the Critical Mach Number M_{cr}.

Let us look at the picture of pressure distribution along the chord of a symmetrical profile at a given angle of attack for various Mach numbers (Fig. 15). If at small Mach numbers the values of the pressure coefficient $\bar{p}$ are small, then with an increase in the speed of the incident flow the rarefaction on the upper profile contour increases and the curve of the pressure distribution is displaced upward. When local supersonic zones and compression shocks are

formed on the profile, i.e., for Mach numbers greater than critical, there is a zone of flow with V > a. This zone is enclosed by the normal compression shock. The formation of the shock causes a decrease in the rarefaction on the upper profile. When there is a further increase in the Mach number, the region of supersonic speeds broaden and the shock gradually is displaced to the rear. Decreasing the rarefaction becomes much more significant. The subsequent increase in the Mach number results in the shock being formed on the lower surface as well, where the rarefaction becomes greater. With even higher values for the Mach number, both shocks reach the trailing edge and the entire profile is surrounded by a supersonic flow. /31

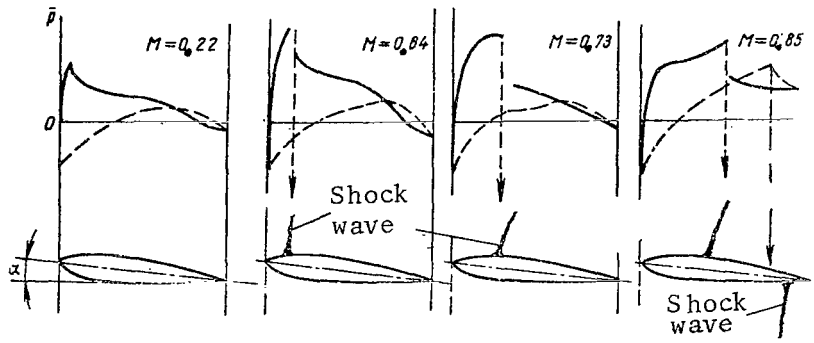

Figure 15. Representative Picture of the Pressure Distribution on a Symmetrical Profile (solid line -- upper surface, broken line -- lower surface).

Examination of the picture of pressure distribution gives proof of the fact that an increase in the Mach number substantially changes both the characteristics of the curves of pressure distribution and the moment characteristics of the wing.

CHAPTER II /32

AERODYNAMIC CHARACTERISTICS OF THE WING AND AIRCRAFT. THE EFFECT OF AIR COMPRESSIBILITY.

§ 1. The Dependence of the Coefficient c_y on the Angle of Attack

The dependence of the lift coefficient c_y on the angle of attack α is an important aerodynamic characteristic of the wing and the aircraft. The shape of the wing (for a specific number of profiles) in planform has a significant effect on the character of the change of the coefficient c_y for the airfoil at high angles of attack after the local flow starts to break away. Turbojet passenger aircraft have swept wings, and it is these which we shall discuss.

Figure 16 shows a graph for the change of the coefficient c_y as a function of the angle α of the airfoil with the sweep angle $\chi = 35°$. According to this graph we may evaluate the lifting ability of the airfoil and determine the angles of attack at which flight occurs. Depending on the flight speed and altitude for various flight weights, the required values of c_y are determined for horizontal flight.

The performace of an aircraft at high angles of attack, the causes for flow separation (burble) and other characteristics are also determined and explained by the dependence of c_y on α.

At high angles of attack burbling begins which distorts the picture of the flow and introduces a certain decrease in the mean value of the expansion above the airfoil, the increase in c_y slows down, and beyond a /33 certain angle of attack called the critical angle of attack, there is no longer an increase, but rather a decrease in c_y.

At high Mach numbers (flight cruising speeds), analysis of the dependents $c_y = f(\alpha)$ must be carried out with allowance made for the affect of compressibility, which changes this characteristic to a certain degree.

In swept airfoils, variations in the coefficient c_y with respect to the angle of attack have their own characteristics. As can be seen from Figure 16, at angles of attack from -1° to 10 - 12° (for small Mach numbers), there is a linear characteristic of increase in c_y. However, at angles of attack greater than 10 - 12° the proportionality is eliminated between the increase in the angle of attack and the increase in c_y; in addition,

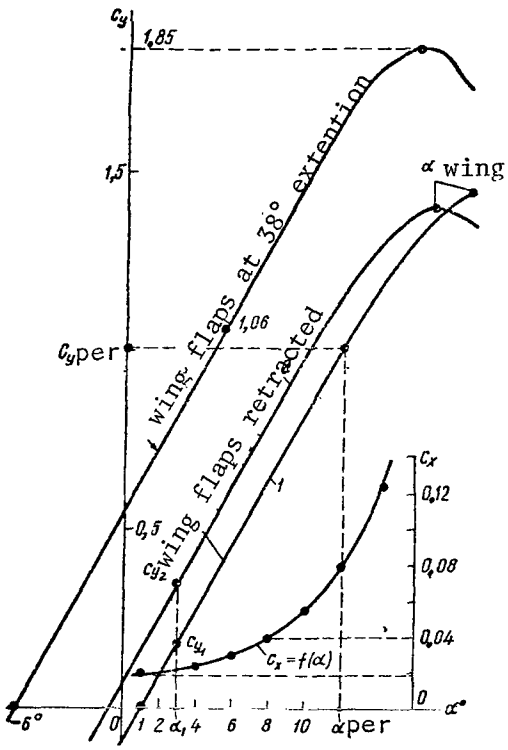

Figure 16. Graphs for the Coefficient c_y for a Swept Airfoil at Small Mach Numbers (1 - wing with geometric twist of 3°, 2 - without geometric twist) and the Coefficient c_x for the Aircraft as a Function of the Angle of Attack.

the increase in c_y slows down. This is due to the onset of burbling. At angles of attack from 17 to 20°, the lift coefficient reaches its maximum of $c_{y\,max}$. The change in the dependents of $c_y = f(\alpha)$ at this portion is a function of the shape of the leading edge of the airfoil. The wings in passenger aircraft have a blunted leading edge, so that the change in c_y in the zone $c_{y\,max}$ is smooth.

Swept wings (as compared to normal wings) have lower values for the coefficient c_y due to the flow around the wing at a velocity V_{ef}, which by creating lift becomes a component of the speed V_{pos} (see Figure 33). When the speed of the flow around the wing does not correspond to the flight speed, there arises a lateral displacement of the air particles in the boundary layer which, for the central sections of the wing, is equivalent to the effect which is obtained when the boundary layer is blown away or drawn off (see Chapter V, § 8). The separation of air particles from the upper surface is protracted to very substantial angles of attack, and before they are reached there is a steady increase in the coefficient c_y for the central portion of the wing.

Because of the great inclination of the curve $c_y = f(\alpha)$ to the horizontal axis in swept wings (as compared to normal wings), the increase in c_y as the angle of attack is increased by 1° it is less than that for a normal wing, i.e., less than the gradient of the increase for the lift coefficient. This also determines the lower lifting ability of swept wings as compared to normal straight wings.

For swept wings, within the range of angles of attack -1.0° - (10-12)°

(linear flow of the relation $c_y = f(\alpha)$ on each degree of increase α) the coefficient c_y increases by approximately 0.09 - 0.11.

The angle of attack at which the decreased growth of c_y is encountered and the characteristic vibrations in aircraft are observed is called the permissible angle of attack α_{per}, while the lift coefficient corresponding to it is $c_{y\ per}$ (Figure 17). The vibration in the aircraft begins after the burbling begins at the wing tips and the vortex flow strikes the tail assembly. On the curve (Figure 17) reflecting the total change in c_y for the wing as a function of α, the angle of attack corresponding to the onset of vibration is determined through the start of local flow separation at the wing tip (in the figure, this corresponds to the point where Curve 2 begins to deviate from the straight line). When $c_{y\ max}$ is reached by the wing tips, in spite of the subsequent sharp decrease in c_y at these tips, c_y for the entire wing begins to increase as the angle of attack does, although slower than at the beginning of separation. The increase in c_y takes place due to the separation-free flow at the central portion of the wing which occurs at high angles of attack. For high Mach numbers, the critical angle of attack may reach 30-35°. /34

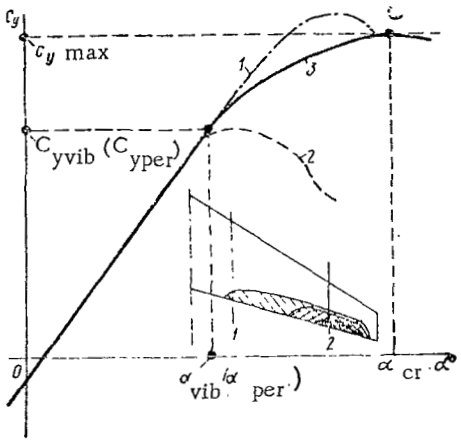

Figure 17. The Coefficient c_y for Various Parts of a Swept Wing as a Function of the Angle of Attack: 1 - central portion; 2 - wing tip; 3 - wing as a whole.

The aircraft's moving into the vibration zone indicates that low speeds have been attained, and in this case the vibration is a warning for the pilot.

In the zone of high angles of attack, there is a smooth change in c_y, especially close to its maximum. As a result of this, in the shift to supercritical angles of attack, swept wings have less of a tendency toward autorotation than do straight wings. In general, the swept wings on transport aircraft have less of a tendency toward spin.

Because of geometric twist, the running value of the coefficient c_y for the characteristic angles of attack during takeoff, climb, horizontal flight, etc., decreases. As can be seen from Figure 16, for the same angle of attack α_1, the wing's lift without geometric twist is better, and $c_{y2} > c_{y1}$. This is why flight in aircraft with wings having geometric twist is performed at greater angles of attack than with wings without this twist.

§ 2. The Effect of the Mach Number on the Behavior of the Dependence $c_y = f(\alpha)$

Air compressibility affects the dependence of the coefficient c_y on the angle of attack. Because of compressibility, an increase in the flight Mach number of more than 0.4 - 0.5 is accompanied by a qualitative change in the character of flow around the wing, because the speed of the flow on the wing increases, as a result of which for one and the same angle of attack the coefficient c_y increases, i.e., there is an improvement in the lifting capability of the wing. This is clear from Figure 18 (in which, for example purposes, the angle $\alpha = 4.5°$ has been selected). The angle of attack at which vibration begins decreases with an increase in the Mach number, because the vibration and the flow separation begins sooner than at low Mach numbers. Therefore, the value $c_{y\ vib}$ also decreases with an increase in the Mach number. For example, at M = 0.65, the coefficient $c_{y\ vib} = 0.99$, while at M = 0.85 it will equal 0.52 (Figure 19). In addition, $c_{y\ max}$ also decreases sharply. If from M = 0.65 the coefficient $c_{y\ vib}$ differs slightly from $c_{y\ max}$, then at M = 0.85 the value $c_{y\ vib}$ will be substantially less than $c_{y\ max}$. Flight accompanied by vibration usually precedes the onset of instability in the aircraft with respect to overload, while at certain values greater than c_y, the vibrations can lead to stalling at certain Mach numbers. Therefore the value c_y at which vibration begins is vital for flight purposes.

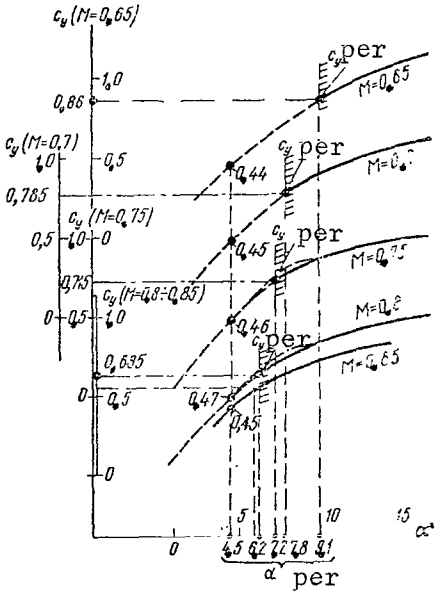

Figure 18. The Affect of the Mach Number on the Dependence $c_y = f(\alpha)$: - - - wind-tunnel tests; ——— flight tests.

If for M = 0.4 - 0.5 the angle of attack for the onset of vibration (see Figure 19) equals 12-13°, then for M = = 0.8 - 0.9 it decreases to 5-7°, and $c_{y\ vib}$ also decreases. This is especially dangerous at high Mach numbers because at the same time as the onset of vibrations, stalling may set in.

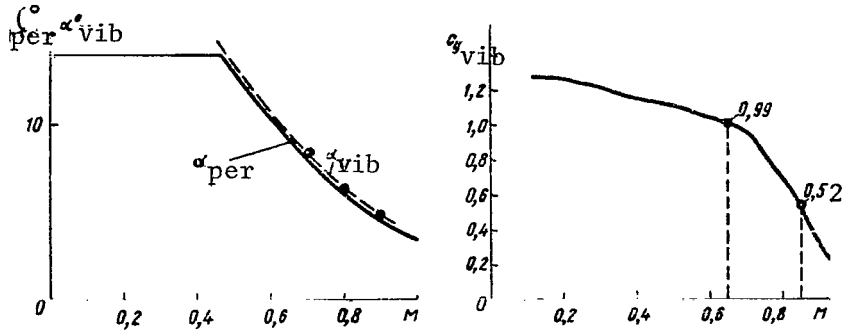

Figure 19. The Dependence of α_{vib} and $c_{y\ vib}$ on the Mach Number.

In the event that the shift to higher c_y is not accompanied by the characteristic vibration (of individual sections of the wing), to forewarn the pilot that this shift has occurred, special tubulence sensors are attached to the wings. They trap the local flow separations on the wing and transmit the vibration to the control wheel. This, for example, is what was done on the British turbojet Comet, on which the sensors are set symmetrically on the leading edge of the center section of the wing (Figure 20). On the pilot's instrument panel there is a special instrument which signals the pilot ahead of time (before $c_{y\ vib}$ has been reached) that the aircraft is shifting toward this regime (see Chapter XI, § 15).

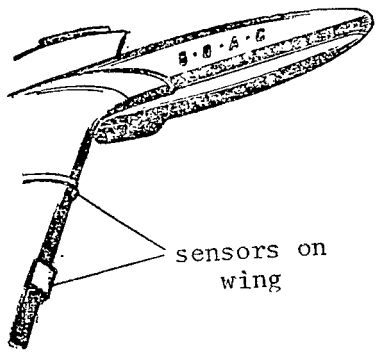

Figure 20. Positioning of Sensors on the Wing of the Comet Aircraft.

§ 3. The Permissible Coefficient $c_{y\ per}$ and its Dependence on the Mach Number

Flight safety is achieved in turbojet aircraft at high altitudes and Mach numbers through restricting the increase in the lift coefficient by the determined permissible values of $c_{y\ per}$. This is necessary to maintain longitudinal stability in the aircraft. Horizontal flight must be performed at an altitude and speed in which the value $c_{y\ hor}$ does not exceed $c_{y\ per}$ for a normalized vertical wind separation. The value $c_{y\ per}$ is selected such that it is always somewhat less than $c_{y\ vib}$ or matches it (Figure 18). From Figure 21 it can be seen that, for example, for a Mach number of 0.65 the coefficient $c_{y\ per}$ = 0.86, for M = 0.80 it equals 0.635, etc. The less the degree of

/37

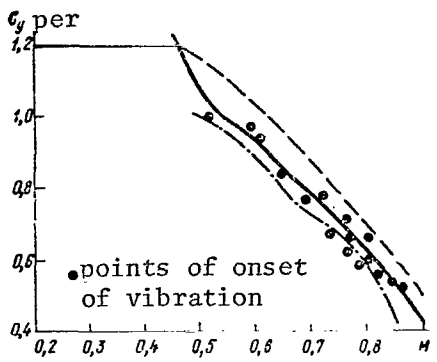

Figure 21. The Coefficient $c_{y\ per}$ as a Function of the Mach Number (angle of sweep $\chi = 35°$): -.-.-.- first-generation aircraft; ------ second-generation aircraft.

sweep of the airfoil, the greater the value $c_{y\ per}$. Careful selection of the profiles permits improving the conditions for flow around the wing and yields higher values of $c_{y\ per}$.

Such selection of profiles is especially characteristic of second-generation turbojet aircraft.

With high values for the Mach number, the coefficient $c_{y\ per}$ decreases to almost half its value, and at M = 0.85 it reaches as low as 0.54. In the zone of small Mach numbers (up to 0.46), a value of $c_{y\ per}$ = = 1.12 -1.2 is used, which permits determination of the lowest permissible speed for an aircraft with smooth wings (wing flaps retracted).

Further, in examining horizontal flight and the stability and handiness of the aircraft, we shall return to $c_{y\ per}$ and, in addition, we shall consider α_{per} and its representative values.

§ 4. Dependence of the Coefficient c_y on the Mach Number for Flight at a Constant Angle of Attack

In examining the effect of air compressibility on the lifting properties of the airfoil in § 2, we noted that for a constant (flight value) angle of attack, each Mach number is matched by a specific value of c_y.

As can be seen from Figure 22 (the curve for $\alpha = 4.5°$), the coefficient c_y increases constantly up to a value of M = 0.83, and then decreases. The reason for such a change in c_y is due to the effect of air compressibility on the pressure distribution along the profile (see Figure 9). Even with a Mach number of 0.4 in the vein flowing over the profile, an increase in velocity is accompanied by a marked decrease in air density, which leads to /38 an additional increase in the expansion above the upper surface (§ 10 of Chapter I). On the lower surface, the affect of air compressibility for these Mach numbers has a lesser effect, so that initially there is an increase in the coefficient c_y. During the formation of a compression shock, the lifting capability of the airfoil decreases. Shock-induction separation leads to a decrease in expansion on the upper portion of the airfoil profile, and c_y decreases. At a given Mach number, when there is a shock on the lower surface as well, it begins moving back, at first slowly

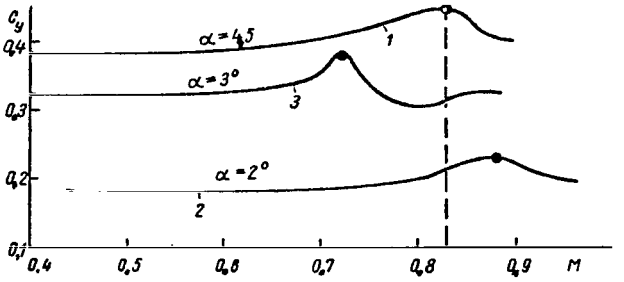

Figure 22. The Effect of Air Compressibility on the Coefficient c_y at a Constant Angle of Attack: 1,2 - swept wing with geometric twist; 3 - non-swept wing.

and then rather rapidly. As a result, on the lower surface the expansion zone will increase as the result of which the lift and, consequently, c_y as well will start to decrease. Later, as a given Mach number, the shock on the upper surface will also start to move back faster and faster, which will entail an increase in the expansion zone and the coefficient c_y. The values of the Mach number at which we observe the initial increase in c_y and its subsequent drop and renewed increase ("spoon") depend on the angle of attack for the profile and the airfoil as a whole. As can be seen from Figure 22, for smaller angles of attack (2-3°), the flow c_y is smoother with respect to the Mach number and the "spoon" is only slightly expressed.

This feature of the change in c_y with respect to the Mach number -- the "spoon" -- explains the "inverse reaction" of an aircraft (in banking) to declination in the control wheel (Chapter XI, § 22).

§ 5. The Affect of the Mach Number on the Coefficient c_x

Let us analyze the formula for drag

$$Q = c_x S \frac{\rho V^2}{2},$$

where S is the wing area.

If the angle of attack α is maintained constant, at small Mach numbers drag will vary proportionately to the square of the speed, while the drag coefficient c_x at these Mach numbers will be practically independent of speed and will vary only with respect to the angle of attack. As we can see from Figure 16, for α = 6-8° the coefficient c_x = 0.038 - 0.05 (at small altitudes and speeds). However, the dependence of c_x on only the angle of attack is observed at speeds at which the effect of air compressibility may be ignored. With an increase in flight speed, however, when compressibility does start to have an effect, the coefficient c_x increases, and more substantially the faster the shock stall on the profile developes. The relationship between the

/39

development of the shock stall and the increase in the coefficient c_x may be considered from Figure 23. Under Mach = 0.7, the coefficient c_x is practically changeless. After the flight (flow) Mach number exceeds its critical value, local compression shocks begin forming on the wing, wave drag appears, and a sharp increase in the curve c_x begins. This makes it clear that the greater the airfoil angle of attack (or the greater the flight c_y), the lower the critical value for the Mach number. With an increase in the Mach number, the compression shocks are displaced toward the trailing edge and become more powerful. At Mach = 1.1 - 1.15, a normal shock appears in front and shocks appear on both the top and bottom of the trailing portion of the profile.

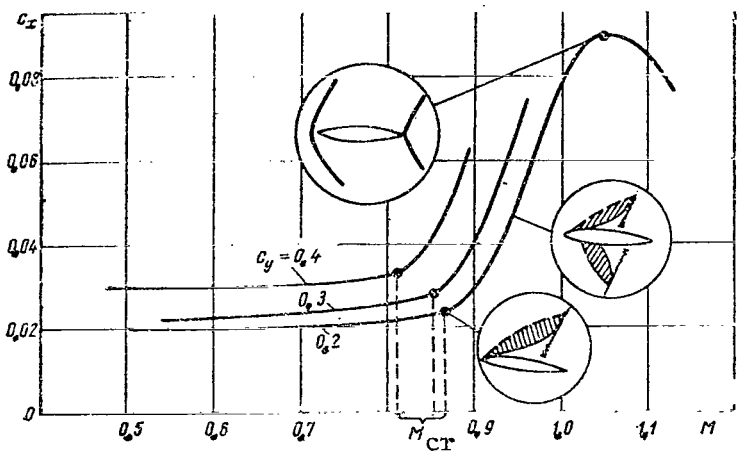

Figure 23. Dependence of the Coefficient c_x on the Mach Number for a Swept Wing.

It must be noted that an understanding of the critical Mach number, as related to the appearance of the local speed of sound at any point on a swept wing, has less of a practical value than it does for a straight wing. In general, the appearance of the local speed of sound on straight and swept wings does not immediately have a significant effect on the aerodynamic properties, and will not be noticed by the pilot.

The critical Mach number for a swept wing and the aircraft as a whole /40
is usually related to changes in the total aerodynamic characteristics and this is understood to mean that flight Mach number at which the pilot becomes aware of the effect of air compressibility on the handling qualities of his aircraft, i.e., changes in the stability and handiness. The critical Mach number as determined from these conditions is M_{cr} = 0.82 - 0.88. At such a Mach number, aircraft instability in terms of speed developes (the "spoon" on the balance curve) and the reverse reaction (in terms of banking) to declination of the rudder also appears.

In flight practice, concepts are used such as the so-called limiting Mach number, which the pilot must know absolutely. It is usually equal to 0.86 - 0.9. This Mach number can reasonably safely be substituted for the critical Mach numbers discussed earlier.

It should be pointed out that in aerodynamic calculations, the critical

Mach number is sometimes taken to be a flight Mach number whose increase by 0.01 leads to a 1% increase in the aircraft's coefficient c_x. According to the latest formulas, the Mach number M_{cr} = 0.78 - 0.80 for cruising values c_y = 0.25 - 0.30. For c_y = 0.35 - 0.5 at ceiling altitudes, depending on the takeoff weight the value M_{cr} decreases 0.70 - 0.74.

As was stated above, when the Mach number is increased above M_{cr}, a large supersonic zone of flow appears on the profile, the compression shock is moved back and expansion in the tail portion of the profile is increased and initiates an increase in the coefficient c_x. For non-swept wings, for example, this phenomenon occurs at Mach numbers 0.04 = 0.1 below M_{cr}.

For a further increase in the Mach number above the critical value, the coefficient c_x increases as a result of the increase in the local speeds on the lower profile surface, where a compression shock is also formed. A more intense increase in c_x in non-swept wings occurs in the range of Mach numbers from M_{cr} to M = 1; with a shift beyond M = 1, however, the coefficient c_x usually decreases. For swept wings, the maximum value of c_x corresponds to the Mach number M = 1.1 - 1.15.

It is known that wing drag is compounded from the profile drag Q_p and the induced drag Q_i; the formation of compression shocks on the wing adds the wave drag Q_w to these. With respect to this, the inverted form of the formula for the drag coefficient will be the following:

$$c_x = c_{xp} + c_{xi} + c_{xw},$$

where c_{xp} is the coefficient of profile drag for zero lift, and is compiled from the drag of the air friction on the wing surface and the drag caused by the difference between air pressures on the leading and trailing portions of the wing. The profile drag for the wing at small Mach numbers can best be established from friction whose value is only slightly dependent on the angle of attack*; at high angles of attack the separation drag is added to the friction drag and the coefficient increases sharply: $c_{xp} = c_{x\,fric} + c_{x\,pres}$; /41

c_{xi} is the coefficient of induced drag, which is a function of the wing lift; it is directly proportional to the square of the lift coefficient and inversely proportional to the wing aspect ratio:

$c_{xi} = \frac{c_y^2}{\pi\lambda}$ (here $\lambda = \frac{l^2}{S}$ - wing aspect ratio, l - span, and S - Wing area);

* A.P. Mel'nikov. High-Speed Aerodynamics (Aerodinamika bol'shikh skorostey), Voyenizdat, 1961.

c_{xw} is the wave drag coefficient.

Induced and wave drag are by nature pressure drags. When wave drag developes, the coefficient c_x increases 3-6 times for straight wings and 40-70% for swept wings as compared to its values for slow speeds.

Thus, the onset of compression shocks leads to an intense increase in the coefficient c_x because wave drag is added to the normal profile drag and induced drag.

§ 6. Wing Wave Drag

It was established earlier that an increase in the flight speed above critical leads to the appearance of a new, additional form of drag called profile wave drag.

To explain the nature of this drag, let us once more examine the picture of the pressure distribution along the upper wing surface for subsonic flow at sub- and supercritical flight speeds (Figure 14 and 24). As can be seen, in Figure 24 one section of the expansion vectors sort of "draw" the profile forward, while the other draws it back. To evaluate what would happen to the wing under the affect of these "pulling" forces, all expansion vectors must be projected in the direction of flight. When this is done we see that at subcritical speeds the forces "pulling" forward are negligibly less than those "pulling" back (Figure 24a). With an increase to supercritical speeds, the pressure distribution picture changes (Figure 24b), as a result of which the forces "pulling" the profile forward decrease (expansion becomes less at the bow of the profile) while the forces "pulling" back increase (because expansion on the trailing slope of the profile increases by an absolute value). From the figure it is clear that the difference in the projections of the vectors of the "pulling" forces directed to the rear increases, causing an increase in drag. However, because the extent of the supersonic zones over and under the wing increases as flight speed increases, there is an even greater displacement of the largest expansion toward the rear and the trailing edge. The forces "pulling" the profile forward increase at the same time the pressure on the leading edge of the profile increases. To sum up, the wing drag continues to increase. Thus, the wave drag is by nature a pressure drag because it is dependent on the increase in the pressure difference in front of the wing and behind it.

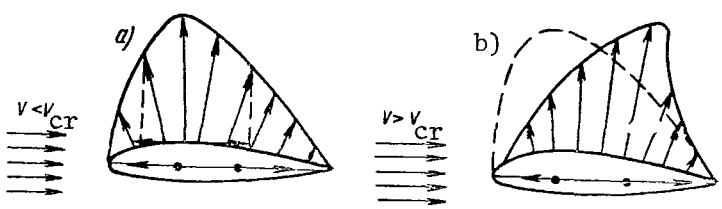

Figure 24. Examples of Wave Drag.

/42

Therefore, in aerodynamics wave drag has come to mean the additional drag

caused by an increase in the pressure differences in front of the wing and behind it when there are supersonic zones of flow and compression shocks on the airfoil profile*.

This drag is called the wave drag because the process of the development of supersonic zones of flow is accompanied by the development of shock waves or compression shocks.

From the energetic viewpoint, wave resistance is the result of the deceleration of air flows on the compression shocks. When this occurs, the kinetic energy of the flow is irreversibly consumed in heating the air in the shock.

As can be seen from Figure 25b, in the range of cruising flight Mach numbers, the value of the wave drag c_{xw} = 0.004 - 0.012 or for the mean value c_x = 0.025, it will equal 25 - 50% (for aircraft).

At supersonic flight speeds (Mach ≥ 1 - 1.2, Figure 25a), air deceleration on the bow and tail compression shocks decreases because the angles of inclination of these shocks decrease, which means that the wave drag itself decreases.

At supercritical Mach numbers, aircraft drag increases intensely because it is a function of both c_x and V^2. From the same figure we see that at a constant angle of attack, the drag force below M = 0.5 increases as a parabola, /43 while beyond this Mach number this lull does not hold, and the curve deviates from the square parabola, which is the result of the effect of compressibility and the development of compression shock.

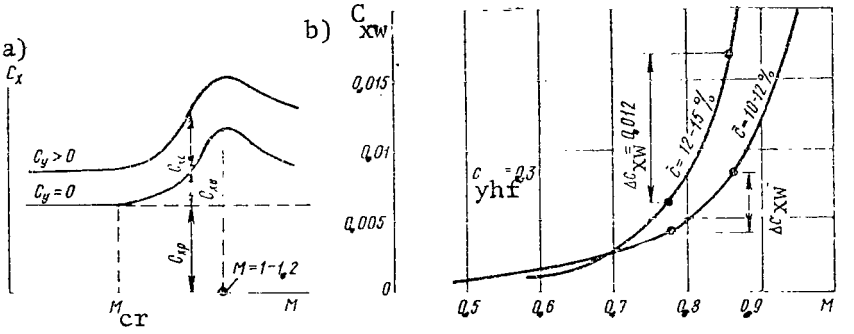

Figure 25. Dependence of the Coefficient c_x on the Mach Number (a) and the Effect of the Relative Profile Thickness on Δc_{xw} for the Wing (b).

* A.P. Mel'nikov. High-Speed Aerodymamics (Aerodinamika bol'shikh skorostey), Voyenizdat, 1961.

§ 7. Interference

The increase in aircraft flight speeds has led to an increase in the importance of interference, i.e., the combined effect of various parts of the aircraft such as the wing and the fuselage. Usually interference leads to an substantial increase in drag, especially in the zone of transonic flight speeds.

It has been experimentally established that "positive" interference can be achieved. This is the interference which aids in decreasing the additional drag resulting from the points where the various aircraft components are joined. Turbojet passenger aircraft are basically low-wing aircraft. When the wing and fuselage are joined in this way, the use of fairings helps to smooth the junction point of the wing and fuselage to a certain degree. Positioning the engines in the base of the wing (see Chapter IV, § 8) as was done on the Tu-104, Tu-124 and Comet aircraft creates an ejector effect -- an "active fairing" -- at the junction point for operating engines.*

Another way of decreasing the drag is using the "rule of area," which is also applicable for subsonic aircraft.

With respect to this rule, drag in flight vehicles proves to be minimal when the law of variations in cross-sections with respect to length corresponds to the law of variations in cross-sections with respect to the length of a body of revolution of least drag. It is well known that drag from the combination of the wing and fuselage (and other parts of the flight vehicle) will be the same as equivalent drag, i.e., drag having the same law for variations in cross-section with respect to length of a body of revolution. Therefore minimal drag may be achieved through decreasing the cross-section of the fuselage ("squeezing"), at the point where it joins the wing, by a value equal to the area of the corresponding wing cross-sections (Figure 26). /44

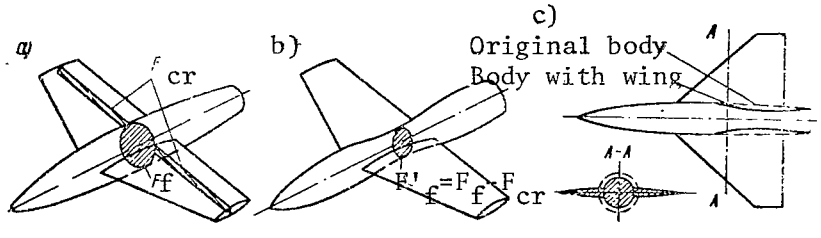

Figure 26. Examples of the Use of the "Area Law": a - "fuselage - wing" combination without allowance for the area law; b and c - the same combination with allowance for the "area law."

* S.M. Yeger. Designing Passenger Jet Aircraft (Proyektirovaniye passazhirskikh reaktivnykh samoletov). Mashinostroyeniye, 1964.

The "area law" is also applicable to the junction of engine nacelles, externally suspended fuel tanks and other aircraft components. Thus, for example, on the Tu-104 and Tu-124 aircraft having wings with a relatively high wing aspect ratio, the wing and fuselage interference is somewhat decreased by the substantial distance of the wing tips from the fuselage; as a result, instead of thickening the fuselage behind the wing, drop-shaped nacelles are installed on the wing. This yields a smoother change in the volume of the aircraft along its length without modifying the fuselage.

On the Convair 990, there are four nacelles which are used to carry fuel. As a result this aircraft has achieved a maximum cruising Mach number of 0.91.

It is felt that allowance for the "area law" in designing aircraft can improve their flight qualities by 20-25%. In some cases, however, observance of this law has proven unsuitable due to complications and difficulties in designing the fuselage which have resulted in the need for curvature of its power plants.

§ 8. The Aircraft Polar. The Effect of the Landing Gear and Wing Mechanization on the Polar

The polar of an aircraft serves in evaluating the aircraft's aerodynamics. It offers a graphic representation of the values of the coefficients c_y and c_x at various angles of attack, as well as indicating their variations when these angles change.

Figure 27 shows the polars of one aircraft obtained as the result of wind tunnel testing and refined with respect to data from flight testing. Let us determine the characteristic angles of attack and their corresponding aerodynamic parameters. The point of intersection of the polar a with the axis of the abscissa is determined by the zero-lift angle of attack $\alpha_0 = 1°$ and its corresponding coefficient $c_{x0} = 0.018$ (for a relative airfoil profile thickness of $\bar{c} = 10 - 12\%$); for $\bar{c} = 12 - 15\%$ the coefficient $\bar{c}_{x0} = 0.021 - 0.023$. The small value for c_{x0} is obtained through the creation of a well streamlined shape for the aircraft with a small center section for the fuselage and engine nacelles. /45

The aerodynamic tests as to the degree of refinement in the aircraft is its efficiency. Modern aircraft have a maximum efficiency of $K = 15 - 18$ at the optimum angle of attack of 5-7° and Mach numbers of $M < 0.5$. An aircraft's lift drag ratio increase with an increase in the angle of attack from α_0 to the optimal α_{opt}, because at this point c_y increases faster than c_x. Starting with an angle of 5-7°, the coefficient c_x increases more rapidly (due to the increase in the induced drag) and therefore the performance drops. Later it will be shown that α_{opt} is the division point between two flight /46

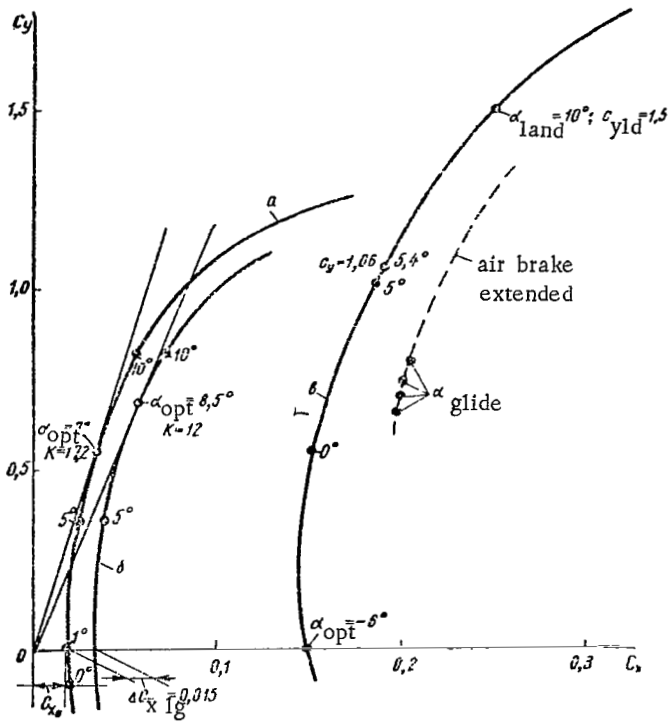

Figure 27. Aircraft Polars: a - landing gear and wing flaps withdrawn; b - landing gear down; c - landing gear and wing flaps extended in landing configuration.

regimes: the first and the second. For the polar a (see Figure 27), $\alpha_{opt} = 7°$ at $c_y = 0.55$, while K = 17.2.

When the landing gear is lowered, the polar moves to the right (polar b in Figure 27) because the coefficient c_x increases to the value $\Delta c_{x\ lg}$. After the landing gear is retracted, the well doors are normally closed so that $\Delta c_{x\ lg} = 0.015 - 0.020$ and the lifting ability of the wing does not change. As a result the setting for the angle of attack for polar b remains the same as for polar a. The maximum performance for an aircraft with landing gear extended decreases in our case to 12, while α_{opt} increases to 8.5°.

When the landing gear and wing flaps are extended (in landing configuration) the polar moves to the right and upward (polar c in Figure 27), and the coefficient c_y increases throughout the range of angles of attack, the zero-lift angle of attack becomes negative ($\alpha_0 = -6°$), and the maximum performance of the aircraft decreases as a result of the fact that the coefficient c_x increases to a greater degree than the coefficient c_y.

When the wing flaps are in the takeoff configuration, the maximum performance (landing gear down) decreases to 10-12 (Figure 65).

In gliding toward the landing with landing gear and wing flaps down in the landing configuration, the performance decreases to 7-8. Extending the air brake moves the graph of the polar to the right, as the result of which the performance decreases substantially, particularly in gliding at angles of attack of 2-3°, at which the landing run is made. Displacing the hinged flap spoilers causes a sharper drop in the aircraft performance (see Figure 107).

§ 9. The Effect of the Mach Number on the Aircraft Polar

For each flight Mach number we may construct a polar by determining for this value c_x and c_y with an allowance made for the effect of compressibility and thereby obtain the polar net (Figure 28a). Earlier it was established that at subcritical flight speeds the wing coefficient c_x is almost invariable, while the lift coefficient c_y increases starting at M = 0.5 - 0.6. Therefore, with an increase in the Mach number to M_{cr}, the polar is pulled forward because of the increase in c_y and in the region of high angles of attack is simultaneously shifted to the right due to the increase in c_x as a result of an increase in the induced drag. This is clearly shown in polars for Mach numbers 0.8 and 0.84 (wing with $\bar{c}$ = 12 - 15%).

As is well known, aerodynamic performance /47

$$K = \frac{c_y}{c_x} = \frac{1}{\tan\theta}.$$

At super-critical flight speeds at which the wave drag increases substantially, for a specific Mach number the polar moves to the right and increases the shift to that side (in Figure 28a, this corresponds to Mach number of M = 0.84) as a result of a decrease in c_y. If, however, the Mach number is so great that there is wave drag at almost every angle of attack, this Mach number (for any c_y) has an increased value of c_x and the polar proves to be only shifted to the right (in Figure 28a, the polar for the Mach number 0.9). This bears witness to the decrease in the maximum performance of the aircraft, as can be seen in the figure, in which are given the tangents to the polars and the angles for performance $\theta_2 > \theta_1$.

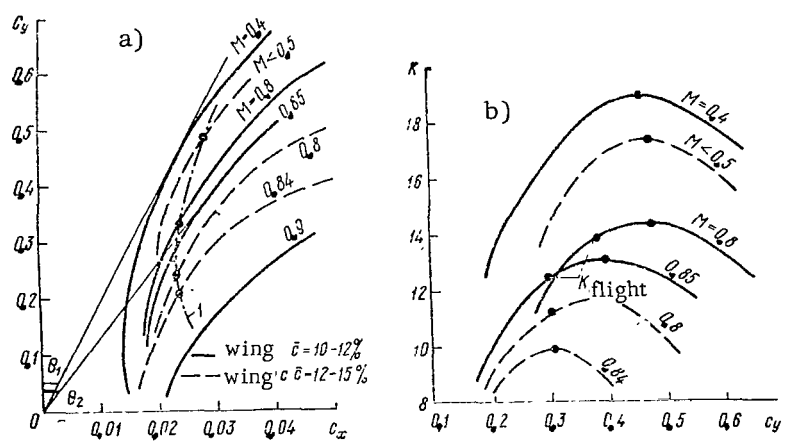

Figure 28. Aircraft Polars and Dependence of Aerodynamics Performance K on Mach numbers.

In arranging the polar net, we may construct a graph for the dependence of performance on c_y for various Mach numbers (Figure 28b). Usually maximum performance is obtained for values of c_y which are 20-30% greater than the

value for c_y in horizontal flight. If at M < 0.5 the maximum performance K = 15-17, then at M = 0.8 it will equal approximately 12-14.5. As can be seen from Figure 29, for Mach numbers M = 0.8 - 0.84, K_{max} = 12-14 and only at high Mach numbers does it decrease to 11-12. High aerodynamic performance in an aircraft has a favorable effect on the volume of fuel consumed per kilometer.

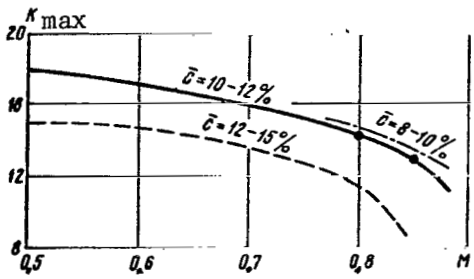

Figure 29. Maximum Aerodynamic Performance as a Function of Mach Number: ----- first-generation aircraft; ——— various second-generation aircraft.

The affect of wing sweep is that with/48 an increase in the angle of sweep, the aerodynamic performance decreases at low flight speeds and increases at high flight speeds. The parameters for second-generation aircraft wings at cruising Mach numbers of M = 0.8 - 0.85 have been selected such that K = 13-14 is achieved (Figure 29).

It is well known that for each Mach number, a high-speed aircraft has its own relation between the coefficient c_x and c_y. If for various Mach numbers we introduce into the polar network values of c_y for horizontal flight (for specific weight and altitude) and then join these points, we obtain the polar for horizontal flight regimes (the dot- and dash line in Figure 28a), which establishes a relationship between c_x, c_y, the Mach number and the horizontal flight altitude. It is clear from the picture that this polar intersects all the working polars for Mach numbers from 0.5 to 0.84. The higher the Mach number, the lower the c_y at which this intersection occurs. In other words, the higher the flight Mach number, the lower the value of c_y required for horizontal flight.

CHAPTER III

SOME FEATURES OF WING CONSTRUCTION

§1. Means of Increasing the Critical Mach Number

The increase in drag as the Mach number M_{cr} is raised is an unusual barrier which makes it difficult to achieve high flight speeds. Therefore, tests have been run on aerodynamic shapes of aircraft at which the shock stall would begin at the highest possible flight Mach number and would be maintained as long as possible smoothly, i.e., so that means of increasing the critical Mach number for the profile could be achieved.

The critical Mach number for the profile may be determined according to the following empirical formula:

$$M_{cr}=1-0.7\sqrt{\bar{c}}-3.2\bar{c}c_y^{1,5},$$

where $\bar{c}$ is the relative thickness of the profile;
c_y is the lift coefficient for the angle of attack under consideration.

Let us bear in mind that the characteristic parameters for the airfoil profile are (Figure 30):

relative thickness $\bar{c}\%$ - the ratio of the maximum profile thickness c_{max} to the chord b;

the position of the maximum profile thickness $\bar{x}_c\%$ - the relative distance of the maximum profile thickness x_c from the nose to the chord b;

the relative profile curvature $\bar{f}\%$ - the ratio of maximum buckle f to the chord b;

the distance from the profile nose to the point of maximum profile curvature x_j, expressed in units of the chord b, - $\bar{x}_f\%$.

Let us examine the effect of each of these parameters on the M_{cr} number.

The effect of $\bar{c}$. The profile thickness has a distinct effect on the value of the drag. The greater it is, the greater the degree to which the air stream surrounding the profile is compressed, and consequently the sooner the shock stall will occur at lower Mach numbers. In contrast, decreasing the profile thickness displaces the moment when the shock stall occurs to a higher Mach number. Figure 31 gives a clear example of the degree to which the thinness of the profile results in a greater critical Mach number M_{cr}.

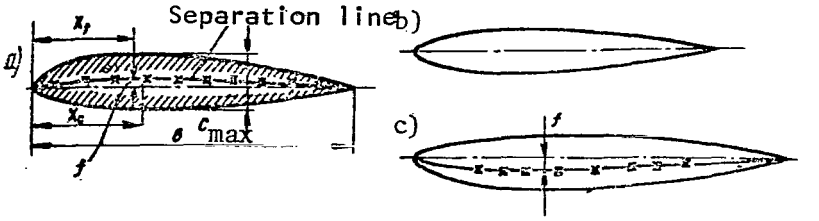

Figure 30. Geometric Parameters and Shapes of an Airfoil Profile: a - profile with positive curvature; b - symmetrical profile; c - "inverted" profile with negative curvature (Douglas DC-8).

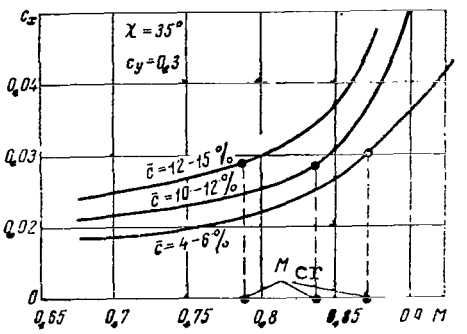

Figure 31. The Effect of Airfoil Profile Thickness on the Coefficient c_x for Various Mach numbers.

Aircraft wings carry fuel, with the result that the relative profile thickness is 10 to 15%. This is necessary to obtain sufficient volume and maintain wing strength.

As an example, let us determine the critical Mach number for profiles with relative thicknesses of 10 and 15% if $c_y = 0.3$. Calculations show that for $\bar{c} = 10\%$, $M_{cr} = 1 - 0.7\sqrt{\bar{c}} - 3.2\bar{c}c_y^{1.5} =$ /50

$= 1 - 0.7\sqrt{0.10} - 3.2 \cdot 0.1 \cdot 0.3^{1.5} = 0.722$,

while for $\bar{c} = 15\%$ $M_{cr} = 1 - 0.7\sqrt{0.15} -$

$- 3.2 \cdot 0.15 \cdot 0.3^{1.5} = 0.651$. As we can see from this example, the lower the relative profile thickness, the greater the critical Mach number.

When there is a change in the angle of attack, and consequently the value c_y (for example, let us take $\bar{c}_y = 0.4$ and $\bar{c} = 10\%$), we obtain a different value for the critical Mach number M: $M_{cr} = 1 - 0.7\sqrt{0.10} - 3.2 \cdot 0.10 \cdot 0.4^{1.5} =$

$= 0.691$. Thus, an increase in the Mach number (c_y) has led to a decrease in M_{cr} from 0.722 to 0.691. This is explained by the fact that as the angle of attack increases, the upper air stream is compressed stronger by the profile. The straight-away sections in the stream decrease more intensely, as a result the velocity increases more sharply, and the speed of sound is attained at a lower Mach flight number. This is why an increase in the flight altitude (an increase in c_y) decreases the critical Mach number.

Second-generation aircraft have airfoil profiles from $\bar{c}$ = 10-12%, which makes it possible to increase the cruising Mach flight number to 0.8 - 0.85

without a substantial increase in drag. Usually the optimum cruising flight speed corresponds to M_{cr} or less.

The effect of a positive maximum thickness and the relative profile curvature. It has been experimentally established that with identical wing thicknesses, the profile which has a higher critical Mach number M_{cr} is the one in which the maximum thickness is closer to the center, i.e., for $\bar{x}_c$ = 35-50%. This is explained by the fact that with such a value for $\bar{x}_c$, there is a smoother profile contour, and consequently a smoother change in pressure and velocity along it (Figure 32).

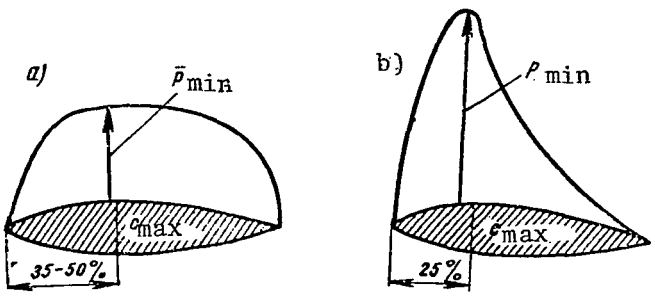

Figure 32. Effect of the Position of the Maximum Airfoil Profile Thickness on the Critical Mach Number M_{cr}: a - profile without rarefaction peak; b - profile with rarefaction peak.

A decrease in the profile curvature has a favorable effect on the aerodynamic characteristics at high flight speeds. A symmetrical profile (Figure 30,b), in which $\bar{f}$ = 0, other conditions being the same, as a higher critical Mach number. However, in such profiles the values for $c_{y\ max}$ are small (by comparison with asymmetric profiles), so that their use on transport aircraft is difficult. Recent years have shown a broader use of the so-called "inverted" profile, i.e., a profile having negative curvature (Figure 30,c). These profiles, usually used in the basic section of the airfoil, satisfactorily solve the problem of the highly complex interference between the wing and the fuselage, creating smooth flow. The physical nature of the effect of relative curvature on the value M_{cr} is the same as the effect of the thickness.

Decreasing the maximum profile thickness, shifting it to the middle of the chord, and decreasing the profile curvature all increase the value of the critical Mach number by a total of 0.02 - 0.06. /51

The effect of wing sweep. The optimum effect in increasing the critical Mach number is achieved through the use of swept wings.

As wing sweep increases to 35°, the critical Mach number increases by 0.07 - 0.08 as compared with the critical Mach number for a straight wing or profile. Let us see how this is achieved.

The lift of the wing and the tail assembly is determined by the value of the aerodynamic force of the pressures arising as a result of changes in the local flow velocities induced by the external contours of the profile across the entire wingspan or tail span.

Let us expand the flight speed V_{pos} over two components: one, perpendicular to the leading edge* of the wing -- V_{ef}, and the other directed along the leading edge of the wing -- V_1 (Figure 33,a). The component V_{ef} (effective speed) determines the value of the local speeds and expansions along the profile, and consequently the value of the lift as well. The component V_1 is not involved in the creation of the aerodynamic pressure forces. It does have an effect on the boundary layer and, consequently, on the flow separation. In conjunction with the fact that V_{ef} is always lower than V_{pos}, the local speed of sound will be achieved later and, consequently, the critical Mach number will be greater. The shock stall on the profile will set in at a higher flight speed. This means that the critical Mach number in swept wings will always be greater than in straight wings or the profile.

The critical Mach number for a swept wing, with allowance made for the effect of flow characteristics on the pressure distribution along the span, /52 may be determined from the formula:

$$M_{cr\chi} = M_{cr.prof} \frac{2}{1 + \cos \chi},$$

where χ is the angle of sweep for the wing.

For wings having a sweep of 35° ($\cos 35° = 0.82$), the formula assumes the following form: $M_{cr\chi \cdot 35°} = 1.1\, M_{cr.prof}$. For example, for a relative profile thickness of 10%, we obtain a Mach number $M_{cr\chi \cdot 35°} = 0.795$. We must bear in mind that the empirical formula for determining the critical Mach number offers an error of 15-20%.

Along its span, the aircraft wing has changing values relative to the thickness. Therefore, the critical Mach number also has various values.

The effect of wing sweep, by increasing the critical Mach number, is decreased at the point where the central section of the wing joins the fuselage. Here the wing is subjected not to oblique airflow (resulting from decomposition of the incident flow into two components), but to straight airflow. The critical Mach number is increased through increasing the sweep of the central portion of the wing along the leading edge. Thus, if the angle $\chi = 30\text{-}35°$, in the central section of the wing it reaches 40-45°, i.e., the wing is given a "crescent" shape in planform. The Tu-104 and Tu-124 aircraft have a slightly expressed "crescent" shape. /53

* Strictly speaking, V_{ef} is perpendicular to the aerodynamic center line MN, and the component V_1 is directed along this line, because the wing is looked upon as tapering. Our allowance has been made for simplicity in explanation.

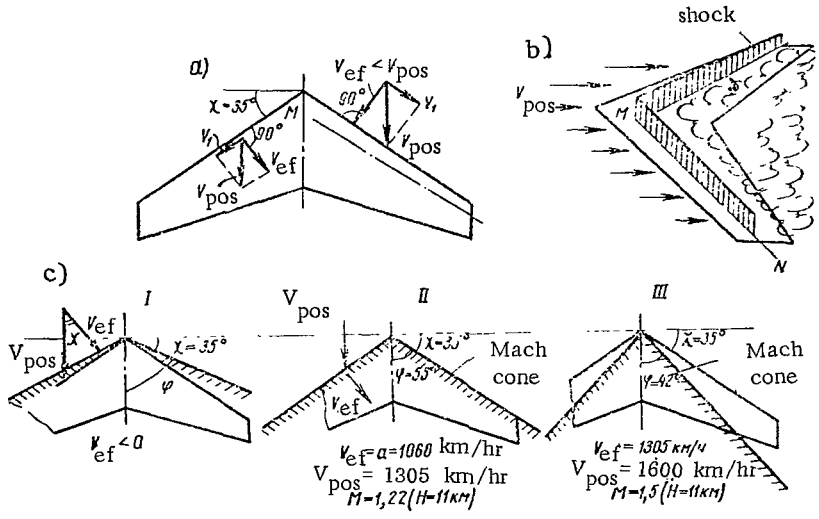

Figure 33. Development of Flight Speed on Swept Wing and Possible Positions of the Leading Wing dge Relative to the Mach Cone: I - subsonic leading edge -- wing located within cone (subsonic flow); II - sonic leading edge (flow at the speed of sound); III - supersonic leading edge (supersonic flow).

The critical Mach number for the wing in passenger aircraft is below unity. For clarity in representation, we will show that for a wing with thin profiles ($\bar{c}$ = 4-6%), at an angle χ = 55-60° the critical Mach number, determined according to the formula already presented, may be greater than unity. However, for an isolated profile, as has already been noted, this is impossible.

The shock stall in a swept wing occurs later, and not simultaneously throughout the wingspan, and less intensely than on a straight wing; in addition, it does not lead to a sharp change in the total aerodynamic characteristics of the aircraft.

At various points on the wing, the shock stall developes in different ways. Recent studies have shown that in the center of the wing the shock stall begins later than at the tips, but because of this increases more intensely. As a result, the negative effect of the central portion of the wing is felt not so much in the sense of a decrease in the critical Mach number as a more rapid increase in the wave drag than at the wing tips, although it starts to increase sooner on the tips.

There is substantially less wave drag in a swept wing than in a straight one, which may be clarified thusly.

Let us assume that local compression shocks arising in profiles from which the wing is shaped start at the line MN (Figure 33,b). In each profile, the local shock will be normal, while for the whole wing the total shock, also located along the line MN, will be oblique (with respect to the incident flow). As has already been stated, the shock stall developes more weakly when there is an oblique shock.

The shock front is located along the leading edge of a swept wing at the instant when V_{ef} becomes equal to the local speed of sound. On a wing with a sweep angle $\chi = 35°$, this occurs at a flight Mach number equal to 1.22. Let us show this.

As can be seen from Figure 33,a, the speed $V_{ef} = V_{pos} \cos 35°$. Let us equate it to the speed of sound: $a = V_{pos} \cos 35°$, i.e., $a = 0.821\, V_{pos}$; then $M = \frac{V_{pos}}{a} = \frac{V_{pos}}{V_{pos} 0.821} = 1.22$. Thus, a wing with $\chi = 35°$ may be used also for flights at low supersonic speeds.

As can be seen from Figure 33,c, a Mach cone forms at the tip of the angle forming the leading wing edge when a swept wing encounters supersonic flow. This Mach cone assumes the form of an oblique compression shock. If the leading wing edges lie within the Mach cone, they are called subsonic. With respect to the degree to which the surface of the Mach cone approaches the leading edge, the wave drag ratio increases and reaches it highest value /54 at the instant when the leading edges meet the cone surface. When there is a further increase in the speed, the leading edges of the wing go beyond the boundary of the Mach cone, after which the surfaces of the Mach cone move away from the edges. In this case, the leading edges are called supersonic.

Passenger aircraft designed in recent years have an optimum angle $\chi = 20\text{-}35°$ and a mean relative thickness of 10-12%. The use of a greater sweep angle (particularly one equal to 45°) is inadvisable in terms of a weight-drag ratio for the wing because of the onset of torque and, additionally, because of poorer takeoff and landing conditions caused by a lower value for $c_{y\ max}$.

Use of a wing with a 35° sweep results in a 10-25% drop in wave drag for flights at M = 0.80 - 0.85, which substantially decreases the overall drag. At the same time it becomes possible to maintain the lift-drag ratio for the aircraft within limits of 13-15. The effect of the sweep angle on the coefficient c_x is given in Figure 34.

In addition to the parameters already discussed, the wing aspect ratio λ also has a determining effect on the critical Mach number. A substantial increase in the critical Mach number results for $\lambda = 1 - 1.5$. In wings with small aspect ratios ($\lambda = 1.5 - 2.5$), the critical Mach number is greater than in wings with high aspect ratios ($\lambda = 5\text{-}8$). This is explained basically by the so-called end effect.

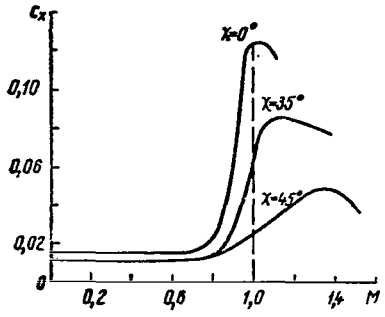

Figure 34. The Effect of the Sweep Angle on the Dependence $c_x = f(M)$.

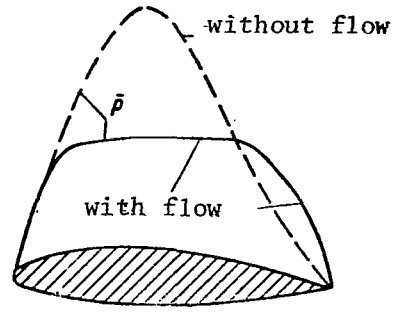

Figure 35. The Effect of Airflow Past the Wing Tips on Pressure Distribution over the Upper Surface.

During flight, pressure below the wing is greater than above it. Therefore, there is an overflow of air at the wingtip from the region of greater pressure toward that of lesser pressure, i.e., a certain pressure balance takes place, thanks to which the maximum rarefaction over the wing decreases (Figure 35). The influence of the end effect is substantial only close to the /55 wingtip. If the wing aspect ratio is decreased, the relative length of these sections increases and the end effect is spread over a large section of the wing.

For passenger aircraft at an angle $\chi = 35°$, the optimum $\lambda = 6\text{-}8$; therefore the critical Mach number in this case undergoes no change.

§ 2. Features of Flow Around Swept Wings

In the preceding section, which examined the development of the speed V_{pos}, we simplified the picture of the flow around a swept wing. Actually, however, this picture assumes a complex spatial scheme. Let us spend some time discussing the various basic moments. To this end, let us examine air streams flowing around the middle and end portions of the wing (Figure 36). As a result of the spatial character of the flow of the stream as we approach the center section of the wing, it becomes wider. As a result of the constant air consumption along the stream, this leads to a decrease in speed in the center section of the profile, and consequently to a decrease in the rarefaction over the rising part of the profile in the middle of the wing. On the descending part there is a constriction of the stream and a consequent rise in speed and increase in rarefaction. Thus, in the middle section of the wing the rarefactions decrease on the rising section of the profile, while they increase on the descending section.

At the tips of swept wings, the picture is reversed. Here the streams approaching the wing are first constricted, which leads to an increase in velocities on the rising profile section. As a result, rarefactions on the

leading profile sections increase. As the profile descends, the stream starts broadening, which leads to a decrease in velocities and rarefaction.

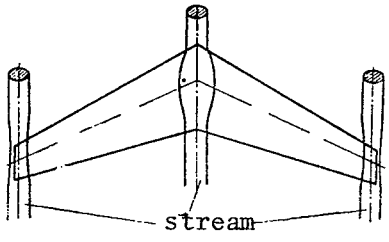

Figure 36. Representative Character for the Flow of Air Streams in the Middle and at the Ends of a Swept Wing.

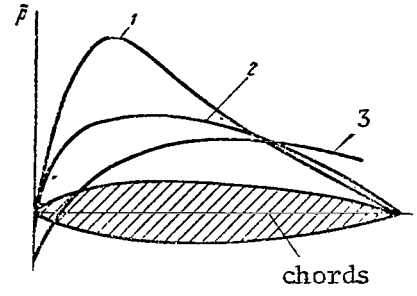

Figure 37. Representative Picture of Pressure Distribution at Various Sections along the Wing: 1 - at the tips; 2 - in the middle of the semi-span; 3 - in the central section.

Figure 37 shows that at the center sections of the wing, the maximum rarefaction is displaced to the rear, whereas at the tip sections, in contrast, the greatest rarefaction is found at the leading part of the profile. In addition, the value of the rarefaction peak is higher at the tips than in the center and base sections. Therefore, the tip sections of the wing are more loaded (have greater lift) than due the base sections. /56

The observed feature of pressure distribution along the chord of the wing leads also to another distribution of load along the span (in contrast to straight wings).

Figure 38 shows the load distribution along the span of swept and straight wings, as well as changes in the maximum values of the coefficient $c_{y\ sec\ max}$ for various wing sections*.

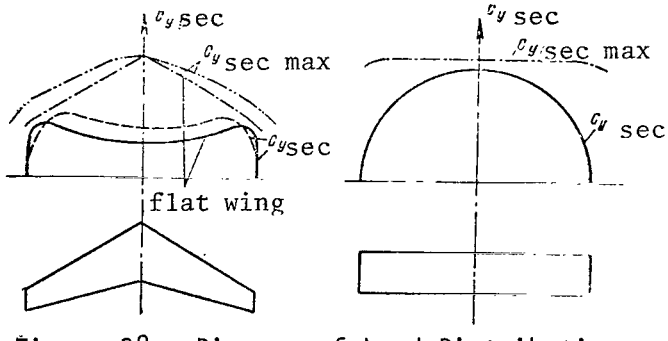

Figure 38. Diagram of Load Distribution Along the Span of a Swept and a Straight Wing: -..- geometric twist; -.- aerodynamic twist; —— flat wing.

The difference in the characteristic for the change in $c_{y\ sec\ max}$ in straight and swept wings is explained in the following manner. The overflow of air past the wing tip from the lower to the upper surface in a straight wing has an effect only on a

* Pashkovskiy, I.M. Characteristics of Stability and Controllability in High-Speed Aircraft (Osobennosti ustoychivosti i upravlyayemosti skorostnogo samoleta). Voyenizdat. 1961

small section, as a result of which the value $c_{y\ sec\ max}$ is identical almost everywhere on the span and only toward the wing tips does it start to decrease. In swept wings, however, the decrease in $c_{y\ sec\ max}$ from the base to the tip is related not only to the overflow of air past the tip but also with the nonsimultaneous increase in the flow separation along the span. This separation is highly dependent on the air overflow in the boundary layer due to the component V_1 (see Figure 33,a). Therefore, the end sections of the swept wing undergo separation before all the others, i.e., they are the first to attain the values $c_{y\ sec\ max}$. /57

As can be seen from the figure, the end sections of the swept wing achieve $c_{y\ sec\ max}$ faster than do the sections of the center and base portions of the wing. In straight wings, on the other hand, $c_{y\ sec\ max}$ is reached earlier in the center section of the wing.

Therefore, with an increase in the angle of attack the flow separation reaches the end sections of the swept wing and the center sections of the straight wing sooner. In addition, the overall end flow separation on the swept wing facilitates the speed V_1, which causes the boundary layer to move toward the wing tip and causes it to thicken. The boundary layer seems to be in a sense sucked from the center section and built up at the ends of the wing. The "swelling" of the boundary layer and the premature separation at the wing tips is one of the basic drawbacks of swept wings.

The end flow separation leads to the development of the pitching moment, which affects the longitudinal stability of the aircraft adversely, especially at slow flight speeds. Flow separation in the aileron zone leads to a drop in the laterial handiness.

Along with end flow separation, at low flight speeds (greater than the angle of attack), such a separation is possible also at high speeds at low angles of attack, which is explained by the interaction of compression shocks with the boundary layer during flight at high altitudes. As in well known, at high altitudes flight is performed at high angles of attack (to obtain the necessary value for c_{yhf}). With an increase in the angle of attack, the value for the critical Mach number decreases. When the angle α increases due to vertical gusts, compression shocks may form earlier (because the critical Mach number is low), which aids in the development of flow separation. In all these cases, during separation there is the characteristic vibration, and in some cases there is even pitching down.

Redistribution of load along the span of a swept (in contrast to a straight) wing always leads to a displacement of the equivalent aerodynamic force of the wing backward or forward along the chord, and therefore is accompanied by a change in its longitudinal moment.

As can be seen from Figure 39, when the wing is swept, each section is

displaced relative to each other in such a way that in toto the points of application of the increasing aerodynamic forces for these sections form a line which is inclined along the perpendicular to the axis of the wing (the axis oz) by angle χ. The distance from the axis oz to the points of application of the aerodynamic forces for these sections differ according to span. In straight wings, on the contrary, the points of application of the increasing aerodynamic forces for the sections lie practically on a straight line parallel to the axis, i.e., they are equidistant from the laterial axis of the wing in all sections across the span. This feature for the load distribution along the span in swept wings changes substantially either with a change in the angle of attack or a change in the Mach number. /58

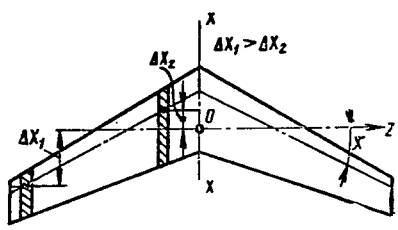

Figure 39. Example of the Effect of Load Distribution Along the Span on the Longitudinal Moment of a Swept Wing.

From Figure 40 we see that an increase in α leads to a greater load on the central section of the swept wing and a lightening of its end sections. In this case, the pressure center for the wing shifts forward along the chord, which creates a tendency toward pitching. The onset of pitching corresponds to the moment of the onset of separation, which starts at that section of the wing where the aileron are located.

If there is a change in the Mach number and α remains constant, there is also a redistribution of load along the span. This is accompanied by an unequal development of shock stall on the wing in the process of reaching and surpassing critical speed. As we can see from Figure 40, an increase in the flight speed up to critical leads first to a certain loading of the end sections of the swept wing. Then, with the development of the shock stall at a Mach number somewhat greater than M_{cr}, the end sections start losing their load. The initial increase in the loading of the end section leads to the development of a slight diving moment, i.e., to a change in the longitudinal stability*. Subsequent changes in the load distribution are brought about through the propagation of the shock stall along the upper wing surface to the base and middle sections of the cantilevers, as well as the development of the stall on the lower wing surface. All this leads to a certain displacement of the wing pressure center (p.c.) forward along the chord and the appearance of a pitching moment at Mach numbers greater than critical, but less than unity (sonic speeds).

Distinct changes in the load distribution along the span of a swept wing may also lead to its flexible deformation (buckling and twisting). In the event of deformation, the local angles of attack at various points along

* Pashkovskiy, I.M. Characteristics of Stability and Controllability in High-Speed Aircraft (Osobennosti ustoychivosti i upravlyayemosti skorostnogo samoleta). Voyenizdat. 1961

the wing change dissimilarly, because the degree of these changes is a function of the aerodynamic forces acting on the wing. These latter, in turn, are functions of the angle of attack, flight speed and Mach number.

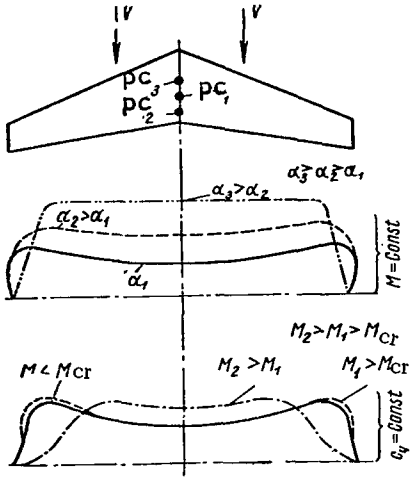

Figure 40. Change in the Load Distribution Along the Span of a Swept Wing as a Function of the Angle of Attack and the Mach Number.

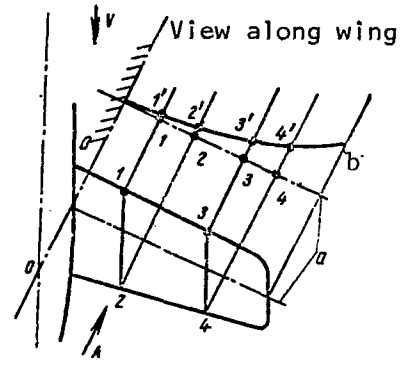

Figure 41. Decrease in Angle of Attack for Bend in a Swept Wing: a - non-deformed flexural axis; b - flexural axis of cranked wing.

In the event of buckling of a swept wing (Figure 41) relative to the 0-0 axis, the points 1 and 3, lying close to this axis, will have less of a vertical displacement than points 2 and 4. As a result of this, the chords 1-2 and 3-4 are turned relative to the flexural axis by a certain angle, and /59 the entire wing turns to the side of the decrease in the angle of attack. Thus, for a wing with normal sweep, in the event of twisting induced by aerodynamic loads directed upward from below, there is always a decrease in the angle of attack of the wing section the closer this given section is to the end of the wing. This also aggravates pitching, in that the end sections have smaller angles of attack and, consequently, lower values for $c_{y\ sec}$. This fact, along with the forward displacement of the pressure center as the angle of attack and speed increase, may also lead to aircraft instabilities within a specific range of Mach numbers.

§ 3. Wing Construction in Turbojet Passenger Aircraft

In designing aircraft for cruising Mach numbers of 0.8 - 0.85, strict attention must be given to the selection of wing parameters. We are already familiar with certain parameters, and now we shall continue our examination.

It has been established that for subsonic passenger aircraft, the optimum

parameters are an angle of $\chi = 35°$ and a wing aspect ratio of $\lambda = 6\text{-}8$. With such values for λ, flight distance is substantially increased.

Narrowing the wing in planform $\eta = \frac{b_{bas}}{b_{end}}$ is decided through the selection /60 of conditions yielding best stability characteristics and characteristics of longitudinal stability, so as to eliminate separation flows at the wing tips. For a 35° sweep, the optimal selection is $\eta = 3.5 - 4.5$*.

The remaining wing parameters are selected from calculation of the optimal lift properties for the wing.

It has been established that the dependence of the coefficient c_y (as well as the coefficient for the longitudinal moment m_z, Figure 140) on the angle α proceeds linearly to α_{vib}, at which point there are local flow separations on the wing and this relation is no longer valid. This leads to the fact that at high angles of attack there is a decrease in longitudinal stability (in Figure 140, this corresponds to the so-called "balance point"). The disruption in longitudinal stability is quite representative of swept wings. It is troublesome not only in that it affects the longitudinal stability of the aircraft adversely, but in addition the flow separation from the wing tips decreases the effectiveness of the ailerons and asymmetric separation may result in pitching down.

Therefore, in establishing the aerodynamic arrangement of the swept wings in passenger aircraft, maximum cruising flight speeds and minimum landing speeds are achieved through holding the development of the flow separation to the highest possible angles of attack and the highest Mach numbers. The following means are used to achieve this.

1. The aerodynamic twist of the wing -- the selection of the wing design from various profile types, the profiles offering the lowest lift being at the base of the wing, while those with the greatest lift are at the tips. This results from the change characteristic for $c_{y\ sec\ max}$ with respect to the wing dimensions (Figure 38). The selection of profiles with greater lift for the wing tips (with $\bar{f} = 2.5 - 3\%$ and greater) with the reverse positioning of maximum thickness ($\bar{x}_c = 35 - 50\%$) permits a certain increase in $c_{y\ sec\ max}$ at the wing tips and, at the same time, increasing the angle of attack and thereby achieving $c_{y\ sec\ max}$.

Symmetrical profiles (sometimes with slight curvature) or profiles with negative curvature -- "inverted" profiles -- are positioned at the base of the wing.

The DC-8, Convair 880, the Boeing-707 and the VC-10 have "inverted"

---

* Yeger, S.M. Design of Passenger Jet Aircraft (Proyektirovaniye passazhirskikh reaktivnykh samelotov). Mashinostroyeniye. 1964.

profiles in the center sections of the wing. This has not hindered the overall lift of the wing and has made it possible to use profiles with $\bar{c}$ = 12-15% without a significant increase in c_x at high flight Mach numbers.

2. Geometrical twist is the gradual spiral effect (positioning at a smaller angle) of the wing tips and middle wing sections relative to the base at an angle of 2-5° (for example, if the angle is +3° at the wing base, while it is -1° at the wing tip, the twist angle equals -4°). This changes the lift distribution along the span toward the side of greater load for the wing base and unloading for the wing tips. During flight, this type wing may achieve higher angles of attack (calculated with respect to the chord of the base profile) before the wing tips reach separation. Figure 16 shows that the geometrical twist has an affect on the extension of the relation $c_y = f(\alpha)$, moving it to the right. /61

Having established the geometric twist, we must take into account the bending and warping of the wing, as shown in Figure 41, so as to not obtain negative lift at the tips.

It was noted earlier that with geometric twist, the required $c_{y\ lg}$ is achieved at a slightly higher flight angle of attack.

3. Positioning aerodynamic baffles 16-20 cm high (an average of 2-4% of the local wing chord, Figure 42) on the upper wing surface. The baffles separate the wing into portions and hinder the overflow of air in the boundary layer along the wing span, resulting in a decrease in the thickness of the boundary layer in the tip sections. This leads to an increase in the local values for $c_{y\ sec\ max}$ in the end sections (by comparison to a wing without baffles), and consequently aids in holding off the onset of flow separation in these sections until the high angles of attack.

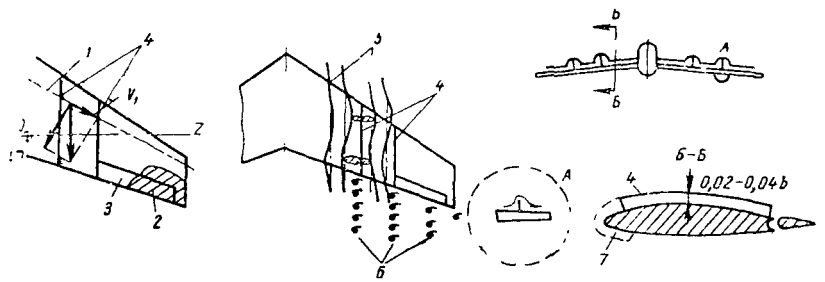

Figure 42. Arrangement of Aerodynamic Baffles on Upper Wing Surface: 1 - line of 1/4 chord; 2 - point of onset of flow separation and burbling; 3 - aileron; 4 - baffle; 5 - air stream (enlarged scale); 6 - vortices separating from wing with baffles; 7 - possible baffle shape.

In the wing section closest to the fuselage (between the baffles and the

fuselage) there is a thickening of the boundary layer and a decrease in $c_{y\ sec\ max}$. Lateral flows arise within the limits of only one section, vortices form at the baffles, and the boundary layer flows off with these. /62

Thus, because of the lateral overflow of air in the boundary layer when the wing is equipped with baffles, the initial flow separation on the wing section between the baffles and the fuselage is maintained and separation from the outer section of the baffles and the wing tips is forestalled. Because the tendency toward separation of the boundary layer weakens, there is an improvement in the lift distribution along the wing span. The separation zone is displaced toward the middle sections and, in some individual cases, even toward the base of the wing. Aerodynamic baffles have been installed on the wings of the Tu-104, Tu-124, Tu-134 and Caravelle aircraft.

A similar effect is created by the pylons which support the engines on such aircraft as the Boeing-707, the Douglas DC-8 and the Convair 880 (see Figure 65). However, pylons behave basically like baffles on the lower wing surface, where there is substantially less cross current in the boundary layer. Only that portion of the pylon which captures the upper wing surface at its nose has an effect on the wing.

The I1-62 has swept wings with so-called "notches" in the leading edge (Figure 43). The "notch" forms a constant vortex cord on the wing surface which acts in the same manner as an aerodynamic baffle, increasing the build up of the boundary layer behind itself with the result that it does not overflow to the wing tip.

There are of course other means for tightening separations from the wing at low speeds, and they will be discussed in Chapter V, § 8.

The Boeing-707, the DC-8 and other aircraft tighten the flow through the use of vortex generators. Their basic purpose is the creation of a system of /63 vortices for activating the boundary layer (Figure 44).

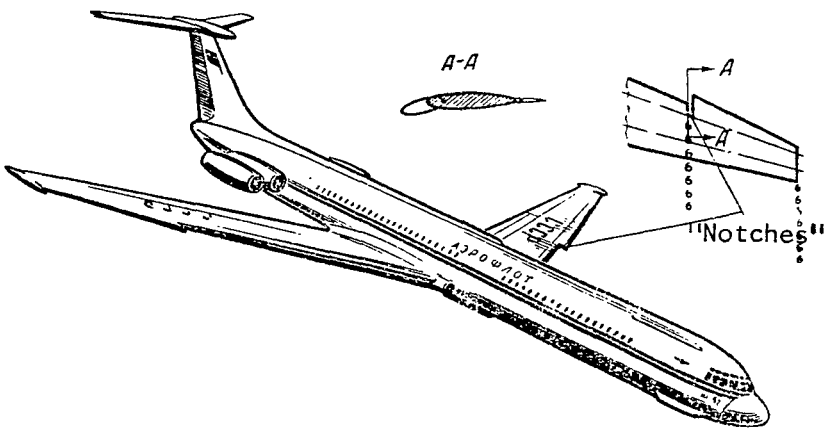

Figure 43. Positioning of "Notches" on the Leading Edge of a Swept Wing.

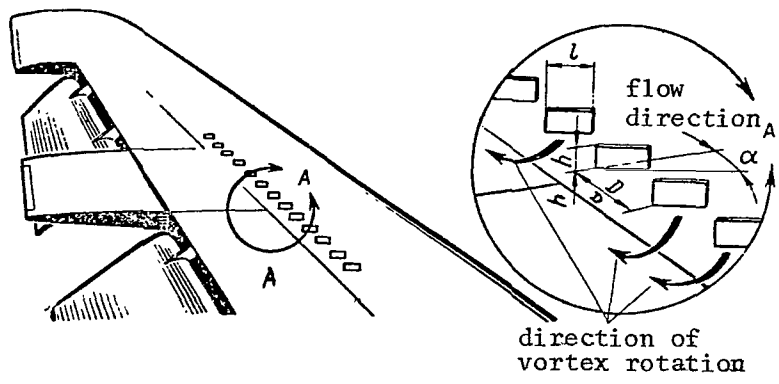

Figure 44. Positioning of Flow Vortex Generators on the Wing of the Boeing-707 (h = 10-12 cm, α = 15°, l = 15-30 cm, D = 40-60 cm).

The principle behind the action of vortex generators is based on the fact that a system of vortices having a parallel influence on the boundary layer flowing around the wing surface at the upper limit causes an increased mixing of the boundary layer with the outer flow. Air particles carried from the outer flow by the vortex displace the particles in the boundary layer and, through mixing with them, are entrapped in the outer layer. There is intensification of the boundary layer which restricts its breaking away from the compression shock. In those instances where break away nevertheless occurs, the vortex system excited by the vortex generators creates in intermixing effect in the separated flow as well, as a result of which the flow separation region is localized and the boundary layer again "adheres" to the wing surface*.

Setting up vortex generators has succeeded in forestalling the development of flow separation at high angles of attack and flight speeds (an increase in the critical Mach number to 0.02 - 0.07). Aileron effectiveness increased because the vortex generators inhibit separation of the boundary layer along the rupture line of the upper wing surface when the aileron is down. Vortex generators set in the base section of the wing (Boeing-707) decrease lift at high angles of attack through flow separation.

In addition, on the Comet-4c there are the so-called sensors (special plates, Figure 20) which break up the flow at the base section of the wing at high angles of attack and by so doing decrease the pitching moment.

In summary, the measures described (including those laid out in Chapter V, § 8) make it possible to design aircraft wings with the shape shown in Figure 45. It must be noted that if along the 1/4 chord line the angle χ = 35°, then along the leading edge the sweep may be somewhat greater (in the /64

* Yeger, S.M. Design of Passenger Jet Aircraft (Proyektirovaniye passachirskikh reaktivnykh samelotov). Mashinostroyeniye. 1964.

figure this corresponds to an angle of $\chi = 41°$ in the base section of the wing and $\chi = 38°$ in the outer wing section).

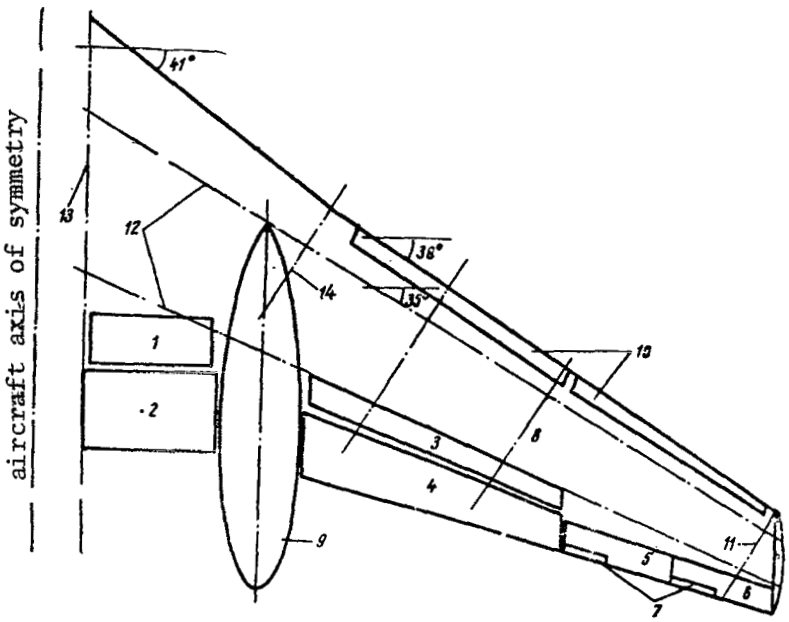

Figure 45. Schematic Diagram of Aircraft Wing: 1 - inside spoiler; 2 - inside flap; 3 - outside spoiler; 4 - outside flap; 5 - inside aileron; 6 - outside aileron; 7 - flettner trim tabs; 8 - intermediate ribs; 9 - landing gear pod; 10 - secondary control surfaces; 11 - tip ribs; 12 - spar axes; 13 - wing stump joint; 14 - wing joint axis.

Tables 3-5 present the values of parameters (in percentage) for the following variations in wing aerodynamic arrangement:

a) for a wing without geometric twist (cruising Mach number M_{cruise} = = 0.75 - 0.78, $\phi_{vib} = +1°$):

TABLE 3

Section	$\bar{c}$	$\bar{x}_c$	$\bar{f}$	$\bar{x}_f$
At wing stump joint	15*	35	1.0	20
At wing joint axis	13	35	3.3	25
At tip rib	12	37	2.5	50

* Relative thickness along flow.

b) for a wing with geometric twist (engines in tail section of fuselage, /65 cruising Mach number M_{cruise} = 0.8 - 0.82, and ϕ_{vib} = +1°, $\phi_{tip\ vib}$ = -1°30'):

TABLE 4

Section	$\bar{c}$	$\bar{x}_c$	$\bar{f}$	$\bar{x}_f$
At wing stump joint	9.75*	35	1.0	30
At wing joint axis	13	35	1.8	35
At tip rib	11.0	35	2.2	35

* Relative thickness along flow.

c) for wing with geometric twist (engines in tail section of fuselage, cruising Mach number M_{cruise} = 0.82 - 0.85, $\phi_{base\ vib}$ = +3°, $\phi_{inter.\ rib}$ = = 0°, $\phi_{tip\ vib}$ = -1°):

TABLE 5

Section	$\bar{c}$	$\bar{x}_c$	$\bar{f}$	$\bar{x}_f$
At wing stump joint	12	56	-0.7	30
Intermediate	11	35	1.2	40
At tip rib	10	35	1.5	45

§ 4. Drag Propagation Between Separate Parts of Aircraft

Total aircraft drag is known to be the composite of drag in the individual sections. For various flight speeds (Mach numbers) diverging drag propagations result between these parts mainly due to the onset of wave drag at the respective Mach numbers. In subsonic aircraft, around half of the total drag is created by the wing. Table 6 shows representative values Δc_x for the basic aircraft components with the engines set in the tail section of the fuselage (the data pertain to horizontal flight at a Mach number of M = 0.8, at which c_x for the entire aircraft equals 0.0305, while c_y = 0.4).

It should be noted that the portion of wave drag for M = 0.8 at c_y = 0.4 (corresponding roughly to the high angle of attack $\alpha \approx 5.5°$) is approximately 20% (Δc_{tail} = 0.006). Having the landing gear down (Δc_x = 0.015 - 0.020) at low flight speeds creates approximately half of the entire aircraft drag.

TABLE 6

/66

Aircraft component	Δc_x	In % of total aircraft	Averaged for remaining aircraft (%)
Wing	0.015	49.5	45-50
Elevator unit	0.0017	5.57	5-6
Rudder-fin unit	0.001	3.28	3-4
Fuselage	0.008	26.2	25-30
Landing gear pods	0.00116	3.8	3-5
Side engine pods	0.0027	8.83	8-10
Center engine intake	0.001	3.28	-
Entire aircraft	c_x=0.0305	100	100

CHAPTER IV

CHARACTERISTICS OF THE POWER SYSTEM

Jet engines and, in particular, turbojet engines generate high in-flight thrust and, consequently, high thrust horsepower (30,000 - 60,000 hp) necessary for propelling aircraft weighing 40 - 160 tons at a speed of 850 - 900 km/hr. /66

Piston and turboprop engines use up all or almost all the energy from the fuel in rotating the propeller. It is the propeller which, driven in its rotation by the engine, creates the thrust. Therefore the propeller is called the prime mover of the aircraft. The power system for piston and turboprop engines comprises both the engine and the prime mover, which create the thrust.

In the operation of a jet engine, however, the thrust is achieved indirectly as the interaction of all the forces acting on the surface of the engine components. The jet engine organically combines within itself the engine in the normal concept of the word and the prime mover.

During test-stand operation of modern turbojet engines, the pressure at the compressor exhaust equals 5-10 atm or more.

The gas temperature at the combustion chamber exhaust is 1,00 - 1,200° abs. The power generated by the gas turbine is 60,000 - 90,000 hp for engines with a thrust from 5,000 to 10,000 kG.

As it exists from the turbine, the gas still has a high amount of heat energy, its pressure is greater than atmospheric, and its temperature equals 800 - 1,000° abs. Through the process of expansion, the thermal energy of the gas at the exhaust nozzle is transformed into kinetic energy, and as a result of the high speed of the gas exhaust, the exhaust thrust is generated.

§ 1. Two-Circuit and Turbofan Engines /67

Attempts by aeronautical engineers to increase engine thrust and decrease fuel consumption led to the creation of the two-circuit and turbofan engines (Figure 46). Fuel consumption in particular decreased by 15-20% by comparison with consumption in normal turbojet engines.

The two-circuit (turbofan) engine is a gas turbine engine in which the excess turbine horsepower, in contrast to the turboprop engine, is transmitted to a compressor or fan enclosed in the circular cowling.

The two-circuit turbojet engine may assume one of several structural designs (Figure 46a and b) which are characterized by the existence of an

additional air circuit through which, after compression, part of the air which has been sucked in is fed to the combustion chamber and turbine bypass directly to the outlet, thereby increasing the mass and decreasing the speed of the jetstream.

Two-contour engines in which the volume of air passing through the supplementary circuit is relatively great while the degree of compression of this air is small are usually called turbofan engines. At present there are in use two-circuit engines of this type and turbofan engines, which are derived/68 through the installation of a fan in addition to the normal turbojet engine (Figure 46c and d). The expediency of creating turbofan engines based on series turbojet engines for civilian aircraft is justified through their great economy and high reliability during use.

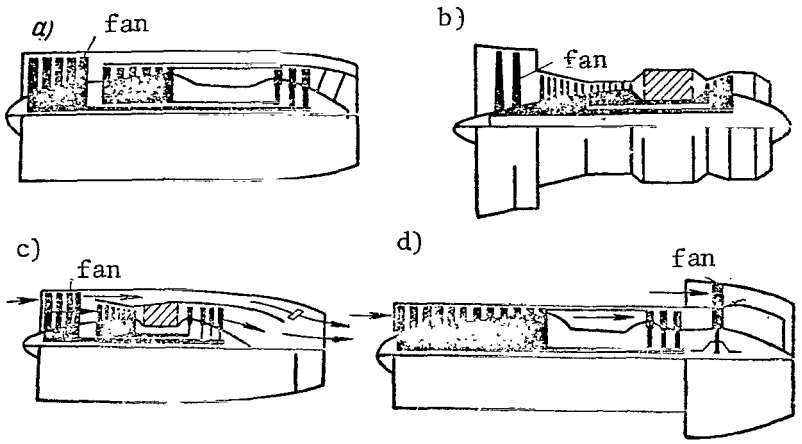

Figure 46. Various Types of Two-Circuit and Turbofan Engines: a - normal scheme (Rolls Royce "Conway" engine); b - two-circuit engine with air displacement from outer contour with gases from the inner contour (Rolls Royce JT8D "Spey"); c - turbofan scheme with forward fan (Pratt-Whitney JT3D); d - turbofan with rear fan (General Electric CJ-805-23).

When a turbojet engine is being designed strictly along the two-circuit plan, optimal parameters are obtained if the design and the parameters of the turbofan engine are to a great degree determined and limited by the parameters of the initial turbojet engine.

Figure 47 shows a simplified schematic of a two-circuit engine. Atmospheric air enters the air scoop through the two layers of blades which form the fan B. From this fan, which is in effect a low-pressure compressor, the air moves on in two separate paths. One part of the air moves along the outer body of the basic engine contour through the second contour C, while the other part moves through the high-pressure compressor D. From there it moves through the combustion chamber E, into which fuel is injected through feed line F and,

finally, after expanding, passes through the high-pressure turbine K and low-pressure turbine H. Then the high-temperature gas exits through the exhaust nozzle, which surrounds the outer ring nozzle with a cold current of air.

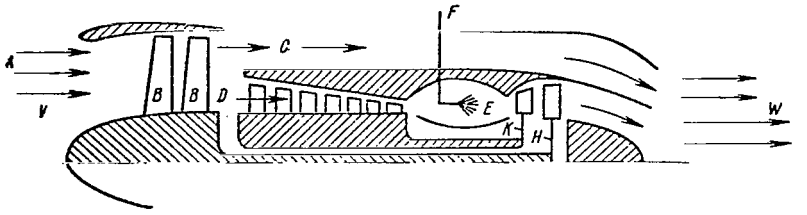

Figure 47. Simplified Schematic Diagram of the Operation of a Two-Circuit Jet Engine.

The air which has been speeded up through the fan of a turbofan engine is exhausted with a slower speed than in the normal turbojet engine or the normal two-circuit engine. The slower the speed of the flow behind the engine, the lower the energy losses will be and the greater the engine's efficiency.

From jet-engine theory we know that the overall efficiency (overall Q-factor) for the power system of any aircraft is determined as the product of the two basic figures: that of the internal (effective) and exhaust (flight) factors.

The effective Q-factor increases with an increase in the air pressure in the engine and with an increase in the gas temperature.

This leads to a substantial decrease in the specific fuel consumption. Because only part of the air passes through the turbine in a two-system turbojet engine, the turbine blades may be shorter than in a turbojet engine with the same overall fuel consumption. For identical blade safety factors, this in /69 turn permits a 100 - 150° temperature increase in the gas in front of the turbine, which gives a decided advantage over the turbojet engine in terms of fuel economy. This is one of the reasons that the two-circuit and turbofan engines have lower specific fuel consumptions.

For propulsive flight efficiency, from the theory of jet engines we are familiar with the following formula:

$$\eta_f = \frac{2}{1 + \frac{W}{V}},$$

where W is the speed of the jetstream; and
V is the flight speed.

When the difference between the speed of the jetstream and the flight speed is decreased, i.e., when there is less of an unused portion of the kinetic energy, the propulsive efficiency increases and reaches its maximum value ($\eta_f = 1$) at a flight speed equal to the speed of the exhaust jetstream. When this is true, the unused portion of the kinetic energy is zero. A clear example is the turboprop engine, in which the speed at which the air is thrust back by the blade is close to the flight speed. However, in turboprop aircraft the flight efficiency drops as the flight speed increases due to a drop in the blade efficiency, and reaches low values at high subsonic speeds.

In two-circuit and turbofan engines, there is an increase in the area of high efficiency, which the turboprop engine has at low flight speeds, up to high subsonic speeds at which the flight efficiency is still too low.

To achieve this, in two-circuit and turbofan engines there is a second circuit from which great masses of air flow at speeds close to the flight speed, which aids in achieving a high flight efficiency as well as a low specific fuel consumption. The specific fuel consumption for a two-circuit jet engine and a turbofan engine is 0.52 = 0.65 kG fuel/kG thrust · hr for H = 0 and V = 0 and 0.75 - 0.85 kG fuel/kG thrust · hr for H = 10-11 km at V = 750 - 880 km/hr.

In designing two-circuit engines, the selection of the two chief variables is vital: the forward or rear positioning of the fan and the ratio of the mass flow of cold air passing through circuit C to the mass flow of hot air passing through circuit D, the so-called two-circuit level $m = G_C/G_D$, whose value may be from 0.23 to 3.5.

The two-circuit level is a vital engine parameter and determines its efficiency, weight and thrust characteristics. The greater the level m, the /70
lower the specific fuel consumption; however, this entails an increase in the engine dimensions and weight. At present the optimum degree is m = 0.6 - 0.7 for civilian aircraft at a flight Mach number of 0.8 - 0.9.

First-generation (Boeing-707-420, and Douglas DC-8) and second-generation (Vickers VC-10 and others) transport aircraft are equipped with the Rolls Royce Conway two-circuit engine in which m = 0.7 - 0.8. The engine thrust for the Conway-509 is 10,200 kG, while the specific fuel consumption at top conditions is 0.725 kG/kG · hr.

Even greater economy may be obtained through mixing flows of high pressure (after the turbine) and low pressure (after the fan) (in the JT8D engine) or after the first compressor stage (the Spey engine) in the exhaust nozzle. When this is done, a relatively low speed of flow is achieved and there is a correspondingly high efficiency. The combination of high thermodynamic and thrust efficiencies has also made it possible to create engines with low specific fuel consumptions. As an example, Table 7 presents some data on the JT8D and Spey engines.

TABLE 7

Flight conditions	Engine type	Thrust kG	Specific consumption kG/kG·hr	H.m.	V, km/hr
Takeoff	JT8D	6350	0,585	0	0
	"Spey"	5150	0,611	0	0
Maximum (climbing)	JT8D	5715	0,57	0	0
	"Spey"	4960	0,6		
Cruising	JT8D	2140	0,838	7500	730
	"Spey"	1680	0,77	7600	870

Tr. Note: Commas indicate decimal points

There are three JT8D engines on the Boeing-727 and two on the DC-9, and there are two Spey engines on the Bak-1-11-200 and three on the Trident aircraft. Soviet two-circuit engines were first installed on the Tu-124.

Replacing normal turbojet engines with two-circuit engines offers an increase in payload and a decrease in the specific fuel consumption and the noise level.

As has already been stated, turbofan engines have the fans placed either forward or behind. When the fan is placed behind, as was done by General Electric (Figure 46d), the design of the forward part of the engine differs in no way from a normal turbojet engine: the compressor, the combustion chamber and the gas turbine are identical. However, with turbofan engines, after the gases have passed through the main turbine they run into one more, the so-called fan turbine, which is mechanically tied in to the main turbine. /71
The blade tips in the fan turbine function as they would in a normal fan and, in the annular gap between the nozzle and the additional turbine, they thrust back a strong flow of air running parallel to the basic gas jet.

The American Convair 990A has four CJ-805-23B turbofan engines (built by General Electric) with the rear fan, each generating a thrust of 7,300 kG. The same engines are used on the French Caravelle-XA in replacement for the obsolete Avon turbojet engines.

The Pratt and Whitney JT3D engine, with m = 1.5, has the fan positioned forward. This type of engine is used on the Boeing-720B and DC-8. Table 8 offers some data on the JT3D engine.

Thus, use of two-circuit and fan engines makes it possible to create aircraft with optimal flight characteristics for various purposes. The increased thrust makes it possible to decrease the takeoff distance for any specific aircraft weight or, in maintaining the takeoff distance, it becomes possible to increase the payload or the fuel reserve.

TABLE 8

Flight conditions	Thrust, kG	Specific consumption kG/kG·hr	H, M.	V, km/hr
Takeoff	8160	0,538	0	0
Maximum (climbing)	7400	0,515	0	0
Cruising	1700	0,79	9100	865

Tr. Note: Commas indicate decimal points.

§ 2. Basic Characteristics of Turbojet Engines

In examining the flight conditions for turbojet passenger aircraft we must know the following basic engine characteristics: thrust, specific thrust, specific fuel consumption, specific weight and maximum-power altitude.

Thrust in turbojet engines is determined in accordance with the following formula:

$$P = \frac{G_{sec}}{g} (W - V) \text{ kG},$$

where G_{sec} is the per-second rate of airflow through the engine, (kG/sec);
$g = 9.81$ m/sec^2 is the acceleration;
W is the speed of the rate of gas flow from the exhaust nozzle (m/sec);
V is the aircraft flight speed (m/sec).

Turbojet engines designed in the last two decades have $G_{sec} = 18 - 260$ /72 kG/sec, which corresponds to a thrust of from 800 - 900 to 10,000 - 13,000 kG, W = 550 - 600 m/sec (stand-still operation), while in flight it reaches high values. Two-circuit engines have a discharge velocity of 520 - 550 m/sec, whereas turbofan engines have only 350 - 370 m/sec.

Specific thrust -- this is the thrust obtained from 1 kG of air passing through the engine per-second:

$$P_{spef} = \frac{W - V}{g} \frac{\text{kG}}{\text{kG/sec}}.$$

Specific thrust characterizes the economy of an engine. In modern turbojet engines, $P_{spef} = 40 - 70$ kG/kG/sec. Specific thrust depends strongly on the compressor efficiency and turbine efficiency, as well as the degree to

which the air has been pre-heated. It determines the relative dimensions and weight of the engine: the greater the specific thrust, the lower the engine dimensions and weight for a given thrust.

Specific fuel consumption -- this is the relative hourly fuel consumed in generating engine thrust:

$$c_p = \frac{G_t}{P} \text{ kG} \cdot \text{fuel/kG} \cdot \text{thrust} \cdot \text{hr},$$

where G_t is the hourly fuel consumption (kG fuel/hr).

The specific consumption indicate how many kG of fuel have been expended in creating 1 kG of thrust in an hour, and also characterizes the engine efficiency. The lower the c_p, the more efficient the engine and the greater the aircraft flight range and duration.

Specific weight of the engine is the ratio of the dry weight of the engine to its thrust:

$$g_{tj} = \frac{G_{tj}}{P} \text{ kG/kG thrust}.$$

In modern turbojet engines, $g_{tj} = 0.19 - 0.35$ kG/kG thrust. For example, for the J-58 engine, the value of the specific weight is $g_{tj} = 0.25$ kG/kG thrust. This means that for a thrust of 13,600 kG, the engine weight is $G_{tj} = 3,400$ kG. As can be seen from these figures, turbojet engines do not overload the aircraft by virtue of their weight. Whereas the weight of the power system for a piston-engine aircraft may sometimes amount to 22 - 25% of the takeoff weight, for turbojet aircraft this value equals only 10 - 12%.

§ 3. Throttle Characteristics

Depending on how it is used and on its rated service life, each engine has several basic modes of operation which differ by the number of rpm's, the /73 temperature regimes, etc. Usually the following operation conditions are distinguished: takeoff, nominal, cruising, and idling.

Practice in aircraft and engine use has resulted in the need for an additional condition which, for the Tu-104 for example, has come to be called the "extreme" condition. As can be seen from the very name itself, this is used in only certain cases, specifically in the event of failure of one of the engines. In this event, because of the engine forcing with respect to the temperature of the supply of additional fuel and the increased revolutions, the thrust increases by 8 to 10% by comparison to takeoff. However, this emergency condition puts an overload on the engine which in turn means that the engine must be overhauled faster than normally.

The takeoff condition corresponds to the maximum permissible number of rpm's and the maximum thrust. Under this condition, the engine components are subjected to the greatest mechanical and thermal stresses, as a result of which their period of continuous use is limited and normally does not exceed 5 - 10 minutes. Takeoff conditions are applied to decrease the takeoff run through increasing the horizontal flight speed, decreasing the aircraft acceleration time and accelerating the breaking clouds in gaining altitude.

The normal rating corresponds to somewhat decreased (by 3-8%) rotation with respect to the takeoff rating. The thrust is approximately 90% of the takeoff thrust. The operation time at a normal rating is substantially longer: it is used in gaining altitude and for near-ceiling flight. During such operation the engine components are subjected to substantially lighter loads.

Cruising performance differs from the two preceding conditions through decreased rpm's (by 10-15%) and thrust (by 25-50%) as opposed to maximum.

The idling period corresponds to the lowest number of rpm's at which the engine can operate stably. Under these conditions, there is little thrust and therefore it is used in landing runs, dropping from high altitudes, etc. The amount of thrust is 300-600 kG at low flight altitudes and 150-300 kG at altitudes of 8,000 - 10,000 m.

The character of the change in engine thrust with respect to rpm's is shown in Figure 48, from which we can see that an increase in the number of rpm's causes an increase in thrust. At low rpm's, the amount of air passing through the engine is also low and as a consequence, the fuel consumption, too, is low. The amount of gases formed is small and develop a negligible exhaust velocity, so that the thrust generated by the engines with this value of rpm's is low, usually 300 - 600 kG. An increase in the rpm's leads to a sharp increase in the air exhaust, the fuel delivery increases, the temperature of gases in front of the turbine increases and, as a result -- thrust increases. The highest thrust may be obtained at the maximum permissible rpm's, i.e., during takeoff or emergency conditions.

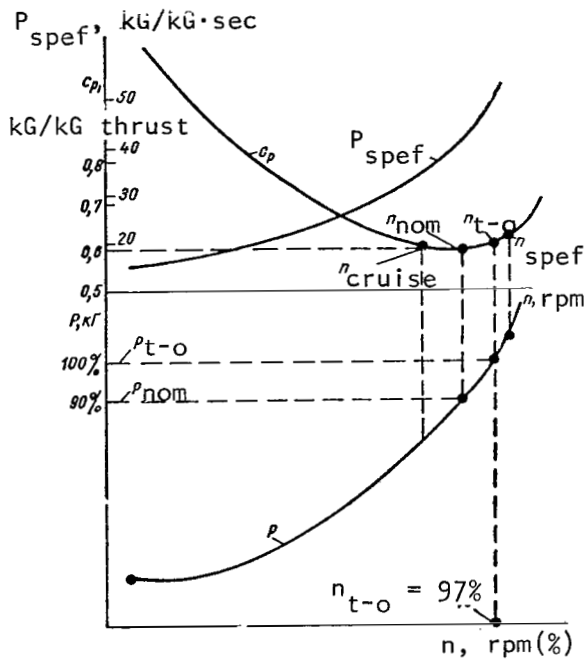

Figure 48. Engine Thrust, Specific Thrust and Specific Fuel Consumption as Functions of the rpm's. $n_{t\text{-}o} = n_{take\ off}$.

Figure 48 also shows the dependence of the specific fuel consumption on the number of rpm's. The change in cp is a function of /74

the degree of compression of the air in the combusion chamber. The more highly compressed the air is, the more fully the heat is used during the process of fuel consumption and the lower the specific fuel consumption will be. Pre-compression of the air depends basically on the compressor (engine rpm's) and on the flight speed. Therefore, when the rpm's are increased, the specific fuel consumption decreases. During normal and takeoff conditions, the specific consumption is close to minimum.

Engine use during cruising rpm conditions yield optimum economy.

§ 4. High-Speed Characteristics

The high-speed characteristics of turbojet engines are the dependence of the engine thrust, specific thrust and specific fuel consumption on flight speed at a given altitude for a selected rule of control.

Let us examine the high-speed characteristics for constant rpm, gas temperature in front of the turbine and flight altitude (Figures 49 and 50). Normally the characteristics are examined for a nominal number of rpm's.

From the formula $P = \frac{G_{sec}}{g}(W - V)$ we can see that the exhaust thrust will /75 be greater, the greater the amount of air which passes through the engine per second and the greater the difference between the gas exhaust speed and the flight speed. In increasing the flight speed from 0 to 700 - 800 km/hr, thrust decreases somewhat, because G_{sec} increases more slowly than the difference W -V drops. With an additional increase in speed, on the other hand, the increase in air exhaust begins to surpass the decrease in the differences between the speeds W and V.

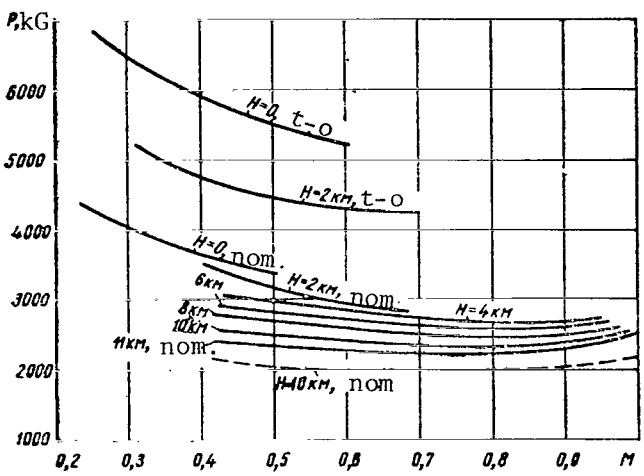

Figure 49. Engine Thrust as a Function of Mach Number (flight speed) for Various Altitudes (standard conditions, the broken line representing a temperature 10° above standard).
T-O = Take-off.

This is explained by the character of the change in thrust with respect to speed. When the flight speed is increased from 0 to 700 - 800 km/hr, thrust decreases by no more than 10-15%. This permits us to consider the available thrust generated by a subsonic turbojet engine to be practically independent of flight speed.

The specific thrust ($P_{spef} = \frac{W - V}{g}$) drops as the speed increases, because the difference between speeds (W -V) decreases (Figure 50a).

The specific fuel consumption increases with an increase in flight speed (Figure 50b). When there is a change in the flight speed from zero to 750 - 850 km/hr, the specific fuel consumption increases by 15-30%. Thus, if for V = 0 the consumption is c_p = 0.89 kG/kG · hr, then at a speed of 850 km/hr it will increase to 1.15 (for the RD-3M engine). For the JT3D turbofan engine, for V = 0, the consumption is c_p = 0.61, whereas for a speed of 880 km/hr it is 0.781 kG/kG · hr (at an altitude of 11 km). /76

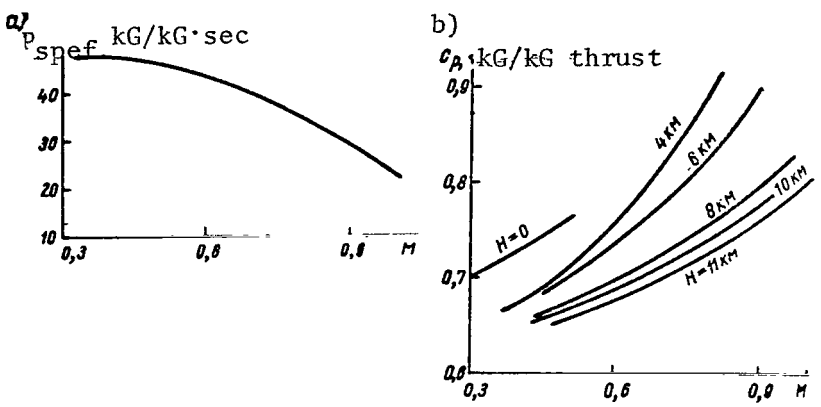

Figure 50. Change in Specific Fuel Consumption (b) and Specific Thrust (a) with Respect to Flight Speed.

In the supersonic speed range, the thrust in a turbojet engine at first rises sharply, reaching its maximum value at a specific speed, then sharply decreases (Figure 51). Thus, for example, the J-79 engine (used in the American F-104 fighter) generates a thrust of 5,700 kG on the ground, which is increased to 7,200 kG through thrust augmentation by afterburning. In flight at altitude, the drop in thrust is compensated by velocity head. During operation with afterburning at an altitude of 11,000 m and a speed of 2,000 km/hr (M ≈ 2), it generates the same thrust as on earth, i.e., 7,200 kG.

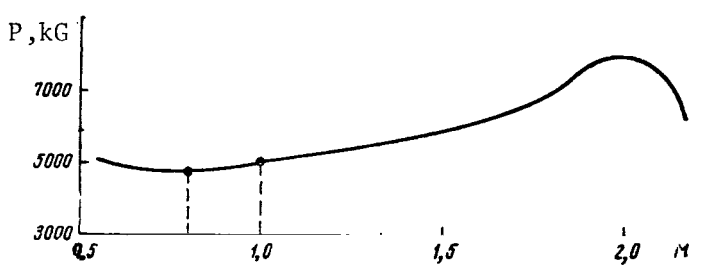

Figure 51. Representative Dependence of Engine Thrust for a Supersonic Fighter on the Flight Mach Number (H = 11,000 m).

§ 5. High-Altitude Characteristics

The dependence of thrust, specific thrust and specific fuel consumption on flight altitude for a constant number of engine rpm's and constant flight speed is called the high-altitude characteristics. /77

The thrust of a turbojet engine decreases sharply with an increase in flight altitude because thrust is directly proportional to the weight rate of airflow, while the rate decreases with altitude due to a drop in air density. The decrease in thrust with altitude occurs in spite of the fact that the specific thrust, i.e., the thrust created by each kilogram of air passing through the engine, increases by approximately half again as much as compared to the ground level.

Up to an altitude of 11,000 meters, because of precompression in the compressor, the weight rate of airflow decreases more slowly than the air density, whereas above 11,000 meters, where the temperature remains constant, it drops more rapidly. The change in engine thrust with altitude may be calculated with respect to the following formula: for altitudes up to 11,000 meters: $P_H = P_0 \cdot \Delta^{0.7}$; for altitudes greater than 11,000 meters: $P_H = 1.44 \Delta \cdot P_0$ (here P_H is the thrust at altitude; P_0 is the ground engine thrust); $\Delta = \frac{\rho_H}{\rho_0}$ is the ratio of densities ($\Delta < 1$).

If we take P_0 as 100%, then at an altitude of 10,000 meters the thrust is approximately 45-50% of the ground thrust, while at an altitude of 20,000 meters it is only 10%. This comments on the lack of maximum-power altitude in turbojet engines. However, modified turbojet engines developing a ground thrust of 10,000 - 13,000 kG have high flight speeds at altitudes of 10,000 - 12,000 meters.

Figure 52 shows the variation in engine thrust in terms of altitude for various rpm's. It should be noted that above the maximum-power altitude boundary the power of piston engines drops more rapidly than does the thrust of jet engines.

Up to an altitude of 11,000 meters the specific fuel consumption c_p decreases, after which it holds constant (Figure 53). The basic principle in /78 the drop in c_p (and the increase in specific thrust) lies in the fact that with a drop in the temperature of the surrounding air the degree of compression in the compressor and the degree of precompression are increased.

The hourly fuel consumption, which is equal to the product of $c_p P$, decreases with an increase in flight altitude by approximately the same intensity as does the air consumption and thrust.

The hourly fuel consumption at an altitude of 11,000 meters is less than one half the ground consumption for the same engine rpm conditions.

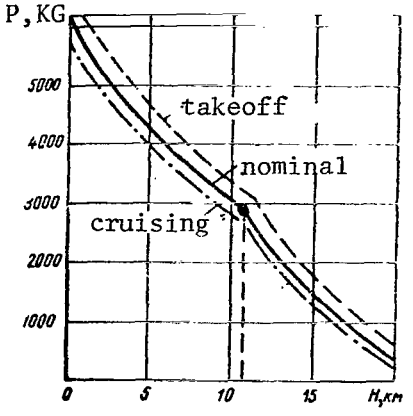

Figure 52. Variation in Engine Thrust in Terms of Flight Altitude (Mach = 0.75).

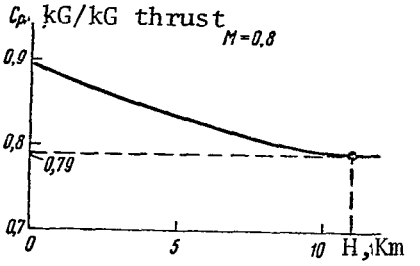

Figure 53. Dependence of Specific Fuel Consumption on Flight Altitude.

Thus, these engines are more effective in operation at high altitudes.

§ 6. The Effect of Air Temperature on Turbojet Engine Thrust

Air temperature, like altitude (pressure), has a significant effect on thrust and specific fuel consumption.

During test-stand trial runs of the engine the measured thrust is reduced to standard conditions, i.e., the so-called reduced thrust is determined for p = 760 mm Hg and t = 15°C. Depending on the control system, the effect of temperature changes on thrust is manifested in different ways. Thus, for example, for turbojet engine with operational rpm's of 4,000 - 5,000, a one-percent temperature increase decreases thrust by approximately 2%. For two-circuit and turbofan engines with 6,700 - 11,000 rpm, a one-percent temperature change varies the thrust by 1 - 1.5%. For example, the thrust in a turbojet engine equals 7,000 kG for t = 15°C and p = 760 mm Hg. A temperature increase of up to t = 25°C has occurred. Let us determine the variation in engine thrust. To do so, let us express the temperature change in a percentage ratio: T_1 = t°C + 273° = 15° + 273° = 288°; T_2 = 25° + 273° = = 298°; 298 : 288 = 1.03, i.e., the temperature increased by 3%. Consequently, thrust decreased by 6%, amounting to 420 kG.

Thus, for t = 25°C, the engine will generate around 6,600 kG of thrust. If the temperature increases to 35°C, the thrust decreases by 13.6%, i.e., the engine will generate only about 6,000 kG of thrust.

When the air temperature increases, thrust increases. This comes about because of the control system on the fuel-supply arrangement in turbojet engines, which increases the fuel supply when temperature drops. An increase in thrust usually occurs when the temperature decreases to +3 - -15°C,

depending on the engine conditions and the control of the fuel pump and regulator.

Let us determine the increase in thrust for a temperature of -15°C if for t = 15°C thrust P = 7,000 kG: T_1 = 288°C, T_2 = 258°C and 288 : 258 = 1.115, i.e., the temperature increases by 11.5%, consequently, the thrust increases by 23%, amounting to 1,600 kG (Figure 54). /79

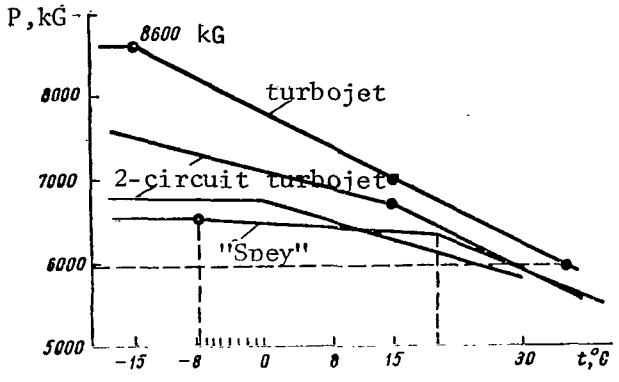

Figure 54. Effect of External Air Temperature on Thrust of Turbojet Engines.

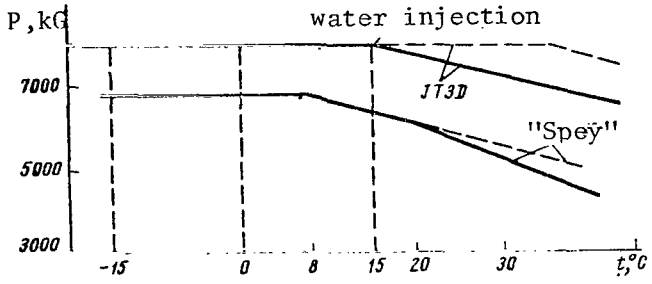

Figure 55. Test-Stand Thrust in the JT3D Turbofan Engine and the "Spey" - type Two-Circuit Turbojet Engine as a Function of the Ambient Air Temperature.

To maintain these engine thrust values at high altitudes, water injection into the compressor is used.

Figure 55 shows the change in thrust in a JT3D turbofan engine with and without water injection. As can be seen from the figure, water injection aids in maintaining the calculated takeoff thrust up to and intake temperature of +35°C. While this holds, the high-temperature flight characteristics for the aircraft change negligibly. In the case of the "Spey" engine, water injection aids in forestalling a drop in its thrust at temperatures greater than 20°C.

§ 7. Thrust Horsepower /80

Thrust horsepower is the available engine power:

$$N = \frac{PV}{75} \text{ hp},$$

where V is the flight speed in m/sec.

Let us determine the thrust horsepower for the engines of an aircraft flying at an altitude of 10,000 meters and a speed of 900 km/hr, if the available engine thrust is 6,000 kG:

$$N = \frac{6000 - 900}{75 \cdot 3,6} = 20\,000 \text{ hp}.$$

However, at flight with the maximum speed of 1,000 km/hr at an altitude of 6,000 m and with an available thrust of 9,000 kG, the thrust horsepower is

$$N=\frac{9000\cdot1000}{75\cdot3.6}=32000 \text{ hp.}$$

The thrust horsepower increases directly proportionately to the speed. When racing the engines on the ground without the aircraft's moving, N = 0, because there is no work being done, i.e., PV = 0. A change in the available horsepower with respect to altitude (rpm's being constant) is shown in Figure 56.

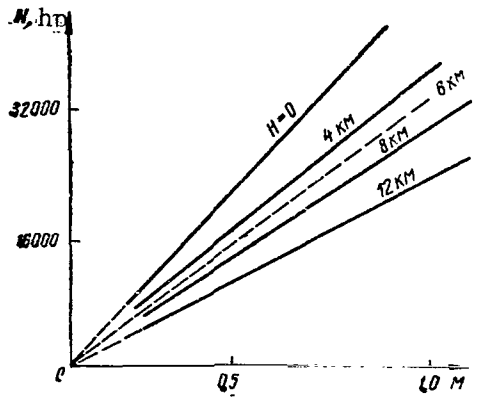

Figure 56. Thrust Horsepower as a Function of Mach Number for Various Flight Altitudes (constant rpm's).

In contrast to piston aircraft, in which the available horsepower decreases with an increase in speed above maximum due to a drop in the propeller efficiency, in jet aircraft it increases with an increase in flight speed. Therefore, rapid flight speeds may be obtained only in aircraft with turbojet engines or other types of jet engines.

Like thrust, the available horsepower is a function of the engine rpm's: the greater the number of engine rpm's (for a specific altitude and flight speed), the higher the available horsepower.

§ 8. Positioning the Engines on the Aircraft /81

The absence of propellers, the relatively low weight for high stress, and their simplicity with respect to design and servicing make it possible to install turbojet and turbofan engines in such a way that their optimal operational conditions and those of the aircraft are achieved.

At present, first- and second-generation turbojet passenger aircraft have their engines mounted on the wing, on pylons below the wing, or in the tail section of the fuselage.

Engine Installation in wings. When the engines are installed in the wing (between the upper and lower plankings), the total drag is reduced. In practice, however, the engine is fastened to the fuselage (in double-engine aircraft), while the air duct extends along the chord in the wing. This leads to a decrease in thrust as a result of a pressure loss in the duct, but in contrast an advantage is the almost "clear" wing (without secondary structures) which results. Engines arranged in this manner (close to the aircraft axis), if one of them fails this creates only a slight turning moment.

Of the disadvantages which result from this arrangement, let us point out the fact that it becomes impossible to make use of the thrust reversal

due to the heat effects of the gas jet on the fuselage (for a double-engine aircraft) and the partial use of thrust reversal (for a four-engine arrangement) (see Chapter IX). The stream of exhaust gases creates substantial noise in the tail section of the fuselage and causes discomfort to the passengers seated in the rear. On the Tu-104 and the Tu-124 (Figure 57), the engines are located in the base of the wing, so that the greater part of the engine pod is hidden behind the wing. In the De Havilland Comet, however, the engines are fully hidden in the wing (Figure 58). The engine's small size makes it possible to design its pods with quite small maximum cross-sections.

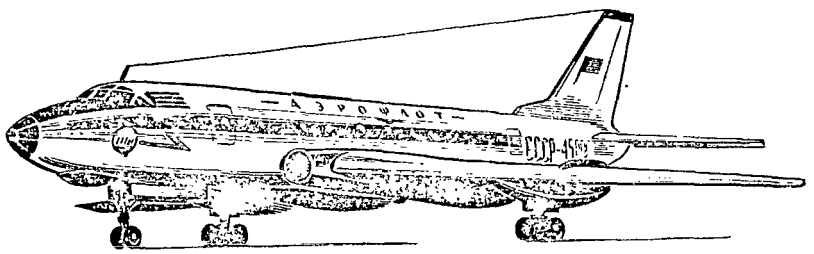

Figure 57. The Tu-124.

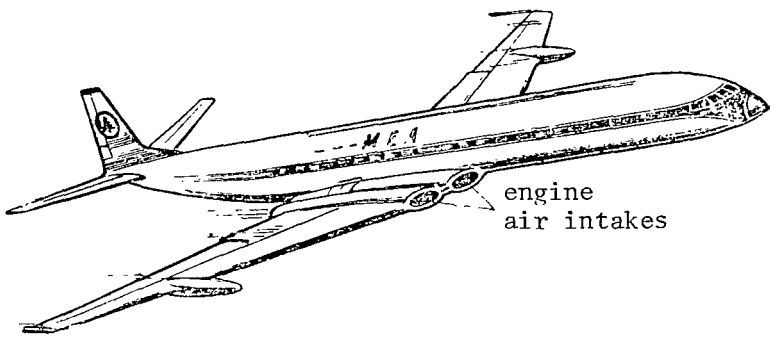

Figure 58. The Comet

Engines located at the base of the wing create positive interference at the most complex aerodynamic point -- the joint between the low-hung wing and the fuselage. The effect of the jetstream causes the formation of an "active /82 fairing" here, i.e., an increase in the "regeneration" of the surrounding flow. This leads to a decrease in drag for the aircraft as a whole*.

However, this engine arrangement requires an increase in the relative thickness of the airfoil profile, which causes a decrease in the aircraft's

* Yeger, S.M. Design of Passenger Jet Aircraft (Proyektirovaniye passachirskikh reaktivnykh samelotov). Mashinostroyeniye. 1964.

high-speed characteristics. The angle at which the engines are installed relative to the longitudinal axis is 3-5° in this arrangement. This inclination is necessary to guarantee that the engine exhaust flow does not hit the elevator unit. In planform, the engines are turned outward by an angle of 2-4°, in order that the exhaust gas jet have less of an effect on the fuselage.

Positioning the engines on pylons beneath the wings. This is done on the American Jets the Boeing-707 and 720, the Douglas DC-8 (Figure 59), and the Convair 880 and 990. Even the newly created Boeing-737 shows a return to the pylon arrangement.

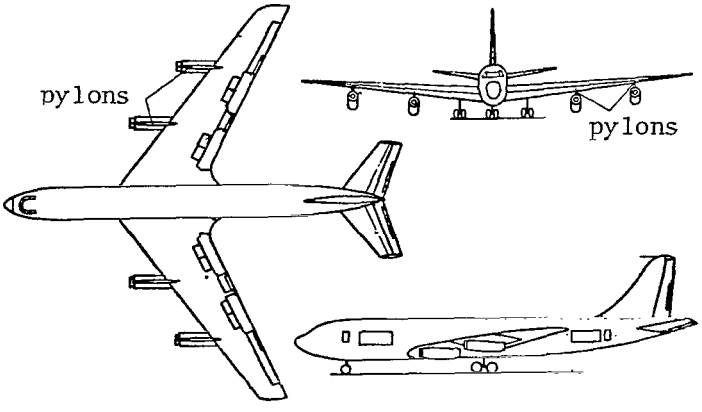

Figure 59. Aircraft with Pylon Suspension of Engines.

In this setup, the positioning of the engines increases aircraft drag slightly, particularly due to negative interference from the wing and pylons. However, the short length of the engine's intake duct when the air admission is well designed minimizes thrust losses and thereby improve the aircraft's takeoff performance.

Suspending the engine from a thin swept wing substantially lightens the wing and decreases its structural weight. However, such a suspension requires increased reinforcement of the engine and its pylon (due to greater inertial loads during aircraft maneuvering) and as a result the wing weight is negligibly decreased. Aircraft with pylon suspension of engines should be used only on concrete runways which have substantially cleaner surfaces, because the engines are only 40-70 cm above /83 the ground. If foreign matter is drawn into the intake duct, the engine compressor may fail. Although positioning the engines to the side of the fuselage makes it possible to effectively use thrust reversal from all four engines, the failure of the outside engine creates a substantial turning moment, which greatly impedes handling the aircraft. This moment, acting in the horizontal plane, causes an intense rolling motion around the longitudinal axis, which (with allowance made for the aircraft's substantial moment of inertia relative to the longitudinal axis) leads to an emergency situation.

The basic advantage of pylon engine suspension is the decreased noise within the passengers' compartment.

Positioning of engines in the fuselage tail section. This arrangement was first used in the French Caravelle passenger aircraft (Figure 60). The following aircraft have also been designed along these lines: the Il-62, the

Tu-134, the DC-9, the BAC-1 11, the Boeing-727, the De Havilland DH.121 Trident and the Vickers VC-10 (Figure 61).

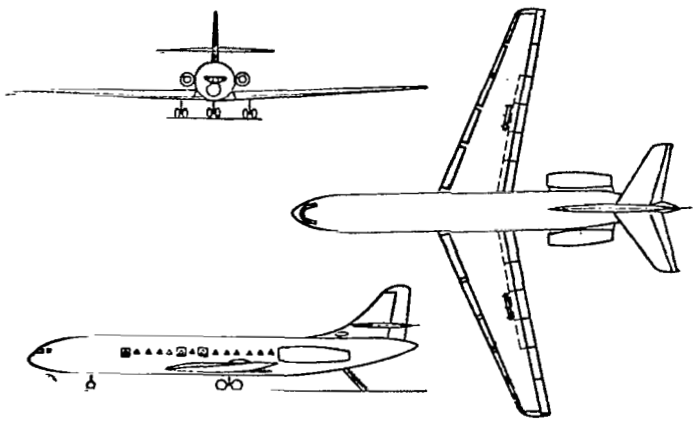

Figure 60. The Caravelle.

Such an engine arrangement yields the "clear wing" and offers maximum mechanization of the wing.

Jet passenger airlines with such engine arrangements have several advantages. The basic advantage is their increased aerodynamic characteristics and increased comfort within the passenger cabin (decreased noise level). The absence of engine pods on the wing results in negative interference being a factor only at the juncture of the wing and fuselage. In addition, conditions are created for designing a wing with an increased critical Mach number and a more effective mechanical high-lift device on the wing. The lack of secondary structures on the wing improves the wing's lift, which in turn permits a drop in the wing area.

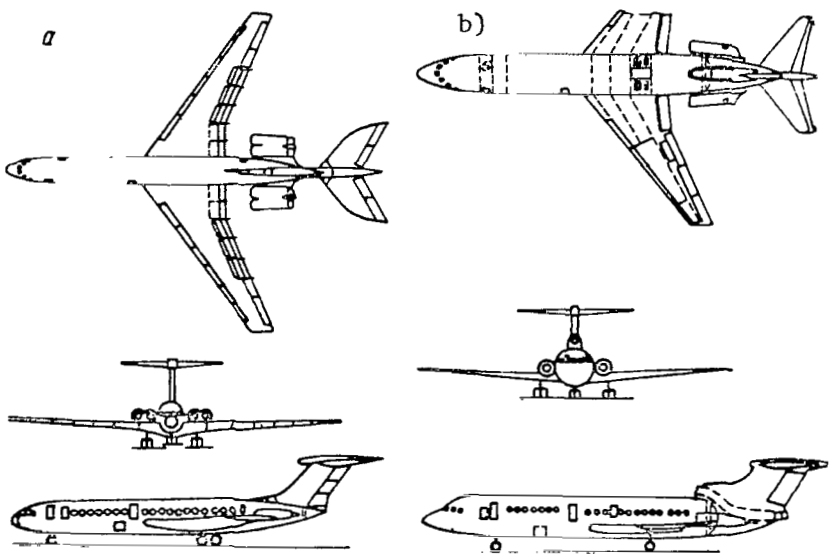

Figure 61. The Vickers VC-10 (a) and the De Havilland DH.121 (b).

Conditions are also created for the operation of the engine air scoops at high angles of attack as a result of downwash, which in a sense "corrects" the flow toward the side engine. During gusts, the entrance angle of the airflow into the air scoop decreases almost to half the airfoil angle of attack, i.e., when the airfoil angle of attack changes by 4°, for example, the direction of the airflow around the air scoop varies by approximately 2°. The air will enter the engine at less of an angle, which substantially decreases the pressure loss at the intake. When the engine is installed in the wing or suspended from a pylon, however, the entrance angle corresponds to the angle of attack at which the aircraft is flying. Here the air circulation around the wing increases the flow intake angle. As is well known, this causes additional losses.*

/84

/85

One of the structural characteristics of this arrangement is the T-shaped tail assembly with its adjustable stabilizer. The elevator assembly, located on the upper section of the vertical fin, is free from the destructive effect of sound-waves created by the sound fields of the engine exhaust (Figure 62). This, too, has a specific effect in decreasing vibration.

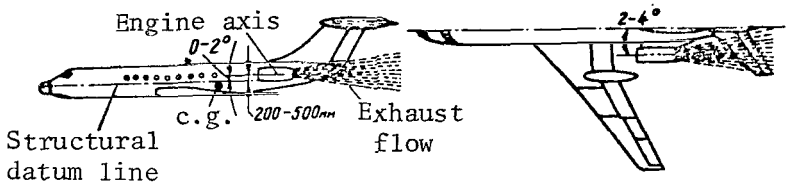

Figure 62. Diagram of the Effect of Engine Exhaust Jets on the Stabilizer and Vertical Fin.

The aerodynamic advantage of the T-shaped tail assembly is that the flow beyond the wing and its resultant separations have little effect on it during horizontal flight.

The engine pods form horizontal surfaces which increase the aircraft's longitudinal stability, in view of which the aircraft's longitudinal stability characteristic progress linearly up to high angles of attack.

At the point of intersection of the horizontal tail surfaces and the elevator for the T-shaped arrangement at high flight speeds, the increase in drag drops as compared to the normal arrangement. This is an example of so-called positive interference, and the effectiveness of the vertical tail surface increases.

The engine pods have a horizontal pylon. The angle at which the pod is set relative to the axis of the fuselage varies from zero to +2°, while in the horizontal plane the pods may be turned out from the fuselage by an angle of 2-4° (Figure 62).

---

* Yeger, S.M. Design of Passenger Jet Aircraft (Proyektirovaniye passachirskikh reaktivnykh samelotov). Mashinostroyeniye. 1964.

When the pod axis is higher than the structural axis of the fuselage and consequently higher than the aircraft's center of gravity, a negative pitching moment is created from the engine thrust.

Moving the engines to the tail section of the fuselage creates the /86
following operational advantages. As can be seen from Figure 63, only a slight portion of the airflow thrust back by the nose wheels is covered by the engine. The jets from the main wheels are covered by the wing both during takeoff and landing. This decreases the possibility that foreign matter will enter the engines off the runway. Ground maintenance of the engine is made simpler through the ease with which the pods can be reached.

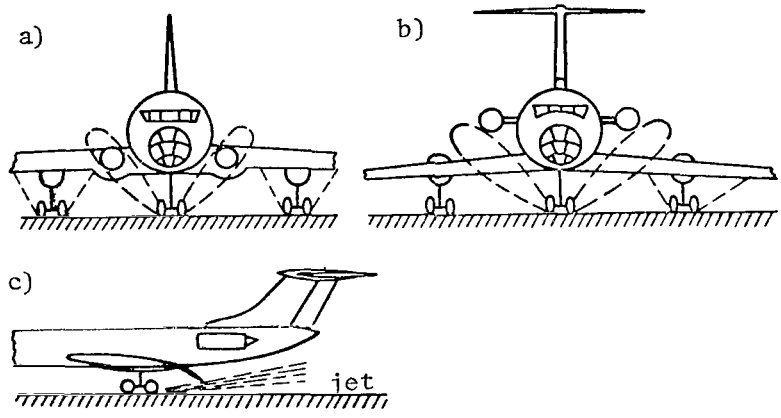

Figure 63. Diagram of the Effect of Airstream Thrown Back from the Landing Gear Wheels: a - engines mounted in wing; b - engines in tail section of fuselage; c - engines on pylons.

When the engines are suspended from pylons, as was stated above, there is no need for long air scoops. However, when the engines are mounted in the wing, as was done in the Tu-104 and Tu-124 and the Comet, the length of the air intake is 4-5 meters, as a result of which losses in air pressure at the intake decrease engine thrust by 3-6%. Moving the engines to the tail, however, decreases losses at the intake and the thrust drop is only 1-2%, which improves the aircraft's takeoff performance.

In conclusion it should be noted that in spite of the numerous advantages derived from installing the engines in the tail section of the fuselage, this arrangement also has its drawbacks. Thus, for example, the engine performance decreases at high angles of sideslip. The diving moment from engine thrust increases both the speed of raising the landing gear nose wheels strut during the takeoff run and the conditions for the control wheel. The need arises for an adjustable stabilizer. There is an increase in the weight of the rudder unit, which supports the elevator unit. The structure of the aircraft

becomes heavier as a result of the reinforcement for the construction of the fuselage tail section due to the additional mass and inertial loads from the engines as well as the need to increase reinforcement for the engines to prevent its breakaway during emergency landing. During charging and fueling-up, the aircraft center of gravity is shifted substantially farther forward, which makes takeoff harder, and during flight requires precise functioning of the automatic equipment which controls the fuel output. /87

Grouping the engines together in the tail section of the fuselage facilitates using them for controlling the boundary layer (see Chapter IV) and, finally, with the power plant arranged in this manner, the distance from the engines to the ground is determined only by the aircraft's landing configuration and the height of the landing gear. This makes it possible to decrease the landing gear height and retain the permissible distance from the ground to the edges of the air scoops.

CHAPTER V

TAKEOFF

§ 1. Taxiing

Aircraft with engines in the tail section of the fuselage or in the wing (along the sides of the fuselage) have satisfactory taxiing properties. The small thrust arm has no adverse effects on the aircraft's maneuvering properties. In fact, all modern jet aircraft have a pedal-controlled leading strut, which makes it easy to perform turns and maintain direction during take off runs and landing runs.

The angle of rotation of the leading strut is 35-45°, while during take off runs and landing runs (with flaps down) it is decreased to 5-6°. The taxiing speed along the ground, during turns and close to obstacles reaches no more than 10 km/hr, while in clear and straight runway sections, it is no more than 50 km/hr.

Landing gears with nose wheels offer good runway stability during taxiing on runways and taxiways. Turns are manipulated through the use of the leading struts, as well as the creation of asymmetrical thrust and partial braking of the right or left landing gear trolley wheel. Turning an aircraft 180° requires a runway 50-60 meters wide, depending on the width of the landing gear wheels. Turbojet aircraft can also taxi over wet grass cover and over unsmoothed snow cover at an airfield. The four to six wheels on each main strut of the landing gear causes an even distribution of load over the airfield surface, and reduced pressure in the pneumatic wheels (up to 4.5 - 6 kG/cm^2) increases ability to travel over dirt airfields. Modern aircraft using concrete landing strips maintain a tire pressure of 6.5 - 9.5 kG/cm^2.

One drawback in the use of aircraft on dirt airfields is the damage to /88
the surface caused by the wheels during taxiing, takeoff and landing, the formation of ruts, and the great amount of dust thrown up from the exhaust of the jet engines, which reduces visibility on the landing strip for pilots of aircraft approaching for a landing.

§ 2. Stages of Takeoff

Takeoff is the aircraft's motion from the moment of starting until it reaches an altitude of 10.7 meters* and has attained a safe flight speed.

---

* This is the presently accepted altitude for complete takeoff according to the ICAO and norms for flight worthiness for civil aircraft in the USSR.

The distance covered by the aircraft from the moment of starting until the altitude of 10.7 meters has been reached is called the takeoff distance.

Aircraft takeoff (Figure 64) consists of two stages: a) taxiing until the speed of lift-off and lift-off itself, b) acceleration from the lift-off speed to a safe speed, with simultaneous climbing.

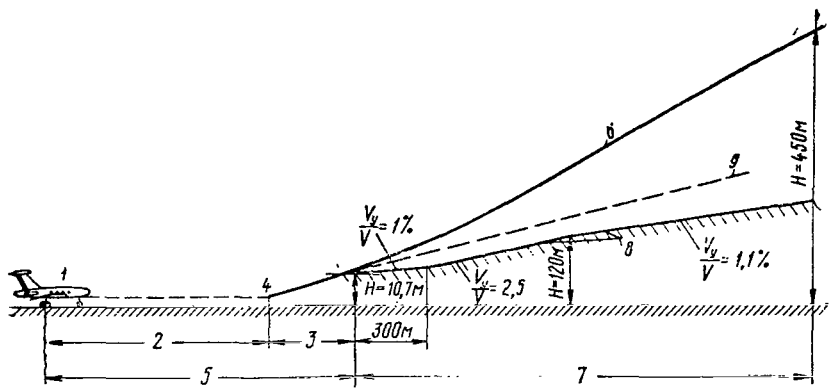

Figure 64. Diagram of Aircraft Takeoff and the Calculated Takeoff Trajectory According to the ICAO: 1 - beginning of run; 2 - takeoff run; 3 - acceleration and climbing; 4 - point of aircraft lift-off; 5 - takeoff distance; 6 - climbing trajectory for 100% engine thrust; 7 - length of calculated takeoff trajectory; 8 - permissible inclinations in trajectory for extended takeoff due to engine failure; 9 - actual trajectory of extended takeoff.

Immediately after lift-off, the aircraft's high thrust-weight ratio permits it to gain altitude and accelerate up to its rate of climb along an inclined trajectory. In this case, the gain in altitude is curvilinear, because its angle of inclination constantly increases.

The holding after lift-off, which is used in the acceleration of piston aircraft prior to beginning gaining altitude, is not applied in turbojet aircraft.

The take-off run up to lift-off speed. As a rule, takeoff is performed /89
with flap deflection, from the brakes when the takeoff regime for the engines is used. To this end, the engines are first put into takeoff rpm's and then the brakes are slowly released. Figure 65 shows a graph of the coefficient c_y as a function of the angle of attack and the aircraft polar for takeoff position of the wing flaps and slats. An aircraft having triple-slotted flaps (high value for $c_{y\ 1\text{-}o}$) was used as an example.

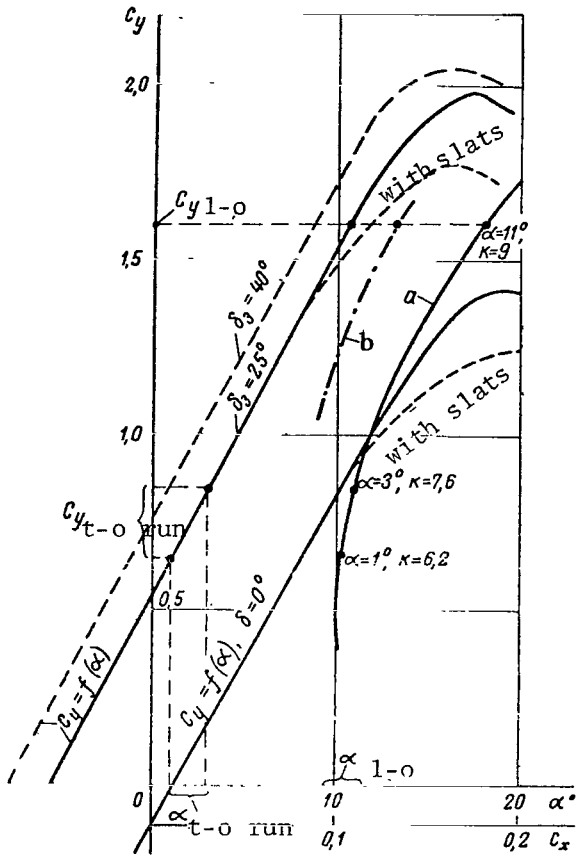

Figure 65. The Dependence of c_y on α and the Polars of an Aircraft having Triple-Slotted Wing Flaps and Slats: a - polar for aircraft with landing gear down and wing flaps deflected at 25°; b - the same aircraft with allowance made for the effect of screening by the earth during the takeoff run (K = 1.6 : 0.134 ≈ 12). Note: T-O = Take Off

At the beginning of the take- /90
off run, direction is maintained by the brakes and directing the nose wheel, and at a speed of 150-170 km/hr, when the rudder becomes effective, it is maintained through the appropriate inclination of the rudder to the side as required. When the proper takeoff angle of attack (9-10°) is maintained, lift-off of the aircraft from the ground occurs without additional movement of the control wheel when lift-off speed is attained. With a lift-off angle of attack of 9-10°, the tail section of the fuselage must be sufficiently far off the runway and a specific sub-critical angle of attack must be maintained. If the pilot unintentionally increases the angle of attack to 11-12°, contact of the tail portion of the fuselage with the concrete must be avoided.

An improperly chosen angle of attack during lift-off may either extend the length of the takeoff run, or, on the contrary, lead to premature lift-off at a low speed. Thus, if the pilot achieves lift-off at a lower angle of attack (for example, with α = 6° instead of 9-10°), i.e., below $c_{y\,1\text{-}o}$, which corresponds to a high speed, the length of the takeoff run increases. In calculating the aircraft lift-off during takeoff, the values normally accepted are α = 8-11° and $c_{y\,1\text{-}o}$ = 1.3 - 1.7 (depending on the design and arrangement of the flaps). For the example shown in Figure 65, we have $\alpha_{1\text{-}o}$ = = 11° and $c_{y\,1\text{-}o}$ = 1.6.

Acceleration from the lift-off speed to a safe speed with simultaneous climbing. Piloting an aircraft during this stage of flight involves the following. After lift-off, maintaining the takeoff angle, the aircraft smoothly shifts into gaining altitude with a subsequent decrease in the angle

of attack. The main wheels are braked, the time for complete braking averaging 0.2 - 0.3 sec. To decrease drag against the aircraft during climbing (after lift-off), the landing gear must be retracted without delay. The aircraft's hydraulic system retracts the landing gear, with opening and closing of the main landing gear doors, in 5-15 sec. The landing gear is retracted at a speed of 20-30 km/hr above the lift-off speed, and at a height not below 5-7 meters. During the process of retraction, the aircraft's speed increases. After the landing gear is retracted, the flaps are in turn retracted at a height not less than 50-80 meters, and the aircraft accelerates to a speed for gaining altitude. The pilot must fly the aircraft during this interval in such a way that before the flaps are retracted, the speed does not exceed the permissible with respect to stability conditions. The time required for retracting flaps deflected at a takeoff angle is 8-12 sec. As the flaps are retracted, a pitching moment is created, so that pressing forces are created on the control wheel which are easily relieved by the elevator trim tabs. This is a case in which the electrical control of the elevator trim tabs is convenient to use. After the flaps are retracted, the engine rpm's decrease to normal and there is a further acceleration up to the climbing cruising speed or to the flight speed along a rectangular root.

§ 3. Forces Acting on the Aircraft During the Takeoff Run and Takeoff /91

Let us examine the forces acting on the aircraft during the takeoff run (Figure 66). The total force of the engine thrust acts in the direction of the aircraft motion. The overall force of wheel friction against the ground $F = F_1 + F_2$ and the aircraft drag Q act against the aircraft's motion, braking it. The difference in the forces $P - Q - F = R_{acc}$ is called the acceleration force. The following forces act perpendicular to the trajectory of motion: lift force Y, force N of the reaction of the ground on the landing gear wheels, and the force of weight G. The force R_{acc} communicates to the aircraft the acceleration

$$j_x = \frac{R_{acc}}{m} = \frac{R_{acc}}{G} \cdot g = 9{,}81 \frac{R_{acc}}{G},$$

where m is the aircraft mass.

The greater the acceleration force and the lower the aircraft weight, the higher the acceleration will be. If instead of R_{acc} we substitute its value into the formula, we obtain

$$j_x = 9{,}81 \left(\frac{P}{G} - \frac{F}{G} - \frac{Q}{G} \right).$$

As the landing gear wheels roll along the ground, friction forces arise whose value is a function of the condition of the runway (type of surface) and

the degree of deformation in the tires. The amount of the force of friction is determined as the product of the loads on the wheels on the friction coefficient f.

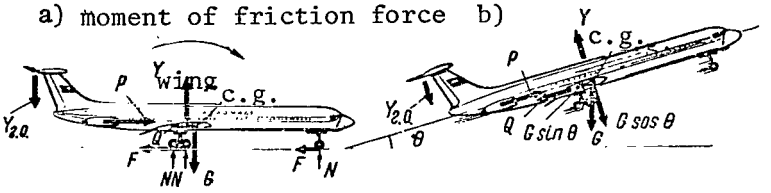

Figure 66. Diagram of Forces Acting on the Aircraft During Takeoff Run (a) and After Lift-Off During Climbing (b).

During the takeoff run, the aircraft wing begins creating a lifting force which rapidly increases and removes the load from the landing gear wheels. The value of the friction force for each moment may be determined according to the following formula: $F = f (G - Y)$. The friction coefficient (or coefficient of adhesion) for dry concrete is $f = 0.03 - 0.04$, and for wet concrete it is 0.05; for dry ground cover and for a cleared snow cover it is 0.07; for a wet grass surface it is 0.10.

The value P/G is the aircraft thrust-weight ratio during takeoff. The greater the thrust-weight ratio, the greater the takeoff run acceleration and /91 the shorter the length of the takeoff run. Increasing the thrust-weight ratio is an effective means of improving takeoff characteristics. For example, when the Conway 550 double-circuit engines with their 7,500 kG thrust were installed on the Boeing-707, the thrust-weight ratio increased from 0.2 to 0.26. A greater thrust-weight ratio is enjoyed by aircraft with two engines (0.28 - 0.33 kG thrust/kg weight), and the least is that of aircraft with four engines (0.22 - 0.26 kG thrust/kg weight).

As can be seen from the formula above, the maximum acceleration is during the first stage of the takeoff run (the aircraft drag force is low).

With an increase in speed the thrust of jet engines decreases, although during the takeoff run it may be considered constant. By comparison with piston engines, the thrust of jet engines during takeoff decreases less significantly and at the end of the takeoff run amounts to 87 - 92% of the static thrust P_0. The drag force during the takeoff run increases from 0 to Q_{1-o} (aircraft drag at the instant of lift-off). At lift-off, Y = G, so that the friction force will equal zero.

Thus, at the end of the takeoff portion, when the aircraft separates from the ground, the acceleration force (reserve thrust) equals the difference between the total engine thrust and the aircraft drag: $R_{acc} = P - Q$.

Aircraft drag at the instant of lift-off (1-o) may be determined according to formula:

$$Q_{1\text{-}o}=c_x\rho S\frac{V^2}{2},$$

where c_x is the drag coefficient for an aircraft with landing gear down and flaps extended in takeoff position at an angle of attack at the instant of lift-off.

For example, for an aircraft with a takeoff weight of 76 tons and a wing area of S = 180 m^2, the thrust during takeoff configuration for a lift-off speed of 300 km/hr (83.3 m/sec) is approximately 17,000 kG. If we assume that at lift-off $c_{x\ 1\text{-}o}$ = 0.07 - 0.075, then

$$Q_{1\text{-}o}=c_{x_{1\text{-}o}}\rho S\frac{V}{2}=0.071\cdot0.125\cdot180\frac{83,3^2}{2}=5500\ \text{kG}.$$

Then the acceleration force R_{acc} = 17,000 -5,500 = 11,500 kG. The mean acceleration at this instant will be

$$j_x=\frac{gR_{acc}}{G}=\frac{9.81\cdot11\,500}{76\,000}=1.48\ \text{m/sec}^2.$$

The lower the value $c_{x\ 1\text{-}o}$ (due to the proper selection of the flap and slat systems), the lower $Q_{1\text{-}o}$ will be and the greater the acceleration force will be for the same assumed engine thrust. For example, for an aircraft with a low takeoff weight (two engines), during the takeoff run below the lift-off speed R_{acc} = 9,000 -5,800 kG, while the mean acceleration j_x = 2.5 - 2.0 m/sec^2/93 In such an aircraft, the takeoff time decreases.

During the climbing portion of flight, under the effect of the force R_{acc} (Figure 66) there will be a further increase in flight speed. For this case we may write the following equation of motion

$$R_{acc} = P - Q - G \sin \Theta = mj,$$

where G sin Θ is the aircraft component weight acting along the line of flight;
m is the aircraft mass.

Decreasing the total engine thrust with an increase in flight speed does not decrease the value of the acceleration force, because as a result of a decrease in the angle of attack, the induced drag for the aircraft decreases. This allows an increase in the speed during the takeoff run portion (achieving the required climbing speed or flight speed along a rectangular root).

The length of the climbing portion with acceleration is a function of the specific load, thrust-weight ratio, and other parameters.

The component G sin Θ initially has a low value, because the angle of inclination of the trajectory during climbing is small (Θ = 6 - 10°; sin Θ = = 0.105 - 0.175).

§ 4. Length of Takeoff Run. Lift-off Speed

The length of the aircraft takeoff run is a function of the lift-off speed and acceleration:

$$L_{acc} = \frac{V^2_{1\text{-}o}}{2j_{x\,ave}},$$

where $j_{x\ ave}$ is the average acceleration value.

The lift-off speed is determined according to formula:

$$V_{1\text{-}o} = \sqrt{\frac{2G}{c_{y_{1\text{-}o}} \rho S}} = 14.4 \sqrt{\frac{\frac{G}{S}}{c_{y_{1\text{-}o}}}} \text{ km/hr},$$

where $\frac{G}{S}$ is the unit load per 1 m^2 of wing area.

The greatest unit load is in four-engined aircraft (the Super Vickers VC-10, 570 kG/m^2; DC-8-30, 560 kG/m^2) and somewhat lower in two-engined aircraft (BAC-111-200, 370 kG/m^2, the Caravelle-XB, 350 kG/m^2); for three-engined aircraft (the Boeing-727 and the De Havilland Trident-1E) it is 450 kG/m^2.

For an average $c_{y\ 1\text{-}o}$ = 1.6 (triple-slot flaps and slats), the lift-off speed for G/S = 450 - 500 kG/m^2 is 220 - 240 km/hr. For an average acceleration of j_x = 2 m/sec^2, the length of the takeoff-run is 1,100 - 1,300 m.

As has already been noted, the swept wing has a lower value for the coefficient $c_{y\ max}$ then does the straight wing. This results in a lower value for $c_{y\ 1\text{-}o}$. All in all, this leads to a substantial increase in $V_{1\text{-}o}$, and consequently in the length of the takeoff run. Therefore, the flaps and slats are used to increase $c_{y\ max}$. Deflecting them to their maximum angle at take-off may, of course, substantially decrease the lift-off speed, but in this event there is also an increase in drag, a decrease in acceleration and, lastly, an increase in the length of the takeoff run. This requires selection of the optimum angle of inclination for the flaps, at which $c_{y\ max}$ increases and, /94

consequently, so does $c_{y\ 1\text{-}o}$, while the aircraft drag increases negligibly. Designers are striving to achieve both the greatest value for $c_{y\ 1\text{-}o}$ and high aerodynamic performance in aircraft. If during takeoff the aircraft has a fineness ratio of 14-15, this makes it possible to solve many problems such as, for example, achieving the continuation of takeoff in the event of the failure of an engine, decreasing noise in the area through a sharper climbing trajectory, the selection of engines with optimal thrust values for a given aircraft, etc. Calculations and flight tests have shown that the optimum angle of deflection for flaps during takeoff is 10-25°. This angle yields the optimum ratio between $c_{y\ 1\text{-}o}$ and c_x, which leads to a marked decrease in the length of the takeoff run. We must once more take note that $c_{y\ 1\text{-}o}$ is selected from the condition of a sufficient reserve with respect to the angle of attack prior to lift-off ($c_{y\ max}$), so as to eliminate sideslip. According to norms of airworthiness, the aircraft lift-off speed must be no less than 20% greater than the brakeaway speed (see how it is determined in Chapter XI, § 14).

§ 5. Methods of Takeoff

Earlier we established that acceleration during the takeoff run and consequently the length of the takeoff run are functions of the difference in the available thrust and the overall aircraft drag. The engine thrust during the takeoff run up to the lift-off speed of 220-240 km/hr varies insignificantly (by 6-8%). The overall aircraft drag during this portion of takeoff is the sum of the aerodynamic drag (which increases as the angle of attack increases) and the friction force of the wheels (on the runway surface), which decreases as a result of a lessening of the load on the wheels then increase in wing lift. Therefore, the pilot must select an angle α (different for each aircraft) at which the total drag will be minimal and, consequently, the takeoff run will be shortest. Due to the lack of airflow of the slipstream from the propellers, the effectiveness of the pitch control at the beginning of the takeoff run is below that of a prop-driven aircraft. The required longitudinal moment for lift-off of the nose wheel is created by the elevator only at a rather high speed, close to the take-off speed. As a result of this, the greater part of the take-off run for a turbojet aircraft is achieved in standing configuration. The angle of attack during the takeoff run is a function of the angle ϕ of the wing setting; if, for example, the setting angle $\phi = 1°$, then $\alpha = 1°$ also. However, the wings of modern aircraft have geometric twist (Chapter II, § 1), which creates an angle α which varies along this span. In the graph shown in Figure 65, the value $c_{y\ t\text{-}o}$ corresponds to the average for a takeoff run of $\alpha = 1 - 3°$. /95

By the longitudinal position of the aircraft (the angle of the aircraft's longitudinal axis), i.e., the angle of attack, the pilot may control in achieving a speed at which the effectiveness of the elevator is sufficient to initiate lifting the aircraft's nose (front landing gear strut). Often

this speed is selected from the condition of achieving rudder efficiency in order to prevent the aircraft from turning on the main landing gear struts with nose raised in the event of engine failure during the takeoff run. In this event, the rudder should parry the turning moment from the asymmetric thrust of the operating engines. Usually, after lift-off of the front strut, the aircraft tends to progressively increase the pitch angle under the effect of the increasing wing lift. Therefore, initially the control wheel is brought back toward oneself, and then commensurably moved away, in an attempt to maintain the aircraft at an angle of attack of 3-4°. The length of the takeoff run is a function basically of the accurate setting of the angle of attack. During the takeoff run, minor deviations from the optimum α, at which drag is minimal, do not lead to a substantial increase in the length of takeoff run.

There are two ways of putting the aircraft into the takeoff angle of attack. The first consists of the nose strut's lifting off at the instant when elevator efficiency is achieved. The aircraft achieves an angle of attack of 3-4° and the rest of the run takes place on the main landing gears. Smoothly operating the elevator, the pilot maintains the angle of attack during the takeoff run and at the instant of lift-off he creates the takeoff angle of attack.

In the second way, which has only recently gained acceptance, the entire takeoff run is performed in the standing configuration, and when a speed close to the lift-off speed ($V_{l\text{-}o}$ - 15 - 20 km/hr) is achieved, the control wheel is smoothly but vigorously pulled toward oneself (in 4-5 sec), by which motion the pilot lifts the front strut off and, without maintaining the aircraft in a two-point configuration, puts it into the takeoff angle of attack. Separation occurs practically from three points without any perceptible overload during the process of rotating the aircraft relative to the lateral axis and increasing the pitching angle. In this way the pilot maintains complete control of the takeoff run, the speed and the operation of the engines. Usually during the takeoff run, the navigator states the aircraft speed over the intercom at each 10 km/hr, starting at a speed of 150 km/hr, while the pilot directs all his attention straight ahead. A controllable leading strut simplifies maintaining the direction during the first stage of /96
the takeoff run, before the rudder becomes responsive, which almost eliminates the use of the brakes in the main landing gear trolley.

In the second method of piloting, the takeoff distance remains practically the same as in the first, but the takeoff run is somewhat shorter due to the higher speed. Also, takeoff with a side wind is facilitated, since the controllable nose wheel in combination with the rudder makes it possible to hold a fixed direction up to the moment of separation without increasing the takeoff run length (in aircraft with uncontrolled nose wheel, the run length is usually increased due to the asymmetrical braking of main landing gear trucks). After the aircraft breaks away, the side wind causes it to turn against the wind; for example, with a wind speed of 18-20 m/sec, the rotation angle is 18-20°.

Flying investigations have shown that the required rotation of the front wheel does not exceed 4-5° with a side wind up to 20 m/sec. This allows the maximum permissible side wind during takeoff to be increased, for example, a wind at 90° to the runway can be up to 15-18 m/sec, and also simplifies the takeoff maneuver.

Up to the present time, no single opinion has developed among pilots as to the way in which the control system of the front gear should be constructed. The predominant opinion is that the rotation of the wheels should be controlled by the rudder pedals (as on the TU-124 aircraft), freeing the pilot's hands for operation of the elevator control lever, motor throttles, etc. However, it is known that when the takeoff speed reaches 150-200 km/hr and the rudder begins to be effective, it is more expedient to use the rudder alone to maintain the takeoff direction, disconnecting the front landing gear, which is not always technically possible if the gear is controlled by the pedals. Therefore, the wear rate of the rubber tires on the front landing gear may be increased. A second plan is that of independent control of rotation of the front landing gear, not connected to the operation of the rudder (TU-104 aircraft).

Let us analyze the technique of performing a takeoff using the second method (separation from three points). It is recommended that the elevator trimmer lever be set at 0.5-0.8 divisions forward in advance, in order to increase the load on the stick from the elevator at the moment of separation. Thus, these actions are in opposition to the established tradition, according to which the trimmer control is moved 0.5-1 divisions back in order to decrease loads at the moment of lifting of the front gear and separation of the aircraft. Before beginning the takeoff run, the stick is pushed forward approximately to the neutral position. Holding the aircraft with the brakes, the engines are set at takeoff regime. After making sure that the operating regime of the engines corresponds to the norm, the brakes are released and the takeoff run is begun, during which the required direction is maintained by controlling the front landing gear. The effectiveness of control of the front landing gear is higher, the more strongly the wheels are forced down to the runway. When sufficient effectiveness of the rudder has been achieved to maintain the takeoff course, generally 60-70% of the maximum speed, control of the front wheels can be disconnected (if this is possible in the aircraft). When the takeoff is being performed with a side wind, in order to prevent wind banking at the moment of separation, the aileron control must be turned "against the wind" by 30-80° with a wind speed of 8-18 m/sec before separation. After separation, the rate of increase in the pitch angle must be slightly decreased and the stick smoothly moved to the neutral position. /97

§6. Failure of Engine During Takeoff

Main takeoff characteristics of aircraft with one engine inoperative. As we know, one of the main requirements placed on passenger aircraft is the possibility of continuing takeoff and climb in case of engine failure. A

knowledge of the takeoff characteristics of an aircraft and timely usage of the piloting recommendations in case of engine failure will guarantee a successful continuation of the flight.

The takeoff characteristics of an aircraft with one inoperative engine include the following: a) the length of the takeoff run from the starting point to the moment of engine failure; b) the length of the takeoff run from the moment of engine failure to the moment of separation; c) the inclination of the trajectory during the climbing sector with acceleration; d) the inclination of the trajectory during the climbing sector with landing gear up; e) the critical engine failure speed (the speed of interruption of takeoff) V_{cr}; f) the safe takeoff speed V_{sto}.

If we know the length of the takeoff run of the aircraft from the start position to the moment of engine failure and the length of the run from the moment of failure to complete aircraft halt, which make up the distance for interruption of takeoff, we can determine which airfields are safe for operation of a given aircraft, which type of approaches to the runway should be used, how the aircraft should be piloted with an inoperative engine, etc.

In order to assure safety during continuation of the takeoff and climb with one motor inoperative, it is necessary that the angle of inclination of the takeoff trajectory and climb to altitude measured during tests be greater than the minimum permissible angle (Figure 64). As we can see from the figure, after the landing gear are raised the inclination of the trajectory should be no less than 2.5%, corresponding to an angle $\Theta = 1^\circ$ 30 min ($\sin \Theta = V_y/V = 0.025$ and $\Theta = 1^\circ$ 30 min). The end of the operation of raising the landing gear should correspond approximately to the moment of passage of the takeoff distance (H = 10.7 m) plus 300 m.

In case of an engine failure during takeoff, the available thrust decreases, the flying quality of the aircraft becomes worse and piloting becomes more difficult due to the asymmetrical nature of the thrust and the /98
low flight speeds, decrease in controllability and decrease in rate of climb.

The decrease in available thrust leads to an increase in the dependence of the flying characteristics of the aircraft on temperature and air pressure. Therefore, the vertical speed of the aircraft with one engine inoperative, characterizing the possibility of continuing the takeoff and climb under design conditions (p = 730 mm Hg and t = +30°C) are slightly less than under standard conditions (p = 760 mm Hg and t = +15°C).

The following speeds are characteristic for continued and interrupted takeoffs: a) the critical speed of engine failure, V_{cr}, is the speed corresponding to the "critical point" during the takeoff run, at which failure of one of the engines is possible. In case of failure of one engine at this point, the pilot can either end the takeoff run within the distance

available, separate and continue his flight, or end his takeoff run and stop within the interrupted takeoff distance; b) the safe takeoff speed V_{sto}, is the speed at which the aircraft begins to climb after separation and acceleration with one engine inoperative. According to the norms of the ICAO, this should be 15-20% (depending on the number of engines on the aircraft) greater than the separation speed for the takeoff configuration of the aircraft: $V_{sto} \geq (1.15\text{-}1.2)\ V_{S_1}$ (see Chapter XI, §14).

If the speed of separation is less than the safe speed of the aircraft, the aircraft is held after separation with acceleration to V_{sto}, then the climb to altitude is begun.

The main characteristic indicating to the pilot that an engine has failed is the appearance of a tendency of the aircraft to turn and bank toward the engine which has failed. Also, failure of an engine can be determined from the drop in oil pressure and fuel pressure, decrease in engine rotating speed indicated by the tachometer, etc.

In order to make it possible for the pilot to decide to continue the takeoff or interrupt the takeoff, the pilot should know the critical speed for engine failure and for interruption of the takeoff.

During the process of aircraft testing, interrupted and continued takeoffs are usually performed with one engine switched off during various stages of the takeoff. When this is done, the length of the takeoff run to separation of the aircraft and the length of the trajectory to altitude 10.7 m are measured if the takeoff is continued, as well as the length of the run to halt if it is interrupted. When an interrupted takeoff is performed, first the engine is turned off, then after 3 sec (reaction of pilot to failure) the operating engines are reduced to the idle, the spoilers are extended and the braking parachute is released and intensive braking is begun. The transition to the idle is made due to the necessity of maintaining pressure in the hydraulic system controlling the spoilers and landing gear.

When a continued takeoff is performed, the pilot, after the engine is /99
turned off, continues his acceleration to the separation speed and acceleration to the safe flying speed. The data produced by these tests are used to construct graphs of the dependence of takeoff run, distance of continued flight to H = 10.7 m and distance of interrupted takeoff on speed (Figure 67). The critical speed for engine failure (point B) corresponds to point A of the intersection of the curves for interrupted and continued takeoffs. Here also the so-called runway balance line in the direction of the takeoff course (point C) is determined, which in case of an engine failure during takeoff provides for continuation of the takeoff or stopping

of the aircraft (by braking) within the length of the runway after the takeoff is interrupted. /100

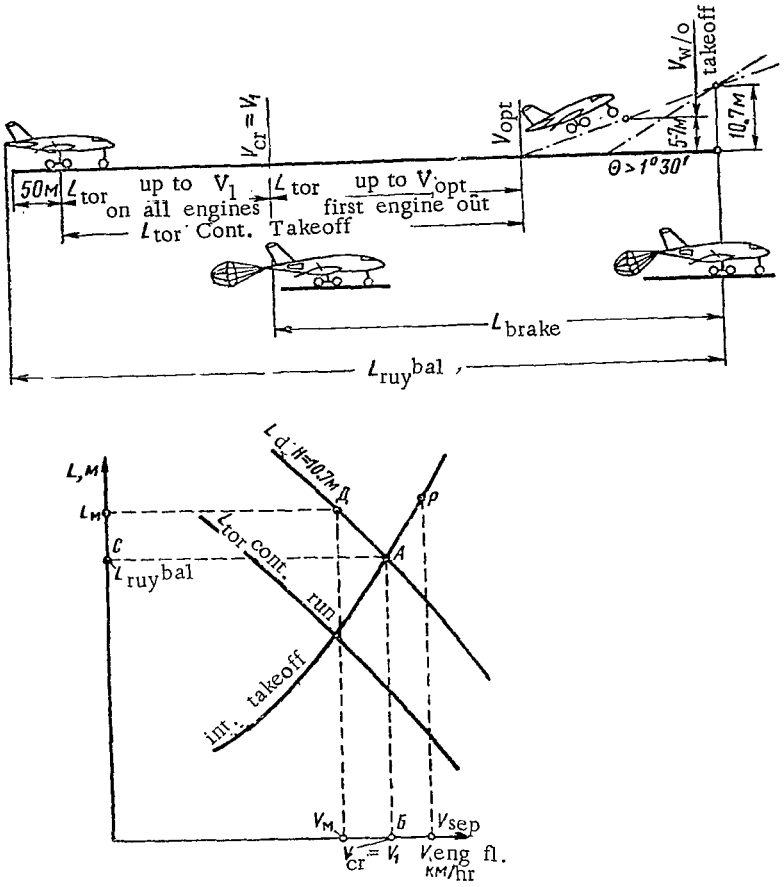

Figure 67. Diagram for Determination of Balance Runway Length and Critical Speed of Engine Failure

If the takeoff is continued, acceleration of the aircraft to the safe takeoff speed should be performed at an altitude of 5-7 m (above the runway), at which point the landing gear should begin to be raised. At 10.7 m, the landing gear should be almost all the way up (takeoff distance).

The complete raising of the landing gear should be completed after the takeoff distance plus 300 m (reserve) have been covered.

In case of interruption of the takeoff, the run should be completed on the runway.

The critical speed for engine failure is the maximum speed, upon reaching which the pilot can interrupt the takeoff or continue it with equal safety. If the takeoff is continued at $V_M < V_{cr}$ (Figure 68), the continued takeoff distance L_M to altitude 10.7 m is greater than the balanced runway length; this is particularly dangerous if this length includes the 400-m terminal safety strip. This is a paved concrete strip (in case the aircraft rolls beyond the actual runway during an interrupted takeoff).

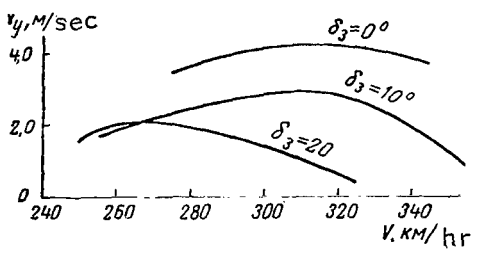

Figure 68. Vertical Speed of Aircraft During Climb with One Inoperative Engine As a Function of Flight Speed (Aircraft with Two Engines, G_{to} = 35 t, Landing Gear Up, H = 900 m)

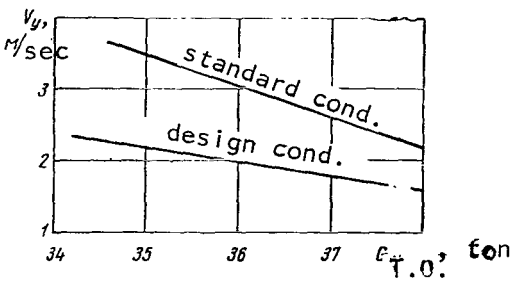

Figure 69. Vertical Speed As a Function of Takeoff Weight of Passenger Aircraft (Aircraft with Two Engines, Specific Loading 360 kg/m^2, One Engine Inoperative, Available Power 0.14 kg thrust/kg Weight)

In case of an interrupted takeoff at the separation speed $V_{sep} > V_{cr}$, the braking distance will also be increased (point P) and the aircraft will roll beyond the end of the airfield.

The best case is equality of critical speed and separation speed, since this facilitates piloting of the aircraft considerably and makes it possible to interrupt the takeoff safely right up to the moment of separation of the aircraft.

Let us now analyze the selection of a safe speed for continuing of the takeoff (Figure 68). Usually at speeds of 280-320 km/hr, the maximum vertical speed is achieved with the flaps in the takeoff position. However, acceleration of the aircraft from V_{sep} = 220-260 km/hr to a speed of 280-320 km/hr requires a great deal of time and lengthens the takeoff distance. Therefore, in order to avoid increasing the takeoff run length unnecessarily, leaving it within limits of 600-800 m, the safe takeoff speed is selected as 10-15 km/hr greater than the separation speed, if this will provide a climb trajectory angle of no less than 2.5% for an aircraft with landing gear up. With an average acceleration of 1 m/sec^2, 3-4 sec are

required to increase the speed of the aircraft by 10-15 km/hr (2.8-4.2 m/sec). During this time, the aircraft can climb 5-7 m. The critical speed of engine failure for an aircraft with a given weight under given concrete atmospheric conditions for the balanced runway length has a unique value. However, it is known that the engine thrust depends strongly on temperature of the surrounding air and atmospheric pressure, and, for example, decreases below the standard thrust with increasing temperature, so that the excess available thrust decreases. This means that the takeoff run length and takeoff distance increase, the vertical speed decreases (Figure 69), the angle of inclination of the aircraft trajectory with a continued takeoff with one engine inoperative decreases. /101

In order to go beyond the limitation with respect to trajectory inclination, the angle of inclination of the flaps must be decreased, or if this is insufficient, the takeoff weight must be decreased.

The operating instructions of every aircraft include graphs and nomograms which can be used to determine the takeoff characteristics in case of engine failure during the takeoff run. For this purpose, first of all on the basis of the fact that the trajectory inclination of a continued takeoff should be no less than 2.5%, the permissible takeoff weight is determined for each selected flap angle and actual air temperature (Figure 70). Then, using the nomogram (Figure 71) for the same atmospheric conditions and the weight which has been determined, the balanced runway length is found (point K). Then, using the nonogram (of Figure 72), the critical engine failure speed (takeoff interruption) is found, as well as the safe speed for continued takeoff. Figure 72 shows a nomogram for determination of the critical speed. The same form of nomogram as on Figure 72 is constructed in order to determine the safe speed for continued takeoff, takeoff run length, separation speed, etc.

The nomograms on Figures 70-72 correspond to the norms of the ICAO. The arrows on the nomograms show the path for determining desired quantities.

Piloting of an aircraft with one engine inoperative after separation. Separation of an aircraft with one engine inoperative occurs at the same speeds as with all engines operating. The effectiveness of the ailerons is decreased. Therefore, the pilot should accelerate the aircraft to a safe speed, exceeding the separation speed by 10-15 km/hr. This speed is also called the best takeoff speed, since it provides sufficient transverse controllability and allows a climb to be performed at V_y:V = 2.5%. /102

Acceleration after separation should be performed near the ground, since the aerodynamic influence of the surface is favorable and the inductive drag of the aircraft is decreased. At V_{sep} + 10-15 km/hr with flaps deflected by 10-25°, α = 7-9° and the aerodynamic quality is 12-13; the inductive drag (c_y = 1.15-1.3) is approximately equal to one-half of the

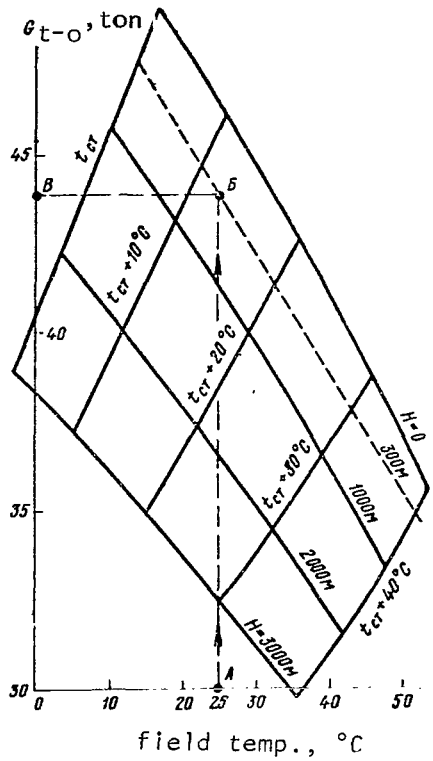

Figure 70. Nomogram for Determination of Permissible Takeoff Weight from Condition of Production of Trajectory Inclination of 2.5% in Continued Takeoff

entire drag of the aircraft. With quality values of 12-13, the thrust consumption of the aircraft is always considerably less than the available thrust and the aircraft can be either accelerated or transferred into a climb.

We can see from Figure 65 that for an angle α_{sep} = 11°, the aerodynamic quality of the aircraft K = 9, while considering the influence of the earth it is increased to 12. At 10-15 m, the influence of the earth decreases sharply, and by this time the aircraft is already flying at the safe speed (in our example this corresponds to α = 8° and K = 9). The airborne sector of aircraft acceleration during which it climbs to 5-7 m, is 600-800 m, and the vertical speed V_y = 1.5-2.5 m/sec (depending on atmospheric conditions). Upon achieving the safe altitude after acceleration, the landing gear must be raised, in order to decrease the drag. 6-8 sec after the landing gear begin to come up, the drag of the aircraft is decreased significantly and the excess thrust can support a climb with higher vertical speed, increasing the safety of continuation of the flight. Therefore, if the landing gear are raised quickly, this should be done during the acceleration sector, although the flying altitude will still be quite low. Raising the landing gear increases the vertical speed by 0.5-1.0 m/sec, i.e., the climb will occur at V_y = 2-2.7 m/sec (depending on the aircraft weight). /103

Climbing up to 100 m altitude should be continued at constant speed. At this altitude, the aircraft can be accelerated to the permissible flight speed with mechanical devices retracted, and the flaps can be raised. In order to avoid a loss in altitude, it is recommended that the flaps be raised in two to three partial movements. After the flaps are raised, the engines should be set in the nominal regime. The direction of flight can be maintained with one engine inoperative by deflection of the pedals and creation of a 2-3-degree bank toward the engine still operating.

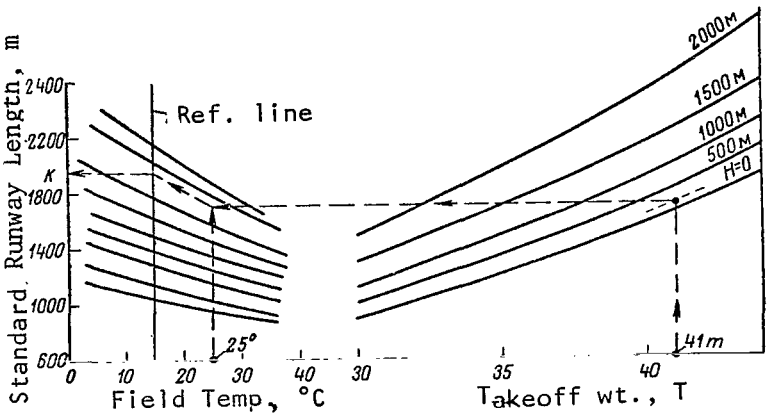

Figure 71. Nomogram for Determination of Balanced Runway Length

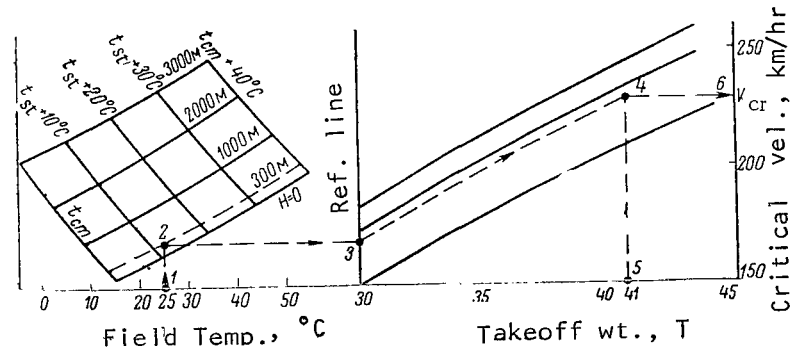

Figure 72. Nomogram for Determination of Critical Engine Failure Speed

Flight trajectory with one engine inoperative. As we noted above, the angle of inclination of the trajectory during the flight sector after the landing gear are raised should be no less than 1° 30 min, i.e., 2.5%. However, depending on the concrete conditions in which the aircraft is being operated, this trajectory inclination may vary. /104

Under standard conditions, the aircraft has great vertical speed, so that it is not difficult to provide the necessary trajectory angle. The problem is somewhat more difficult under design conditions, and particularly at high air temperatures, at which the vertical speed during takeoff with one engine inoperative is sharply decreased.

Usually, the first marker beacon is located 900-1000 m from the runway, and has a tower 10-12 m high. If the takeoff is continued, the aircraft

will fly over this point with landing gear almost up at 20-25 m. Errors in piloting techniques and instrumental errors, as well as failure to follow the flying instructions may result in reduced altitude of flight over this beacon. It is therefore required that the approach to the runway be open in order to avoid collision of aircraft with obstacles in case of a continued takeoff.

§7. Influence of Various Factors on Takeoff Run Length

During the process of flying operations, the length of the takeoff run may differ from the values calculated for standard conditions under the influence of changes in engine thrust, aircraft weight, temperature, density and pressure of the air, position of the flaps, speed and direction of the wind.

Engine thrust has a clearly expressed dependence on engine rotation speed. For example, if the rotating speed is decreased from the takeoff to the nominal speed, the thrust is decreased by 5-7% (see Figure 52). Therefore, a decrease in rotating speed may increase the takeoff run length considerably. During takeoff at the nominal regime, the takeoff run length is increased by 10-12%, and flight safety in case of an engine failure is decreased.

The takeoff weight influences the takeoff run length as follows: 1) with an increase in weight, the separation speed increases; 2) with the same engine thrust, an increase in weight leads to a decrease in performance, and consequently to a decrease in acceleration during the takeoff run. As a result, the length of the run is increased.

The air temperature influences the takeoff run length in two directions. First of all, the air temperature influences the thrust of the engine, and, secondly, it influences the true separation speed. Increasing the temperature causes a decrease in thrust, and consequently of acceleration during the takeoff run, which increases the takeoff run length. Also, increasing the temperature causes a decrease in density and, consequently, an increase in the separation speed. For example, an increase in air temperature of 10° increases the takeoff run length by 6-7%. /105

Pressure and density of the air. If the air temperature is constant, but the pressure changes, the density of the air will also change; as the pressure changes, the density changes by the same factor, since

$$\rho = 0.0473 \frac{p}{T},$$

where p is the air pressure, mm Hg;
T = 273 + t is the absolute temperature;
t is the temperature of the surrounding air in degrees Centigrade.

This formula allows us to determine the density in case of a simultaneous change of temperature and air pressure. A decrease in density leads to an increase in the separation speeds and a decrease in the thrust of the engine due to the decrease in the air flow by weight through the engine. With decreasing thrust, the mean acceleration j_{xav} decreases and, in the final analysis, the takeoff run length increases. A decrease in pressure of 10 mm Hg leads to an increase in takeoff run length of 3-4%. Thus, during takeoff under nonstandard conditions (t = +30°C and p = 730 mm Hg) the takeoff run length is increased by 30-32%.

Wind speed and direction. The length of the takeoff run with a wind is determined by the following formula:

$$L_{tor} = \frac{(V_{sep} \pm W)^2}{2j_{av}},$$

where W is the head wind component of the wind (the "plus" sign is taken with a tail wind, "minus" -- with a head wind).

The takeoff, as a rule, is performed against the wind, so that the run length and takeoff distance are minimal. Separation occurs at a given air speed V_{sep}. With a head wind, the separation speed of the aircraft relative to the ground is decreased by the value of the wind speed. Therefore, less time is required for a takeoff run with a head wind than in calm air, and the takeoff run length is decreased; while with a tail wind it is increased. For example, if the head wind speed is 5 m/sec (18 km/hr), the aircraft need be accelerated to only 222 km/hr ground speed, at which time the air speed will be 240 km/hr, i.e., the separation speed is reached, and the takeoff run is shortened. A headwind of 5 m/sec decreases the takeoff run length by an average of 15-17%, while a tail wind of this same speed increases the length by 18-20%. When taking off with a side wind, the aircraft tends to turn into the wind, particularly during acceleration with the front landing gear up. The reason for this rotation is the fact that aircraft with turbojet engines have large vertical tail surface area, located at a considerable distance from the main landing gear.

A quantitative estimate of the influence of various factors on the length of the takeoff run can be made using nomograms, with which the pilot can determine the takeoff run length under the concrete takeoff conditions involved. /106

§8. Methods of Improving Takeoff Characteristics

As we analyzed above, the length of the takeoff run depends on the separation speed and acceleration during the takeoff run. In turn, the separation speed depends on the specific loading per 1 m^2 of wing area and $c_{y\ sep}$, while the acceleration depends on the excess thrust available.

A decrease in specific loading on the wing is the most effective method of decreasing V_{sep} and L_{tor}. However, this always involves a decrease in the useful weight carried, since with the surface area of the wing constant, a decrease in takeoff weight can be achieved only by decreasing the useful load. A decrease in the weight carried in a passenger aircraft means a decrease in operational economy. Therefore, this means of decreasing the takeoff run length is used to a limited extent, particularly since the tendency to use the maximum possible flight range requires an increase in specific loading on the wing.

The most acceptable method of decreasing the takeoff run length is an increase in the lifting force of the wing using the wing mechanisms.

As we know, the main means of mechanization of the wing consists of the flaps. All modern jet passenger aircraft have extendable (sliding) slit type wing flaps[1]. The effectiveness of the flaps (magnitude of increase in Δc_y) increases as the slide (outward movement) of the flaps and angle of flap deflection are increased. With low angles of flap deflection, the lifting force is primarily increased without any essential increase in drag, and the aerodynamic quality is decreased only insignificantly. These angles can be used for takeoff during high temperature conditions, when the length of the takeoff run can be retained within the required limits in spite of the decrease in quality. The lower drag during the takeoff run allows a considerable acceleration to be achieved.

Usually, attempts are made to produce the maximum aircraft aerodynamic quality with the flaps deflected to the takeoff position, since the quality determines the thrust consumed and the excess thrust which accelerates the aircraft during the takeoff run. For aircraft with takeoff weights of 55-80 and aerodynamic quality of 12-14, a thrust of consumption of 5000-6000 kg is required, and with a total available thrust of 13,000-28,000 kg, the excess thrust provides rapid (25-30 sec) acceleration of the aircraft to the separation speed; the takeoff run length is 1000-1200 m. /107

Long experience of passenger aircraft operation has proven the usefulness of the method of decreasing takeoff run length by increasing the available power (greater excess thrust). The Boeing 727 aircraft carries a

[1] S. M. Yeger, *Proyektirovaniye Passazhirskikh Reaktivnykh Samoletov* [Design of Passenger Jet Aircraft], Mashinostroyeniye Press, 1964.

three-slit flap (Figure 73) which, together with the slit type slat and Kruger slat (front flap) makes it possible to produce $c_{y\ max} = 2.7$ with the maximum angle of flap deflection. This in turn allows rather high values of c_y to be achieved with lesser angles of deflection, corresponding to the takeoff position of the flaps ($c_{y\ sep} = 1.6\text{-}1.8$).

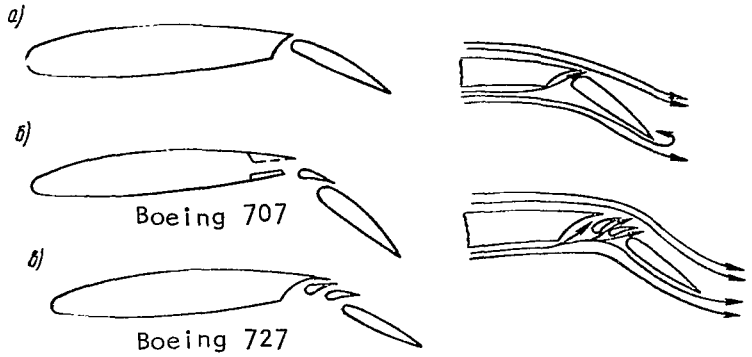

Figure 73. Diagram of Extendable Flaps: a, Single-slit (flow separation begins at $\delta_3 = 35\text{-}40°$); b, c, Multi-slit (flow separation delayed to δ_3 - 50-60°)

The multi-slit flap, due to the increase in curvature of the profile and the pumping effect of the slits, delays flow separation to larger angles of attack, which allows rather high values of c_y to be produced during takeoff and landing. The increase in the lifting force of the wing with flaps down results from a change in circulation around the wing with increasing flow speed over the upper surface of the wing.

However, at large angles of attack, flow separation at the upper surface begins at the front of the wing profile, which is combatted using front slats or deflectable leading edges of the wing. Slit type slats (Figure 74, a), which allow air to flow through the front slit, intensify the boundary layer behind the peak of rarefaction on the wing profile and increase the energy of the flow, so that separation of the flow is delayed at high angles of attack.

When Kruger slats are opened (Figure 74, c) the effective aerodynamic curvature of the provile is increased in the front portion, as a result of which the load-bearing characteristics of the profile are improved. Since /108
this increases the suction force pulling forward, the drag of the wing with the front slat open increases only slightly, and the aerodynamic quality of the wing remains essentially unchanged.

The same effect can also be achieved by tilting the forward edge of the wing downward (Figure 74, b).

Thus, there is a rather large number of methods of increasing c_y and, consequently, decreasing the separation speed and length of the aircraft takeoff run.

One promising method is the usage of the gas streams from the jet engines. Experiments have shown that if the gas stream is directed downward, it can supplement the lifting force of the wings. As a result, the aircraft can be separated from the earth almost without a takeoff run. During the landing, this same gas stream carries a portion of the flying weight of the aircraft and allows the aircraft to be landed at low speeds.

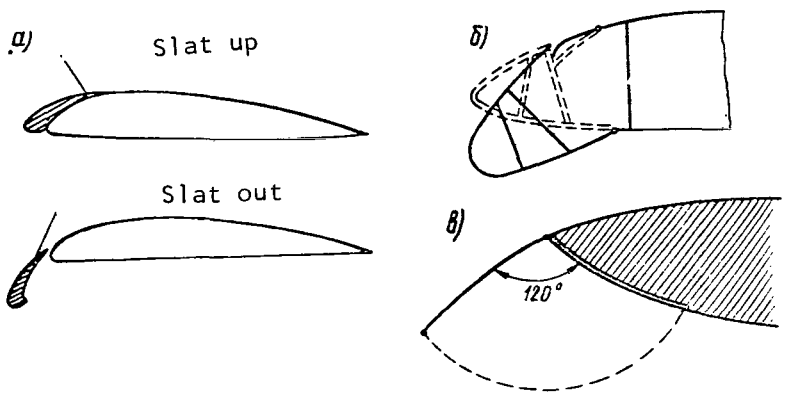

Figure 74. Diagram of Slit Type Front Slat (a), Deflectable Front Portion of Aircraft Wing of "Trident" Aircraft (b) and Kruger Front Slat (c)

The reaction flap (Figure 75), a device consisting of a slit along the rear edge of the wing through which a stream of air flows at a certain angle β to the chord, driven by the compressor of the jet engine, is quite important for heavy transport aircraft. This device changes the nature of flow around the wing, causing a significant increase in lifting force. The value of c_y increases due to the pumping of gas jets in the boundary layer from the upper surface of the wing and the reaction of the outflowing gas stream. The force of the reaction of the stream is divided into components N_y and N_x. The component N_y increases the lift of the wing, while N_x produces additional thrust. The lifting factor of a wing with a reactive flap is equal to the sum of the lift factors of the aerodynamic effect of the flow over the wing and from the reaction of the outflowing gases. /109

The usage of the reactive flap allows a broad range of flight speeds to be used and simplifies the problem of takeoff and landing.

Systems are known for controlling the boundary layer, which either remove or inject air. As we know, flow separation of the wing due to an increased boundary layer thickness decreases coefficient c_y. By using removal or injection in the boundary layer, the beginning of separation can be delayed to higher angles of attack, which makes it possible to increase the lift of the wing, decrease the takeoff and landing speed of the aircraft and reduce the takeoff and landing run length (and consequently the length of the runway). For example, a boundary layer blowing device decreases the landing speed by 20-25%. This type of boundary layer control system (BLAC) was used on the C-130C "Hercules" heavy turboprop transport. With this system, the lifting force of the wing is increased more than when the boundary layer is drawn off by suction. Four gas turbine reaction engines located in two gondolas beneath the wing were used to supply compressed air to the system. The air is collected in the rear portions of the gondola and fed by four centrifugal compressors to a network of airlines (common system for wing and tail surface). Many small lines connect the main distributing line with a common collecting chamber, from which the air is ejected on the upper surfaces of the flaps and ailerons through slits. The landing speed of the aircraft was decreased from 170 to 110 km/hr, while the takeoff distance was reduced from 1280 to 853 m, and the landing distance was reduced from 427 to 250 m.

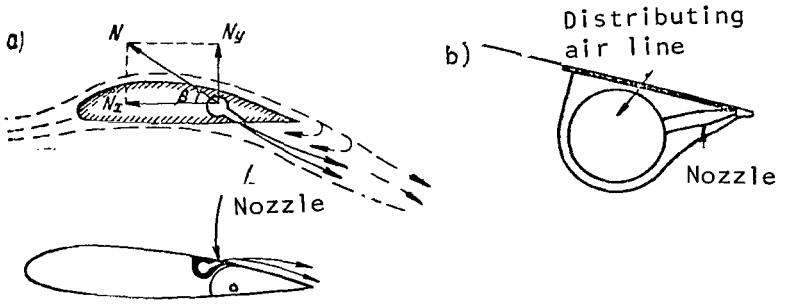

Figure 75. Reactive Flap on Wing (a) and Air Feed System for Boundary Layer Injection at Wing Surface (b)

A BLAC system is also installed on the English Blackburn NA39 "Buckaneer" military turbojet aircraft. The experimental Boeing 707 aircraft used a system for boundary layer injection in the area of the flaps using air taken from the engine compressors. During the tests, a decrease in landing speed from 220-240 to 150-160 km/hr was achieved, i.e., by approximately 30%. /110

Turbofan engines expand the possibility for using BLAC in passenger jet aircraft, since the removal of considerable masses of air from the outer channel does not disrupt the operation of the engine.

The placement of a slat on the front edge of the wing and injection of the boundary layer at the flaps and ailerons can produce a considerable decrease in landing and takeoff speeds and allow the length of runways to be decreased by 30-40%. The placement of a slat on the wing of a jet aircraft, in addition to decreasing takeoff and landing speeds, also improves its maneuverability at high speeds, since it delays the point of flow separation to higher angles of attack. Practice has shown that slats can be used up to M = 0.9.

A laminar flow control system is in the stage of development. It has been experimentally established that the transition of laminar flow to turbulent flow can be prevented by sucking the slow, turbulization-inclined boundary layer away from the wing surface through a large number of thin slots cut in the wing covering. This is called laminar flow control. Investigations performed in the USA[1] have shown that this method can increase the profile drag coefficient of a swept wing to a value near the drag coefficient of a plate with laminar flow, i.e., decrease it by approximately six times.

Laminar flow control by sucking away the boundary layer, naturally, increases the load-carrying capacity of the wing. However, the usage of lfc to increase c_y alone is not expedient, since this problem can be more simply solved by injection into the boundary layer. The production of high aerodynamic quality (increased by a factor of 1.5 times) both during takeoff and during flight, allows the takeoff and other characteristics of the aircraft to be improved. Calculations have shown that for an aircraft like the Lockheed C-141 with a takeoff weight of about 120 t and a cruising speed of 850 km/hr, laminar flow control can increase the flight range by 30-33%. With this flight range, the takeoff weight of the aircraft can be decreased by 18-20% by decreasing the fuel reserves carried.

In conclusion for this chapter, we note that an improvement of takeoff (as well as landing) characteristics of passenger jet aircraft -- decreased takeoff run length and separation speed -- makes it possible to expand the network of airfields and connect area and administrative centers. It is always easier to find areas for small airfields than for large airfields. /111
Better takeoff and landing characteristics of aircraft will also provide a lower "minimum weather" (see Chapter IX, §8).

At the present time, considerable attention is being turned to the creation of special passenger jet aircraft with short takeoff and landing characteristics.

[1] S. M. Yeger, *Proyektirovaniye Passazhirskikh Reaktivnykh Samoletov* [Design of Passenger Jet Aircraft], Mashinostroyeniye Press, 1964.

Chapter VI. Climbing

§1. Forces Acting on Aircraft

Climbing refers to straight and even (constant velocity) flight of an aircraft in an ascending trajectory. During the climb, the forces acting on the aircraft include the force of gravity G, the force of the thrust P, lifting force Y and drag Q (Figure 76). /111

Forces Y and Q are arbitrarily considered to be applied to the center of gravity of the aircraft, although they are actually applied at the center of pressure. This arbitrariness is permitted for forces Y and Q, since the aircraft is balanced by deflection of the elevator. Force P for simplicity of discussion will be considered to be applied through the center of gravity. The direction of the effect of the forces is as follows: force G acts vertically downward, force P -- forward at a certain angle β to the direction of flight, force Y -- perpendicular to the direction of flight and force Q -- opposite to the direction of flight.

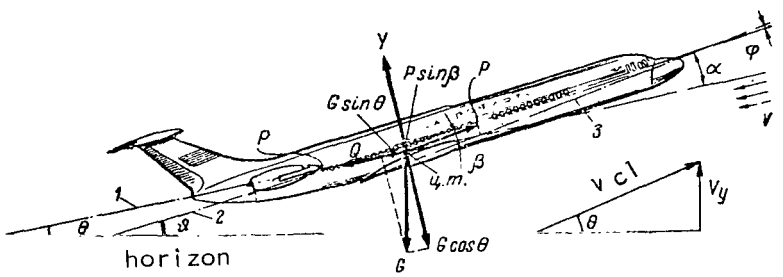

Figure 76. Diagram of Forces Acting on Aircraft in Stable Climb: 1, Climb trajectory; 2, Longitudinal axis of aircraft; 3, Chord of wing

The flight trajectory of the aircraft is inclined to the horizontal at a certain angle Θ, called the climbing angle. The following dependence exists between the pitch angle ϑ, the climbing angle Θ, angle of attack α and angle of wing setting (angle included between longitudinal axis of aircraft and wing chord): $\vartheta + \phi = \Theta + \alpha$. For modern aircraft, angle ϕ = 1-3°, angle α = 2.5-5°, the pitch angle (the angle included between the axis of the fuselage and the horizontal) in flight can be determined using the gyrohorizon. During a climb, the climbing angle is less than the pitch angle. /112

Force P does not correspond to the flight trajectory, forming with it a certain angle β. The magnitude of this angle is influenced by the angle of motor setting relative to the longitudinal axis of the aircraft. As we explained earlier (chapter 4, §8) the angle of motor setting may be from zero to five degrees. Angle β can be determined as follows. Let us analyze the climb during the first moments after takeoff. Let us assume that force P forms an angle of 5° with the longitudinal axis of the aircraft, the velocity in the climb is 520 km/hr, and the vertical speed is 16 m/sec. The climbing angle can be determined as follows (Figure 76):

$$\sin\Theta=\frac{V_y}{V_{c.t}}=\frac{16}{144.2}=0.1108,$$

i.e., $\Theta \approx 6.5°$. Then pitch angle $\vartheta = \Theta + \alpha - \phi = 6.5° + 3° - 1° = 8.5°$ (we assume $\alpha = 3°$ for $V_r = 520$ km/hr, and the angle of wing setting $\phi = 1°$). Since the difference between angles ϑ and Θ for this case is 2°, force P corresponds to the climbing trajectory, angle $\beta = 7°$. In this case, the component P sin β is added to the lifting force. The magnitude of this component may be rather high. For the quantities here being analyzed in an aircraft with four motors with a thrust of each motor of 8,000 kg, we produce P sin $\beta = 32{,}000 \cdot 0.122 = 3900$ kg. This force is added to the lift Y = 80-85 t.

As the altitude increases, the vertical speed decreases, but the true velocity in the climb increases. Therefore, the lift angle is continually decreased. We can therefore write the following two equations for a stable climb:

$$Y=G\cos\Theta;$$
$$P=Q+G\sin\Theta.$$

We can see from the first equation that the lift during a climb equalizes only a portion of the weight of the aircraft. The other portion of the aircraft weight (G sin Θ) is balanced by the motor thrust. For example, for an aircraft weighing 38 t with a climbing angle $\Theta = 7°$, component G sin $\Theta = 38{,}000 \cdot 0.122 = 4630$ kg, and for an aircraft weighing 80 t this figure is 9770 kg.

If the available engine thrust for an aircraft with a takeoff weight of 38 t is 6700-7000 kg in the nominal operating mode (near the earth), more than one half of this thrust is expended to balance the weight of the aircraft, while the remaining thrust is expended in overcoming drag. The climbing angle Θ can also be determined from the second force equation:

$$\sin\Theta=\frac{P-Q}{G}=\frac{P}{Q}-\frac{Q}{G}=\bar{P}-\frac{1}{K},$$

/113

where P - Q = ΔP is the excess thrust; $\bar{P}$ is the thrust factor of the aircraft: the ratio of engine thrust to aircraft weight; Q/G is a quantity inverse to quality.

At climbing angles of 6-8°, the value of cos Θ ≈ 1, and the first equation can be written as follows:

$$Y=G\cos\Theta\approx G.$$

In order to determine angle Θ, we must use the Zhukovskiy curves for consumed and available thrust. Figure 77 shows the definition of ΔP_{max}, at which the maximum climbing angle is achieved. The maximum excess thrust is produced at the most favorable flight velocity, corresponding to the maximum aerodynamic quality of the aircraft and the steepest climbing angle. For aircraft with specific loads of 350-370 kg/m^2, the most suitable speed is 360-370 km/hr, for specific loads of 500-550 kg/m^2 -- 400-450 km/hr. The excess thrust produced under these conditions at nominal engine operation will provide a climbing angle Θ = 6-8°.

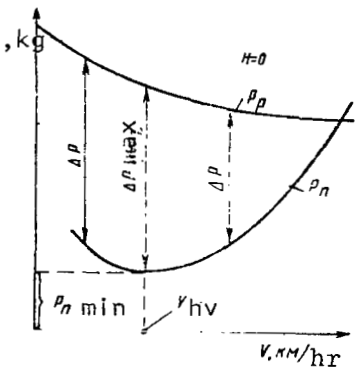

Figure 77. Determination of Maximum Excess Thrust Using Zhukovskiy Curves

§2. Determination of Most Suitable Climbing Speed

The vertical speed in a climb is determined by the formula $V_y = V \sin\Theta$. Replacing sin Θ with the excess thrust and weight (we know from aerodynamics that ΔP/G = sin Θ, we produce

$$V_y=\frac{V\Delta P}{G}\ \text{m/sec}$$

In order to produce the maximum rate of altitude increase (since it is this quantity, not the climbing angle which is of the greatest practical interest), we must know the maximum value of the product ΔPV, which represents the excess power: ΔN = ΔPV.

For turbojet aircraft, the maximum values of the product ΔPV kg·m/sec is determined, and the vertical velocities are calculated (Figure 78).

If we have the maximum values of the product $\Delta PV/3.6$(kg·m/sec), we can determine the maximum V_y for various weights. /114

The velocity along the trajectory at which the maximum rate of altitude increase is achieved is called the climbing speed V_{cl}. It is higher than the speed at steepest climb which, as we showed in the preceding paragraph, corresponds to the most suitable aircraft velocity (maximum quality).

The climbing speed can be easily determined also using Zhukovskiy curves for power consumed and available (Figure 79) (the available thrust power was analyzed in Chapter IV,§7, and the graph of power consumption for various flight altitudes is constructed like the graph for thrust consumed). In order to do this, we must draw a tangent parallel to line N_p of power to the curve for power consumed. At the point of contact, the excess $\Delta N_{max} = P\Delta V$ and velocity corresponding to this excess power are determined.

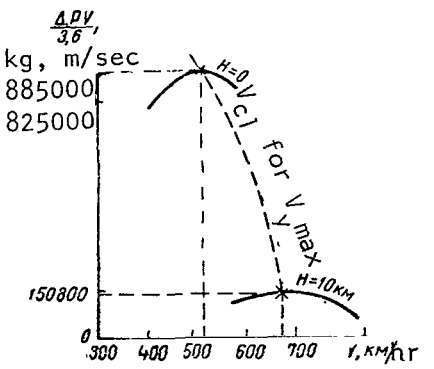

Figure 78. Excess Power As a Function of Flight Velocity (G_{tl} = 52 T, specific load 390 kg/m^2)

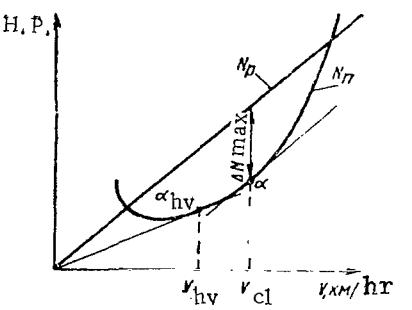

Figure 79. Zhukovskiy Curves for Power

For aircraft with wings swept at 30-35°, the maximum rate of altitude increase is produced for practically all takeoff weights (from the maximum permissible to the minimum with small commercial load) is produced at indicated speeds of 480-550 km/hr at the earth. This speed must be maintained up to 5000-6000 m. If this is done, the maximum rate of altitude increase will be achieved at all altitudes. As the altitude increases, the true flight speed will increase (for example at H = 6000 m and V_{ind} = 520 km/hr, V_{tr} = 700 km/hr).

Many flying investigations have shown that in order to retain maximum vertical speed, the indicated speed must be decreased beginning at 6000-7000 m by an average of 15-20 km/hr per 1000 m. Figure 78 shows that the product ΔPV has a smoothly sloping upper portion in the zone of maximum values, so that a deviation of the indicated climbing speed of ±20 km/hr from the most favorable value (pilot error) changes the vertical speed insignificantly, and the time to climb and fuel expenditure over the climb remain practically unchanged from the most favorable values. /115

The maximum vertical speeds of aircraft with two and three motors are 17-25 m/sec (at the earth), decreasing with increasing altitude to 8-10 m/sec at 8000-9000 m. For aircraft with four motors, the vertical speeds are 12-15 m/sec at low altitude and 5-8 m/sec at high altitudes. The greatest decrease in vertical speeds is observed at altitudes of over 10,000 m. The flight altitude at which the vertical speeds equal 0.5 m/sec corresponds to the practical ceiling of the aircraft. The height of the practical ceiling of a passenger aircraft is 12,000-13,500 m. The height of the practical ceiling (without consideration of maneuvering in the area of the airfield after takeoff) can be reached by an aircraft in 43-45 min.

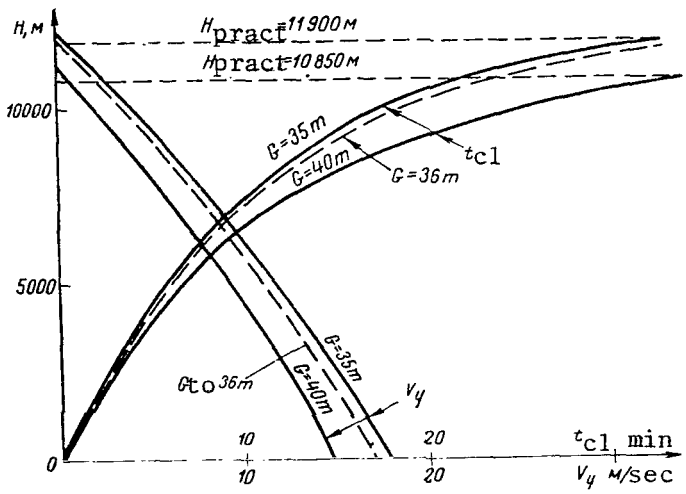

Figure 80. Vertical Speed and Time of Climb for An Aircraft with Two Motors (nominal mode, power factor P = 0.3)

Climbing at the nominal engine mode is the most economical (Figure 80), since the maximum difference between available and consumed power is produced, and the specific fuel consumption will be near minimal. A decrease in the operating mode of the engines in a climb leads to an increase in specific fuel consumption, a decrease in available power and rate of altitude increase of the aircraft, an increase in climbing time, and as a result an increase in the total fuel expenditure required to perform the climb. A modern passenger /116

aircraft reaches an altitude of 10,000-11,000 m in 18-25 min, covering 200-250 km and expending 2000-4000 kg of fuel (the higher values correspond to three- and four-motor aircraft).

§3. Velocity Regime of Climb

Climbing at the maximum rate of altitude increase is most economical. In this case, up to 10,000-11,000 m the climb occurs at an indicated speed of 460-440 km/hr (with corresponding lower true velocity), and upon reaching the indicated altitude the pilot accelerates the aircraft at the nominal regime to an indicated speed of 500-550 km/hr in 4-5 min for subsequent horizontal flight at the maximum cruising regime. Thus, acceleration of the aircraft at these altitudes, where the excess thrust is slight, requires additional time. Operational tests of many turbojet passenger aircraft have shown that at times it is more expedient (from the point of view of cost) to climb to altitude in the so-called high speed regime.

To do this, the aircraft is turned in its final flight direction, then accelerated to an indicated speed of 600-670 km/hr and the climb is performed at this speed until the air speed reaches 800-880 km/hr (according to the thin needle). At this point, the rate of altitude increase of the aircraft is decreased to 12-14 m/sec, while the indicated speeds are considerably higher than the most favorable speed.

When an air speed of 800-880 km/hr is reached, further climb is continued at this speed. The rate of altitude increase decreases to 2-3 m/sec as altitudes of 10,000-11,000 m are reached. The aircraft arrives at its assigned altitude with sufficient true velocity, so that almost no additional acceleration is required. After the transition to horizontal flight, the cruising operating regime of the motors is instituted.

Climbing at the high speed regime decreases the duration of the flight, but increases slightly the fuel expenditure. The problem is that as speeds of 600-880 km/hr are maintained, the vertical speed is decreased at all altitudes and the time which the aircraft spends at low altitudes is increased, leading to an increase in fuel expenditure in the climb. Therefore, the high speed climb method is generally recommended for flights over short distances, 50-60% of the maximum range of the aircraft with full fuel load. The additional /117
fuel expenditure in these flights requires no decrease in commercial load.

The distance which the aircraft travels in the horizontal direction during the climb in the high speed regime is 50-100 km greater than during the climb at maximum rate of altitude increase. The polar curve on Figure 81 characterizes these two climbing methods. As we can see from the figure, the vector corresponding to the speed of 500 km/hr is directed more steeply upward, corresponding to vertical speeds of 15-17 m/sec, while at 650 km/hr the vertical speeds produced are less, but the horizontal range is greater.

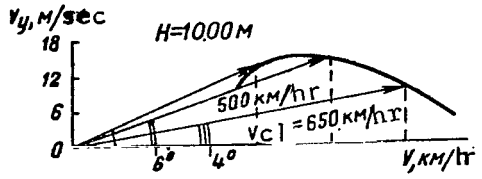

Figure 81. Polar Curve of Climbing Speeds

§4. Noise Reduction Methods

The noise of turbojet passenger aircraft is caused by: oscillations of cold air flowing around the aircraft and mixing of the cold air with the pulsating, hot gas jets from the engines and oscillations of air compressed in the compressors of the engines.

The frequency spectrum of this noise is significantly different from the noise created by piston and turboprop motors. Whereas the noise spectrum of turboprop engines is characterized by high sound pressures in the low frequencies, the noise spectrum of turbojet engines contains predominantly high frequency sound. This makes the noise created by a turbojet engine more unpleasant to human hearing. The noise created by an ordinary turbojet at over 35% thrust is greater than the noise resulting from the efflux of the jets.

The usage of two circuit turbojet motors allows the noise level to be decreased during takeoff by 8-10 db (decibels), although the noise level is still quite high. Existing engineering methods of noise reduction -- dampers at the input pipes (JT8D engine) and exhaust nozzles (JT3D and Conway engines, etc.) are not effective, and decrease the noise very slightly. For example, a muffler on the output nozzle consisting of nine tubes decreases the noise level by 5.5 db, but also decreases the efficiency of the engine. Installation of perforated sheets and a screen around the air intake also provide some decrease in noise level at the input to the compressor or fan.

Therefore, in order to decrease the noise to the required level (at high power, the noise from the turbine and exhaust jet, at low power -- from the compressor), special methods of piloting after separation and during landing must be used. As we know, foreign aircraft (the Boing 707, Caravelle, etc.) employ the so-called low noise takeoff and landing method (takeoff and landing using the steepest trajectories with engines throttled over listening check points), i.e., the decrease of noise at ground level is based on rapid removal of the noise source from ground level. The initial climb is achieved on steep trajectories at safe speed with decreased engine power. This is aided by improved engine design and high mechanization of the wing. /118

In order to determine the influence of the noise of an aircraft taking off on the population in the region of an airport, the quantity known as perceived noise level is often used. It has been established that the maximum permissible perceived noise level acting on the organs of hearing for several seconds $P_{N_{max}}$ = 112 PN db (here PN db is the unit of measurement of the noise). Noise levels over 112 PN db is said to be above the "tolerance limit" for man.

At many large airports in Europe and the USA, limitations have been placed on the noise created by aircraft taking off and landing. The apparatus measuring the noise level is placed directly beneath the flight path of the aircraft. If the maximum permissible noise level is exceeded, the airline companies are forbidden to continue operating the aircraft.

Let us analyze the specifics of aircraft flight along a steep trajectory. As we can see from the formula $\sin \Theta = V_y/V$, in order to produce the maximum angle Θ, we must provide a combination of vertical speed and speed along trajectory such that the value of $\sin \Theta$ is maximal. Flight tests are usually performed to determine the steep climbing speed, during which the flaps are left down at low speeds after takeoff in order to increase flight safety. Therefore, the steep climbing speed is generally 40-50 km/hr higher than the separation speed and practically corresponds to maximum aircraft aerodynamic quality for the takeoff wing setting angle.

As is known, the flight regime with maximum trajectory inclination Θ corresponds to the maximum excess thrust ΔP and, consequently, the maximum value of $\sin \Theta$:

$$\sin \Theta_{max} = \frac{\Delta P_{max}}{G}.$$

Therefore, if the most favorable aircraft speed (K_{max},Θ_{max}) is about 350-360 km/hr for flaps up, due to the placement of the flaps in their landing position, this speed is decreased to 300-310 km/hr. The climb after takeoff on the steep trajectory is performed at the most favorable speed with flaps down. /119

During testing of one aircraft, the following method was developed for steep climbing (Figure 82). With flaps down in the takeoff position (10°), V_{sep} = 260 km/hr. After separation, at an altitude of 5-10 m, the landing gear was raised and the speed increased to 300 km/hr (at 50-60 m). The climb was continued to 300 m at this speed with the motor operating in the takeoff mode, after which the motor was shifted to the nominal regime. Whereas the climbing angle of the trajectory at the takeoff regime Θ = 8-9°, at the nominal regime it is decreased to 6.5-7°. At an altitude of 500 m, the aircraft was decelerated by decreasing the vertical speed and the flaps were raised. The flight was performed at a pitch angle of 14-16°.

During the landing, it is impossible to reduce noise by increasing the steepness of the gliding trajectory, since the rate of descent is fixed by the operating conditions of the landing system. However, since the engines are operating at reduced power, the initial noise level is decreased.

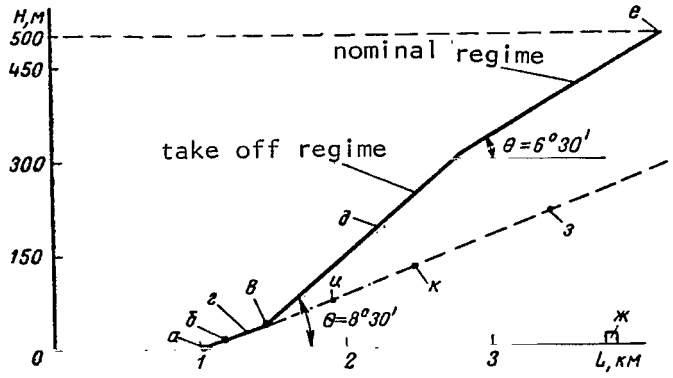

Figure 82. Optimal Climbing Trajectories for Noise Reduction at Ground Level: a, Separation, V = 260 km/hr; b, Beginning of lifting of landing gear; c, Landing gear up; d, Acceleration to V = 300 km/hr; e, Flight sector at V = 300 km/hr; δ_3 = 10°; f, Beginning of acceleration for raising of flaps; g, Listening point; h, Flight trajectory with continuous acceleration; i, Point of beginning of lifting flaps; j, End of lifting of flaps

The influence of noise from an aircraft taking off is particularly noticeable if there is a populated point along the flight path at less than 4-5 km from the starting point of the aircraft. In such cases, tests must be made to determine under which conditions and operating modes of the engines permissible noise levels can be provided (in particular, 110-112 PN db for takeoff during the day and 102 PN db at night, the "tolerance limit" for noise being considerably lower at night). The nomogram on Figure 83 is /120 constructed from the results of flying tests on aircraft with two engines with maximum takeoff weight under standard conditions of 38 T. The sloping lines of the nomogram are the trajectories in steep climb situations.

The zero point on the nomogram corresponds to the beginning of the aircraft takeoff run. On the right we have a table of operating regimes of the engines and the corresponding noise levels perceived on the ground. The dotted line shows an example of determination of the altitude of change in engine operating regime and the necessary regime during takeoff of an aircraft weighing 38 T when the edge of a populated point is located 3.3 km from the beginning of the takeoff run (the takeoff is performed during the day, standard conditions, no wind). To do this, we draw a line from point A, corresponding to a distance of 3.3 km, upward to the point of intersection with the 38 T weight line (point B), then draw a horizontal line. Point C determines the altitude (230-240 m) at which the operating regime of

the engines must be reduced to 88-89% (point D), corresponding to the maximum permissible noise level for daytime, 112 PN db. If the regime is not changed, the noise level is 117 PN db (point D).

After flying over the populated point or an increase in altitude of 500 m, the engines must be shifted to the nominal operating regime.

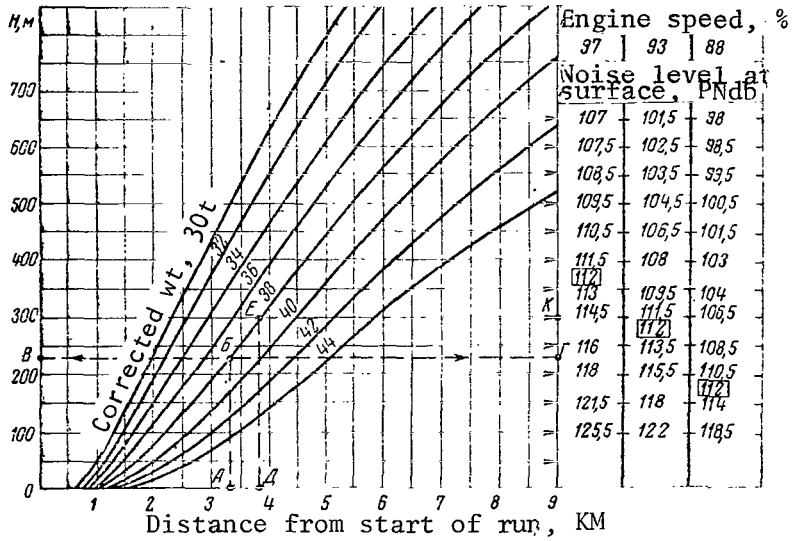

Figure 83. Nomogram for Determination of Altitude of Change in Operating Regime of Motor (conditions of initial climb: V_{ind} = 300 km/hr, n = 97%, δ_3 = 10°)

As we can see from the same nomogram, with the same aircraft, but with a separation distance to the populated point of 3.8 km (point E), it is sufficient to establish the nominal regime (point I) and maintain an altitude of 300 m (point F) in order to produce a noise level of 112 PN db in the daytime. /121

When the air temperature and pressure are changed or when there is a wind, special graphs must be used to determine the corrected aircraft weight, since the flying data change. These graphs change for each aircraft in the handbook on flying operations. For example, for the example above at t = +25°C, p = 760 mm Hg with a head wind component of 2 m/sec, the corrected weight $G_{cor} \approx 40$ t with an actual weight of 38 t. The increased corrected weight requires a lower altitude for the beginning of motor throttling. However, the decreased operating regime of the engines after raising the landing gear is not permitted at an altitude of less than 150 m.

In conclusion, we note that the flight speed during a steep climb to altitude with flaps down should provide a sufficient reserve against

separation. The aircraft speeds at which horizontal flight with sufficient controllability is possible is called the maneuvering speed; it must be 1.15 times the minimum speed corresponding to separation. For example, flying tests indicate a minimum speed of 200 km/hr, so that the maneuvering speed is 230 km/hr. The reserve against separation with a steep climb speed of 300 km/hr is 70 km/hr, and the reserve to stall is about 100 km/hr.

§5. Climbing with One Motor Not Operating

If the situation requires a pilot to fly to a reserve airfield after a motor failure on takeoff, with the reserve airfield located 350-400 km distance, a climb must be performed. It will be shown in Chapter VII that the most favorable altitude for ranges of 300-400 km is 5700-6000 m; however, for flight with one motor not operating, the most favorable altitude is 2500-3000 m. An aircraft with a motor out, when climbing at the nominal regime, can attain a vertical velocity component of 3-6.5 m/sec at ground level. This speed decreases with altitude and at 4500-7000 m, the rate of altitude increase is about 0.5 m/sec. It is considered that at this point the aircraft reaches its practical flight ceiling with one motor not operating. For aircraft with three motors, the flight altitude with one nonoperating motor, naturally, is greater than for aircraft with two motors. The time to climb to this altitude is 45-50 min and depends strongly on the actual temperature of the surrounding air. The climbing speed in such cases is 70-100 km/hr less, explained by the decrease in available thrust of 30-50%, so that the maximum of product ΔPY is displaced toward lower values of indicated (as well as true) speed. It is recommended that as the altitude is increased, the indicated speed be decreased by 5 km/hr per 1000 m altitude. Transition of engines from nominal to takeoff regime increases the excess thrust and allows the rate of altitude increase of the aircraft to be increased temporarily, although the time of operation in takeoff regime is limited.

Chapter VII. Horizontal Flight /122

§1. Diagram of Forces Acting on Aircraft

Horizontal flight means straight line, stable aircraft flight without increase or decrease of altitude.

The forces acting on the aircraft were shown in chapter VI. We add that the total aerodynamic force R (equalizing forces Y and Q) is applied at the center of pressure, and is deflected from force Y by certain angle Θ (Figure 84). Inclination of force R is changed by the pilot by using the elevator, deflecting it enough so that force R passes through the center of gravity. Therefore, we will consider for horizontal flight, as for climbing, that all forces are applied to the center of gravity of the aircraft.

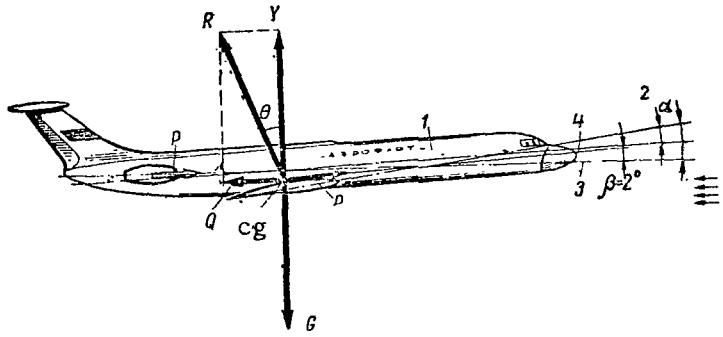

Figure 84. Diagram of Forces Acting on Aircraft in Horizontal Flight: 1, Longitudinal axis of aircraft; 2, Chord line; 3, Direction of aircraft; 4, Direction of thrust

As we know, in order to achieve stable horizontal flight, it is necessary that the following equation be fulfilled:

$$G=Y+P\sin\beta;\ Q=P\cos\beta.$$

These equalities show the conditions of horizontal flight. The first equality shows that the movement of the aircraft is linear and occurs in the horizontal plane. The second is the condition of evenness of motion, i.e., flight at constant velocity. If this condition were not fulfilled, the flight would be /123 unstable (with acceleration or deceleration).

It was stated above that force P may make a certain angle with the chord of the wing. If we assume as an average $\alpha = 3°$, the wing setting angle $\phi = 1°$ and the motor setting angle (in the tail portion of the fuselage) is zero, as we see from Figure 84 angle $\beta = 2°$. Therefore, the force P cos β will be less than force P. In practice, with angle $\beta = 2\text{-}7°$, the value of cos β differs little from unity, so that it can be considered that Q = P. We can also consider that Y = G, since we can ignore the component P sin β, which for cruising thrust values will be less than one percent of the mean flying weight. For example, with an average flying weight of 70 t and a quality of 14, the required thrust P_r = 5000 kg, and P sin 2° = 5000·0.035 = 175 kg, i.e., 0.25% of the average weight. Even if $\phi_{en} = 5°$ (with engines in the rear portion of the wing) and $\alpha = 3°$ and $\beta = 7°$, with the same P_r = 5000 kg we produce P sin 7° = 5000·0.122 = 610 kg. This is 0.87% of the weight of 70 t.

§2. Required Thrust for Horizontal Flight

An aircraft is capable of performing flight at various angles of attack within the speed range from the minimum to the maximum, i.e., at various regimes. Each of these regimes corresponds to a certain air speed (angle of attack), providing the lifting force equal to the weight of the aircraft. This velocity has come to be called the required velocity for horizontal flight, and the thrust necessary for the performance of horizontal flight at this angle of attack is the required thrust for horizontal flight. Thus, in horizontal flight a given angle of attack corresponds to a definite required velocity and thrust. In order to calculate the graphs of required thrust on Figure 85, a graph of the dependence $c_y = f(\alpha)$ and the polar curve of the aircraft with a wing without geometric twist is used. The calculation was performed in the following order: the required thrust in horizontal flight is set equal to the drag: $P_r = Q$. Setting various flight speeds, we determine for each of them the impact pressure and c_y; using the polar curve (for various M numbers) we find the value of c_x corresponding to these speeds. Using the formula $P_r = Q = c_x S\rho(V^2/2) = c_x Sq$, we determine the required thrust.

As we can see from Figure 85, with the most favorable angle of attack $\alpha_{hv} = 6°$ and H = 0, we produce the minimum required thrust, corresponding to the most favorable speed of 360 km/hr and quality K = 15 (from the formula $P_r = G/K$ we produce $K = G/P_r = 35{,}000/2330 = 15$). An increase or decrease in speed leads to an increase in required thrust, since with angles of attack greater than or less than 6°, the aerodynamic quality decreases. /124

For flight at 360 km/hr near the earth the motors must be throttled back so as to achieve equality $P_p = P_r$. In this case, the curve of available

thrust touches the curve of required thrust at point B, corresponding to $\alpha = 6°$. As we can see from Figure 85, for flight with lower speed (V = 300 km/hr) as well as for flight with higher speed (600 km/hr), an increase in engine thrust is required (points C and A).

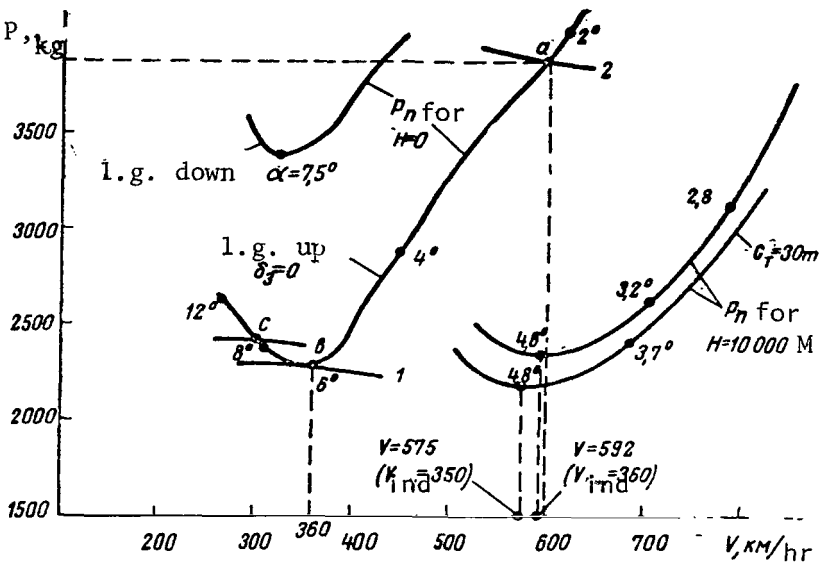

Figure 85. Required Thrust As a Function of Flight Speed (flying weight 35 T): 1, Thrust for flight with V_{hv} = 360 km/hr; 2, Thrust for flight with V = 600 km/hr
1.g. = landing gear

We know that for aircraft with turbojet engines, the maximum excess thrust corresponds to the most favorable speed and, in the example here analyzed V_{hv} = 360 km/hr. In order to achieve ΔP_{max} at the takeoff or nominal regime, an indicated flight speed of 360 km/hr must be maintained.

As the flying altitude is increased (for the same weight, in our example 35 t), the required thrust remains unchanged if the quality is the same. In practice, however, as the indicated speed is retained, K_{max} decreases slightly with increasing altitude (by 0.4-0.6), so that P_r is somewhat higher. In our example (Figure 85), the indicated speed of 360 km/hr at 10,000 m corresponds to a true speed of 592 km/hr (M = 0.5) and a maximum quality of 14.5, i.e., the quality is decreased by 0.5. The angles of attack corresponding to K_{max} are also different for different altitudes due to the influence of the M number on the polar curve of the aircraft. For example, for H = 0, the angle of attack corresponding to the minimum required thrust is 6°, and for H = 10,000 m -- 4.8°. /125

A decrease in flying weight results in a decrease in required thrust for the same angles of attack (and therefore, for the same altitudes). As we can see on Figure 85, at H = 10,000 m for G = 30 t, the minimum P_r is less than the minimum P_r for G = 35 t, and also the speed corresponding to the minimum required thrust is less -- 575 km/hr (V_{ind} = 350 km/hr).

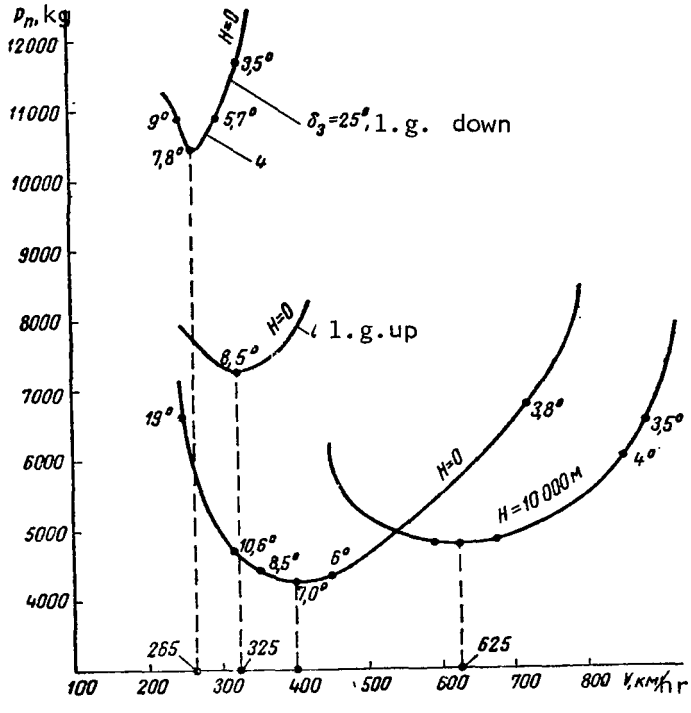

Figure 86. Required Thrust As a Function of Flight Speed (aircraft with three engines)

If we construct curves of required thrusts for aircraft with high weight and specific load (for example with G = 80 t and G/S = 432 kg/m^2), the most favorable speed is increased to 400 km/hr at H = 0 and 625 km/hr at H = 10,000 m (Figure 86).

In order to calculate the curves on Figure 86, we used the dependence $c_y = f(\alpha)$ and the polar curve of the aircraft shown on Figures 16 and 27. The increased α_{hv} is explained by the geometric twist of the wing, about 3°. For /126 clarity, Figure 86 shows the required thrust as a function of flight speed for an aircraft with landing gear and flaps down, when the required thrust is increased due to the decreased quality.

§3. Two Horizontal Flight Regimes

The points of intersection of the curves of required and available thrust correspond to the equality $P_r = P_p$; consequently, forces P and Q, as well as Y and G will also be equal. On Figure 85 for H = 0, these points are marked by the letters a, b and c. Due to the specific features of piloting during transition from one velocity to another, these points differ considerably. For example, at point a the transition to a different speed requires simpler control than at point c. Thus, in order to increase the speed to over 600 km/hr, acceleration must be performed by increasing the thrust (P > Q). In order to decrease the speed, the available thrust should be decreased, since the required thrust in horizontal flight in this case is less than for 600 km/hr. However, in order to move to a different speed at point c, for example, in order to increase thrust over 300 km/hr, the control stick must be pushed forward to transfer the aircraft to a lower angle of attack and, in order to maintain the same flight altitude, the thrust must be initially decreased, then the necessary regime set when the speed begins to increase. The same thing must be done to decrease the flight speed: the thrust must be temporarily decreased, then once more increased, since a decrease in speed causes an increase in required thrust.

Point a corresponds to the first flight regime, point c to the second. The main peculiarity of the second regime is the necessity of double action with the control lever of the motor when flight speed is changed. Therefore, flight should not be performed in the second regime, since it decreases controllability and makes flow separation on the aircraft wing possible.

The boundary between the first and second flight regimes is the most favorable angle of attack for a turbojet aircraft (for a piston powered aircraft it is the most economical). Whereas flights in the second regime had no practical significance for piston powered craft, since flights at angles of attack greater than the economical angle of attack were almost never performed since α_{ec} was near the maximum permissible angle of attack, flights of jet aircraft (particularly at altitudes near the practical ceiling) may occur at regimes near the most favorable.

The established minimum permissible operating speed on the basis of the values $c_{y\ per}$ is usually 50-70 km/hr less than the most favorable speed. We should note that in the following in our analysis of examples we will not consider altitude limitations related to the flying weight of the aircraft (see §8 of this chapter).

In the examples on Figures 85 and 86, the division between the two flight regimes at low altitude consists of the most favorable speeds of 360 km/hr and 400 km/hr. In horizontal flight with V_{hv} the motors must be throttled back so that flight occurs at speeds corresponding to the point of contact of the curves of available and required thrust (on Figure 85, point b). As the flying weight is decreased, the most favorable speed decreases; for example, /127

at 30 t, V_{mf} = 350 km/hr indicated (Figure 85).

Lowering the landing gear and flaps displaces the boundary between first and second regimes considerably toward lower speeds (Figure 86). For example, with flaps down the speed decreases to 325 km/hr (α_{mf} = 8.5°) and with flaps down 25°, to 265 km/hr (α_{mf} = 7.8°). As a rule, the aircraft is brought in for a landing in the first regime.

In order to avoid transferring to the second regime with the aircraft wing mechanics in the takeoff and landing position, the pilot must recall the indicated speed corresponding to the boundary between the two flight regimes.

§4. Influence of External Air Temperature on Required Thrust

As was noted, a change in the temperature of the surrounding air leads to a change in engine thrust (chapter VI,§6). Also, temperature of the surrounding air influences the nature of the dependence of required thrust on flight speed, which appears as a displacement of the curve to the left (with decreasing t) or to the right (with increasing t) and influences the value of required speed for horizontal flight. The external air temperature does not influence the required thrust, since $P_r = G/K$, and $K = c_y/c_x$ depends only on the angle of attack. Let us analyze the reason why the curve $P_r = (V,t°)$ is displaced. We know that in horizontal flight with unchanging angle of attack (or c_y) at different temperatures the following condition should be fulfilled:

$$Y = G = c_y S \rho \frac{V^2}{2}.$$

As the temperature is decreased with constant pressure, the density of the air is increased. In this case, in order for equality Y = G to be fulfilled, the required horizontal flight speed must be decreased (c_y unchanged). As the velocities are decreased, the curves of required thrust will be shifted to the left. As the temperature is increased, on the other hand, the curves of required thrust are displaced to the right, since the required velocities increase (Figure 87).

As we can see from the figure, the same P_{rl} corresponds to a greater required thrust for a temperature 10° higher than the standard temperature, since for t_{st} we have V_{crl}, and for t_{st} + 10° velocity $V > V_{crl}$. /128

The curves of required thrust for conditions other than standard are calculated as follows. At first we find the air density under the new conditions. For example, when the outside air temperature is increased by 10° with pressure unchanged for H = 10,000 m, T = 223°K and p = 198 mm Hg, we produce

$T = 223 + 10 = 233°$, $\rho = 0.0473\ p/T = 0.0473 \cdot 198/233 = 0.0403\ kg \cdot sec^2/m^4$. This value of ρ, according to the standard table, is equivalent to a flight altitude of 10,300 m.

Then, fixing the flight speed, we determine c_y, then take c_x from the polar curve of the aircraft with various M (Figure 28). Using the formula $P_r = c_x Sq$, we determine the required thrust. In determining the M number, we base our calculations on the fact that at T = 233°K, the speed of sound a = 306 m/sec.

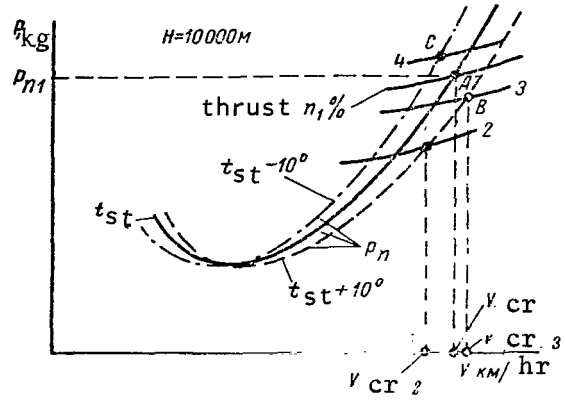

Figure 87. Influence of Surrounding Air Temperature on Required and Available Aircraft Thrust (specific loading 340 kg/m^2)

We must note that as the temperature is increased by more than 10°, the decrease in density (increase in speed) will be greater. For example, with $\Delta t = +30°$ at H = 10,000 m, the decrease in density is equivalent to an increase in flying altitude to approximately 11,000 m.

Let us now analyze the graphs of required thrust (Figure 87).

With standard temperature, in order to produce the velocity V_{cr1} at H = 10,000 m, we must use engine speed n_1%. At this speed, the available thrust will be equal to the required thrust (point A). As the temperature is increased by 10° (by 4.2% of 233°K), the curve of required thrust is displaced to the right, and the curve of P is displaced downward.

The available thrust, depending on the type and design of the motor, may be decreased by 5-8% (curve 2). The intersection of the curves of available and required thrust defines the speed V_{cr2} with unchanged engine operating regime. As we can see from the figure, the true flight speed has decreased, so that the M number is also decreased, since the speed of sound is not 300, but rather 306 m/sec ($M = V_{cr2}/306$). /129

Thus, as the air temperature is increased by 10°, the flying regime changes significantly. If we must maintain the previous M number (i.e., corresponding to t_{st}), we must increase the operating speed of the engines and, as we can see on Figure 87, set in engine speed n_3% (point B). The true flight speed increases and becomes $V_{cr3} = aM = 306\ M$.

If the pilot does not change the operating regime of the engines, as the flight speed is decreased from V_{cr1} to V_{cr2}, the angle of attack and c_y increase. Allowing the aircraft to fly at higher angles of attack is dangerous due to the approach toward $c_{y\ per}$ and the separation limit. Also, under relatively high temperature conditions, the vertical gust reserve is decreased. Therefore, in case such conditions are encountered, the rotating speed of the engine should be increased by an average of 5% for each 5-10° of increase in temperature, or if this is impossible, a lower flying altitude should be requested.

As the temperature decreases, the available thrust increases (curve 4) and the curve of required thrust is displaced to the left. The point of their intersection c defines the new flight speed.

§5. Most Favorable Horizontal Flight Regimes. Influence of Altitude and Speed

The flight range is the distance traveled by the aircraft during the climb, horizontal flight and descent. If flight is performed until the fuel is completely exhausted, the distance traveled is called the technical range. For passenger aircraft, the flight range given is usually that with one hour's fuel reserve if the flight schedule is maintained. (recommended regimes). Since there are various ways which the aircraft can leave the area of the airfield and climb after takeoff, the range of flight covered during the climb to assigned altitude changes significantly. However, the range covered during climb to altitude is relatively slight, so that in the following we will discuss the range of horizontal flight.

The range of the horizontal flight sector depends on the fuel reserve for horizontal flight and on the rate at which it is expended, i.e., the kilometer expenditure c_k -- the expenditure of fuel per kilometer of flight path. Before going over to horizontal flight, the aircraft must take off and climb. The fuel expenditure during the time of takeoff and climb to 9-11 km for two- and three-engine aircraft is 1600-4000 kg.

The fuel expended during takeoff and establishment of nominal flight regime (without consideration of climb) is 250-350 kg, the fuel expended during the descent and landing is 700-1000 kg. In order to determine the quantity of fuel to be used in the horizontal flight sector $G_{f\ hor}$, we must subtract from the quantity of fuel taken on board all supplementary expenditures and the navigational reserve. For example, with a takeoff weight of the aircraft or 44,000 kg and an initial fuel weight of 13,000 kg, 7000-7700 kg of fuel remain for horizontal flight at H = 10,000 m, since about 2000 kg are expended in takeoff and climbing, 800-1000 kg for descent and landing and 2500 kg are held as navigational reserve.

/130

For shorter range flights at the same altitude, the only change is in the quantity of fuel required for the horizontal sector, while the remaining fuel expenditure norms remain approximately unchanged.

The duration of horizontal flight is determined from the relationship

$$t = \frac{G_{f\ hor}}{c_h},$$

where c_h is the hourly fuel expenditure.

The hourly fuel expenditure is the quantity of fuel expended by the aircraft in one hour of horizontal flight. For example, for an aircraft with three engines with a required thrust of 6000 kg and a specific expenditure of 0.8 kg/kg·hr, the hourly rate is 4800 kg/hr.

The relationship between hourly and kilometer expenditures is established from the following considerations: in one hour of flight, the engines burn c_h kg of fuel. However, during this same time the aircraft covers a distance numerically equal to the flight speed V (in calm air). Therefore, the fuel expenditure per km is

$$c_к = \frac{c_h}{V},$$

where V is taken in km/hr. If V is taken in m/sec,

$$c_к = \frac{c_h}{3.6V}.$$

For V = 880 km/hr and c_h = 4800 kg/hr, we produce c_k = 5.46 kg/km.

Both the hourly and kilometer expenditures depend greatly on the specific expenditure of the engines c_p. The relationship between the specific and hourly expenditures is established as follows: for each 1 kg of thrust and one hour of engine operation, c_p kg of fuel are expended, while a thrust of P kg requires the expenditure of P times more fuel. Therefore,

$$c_h = c_P P \text{ kg/hr};$$
$$c_к = \frac{c_h}{V} = c_P \frac{P}{V} \text{ kg/km}$$

In Chapter IV we established that the specific fuel expenditure depends on the rotating speed of the engine, altitude and velocity of flight. /131

Let us now go over to an analysis of flight range. With identical fuel reserve within the limits of possible speeds, various ranges will be produced. For example, in the example outlined above with a fuel load of 13,000 kg, a takeoff weight of 44,000 kg, flight at 10,000 m with a true speed of 810 km/hr (M = 0.75-0.76) and an hourly fuel expenditure of 2500 kg/hr, in calm air a range on the order of 2800-3000 km can be produced. With flight at a high M number (V > 810 km/hr), the range is decreased to 2200-2500 km. Figure 88 shows a flight profile for an aircraft calculated for various horizontal flight speeds, which also illustrates the above.

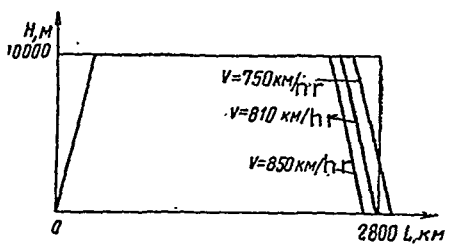

Figure 88. Characteristic Flight Profile of Aircraft to Range at Fixed Altitude

A head wind or tail wind changes the flight range.

Let us analyze the influence of flight speed on the hourly and kilometer fuel expenditures. We can explain this for flight at one and the same altitude, using the Zhukovskiy curves for required and available thrust (Figure 89).

In order to achieve horizontal flight at any given speed (V_{max}, V_1, V_2 and V_{mf}) it is required that $P_p = P_r$. This means that in order to fly at less than V_{max}, the engine must be throttled back so that the curve of P_p passes through points A_1, A_2 and A_3 respectively (Figure 89 a).

The hourly fuel expenditure $c_h = c_P P_p$, but since at any velocity of horizontal flight $P_r = P_p$, $c_h = c_P P_r$. /132

In order to decrease the flying speed, the rotating speed of the engine must be decreased. This results in an increase in specific consumption. However, as the flying speed is decreased, the value of $P_r = G/K$ is also decreased. Thus, as the engine is throttled back, c_p increases, but P_r decreases. The hourly expenditure will depend on the way in which c_p and P change. We find that as the flight speed is decreased, thrust P decreases more intensively than c_p increases. Therefore, c_h also decreases; the minimum

$c_{h\ min}$ will correspond to V_{mf}, at which $P_{r\ min} = G/K_{max}$. With $V < V_{mf}$, c_h begins to increase, since P_r increases. Consequently, the greatest flight duration at any altitude will occur when flying at the most favorable speed.

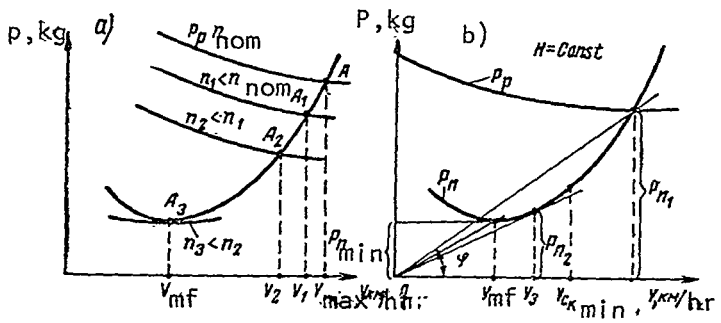

Figure 89. Explanation of Influence of Flight Speed on Hourly and Kilometer Fuel Expenditures

Let us explain how the flying altitude influences the hourly expenditure. In §2 of this chapter we showed that the required thrust is almost identical for the same weight at all flying altitudes up to 10,000 m. However, the required speed increases with altitude. Therefore, the curves of required thrust are displaced toward the area of higher speeds with increasing altitude (see Figure 85).

Since the available thrust of the engine decreases with altitude, the curves of the change in thrust with velocity are displaced downward with an increase in altitude. Therefore, whereas at low altitude the engines must be throttled back, thus considerably increasing the specific expenditure, at 10,000 m less throttling is required and the specific expenditure increases only slightly. When flying at the ceiling, the engines need not be throttled back at all. Therefore, as the flying altitude increases the product $c_p P_{r\ min}$ decreases, which explains the decrease in hourly expenditure. Also, the decrease in c_h with altitude facilitates a decrease in specific expenditure at constant operating speed. Therefore, the longest flight duration for an aircraft with a turbojet engine is produced near the ceiling. Flight duration at high altitude is 2-2.5 times greater than at low altitude. The regime of lowest hourly expenditure is used when flying in a holding pattern or with a strong tail wind (150-200 km/hr) in order to maintain the scheduled time of arrival.

Let us now analyze the way in which the selection of flight speed influences the kilometer expenditure. It was shown above that $c_k = c_h/3.6\ V$. Substituting the value $c_h = c_p P_r$ in this formula, we produce

$c_h = c$

$c_к = \frac{c_h}{V} =$

In Chapter IV we established that th
on the rotating speed of the engine, alt

Let us now go over to an analysis o
reserve within the limits of possible sp
For example, in the example outlined abo
takeoff weight of 44,000 kg, flight at 1
810 km/hr (M = 0.75-0.76) and an hourly
calm air a range on the order of 2800-30
a high M number (V > 810 km/hr), the ran
Figure 88 shows a flight profile for an
horizontal flight speeds, which also ill

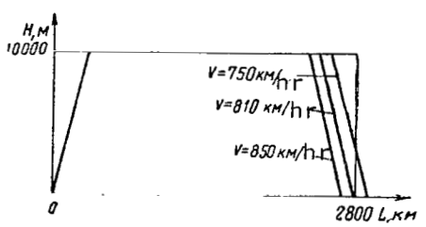

Figure 88. Characteristic Flight Profile of Aircraft to Range at Fixed Altitude

flig

flig
fuel
for
usin
and

at a

it i

that

the engine must be throttled back so tha

points A_1, A_2 and A_3 respectively (Figur

The hourly fuel expenditure $c_h = c_p$
horizontal flight $P_r = P_p$, $c_h = c_p P_r$.

In order to decrease the flying sp
must be decreased. This results in an
However, as the flying speed is decreas
decreased. Thus, as the engine is thro
decreases. The hourly expenditure will
change. We find that as the flight spe
more intensively than c_p increases. Th

If the pilot does not change the operating regime of the engines, as the flight speed is decreased from V_{cr1} to V_{cr2}, the angle of attack and c_y increase. Allowing the aircraft to fly at higher angles of attack is dangerous due to the approach toward $c_{y\ per}$ and the separation limit. Also, under relatively high temperature conditions, the vertical gust reserve is decreased. Therefore, in case such conditions are encountered, the rotating speed of the engine should be increased by an average of 5% for each 5-10° of increase in temperature, or if this is impossible, a lower flying altitude should be requested.

As the temperature decreases, the available thrust increases (curve 4) and the curve of required thrust is displaced to the left. The point of their intersection c defines the new flight speed.

§5. Most Favorable Horizontal Flight Regimes. Influence of Altitude and Speed

The flight range is the distance traveled by the aircraft during the climb, horizontal flight and descent. If flight is performed until the fuel is completely exhausted, the distance traveled is called the technical range. For passenger aircraft, the flight range given is usually that with one hour's fuel reserve if the flight schedule is maintained. (recommended regimes). Since there are various ways which the aircraft can leave the area of the airfield and climb after takeoff, the range of flight covered during the climb to assigned altitude changes significantly. However, the range covered during climb to altitude is relatively slight, so that in the following we will discuss the range of horizontal flight.

The range of the horizontal flight sector depends on the fuel reserve for horizontal flight and on the rate at which it is expended, i.e., the kilometer expenditure c_k -- the expenditure of fuel per kilometer of flight path. Before going over to horizontal flight, the aircraft must take off and climb. The fuel expenditure during the time of takeoff and climb to 9-11 km for two- and three-engine aircraft is 1600-4000 kg.

The fuel expended during takeoff and establishment of nominal flight regime (without consideration of climb) is 250-350 kg, the fuel expended during the descent and landing is 700-1000 kg. In order to determine the quantity of fuel to be used in the horizontal flight sector $G_{f\ hor}$, we must subtract from the quantity of fuel taken on board all supplementary expenditures and the navigational reserve. For example, with a takeoff weight of the aircraft or 44,000 kg and an initial fuel weight of 13,000 kg, 7000-7700 kg of fuel remain for horizontal flight at H = 10,000 m, since about 2000 kg are expended in takeoff and climbing, 800-1000 kg for descent and landing and 2500 kg are held as navigational reserve. /130

For shorter range flights
the quantity of fuel required f
fuel expenditure norms remain a

The duration of horizontal

where c_h is the hourly fuel exp

The hourly fuel expenditur
aircraft in one hour of horizon
three engines with a required t
0,8 kg/kg·hr, the hourly rate i

The relationship between h
from the following considerati
c_h kg of fuel. However, during
numerically equal to the flight
expenditure per km is

where V is taken in km/hr. If V

For V = 880 km/hr and c_h =

Both the hourly and kilomet
specific expenditure of the engi

specific and hourly expenditures
1 kg of thrust and one hour of e

while a thrust of P kg requires
Therefore,

$c_{h\,min}$ will correspond to V_{mf}, at which $P_{r\,min} = G/K_{max}$. With $V < V_{mf}$, c_h begins to increase, since P_r increases. Consequently, the greatest flight duration at any altitude will occur when flying at the most favorable speed.

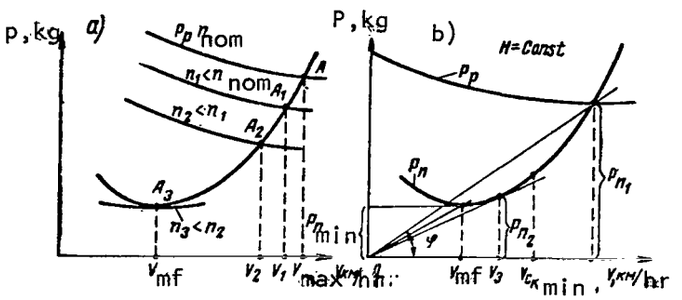

Figure 89. Explanation of Influence of Flight Speed on Hourly and Kilometer Fuel Expenditures

Let us explain how the flying altitude influences the hourly expenditure. In §2 of this chapter we showed that the required thrust is almost identical for the same weight at all flying altitudes up to 10,000 m. However, the required speed increases with altitude. Therefore, the curves of required thrust are displaced toward the area of higher speeds with increasing altitude (see Figure 85).

Since the available thrust of the engine decreases with altitude, the curves of the change in thrust with velocity are displaced downward with an increase in altitude. Therefore, whereas at low altitude the engines must be throttled back, thus considerably increasing the specific expenditure, at 10,000 m less throttling is required and the specific expenditure increases only slightly. When flying at the ceiling, the engines need not be throttled back at all. Therefore, as the flying altitude increases the product $c_p P_{r\,min}$ decreases, which explains the decrease in hourly expenditure. Also, the decrease in c_h with altitude facilitates a decrease in specific expenditure at constant operating speed. Therefore, the longest flight duration for an aircraft with a turbojet engine is produced near the ceiling. Flight duration at high altitude is 2-2.5 times greater than at low altitude. The regime of lowest hourly expenditure is used when flying in a holding pattern or with a strong tail wind (150-200 km/hr) in order to maintain the scheduled time of arrival.

Let us now analyze the way in which the selection of flight speed influences the kilometer expenditure. It was shown above that $c_k = c_h/3.6\,V$. Substituting the value $c_h = c_p P_r$ in this formula, we produce

$$c_к = \frac{c_p}{3,6} \cdot \frac{P_r}{V}.$$

In order to simplify our discussions, let us assume that c_p remains constant with changing flight speed, i.e., consider that neither a decrease in engine thrust nor a decrease in the velocity itself influences c_p. Then it follows from the last expression for c_k that the minimum kilometer expenditure will occur at the speed for which the quantity P_r/V is minimal. In order to determine this speed, we use the graph on Figure 89 b. The quantity $P_r/V = \tan \phi$ (angle ϕ is formed by the horizontal axis and a ray from the coordinate origin to any point on curve P_r). When flying at V_{mf}, $\tan \phi = P_{r\ min}/V_{mf}$, and when flying at V_{max}, $\tan \phi = P_r/V_{max}$. /133

We can see from the figure that with decreasing flight speed, angle ϕ decreases and reaches a minimum at a speed corresponding to the point of contact of the ray to the curve of required thrust. This speed, at which P_r/V is minimal, will be called speed V_3. With a further decrease in speed, angle ϕ begins to increase, i.e., P_r/V is increased. Thus, if we consider the specific expenditure constant as the speed is changed, $(P_r/V)_{min}$ and consequently also the minimal kilometer expenditure will be produced at speed V_3. As we can see, V_3 is always greater than V_{mf}.

Let us now consider that the specific expenditure is not constant with changing speed and consider the influence of throttling of the motor on c_p. If flight is performed at V_{max}, we have high P_r/V and nominal motor operating speed, so that c_p here is minimal. When we decrease the speed (decrease motor operating speed), we decrease P_r/V, but due to the throttling of the motors, c_p increases. At V_3, the value of P_r/V is minimal, but here c_p is increased, since the engines are considerably throttled. Comparing these two extreme positions, we might conclude that somewhere between V_{max} and V_3 there should be a speed at which $c_p P_r/V$ is minimal. This speed is slightly greater than V_3 and is called the speed of minimal kilometer expenditure. For $H = 0$ with a specific loading of 350-420 kg/m^2, this speed is approximately 450-520 km/hr.

We can see from Figure 90 that as the altitude increases, the true speed corresponding to the minimal kilometer expenditure also increases. We can see from Figure 91 that the minimal kilometer expenditure decreases up to 10,800 m, then begins to increase. The decrease in kilometer expenditure of

fuel with increasing altitude is facilitated by the decrease in the quantity P_r/V resulting from the increased flight speed and decreased specific fuel expenditure. /134

In this example, the altitude of 10,800 m at which the minimum kilometer expenditure is produced is called the most favorable altitude. For turbojet aircraft it is 1000-1200 m below the practical ceiling, at which a considerable wave drag is created due to the high angles of attack. Transition to lower altitude, i.e., to lower angles of attack, decreases this drag component significantly and increases the aerodynamic quality. Let us show that the kilometer expenditure depends on quality:

$$c_к = \frac{c_p}{3{,}6} \cdot \frac{G}{KV}.$$

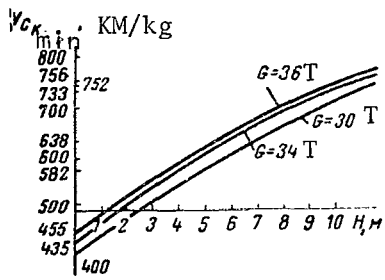

Figure 90. Speed of Minimal Kilometer Expenditure of Fuel As a Function of Flying Altitude (aircraft with two engines)

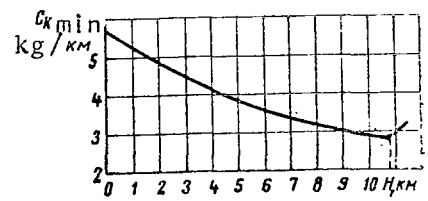

Figure 91. Influence of Flight Altitude on Minimal Kilometer Fuel Expenditure

We can see from the formula that the kilometer expenditure is inversely proportional to the quality. Now we can formulate a definition of most favorable flight altitude: the altitude corresponding to $(KV)_{max}$, called the most favorable altitude or the altitude of least kilometer expenditure.

The dependence of the altitude of the practical ceiling and the altitude of minimal kilometer expenditure on flying weight of a TU-124 aircraft is shown on Figure 92, while Figure 93 shows the dependence of the minimal kilometer expenditure for this aircraft on flight speed. We can see from this last graph that the minimal kilometer expenditure is produced at

V = 752 km/hr. This is the speed $V_{c_{k\ min}}$ at the most favorable altitude. Flights at lower and higher speeds and at other altitudes cause increases in kilometer expenditure.

It has been established that at speeds 5-8% (30-50 km/hr) higher than $V_{c_{k\ min}}$, the kilometer expenditure is increased by an average of 1% (for example, if $c_{k\ min}$ = 3 kg/km, it will be increased to 3.03 kg/km), and that this is the optimal regime for long-distance flights. This cruising regime is the most economical as concerns total transportation cost, since it consumes little fuel, allowing higher commercial load to be carried. /135

For medium range flights (1300-1500 km), the highest cruising regime is recommended, in which the kilometer expenditures are higher but the increased fuel load does not require a decrease in commercial load, but the increase in speed does decrease the flying time, as a result of which the cost of transportation is decreased. These regimes correspond to flying altitudes of 7000-9000 m and maximal indicated speeds, or maximum permissible M number at higher altitudes.

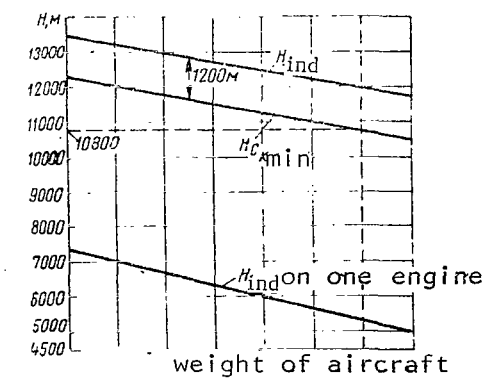

Figure 92. Height of Practical Ceiling and Height of Minimal Kilometer Expenditure of Fuel As a Function of Flying Weight (TU-124 aircraft)

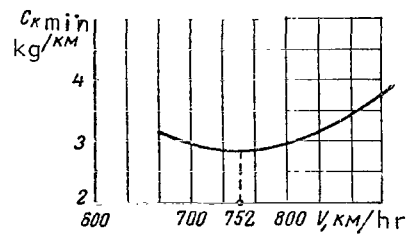

Figure 93. Minimal Kilometer Expenditure of Fuel As a Function of Flight Speed (aircraft with two engines)

§6. Definition of Required Quantity of Fuel

In order to determine the fuel expenditure in flights to various distances at various altitudes with various winds, a special graph must be used (Figure 94). In calculating this graph, we assume the mean cruising regime of engine operation, with a kilometer expenditure of one percent

greater than the minimal. This is sufficient to provide a fuel reserve in case the flight is performed at higher or lower speed than the minimal expenditure speed. The climbing and descending regimes for the aircraft are identical in practically all cases. Therefore, the expenditures of time and fuel for these portions of the flight can be considered constant, dependent only on the flying altitude. The distance traveled by the aircraft during the climb and descent also depends only on altitude.

When it is necessary to determine the flight range or fuel reserve precisely under special conditions (special flights), a graph of this type must be constructed for the regime selected. Figure 94 allows us to determine without calculations the range of an aircraft for a given quantity of fuel for any point. For example, point 4 corresponds to a fuel reserve of 7750 kg and a flight range (calm wind) of 2220 km at H = 10,000 m. /136

The lower portion of the graph presents corrections considering the influence of wind.

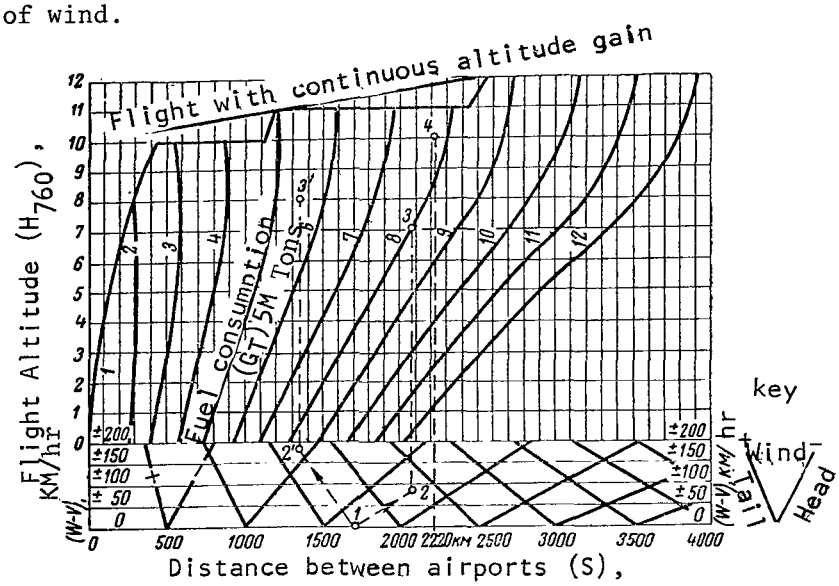

Figure 94. Total Fuel Expenditure As a Function of Distance, Altitude and Wind

If we must determine the fuel expenditure for flight of 1700 km at 8000 m with a tail wind of 175 km/hr, we move from point 1, corresponding to S = 1700 km along the inclined lines for wind to point 2' corresponding to a tail wind of 175 km/hr. Then we move vertically upward to the assigned altitude of 8000 m (point 3') and here read the fuel expenditure: 5500 kg. Adding the navigational reserve, we produce the quantity of fuel which must be placed into the fuel tanks of the aircraft. For a flight of the same range with a head wind of 80 km/hr (point 2) at 7000 m, 8000 kg will be required (point 3).

In processing the material of flying tests with respect to fuel reserves, we usually determine the flying altitude most suitable as concerns total flight cost. Table 9 presents these altitudes for one passenger aircraft.

As we can see from the table, even at 200-400 km range, the flight should be performed at 4500-7000 m, since this will produce minimum fuel expenditure. Flights over these ranges at 1200-1500 m (the altitude of the IL-14 aircraft) are inefficient, since due to the comparatively low true flying speeds (570-600 km/hr, indicated speed 480-550 km/hr) the kilometer expenditure is rather high. /137

TABLE 9

Distance, km	200	300	400	500—700	800—1000	Over 1000
Most favorable altitude, m	4500—5400	5700—6000	6000—7000	7000—8000	8000—9000	10000—11000

§7. Flight at the "Ceilings"

With decreasing flying weight of the aircraft, the height of minimal kilometer expenditure (most favorable altitude) increases (Figure 92). This dependence is used when flying at the "ceilings." The weight of the aircraft when flying to maximum range can be reduced by 10-25 t (by 10-30% of initial weight). In order to keep the aircraft flying at all times at $c_{k\ min}$, the altitude must be gradually increased as the fuel is consumed. The density should be decreased in proportion to the decreasing flying weight. This type of flight is called flight at the ceilings. This is the way in which maximum range can be attained. During the process of such a flight, the aircraft will remain continuously at 1000-1200 m below its current practical ceiling.

We should note that civil aircraft perform flights at assigned altitudes. However, it is of interest to the pilot to know the specific nature of flight at the ceilings, since he may find this flight necessary, for example, when flying along other than established airlanes and in other cases when maximum range must be attained.

Let us analyze the performance of a flight at the ceilings (Figure 95) using a TU-124 aircraft. The initial altitude for this type of flight will be 10,500 m. This altitude (permissible on the basis of the condition of the effect on the aircraft of a 10-m/sec vertical gust) will correspond to an actual aircraft weight at the beginning of the flight of 36 t (we will consider that the flight is not along an established airlane).

At this altitude (ρ = 0.0395 kg·sec^2/m^4, fuel weight 8400 kg), the pilot

should establish a horizontal flight speed of $V_{c\ k\ min}$, which in this case corresponds to M = 0.7. This air speed will be maintained throughout the entire flight. After approximately 2 hr 36 min, the pilot has expended about 5200-5400 kg fuel, i.e., 15.5% of the initial weight. The air density should be decreased by the same factor: $0.0395 \cdot 84.5 = 0.0334$ kg·sec^2/m^4 (84.5% density at H = 10,500 m), meaning that the aircraft will actually have risen to an altitude of 11,800 m (see standard atmosphere table), i.e., will have climbed by 1300 m, with a vertical velocity component of $1300/156 \cdot 60 = 0.139$ m/sec. It is difficult to maintain this speed using the variometer, piloting the aircraft by referring to the thin needle of the KUS-1200 speed indicator. In practice, it is easier to maintain the M number steady using the M number indicator, since the value of a scale division of this instrument is 0.01. At 10,000-12,000 M, the air temperature, and consequently the speed of sound, remains practically unchanged, so that with constant M number, the true speed will also remain constant.

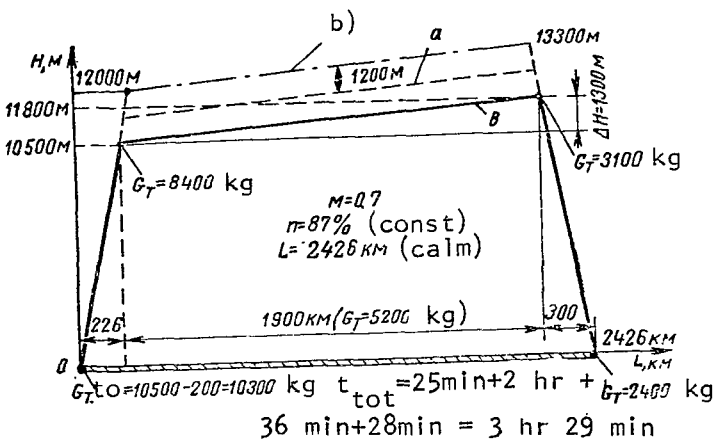

Figure 95. Profile of Flight at the ceilings: a, At most favorable altitudes; b, Ceiling; c, With altitude limited according to flying weight

In this example as the weight is changed for each 1000 kg the flying altitude is increased by 200-220 m. For aircraft with hourly fuel expenditures of 4000-5000 kg, the increase in altitude will be 50-70 m. In flight at the ceilings, the rotating speed of the engines and the M number must be kept constant. If the air temperature changes, the engine rotating speed should be changed by one percent for each 5° (decreasing with decreasing temperature and increasing with increasing temperature).

Flying tests have established that flight at the ceilings can increase the range by 3-8%. Flight at the ceilings can be primarily used in case of engine failure, when it is necessary to continue flying to the assigned destination. It is here that the advantages of this type of flying are most notable.

§8. Permissible Flying Altitudes. Influence of Aircraft Weight

The operation of jet aircraft with high practical ceilings (11,500-13,000 m) has shown that it is not always possible to fly at these altitudes, or even at the altitude of minimal kilometer expenditure (most favorable altitude, Figure 92). The problem is that the flying altitude of a high speed aircraft is selected on the basis of the condition of maintenance of a reserve for overloads in case a vertical wind gust is encountered. Chapter XI. will present an analysis of the effect of a vertical gust on an aircraft, and now let us analyze the influence of aircraft weight on the selection of permissible flight altitude, using the combined graphs $c_{y\ per} = f(M)$ and $c_{yhf} = f(M)$.

Let us analyze the flight of a TU-124 weighing 34 t at 10,000 m at a speed corresponding to M = 0.75, and explain the permissible overload in case of a vertical maneuver from the standpoint of safety.

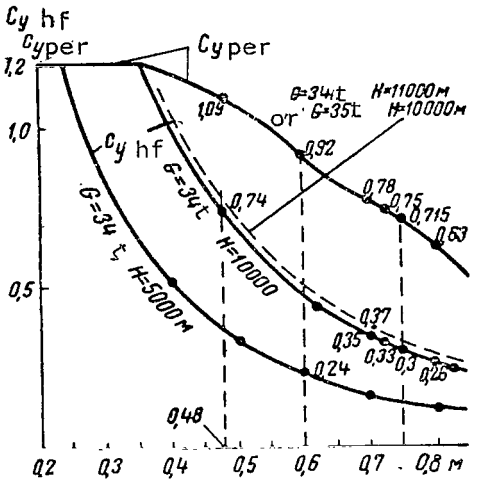

Figure 96. Combined Graphs of Dependences of Coefficients c_{yhf} and $c_{y\ per}$ on M Number of Flight

As we can see from the figure, for these altitudes and M numbers the aircraft will have $c_{yhf} = 0.3$ and $c_{y\ per} = 0.715$. Consequently, the reserve with respect to c_y will be $\Delta c_y = c_{y\ per} - c_{yhf} = 0.715 - 0.3 = 0.415$. In case a vertical gust is encountered or in case of maneuver, this reserve may be expended and the aircraft will find itself at $c_{y\ per}$. This requires that the overload

$$N_{y\ per} = \frac{C_{y\ per}}{C_{y\ h.f.}} = \frac{0.715}{0.3} = 2.4.$$

This will be the value of permissible overload. Each M number (with unchanged weight) corresponds to a definite value of c_{yhf}. By joining the points corresponding to these values, we produce the dependence $c_{yhf} = f(M)$ (Figure 96). As we can see from Figure 96, in the range of numbers M = 0.7-0.75, the reserve with respect to c_y is maximal. With high M numbers, particularly at M > 0.8, the reserve of c_y is decreased. This reserve is also decreased with increasing flight altitude (with unchanged weight) and increasing aircraft weight (at constant altitude).

The reserve of c_y is equivalent to reserve against a vertical gust. In particular, it is required for a passenger aircraft that if an effective indicator gust of 10 m/sec is encountered, the aircraft will reach only $c_{y\ per}$ not encountering stall (see definition in Chapter XI). Therefore, in order to avoid exceeding $c_{y\ per}$ and causing the aircraft to stall, permissible flying altitudes are established as a function of flying weight (Figure 97). If these limitations are not observed, a vertical gust of lower magnitude will bring the aircraft to $c_{y\ per}$ or stall. /140

The decrease in weight resulting from consumption of fuel increases the reserve with respect to c_y and, therefore, the reserve for vertical gusts; therefore, the flying altitude can be increased. In the same way as the altitude is decreased (for example to 5000 m), the reserve with respect to c_y and gusts increases. For M = 0.6 (V = aM = 320·0.6 = 198 m/sec), c_{yhf} = = 0.24 and $c_{y\ per}$ = 0.92 (Figure 96). In this case, the overload permissible with respect to c_y will be $n_{y\ per}$ = 0.92/0.24 = 3.83.

Figure 97 shows a graph of permissible flying altitude (for this example) as a function of flying weight.

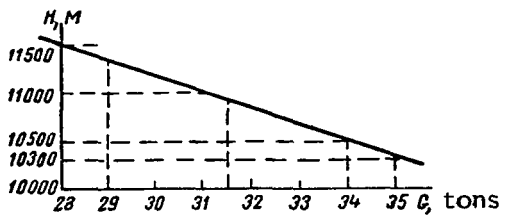

Figure 97. Permissible Flying Altitude As a Function of Aircraft Weight

The standard practice of assigning altitude intervals of 1000 m at altitudes above 6000 m reduces the "resolving capacity" of aircraft as to permissible altitude; therefore, it would be more desirable to use separations of 600 m altitude. The heights of flight at the ceilings correspond to permissible flying altitudes.

The limitation on flying altitude is not the only limitation for a high speed passenger aircraft. The second limitation is the permissible M number for flights at high altitudes (Chapter XI §12). As flying operations have shown, the most favorable cruising flight regimes as to M number and altitude for the first generation of aircraft differ slightly from safe regimes as concerns the conditions of encountering powerful ascending gusts.

§9. Engine Failure During Horizontal Flight

In case of engine failure, if an aircraft cannot continue flying at altitudes ordinarily used (8000-11,000 m). As we know, in flights at altitudes below the ceiling at speeds lower than the maximal, the engines are

throttled to some extent. This is also true of cruising flight regimes at 8000-11,000 m. The necessity of reducing engine speed in these regimes causes /141
an increase in the specific fuel expenditure. In case of failure of one engine, the pilot will be forced to set the remaining engines at the nominal regime (which is permitted for long term operation), which should reduce the specific expenditure. However, in this case the drag is increased due to autorotation of the compressor and turbine of the engine which has failed (for example, at V = 600-620 km/hr at 4000-5000 m altitude, the autorotation drag is 150-300 kg), leading to an increase in the kilometer and hourly expenditures. In case of an engine failure, horizontal flight at altitudes above 6000-7000 m is impossible, and the aircraft will descend to 5500-6000 m (two-engine aircraft, Figure 98). For aircraft with three and four engines in case of failure of one engine, the decrease in altitude is not so great.

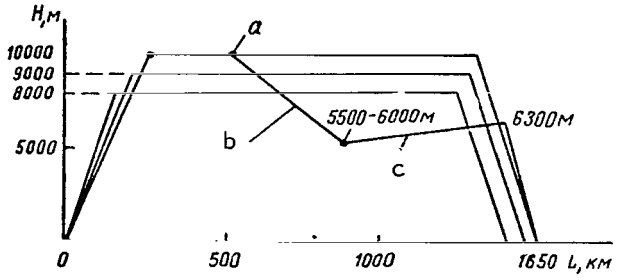

Figure 98. Profile of Flight of Aircraft with Two Engines in Case of Failure of One Engine After 45 min Flying Time: a, Point of failure; b, Descending trajectory (time 37 min, L = 400 km); c, Flight with increasing altitude

The altitude at which the aircraft can fly without further descent will be essentially the initial altitude of flight at the ceilings with one nonoperating motor, if long range flight must be performed and a landing cannot be made immediately after the motor fails.

In case of a motor failure, it is necessary first of all to achieve the least possible rate of vertical descent and secondly to decrease the weight of the aircraft rapidly (using up fuel) in order to make it possible to continue horizontal flight with one nonoperating engine at high altitude. Therefore, the descent should be made at the nominal regime, gradually decreasing the vertical velocity component, which at the beginning of the descent will be V_y = 3-5.5 m/sec. The indicated speed for each aircraft depends on the specific loading on the wing and the power factor. For example, for an aircraft with two engines and a specific loading of 350 kg/m^2, an indicated speed of 430 km/hr was produced. The descent from 10,000-11,000 m to the /142
practical ceiling of the aircraft with one nonoperating engine occurs in 35-45 min. Over this time, the aircraft covers 350-500 km.

If it is necessary to continue the flight, the pilot should shift the aircraft to the regime of flying at the ceilings; then in 60-70 min the aircraft will cover another 650-750 km, with an increase in altitude of 800-1000 m and an average rate of altitude increase of 0.15-0.2 m/sec. Flight

should be performed at M = 0.50-0.55, corresponding at 5500-6500 m altitude to a true speed of 600-650 km/hr. The mean kilometer fuel expenditure for an aircraft with two engines at this stage will be about 3.5 kg/km, which is approximately 0.5 kg/km greater than at 10,000 m with two engines operating. Thus, the flight range with one engine not operating is always less.

A gain in flying range with one engine not operating can be produced only if the initial flying weight was planned (due to unavailability of higher altitudes or other reasons) for a low altitude, for example 6000-7000 m. For example, for the TU-104 aircraft at this altitude at 800 km/hr, the hourly fuel expenditure is 3100 kg/hr, and the kilometer expenditure is 3100/800 = = 3.88 kg/km. In case one engine fails, it is possible to fly at 5000 m and 620 km/hr, the second engine operating at the nominal regime with an hourly expenditure of 2200-2300 kg/hr. In this case the kilometer expenditure will be about 3.6 kg/km, i.e., less than in flight with both engines (for this altitude) and the possible flying range increases.

In all cases in case of failure of one engine, the crew should return to the airfield of origin if possible or land at the nearest available airfield.

§10. Minimum Permissible Horizontal Flight Speed

The most favorable horizontal flight speed is the division between the two flight regimes. However, in establishing the minimum permissible speed, the most favorable speed is not taken into consideration, but calculations are based on $c_{y\ per}$, produced for low M numbers. The value of $c_{y\ max}$, which is used to determine the stall speed, is also not used in this case.

Let us determine the minimum speed of horizontal flight, i.e., the speed corresponding to $c_{y\ per}$, assuming that the wing area is 120 m^2, the aircraft weight is 50 t, and $c_{y\ per} = 1.2$ (from the graph on Figure 96):

$$V = 14.4\sqrt{\frac{G}{Sc_{y\ per}}} = 14.4\sqrt{\frac{50\,000}{120 \cdot 1.2}} = 14.4\sqrt{347} = 268_{km/hr}$$

When values of $c_y > c_{y\ per}$ are achieved, the stability of an aircraft /143
with a smooth wing (flaps up) may be disrupted. In order to prevent a loss of speed and a stall, the minimum permissible horizontal flight speed should be 50-60 km/hr greater than the absolutely minimal speed. In our example, this will be 320 km/hr. After 10 t of fuel have been expended (G_{inst} = 40 t) we produce (according to the last formula) the minimal possible speed of 240 km/hr, so that the minimal permissible speed will be 300 km/hr.

Frequently, in order to avoid the necessity of memorizing many values of minimal permissible speed, flying handbooks show only the value for maximum weight. In our example, this will be 320 km/hr. When flying at this speed, an aircraft weighing 40-50 t or less will have $c_y < c_{y\ per}$ by 30-40%. With normal operation of the aircraft, flying at 320 km/hr is not permissible, since even for circle flights the speed at this weight (S = 120 m^2) should be 350-370 km/hr.

This limitation will provide flight safety.

Chapter VIII. Descent /143

§1. General Statements. Forces Acting on Aircraft During Descent

Descent refers to steady, straight line flight of the aircraft on a descending trajectory. Descent at low power, when the thrust at 8000-10,000 m is flight, will be called gliding. Usually, passenger aircraft descend with the engines operating at 80-86% revolutions, at which the thrust is greater than at the idle (for example, the idle at H = 10,000 m might correspond to 72-74% revolution). The presence of motor thrust increases the descent range and decreases the angle of inclination of the trajectory.

Following his assigned altitude (9000-11,000 m) the pilot begins his descent at 250-300 km from the airfield at a high indicated speed (550-650 km/hr). The time for the beginning of the descent is calculated by the navigator.

In those cases when the flight range is not over 1000-1200 km and fuel economy is of less significance than flying time economy, the descent is performed at the greatest permissible indicated speed or M number.

Figure 99 shows the forces acting on an aircraft during the descent with engines operating. The angle of inclination of the trajectory of the descent from 9000-11,000 m will be Θ = 2.5-3°, the pitch angle $\vartheta \approx$ 2-2.5°. It must be /144 be noted that angle Θ does not remain constant, but rather changes as a function of the vertical component of the descent, which is maintained by the pilot by setting the corresponding engine operating regime.

Operational experience has shown that during a descent from 9000-11,000 m with true speeds of 850-900 km/hr, at first a vertical speed of 8-10 m/sec must be maintained, then gradually decreased so that by 5000-6500 m, when the pressure in the cabin is constant (Figure 100) the vertical speed is not over 5-6 m/sec. At altitudes of less than 5000 m, the vertical speed can be increased to 10 m/sec. We will consider that the thrust of the engines P acts in the direction of movement of the aircraft, although as was stated above there is a certain angle β between force P and the direction of movement of the aircraft. The lifting force Y is perpendicular to the direction of movement of the aircraft, and the drag Q acts in the direction opposite to aircraft movement.

For a stable descent, it is necessary that the aircraft weight component G cos Θ be balanced by force Y, and that force Q be balanced by the weight component G sin Θ and force P, i.e., that the following equality be fulfilled:

$$Y=G\cos\Theta;\ Q=P+G\sin\Theta.$$

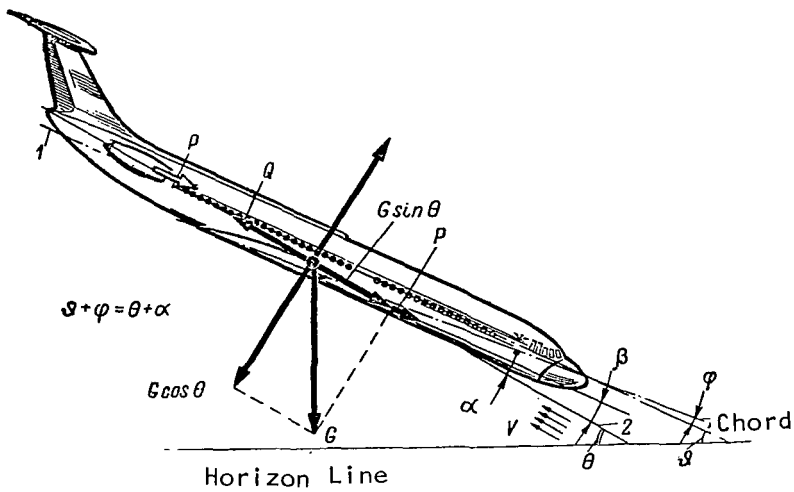

Figure 99. Diagram of Forces Acting on Aircraft During Descent: 1, Longitudinal axis of aircraft; 2, Descent trajectory; ϑ, Pitch angle; Θ, Flight-path angle; ϕ, Rigging angle of incidence; α, Angle of attack

The first equality is the condition for straight line movement, while the second is the condition for constant velocity on the trajectory. /145

§2. Most Favorable Descent Regimes

In order to analyze the most favorable descent regimes from the standpoint of fuel economy, let us use the formula $Q = P + G \sin \Theta$, which characterizes the condition of constant velocity. Let us analyze at first descent with engines throttled.

We will consider that when the engines operate at the idle, the descent occurs only under the influence of the component $G \sin \Theta$, when $Q = G \sin \Theta$.

Let us assume that the flying weight of the aircraft $G = 33{,}000$ kg, force $Q \approx 3000$ kg with a quality of 11 and the flight speed is 810 km/hr. Then $\sin \Theta = Q/G = 3000/33{,}000 \approx 0.091$ and the angle of inclination of the trajectory $\Theta \approx 5°$.

In order to maintain this angle Θ, with a forward speed of $V = 810$ km/hr (225 m/sec) it is necessary to maintain a vertical speed

$$V_y = V \sin \theta = 225 \cdot 0.091 = 20.5 \text{ m/sec}$$

As the flying altitude is decreased, the true speed of the aircraft will decrease and, consequently, in order to retain the constant trajectory angle, the vertical velocity component must be increased to 15-17 m/sec.

With this sort of vertical speed, the total descent time to the holding altitude will be 10-12 min, and the total fuel expenditure 300-400 kg, the descent range 120-170 km (considering the considerable decrease in vertical speed involved at low altitudes).

This method of descent is used when the cabin air pressure regulation can provide normal conditions for crew and passengers. Another descent regime is that in which the engine speed is maintained over the idle (in practice in passenger aircraft the descent at idling regime is just being introduced). When this regime is used for the descent, the fuel expended is 400-500 kg greater than in the regime described above, but satisfactory conditions are maintained for passenger and crew. Table 10 shows the characteristics of the descent regime with least expenditure of fuel for a TU-124 aircraft.

In comparison with the descent regime at the idle, the descent time is almost doubled, and the range is increased by 50-100 km. The vertical velocity components are selected from the condition of maintenance of a constant pressure drop in the passenger cabin. The duration of the landing maneuver (approximately from the region of the third turn, see Chapter IX) is taken as 6 min (according to statistical data from scheduled flights). /146

The next method is descent at the highest speed, in which piloting is performed at the cruising (maximum permissible) M number or maximum indicated speed. In this regime, the descent must be begun 270-300 km from the landing point. The fuel expenditure during the descent is increased, since the engines operate at a regime near the cruising regime for horizontal flight. /147 Table 11 shows the characteristics of the regime of descent at greatest speed (TU-124 aircraft).

§3. Provision of Normal Conditions in Cabin During High Altitude Flying

The cabin of a passenger turbojet aircraft is sealed. In the cabin, the temperature (20-22°C), relative humidity and air pressure are maintained so as to support normal vital activity of the crew and passengers during high altitude flight.

TABLE 10

H, m	V_y, m/sec	V_{ind}, km/hr	Engine speed, %	Descent and landing time, min	Range, km	Fuel expenditure, kg
11 000	8,0	440	80	31	225	700
10 000	7,5	450	80	28,8	200	670
9 000	7,0	455	80	26,4	170	630
8 000	6,5	460	75	23,8	145	590
7 000	6,0	460	75	21,1	120	540
6 000	5,5	465	75	18,2	90	480
5 000	5—10	470	60	15,1	60	410
4 000	10	475	60	13,4	45	380
3 000	10	480	60	11,8	30	350
2 000	10	490	60	10,2	20	310
1 000	10	500	60	8,2	10	270
landing maneuver from H=500m	—	—		6,0	0	250

An excess pressure over the atmospheric pressure is maintained in the cabin (Figure 100). At altitudes between zero and 12,000 m, two pressure regulation regimes are generally used:

a) The regime of constant absolute pressure, during which from ground level to 4500-6500 m, a pressure of 760 mm Hg is maintained;

b) A regime of constant pressure drop (difference between pressure in cabin and atmosphere), in which at altitudes over 4500-6500 m, the pressure in the cabin is 0.5-0.65 kg/cm^2 higher than the atmospheric pressure. With Δp = 0.5 kg/cm^2 at 8000 m, the cabin altitude is 1493 m, at 10,000 m -- 2417 m; with Δp = 0.6, the cabin altitude at these altitudes will be 500-600 m lower.

Each of these regimes has a characteristic rate of change of pressure as a function of altitude.

In the constant absolute pressure regime, the altitude in the cabin remains unchanged during ascent and descent, equal to zero. Therefore, at altitudes from zero to 4500-6500 m at any vertical speeds practically possible (climb or descent) the rate of change of altitude in the cabin is equal to zero. In the constant excess and variable absolute pressure regime, the rate of change of pressure in the cabin is of essential significance for high altitude passenger aircraft during a climb and particularly during a descent, during which vertical speeds may reach 45-70 m/sec (in an emergency situation).

At altitudes over 5000-6000 m, the vertical climbing speeds are usually much less than descending speeds, 10-15 m/sec. /14

TABLE 11

H,m	V_y, m/sec	V_{ind}, km/hr	Engine speed, %	Descent and landing time, min	Range, km	Fuel expenditure, kg
11 000	8,0	480	84	31	270	960
10 000	7,5	520	83	28,8	240	900
9 000	7,0	555	83	26,4	210	830
8 000	6,5	595	82	23,8	175	760
7 000	6,0	600	82	21,1	140	680
6 000	5,5	600	81	18,2	105	600
5 000	5—10	600	80	15,1	65	500
4 000	10	600	79	13,4	45	460
3 000	10	600	77	11,8	30	400
2 000	10	600	76	10,2	20	340
1 000	10	600	75	8,0	10	280
landing maneuver from H-500m	—	—	—	6,0	0	250

The comfort of most passengers varies strongly with the rate of change in barometric pressure. During rapid pressure changes (particularly during descent) the passengers experience unpleasant and painful sensations in their ears. Therefore, the rate of change of cabin pressure W_{cab} should be W_{cab} = 0.18-0.20 mm Hg/sec, according to medical requirements. Maintenance of W_{cab} within these limits at all altitudes over which pressure changes will assure an even rate of pressure increase. The rate of change of cabin pressure is equal to

$$W_{cab} = V_y \cdot \Delta p_H,$$

where V_y is the vertical rate of descent (climb);

Δp_H is the vertical pressure gradient of the atmosphere, mm Hg/m. For H = 0, the gradient Δp_H = 0.09, for H = 8000 m -- 0.038 and for H = 10,000 m -- 0.03 mm Hg/m.

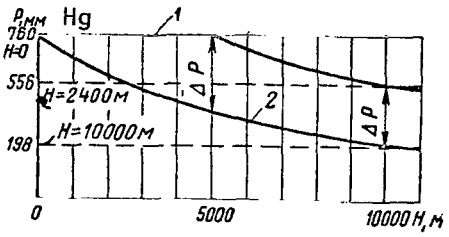

Figure 100. Pressure in Sealed Cabin As a Function of Flying Altitude (pressure drop $\Delta p = 0.5 \pm 0.02$ kg/cm^2): 1, Pressure in cabin; 2, Atmospheric pressure

This dependence can be used to determine the vertical rate of descent or climb for any height, on the basis of the condition of maintenance of normal sensations of the passengers. For example, let us determine the vertical rate of descent of an aircraft for $W_{cab} = 0.18$ mm Hg/sec:

For H = 0

$$V_y = \frac{W_{cab}}{\Delta p_H} = \frac{0,18}{0,09} = 2 \text{ m/sec}$$

For H = 10,000 m

$$V_y = \frac{0,18}{0,03} = 6 \text{ m/sec}$$

Let us now determine the permissible "vertical speed" of the descent in a passenger aircraft with sealed cabin at H = 10,000 m, if the cabin altitude is 2417 m and the vertical pressure gradient for this altitude $\Delta p_H = 0.07$ mm Hg/m: $V_y = 0.18/0.07 = 2.5$ m/sec. However, flying tests have shown that an increase in the vertical velocity component at 10-12 km to 8-9 m/sec and a corresponding increase in the vertical velocity of cabin altitude to 3-3.2 m/sec has almost no influence on the feelings of the passengers. Therefore, the descent can be begun at 250-300 km from the airfield, in order to provide normal landing maneuver.

An improvement in the valves of the cabin altitude system allows V_y to be increased and therefore allows the descent to be initiated 100-120 km from the landing point with the engines operating at the idle, which will provide a savings of 350-600 kg fuel (the descent at the least fuel expenditure regime, the idling regime, analyzed above).

The permissible "vertical velocities" in the sealed passenger cabin of a turbojet aircraft are presented in Table 12.

TABLE 12

Flying altitude, km	0	4	5	6	7	8	9	10	11	12
V_y in cabin, m/sec	2	2	2	2,1	2,2	2,3	2,4	2,5	2,6	2,8

It follows from the above that descent from high altitudes should be performed at a vertical rate of 8-9 m/sec down to 4500-6500 m, then with any vertical rate required, as long as the permissible indicated speed is not exceeded, since the pressure in the cabin will be made constant at 760 mm Hg.

§4. Emergency Descent

We have noted that in sealed cabins of turbojet aircraft the air pressure is 640-540 mm Hg with a pressure drop $\Delta p = 0.50\text{-}0.62$ kg/cm^2 (constant excess pressure regulation regime).

The change in the primary air parameters (pressure, weight density, temperature and humidity) as a function of "altitude" in a sealed cabin is of considerable significance for life support of man in flight. Of primary significance is any change in partial oxygen pressure (p_{O_2}) and its percent content.

The partial pressure of a gas included in the composition of any gas mixture is that portion of the total pressure of the mixture produced by the share of the gas in question. Oxygen enters the human organism, as we know, through the lungs, the alveoli of which are covered by a network of blood vessels. The penetration (diffusion) of oxygen through the walls of the blood vessels into the blood can occur only if the partial pressure exceeds the pressure of the oxygen in the blood. Similarly, removal of carbon dioxide from the organism requires that the partial pressure of carbon dioxide in the blood be higher than in the air in the alveoli of the lungs. Thus, whereas the partial oxygen pressure at which normal gas exchange is assured under surface conditions for the air inhaled is 159 mm Hg, this figure for alveolar air is 105-110 mm Hg. The minimum permissible partial pressure of oxygen in alveolar air, at which blood saturation of 80-85% will occur is 37-50 mm Hg. This pressure corresponds to an altitude of 4.5 km, and this altitude cannot be exceeded without special devices to increase the partial pressure /150
without oxygen starvation. This altitude is the physiological limit for

flight in nonpressurized cabins without oxygen devices. Oxygen starvation, which causes so-called altitude sickness, may occur before this altitude, since it depends to a great extent on the work performed by man. The symptoms of altitude sickness are headache, sleepiness, decreased acuity of vision and hearing, disruption of digestion and metabolism. These symptoms begin to appear quite acutely beginning at 4.5 km due to the decrease in oxygen supply to the cerebral cortex. It is difficult for the organism to compensate for a decrease in the quantity of oxygen in the blood. Therefore, the altitude zone from 4 to 6 km is called the zone of incomplete compensation. Above 6 km the critical zone begins, in which the disruption of mental activity and functions of the organism becomes quite dangerous for survival. In this zone, man loses consciousness and can only be saved by immediate descent or supplementary oxygen supply. The critical zone ends at an altitude of 8 km.

In case of a sudden sharp drop of pressure in the cabin (loss of cabin pressure), oxygen starvation may occur. The time from the beginning of oxygen starvation to loss of consciousness is called the reserve time. It must be used to descend to an altitude providing sufficient oxygen concentration.

In case of a loss of cabin pressurization or in other cases (in particular in case of fire on the aircraft) requiring a rapid descent, the aircraft commander should decrease the flying altitude to 5000 m (safe altitude) in 2.5-3 min or should perform an emergency landing.

An emergency descent should be performed at the maximum possible vertical speed. This can be achieved by increasing the forward speed and the angle of inclination of the trajectory. The greater the forward speed and the greater the angle of inclination of the trajectory, the greater will be the vertical speed. However, the speed of an aircraft is usually limited at high altitudes by the permissible M number, and at altitudes below 6000-7000 m by the permissible indicated speed. Therefore, unlimited increases in forward speed cannot be used, and the forward speed must be maintained within permissible limits.

The next possibility for increasing the vertical speed is to increase the angle of the trajectory Θ. The longitudinal forces must be equal during descent at constant speed. It should be kept in mind that in a turbojet aircraft during an emergency descent, the engines operate at the idle, creating insignificant thrust. We can see from the equation $P + G \sin \Theta = Q$ that $\sin \Theta = (Q - P)/G$, i.e., the angle of inclination of the descent trajectory (with constant aircraft weight) is greater, the greater the drag of the aircraft. An increase in the drag of a turbojet aircraft can be achieved by lowering the landing gear and spoilers. For example, during an emergency descent, c_x of the aircraft is 0.024-0.026 for M = 0.84-0.86. Lowering the landing gear increases c_x of the aircraft by 0.015-0.020. Lowering the spoilers can increase c_x still more. In spite of the high flying altitudes (9000-11,000 m), the impact pressure reaches high values (for example, for

/151

V = 900 km/hr at H = 10,000 m, q = 1300 kg/m^2, while at 6000-7000 m with V_{ind} = 650-700 km/hr it is over 2000 kg/m^2), which makes it difficult to lower and lock the landing gear if they are raised with the flow, or to lower them if they are raised against the flow. Therefore, in order to lower the landing gear the indicated speed must be decreased by 40-60 km/hr. The loss of time to achieve this is compensated for by the considerable increase in angle of inclination of the descent trajectory and, therefore, the decrease in time required for the emergency descent. At the same time, raising the spoiler is practically independent of the impact pressure.

Emergency descent of an aircraft can be divided into three main stages: 1) transition to descent with attainment of the maximum vertical velocity of 35-40 m/sec with landing gear up or 65-70 m/sec with landing gear down; 2) stable descent with these vertical velocities without exceeding the maximum permissible M number at high altitudes or permissible indicated speed at low altitudes; 3) bringing the aircraft out of the descent.

Energetic transition from initial cruising regime to the descent at M = 0.78-0.80 is performed with an overload n_y = 0.6-0.55, and the control should be performed using the overload indicator of the AUAP device (Chapter XI, §15). During this transition, V_y = 35-40 m/sec can be achieved in 12-15 sec, with the M number increasing only to 0.82-0.84 (with landing gear up). With a smooth transition with an overload of 0.9-0.8, the vertical speed will only reach 25-28 m/sec after 35-40 sec, and the M number will be approximately 0.85-0.86, i.e., the rate of increase in M number exceeds the rate of increase in vertical velocity. If this mode of transition is used, the aircraft may quickly reach the maximum permissible M number or exceed it. If the transition is performed with n_y = 0.4-0.3 or less, it becomes difficult to control the increase in vertical velocity, and the aircraft may reach V_y > 35-40 m/sec and subsequently exceed the permissible M number. Therefore, the transition to the descent should be performed with n_y = 0.6-0.55, which (as will be seen below) corresponds to attainment of a vertical speed of 15-17 m/sec in the first 5-6 sec.

The second stage of the descent consists of maintaining a vertical speed of 35-40 m/sec with landing gear up or 65-70 m/sec with landing gear down, with the M number increasing to the maximum permissible value at the same time. The aircraft should continue descent at this M number down to 6500-6000 m. The practically permissible M number is retained for 50-60 sec, then decreases as the maximum indicated speed is reached. Subsequently, as descent is continued at constant indicated speed, the M number drops (by approximately 0.08-0.1 by 5000 m), and the vertical speed decreases from 35-40 to 20-25 m/sec. /152

Flying tests have shown that it is not necessary to attempt to bring the aircraft up to the permissible M number, but rather descent can be formed at an M number 0.02-0.04 less than the permissible, since if the permissible

M number is exceeded, subsequent deceleration of the aircraft will sharply decrease the vertical speed. It cannot be excluded that during the process of a descent the velocity of the aircraft will exceed the permissible value (either permissible M number or indicated speed). In these cases, it is necessary first of all to halt further increase in M number, by slightly decreasing the vertical speed (by 5-7 m/sec), then once more decrease the vertical speed by 5-7 m/sec, and when the M number reaches its permissible value, to re-establish the constant vertical speed of 35-40 m/sec (or 65-70 m/sec with landing gear down).

The third stage in the descent is a smooth transition back to horizontal flight. This must be performed when the safe altitude is reached with an overload n_y = 1.1-1.2, corresponding to a loss of 350-400 m altitude. The transition from the descent (creation of n_y not over 1.2) is achieved by observing the change in altitude, overload and vertical speed, not allowing the maneuver to be performed in less than 300-400 m.

As we can see from Figure 101, the flying altitude of the aircraft with landing gear up decreases by an average of 1000 m each 30-32 sec, and the total time of descent is 2 min 30 sec-2 min 40 sec. With the landing gear down, descent from 10,000 to 5000 m occurs in approximately 2 min. The indicated speed gradually increases from the cruising speed (480-500 km/hr) to the maximum permissible speed (700 km/hr) retaining this latter speed for 20-25 sec from 6500 down to 5000 m (landing gear up).

The M number is increased from the cruising value of 0.78-0.82 to 0.85 (for this concrete case) which it retains for 50-52 sec, then decreases.

The vertical speed increases over 17-20 sec to a value of 35-40 m/sec (landing gear up), then retains this rate down to 7000-7200 m, after which (due to the attainment of an indicated speed of 700 km/hr, which must be maintained by decelerating the aircraft with the elevator) it is decreased. With the landing gear, the vertical speed reaches 65-70 m/sec and retains this level for 50-60 sec.

The overload is decreased during 5-6 sec of the initial transition from its initial value (n_y = 1) to 0.6-0.4, then increases to its initial value and further (depending on the pilot's operation of the stick), remaining between 1.1 and 0.9. /153

The pitch angle ϑ varies from 2° (cruising flight) to -(7-8°) with landing gear up or -(20-22°) with landing gear down.

The angle of inclination of the trajectory in a stable descent is $\Theta = \vartheta + \phi - \alpha$. For example, let us determine angle Θ if the descent is performed at M = 0.86 with V_y = 38 m/sec, where H = 8000 m, the weight of the aircraft is 34 t, the wing setting angle ϕ = 1°; we know from calculation that for these conditions c_y = 0.171, α = 1°, q = 1885 kg/m^2. Then

V = αM = 308·0.86 = 265 m/sec = 955 km/hr, and angle Θ = ϑ = 8°, since

$$\sin\Theta=\frac{V_y}{V}=\frac{38}{265}=0{,}143 \text{ and } \Theta=8°;$$

$$\vartheta=\Theta+\alpha-\varphi=8°+1°-1°=8°.$$

In order to achieve a descent with landing gear down with a vertical speed of 70 m/sec and a forward speed of 955 km/hr, angle Θ = 15-16°. /154

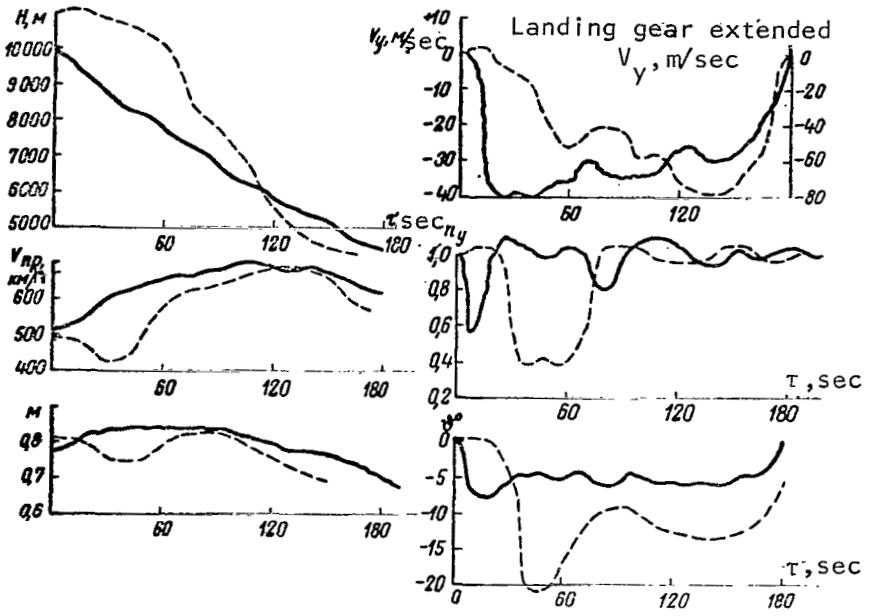

Figure 101. Recording of Parameters During Emergency Descent of Turbojet Aircraft: ———, With landing gear up from H = 10,000 m, M_{init} = 0.78; -----, With landing gear down and preliminary deceleration from H = 11,200 m, M_{init} = 0.8

The method of piloting an aircraft with landing gear up during an emergency descent consists of the following. Before beginning the descent, engines are set at the idle and, by moving the stick rapidly forward, the pilot puts the aircraft in a descent. During this maneuver, the pilot must check the indications of the variometer, overload indicator and M number indicator.

At the moment when V_y = 15-17 m/sec is attained, pressure on the stick must be reduced, pulling it gently back so as to retard the increase in vertical speed slightly. When V_y = 25-30 m/sec is achieved, the stick must be pulled back smoothly to retard the increase in vertical velocity still more, gradually going over to a stable descent at a constant speed of 35-40 m/sec.

During the process of increasing V_y from 30 to 35-40 m/sec, the M number indicator must be watched, to avoid exceeding the maximum permissible value. Subsequently, a constant vertical speed of 35-40 m/sec is maintained using the variometer, and the M number is not allowed to exceed the maximum permissible until the maximum permissible indicated speed is reached (at approximately 6500 m). When the maximum permissible indicated speed is achieved, the descent is continued at this speed until a safe altitude is reached.

The load can be relieved using the elevator trimmer in the process of stable descent when an indicated speed of 580-620 km/hr is achieved, so that a pressure of 5-10 kg is maintained on the control stick. If the force is not relieved by the trimmer, it will reach 50-60 kg. As the indicated speed increases from 480-490 (beginning of descent) to 680-700 km/hr, the elevator trimmer is moved away by 2.5-3°, and the deflection of the trimmer reaches 4-4.5° by the time an indicated speed of 700 km/hr is reached.

As the assigned altitude is reached, the aircraft is brought out of the descent in such a way that it loses no more than 300-350 m altitude in the maneuver. This corresponds to an overload of n_y = 1.16-1.2. At a vertical speed of 5-6 m/sec, the engines can be transferred to the required regime.

Piloting the aircraft during an emergency descent with landing gear down differs only slightly from the above. After the engines are shifted to the idle, the landing gear control lever is moved to the "down" position, and the aircraft is decelerated until the landing gear are completely down (at high impact pressures, this may require 20-22 sec), after which the aircraft is put into the descent by smoothly but forcefully moving the stick forward. Due to the increase in drag resulting from lowering the landing gear, the overload involved in the transition may be slightly less than in the preceding case (the value may reach 0.3-0.4), since the acceleration of the aircraft to the maximum permissible M number occurs somewhat more slowly. /155

When a vertical speed of 22-24 m/sec is reached, the pressure on the stick must be decreased, and at V_y = 35-40 m/sec the rate of increase in vertical speed must be decreased, and a vertical speed must be gradually brought up to 65-70 m/sec.

Chapter IX. The Landing

§1. Diagrams of Landing Approach /155

The descent of an aircraft in the region of the airfield to the altitude of circling flight is generally performed using the outer marker beacon (OMB) or the entrance corridor beacon using the direction finder-range finder system, the on-board and ground based radars.

During the process of the descent, the aircraft is guided to the airfield so that the flying time in the region of the airport is 5-6 min. This allows the fuel expenditure to be decreased (the aircraft flies for a short period of time with landing gear down), and decreases the flying time and cost of air travel.

Therefore, the approach is either direct or uses the shortest path, in which the aircraft is brought in in the region of the third turn (Figure 102). If the approach is direct, at 25-30 km from the airfield the aircraft descends /156 to 400-600 m and decreases its speed to the landing gear down speed. When this altitude is reached, the landing gear are lowered at 12-15 km from the OMB (this range is checked using the range finder or by commands from the earth), and the flaps are lowered by 15-20°. The flaps are lowered completely before entering the glide.

During a descending approach, the speed of the aircraft is decreased in the region of the third turn during the process of descent to the circling altitude, and the landing gear are lowered. The flaps are dropped by 15-20° between the third and fourth turns. The fourth turn is performed with this flying configuration, usually at 12-16 km from the runway, the flaps are deflected fully and the aircraft follows the course to the runway at constant altitude until it enters the glide path.

With forward movement speeds in the descent of 350-500 km/hr and landing speeds of 200-250 km/hr, a jet aircraft will cover considerable distance during the process of descent and speed reduction. Therefore, the extent of the turns and particularly of the straight line sectors between turns will be correspondingly increased. As a result, after the fourth turn the aircraft will be at a considerable distance from the runway (12-16 km).

The inclination of the glide path is generally 2° 40 min-4°, as a result of which the trajectory of the aircraft (after it enters the glide path) is smooth. The glide path is entered at 7.5-8.5 km from the runway.

The OMB is generally located 4 km from the runway, the boundary marker beacon (BMB) at 1000 m from the runway. The altitude over the OMB should be 200 m, over the BMB -- 60 m. For these flying altitudes, the vertical velocity component of the aircraft should be 3-3.5 m/sec.

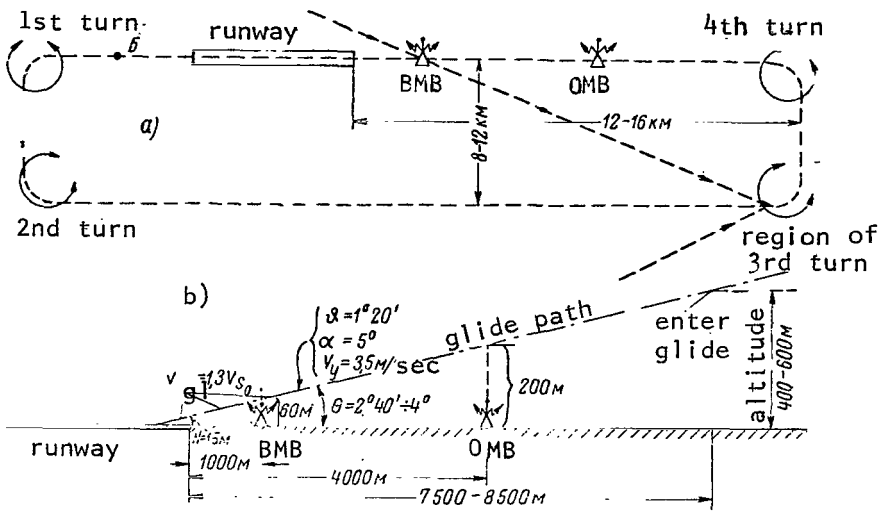

Figure 102. Diagram of Approach to Landing (a) and Glide (b)

§2. Flight After Entry into Glide Path. Selection of Gliding Speed

According to the norms of ICAO, the gliding speed during the descent on the glide path should be 30% greater than the stall speed for the landing configuration of the aircraft, i.e., $V_{gl} = 1.3\ V_{s_0}$ (where V_{s_0} is the stall speed with flaps in the gliding position).

As we can see from Figure 16, for a maximum flap angle of 38°, flow separation on the wing begins at $c_y = 1.85$. For a mean landing weight of 35 t and a wing area of 110 m^2, this corresponds to a stall speed

$$V_{s_0} = 14.4\sqrt{35{,}000/110 \cdot 1.85} = 190 \text{ km/hr.}$$

Then the gliding speed is

$$V_{gl} = 1{,}3V_{s_0} = 1{,}3 \cdot 190 \approx 250 \text{ km/hr.}$$

Before the beginning of leveling off, gliding is performed at constant speed, in this case 250 km/hr. With the standard angle of inclination of the /157

2° 40 min, the vertical rate of descent $V_y = V_{gl} \sin \Theta = 69.5 \cdot 0.0466 =$
$= 3.24$ m/sec (here sin 2° 40 min = 0.0466, $V_{gl} \approx 250$ km/hr = 69.5 m/sec).

Establishment of a constant gliding speed after complete lowering of the flaps facilitates piloting, since it does not require a change in the operating regime of the engines or a decrease in the speed from the moment of entry into the glide path until the aircraft passes over the OMB, BMB and 500-m mark, so that the pilot is less distracted from the instruments.

If the aircraft enters the glide path at 400 m altitude and 8 km range from the runway (Figure 102), flight to the OMB in calm air (the aircraft crosses the beacon at 200 m altitude) requires t = 200: 3.24 ≈ 61 sec.

The difference in altitudes of flight over the OMB and BMB is 140 m, and the time of descent for this difference t = 140: 3.24 = 43 sec. The flying speed of 250 km/hr corresponds to an angle of attack $\alpha = 5°$ (Figure 16). Let us now determine, assuming $\phi = 1°$, the position of the aircraft concerning the landing glide path, i.e., the pitch angle:
$\vartheta = -2°\ 40\ \text{min} + 5° - 1° = 1°\ 20\ \text{min}$.

Thus, the aircraft axis has a positive angle with negative descent angle Θ. If, due to high mechanization of the wing (three slit flaps and secondary control surfaces) the gliding speed is decreased (240-220 km/hr), the pitch angle increases. Therefore, the flying time from the moment the aircraft enters the glide path until it flies over the OMB and BMB at lower speeds is increased, and the pilot's reserve time increases. As a result, the fourth turn can be formed closer to the end of the runway.

As the gliding speed is decreased at the same trajectory angle, the vertical speed is decreased, and with the increasing angle of attack the pitch angle increases, worsening the view from the pilot's cabin.

Let us analyze the engine operation regime required for gliding flight of the aircraft.

With the landing gear down, flaps down and airbrake extended, the aerodynamic quality of the aircraft K = 5-6 and the gliding angle Θ = 9-10° ($\tan \Theta = 1/K = 1/5.5 = 0.183$, $\Theta \approx 10°$), but in this case the engine thrust should be near zero.

Actually, the aircraft descends along the glide path with engines operating at angle $\Theta = 2°\ 40$ min. This angle corresponds to quality

$$K = \frac{1}{\tan \theta} = \frac{1}{\tan 2°40'} = \frac{1}{0.0466} = 21.5.$$

For c_y = 1.06 (angle of attack 5°, Figure 16), we produce c_x = 0.19 (without airbrake). From this value of c_x we must subtract the value of coefficient c_R of required engine thrust, in order to maintain K = 21.5 where c_y = 1.06:

$$K=\frac{c_y}{c_x-c_R},$$ /158

from which

$$c_R=\frac{c_y}{K}-c_x=\frac{1.06}{21.5}-0.19=0.0493-0.19=|0.141|.$$

This value of thrust coefficient corresponds to a thrust consumption $P = c_R qS = 0.141 \cdot 300 \cdot 110 = 4650$ kg, i.e., 2325 kg thrust for each engine (with a two-engine aircraft). This thrust is several times greater than the idling thrust (300-500 kg). If the airbrake is extended, the thrust must be increased (to maintain the gliding angle unchanged, since c_x is increased to 0.226):

$$c_R=\frac{1.06}{21.5}-0.226=0.0493-0.226=|0.177|;$$
$$P=0.177\cdot 300\cdot 110=5840 \text{ kg}$$

As we can see, the thrust is increased by almost 25%.

If after the airbrake is extended the engine operating regime is left unchanged, the angle of inclination of the descent trajectory will be increased to 4° 30 min and the aircraft may come down before the beginning of the runway. In order to determine the new angle of descent, we must first find the quality of the aircraft from the equation $c_R = (1.06/K) - 0.226 = -0.141$:

$$K=\frac{1.06}{0.085}=12.5,$$

and then find the descent angle

$$\tan\theta=\frac{1}{K}=\frac{1}{12.5}=0.08 \text{ and } \theta=4°30'.$$

The effectiveness of the airbrake is quite high, since as c_x is increased the lift of the wing remains practically the same. Therefore, as the landing gear are lowered the aircraft has no tendency to wing stall, but only shows a change in the inclination of the trajectory.

§3. Stages in the Landing

The flight of the aircraft (descent) from 15 m (according to the ICAO norms) consist of the following main stages: 1) gliding from 15 m altitude at $V_{gl} = 1.3\ V_{s_0}$ until leveling off is begun; 2) leveling off until the moment of landing and 3) the landing run.

Figure 103 shows a diagram of the definition of required runway length and a profile of aircraft flight from 15 m downward.

The total length of the horizontal projection of the trajectory of the airborne sector and the landing run is called the landing distance. The required runway length is determined for standard and design meteorological conditions with the maximum landing weight of an aircraft and dry runway. /159

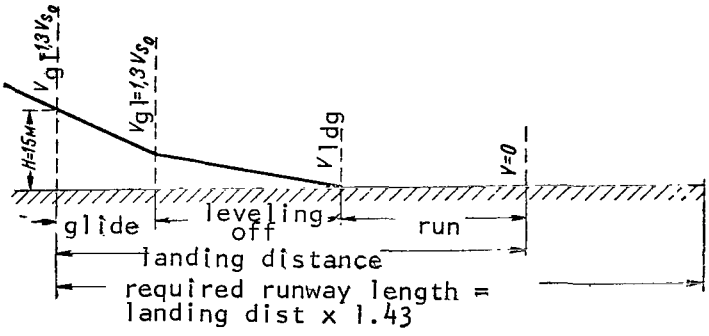

Figure 103. Profile of Descent of Aircraft from H = 15 m

Gliding -- straight line flight of the aircraft on a descending trajectory at constant velocity. Gliding is usually performed at 250-220 km/hr indicated, with an angle of attack α = 5-5.5° and c_y = 0.95-1.1.

Prelanding gliding is not gliding in its pure form, since the engines create approximately 1800-2000 kg thrust each. This thrust is required to retain the aircraft speed and retain good motor readiness in case it becomes necessary to circle once more or for additional thrust to correct the landing pattern. If the airbrake is extended, the engine operating regime must be increased by 5-6%, increasing the safety in case a second circle is required.

When gliding from 15 m to the height where the leveling is begun, the aircraft travels 150-200 m. The vertical speed in the sector is 3-5 m/sec.

With the airbrake extended, the quality is decreased to 4.5-5, and the angle of inclination of the trajectory can be increased when necessary to 9-11°. In this case, the length of the gliding sector from 15 m down decreases to 100-150 m. The vertical speed can be increased to 8-9 m/sec.

Extending the fuselage airbrake creates pitching moment and facilitates balancing the aircraft, since the flaps tend to create a pitching moment in the opposite direction. The aircraft must be balanced so that slight pulling loads are felt on the control stick at all times.

Leveling off. During leveling off, which begins at an altitude of 8-10 m, the movement of the aircraft is curved and the speed decreases. By pulling the stick back, the pilot increases the lift, which becomes greater than the weight component and therefore the trajectory is curved. In /160
practice, during leveling off the aircraft does not fly horizontally, but rather at a slight angle to the ground (0.5-0.8°). In performing this operation, the pilot decreases the angle of inclination of the trajectory and the vertical rate of descent to the point that a "soft" touchdown is provided. This decrease in speed results from two factors: first of all, the angle of attack is increased, increasing drag Q (for stable landing angles of attack 9-10°, the drag increases by 25-30%) and, secondly, before the beginning of leveling off the pilot throttles back the engines and thereby decreases their thrust. Leveling off is completed at an altitude of 1-0.5 m, so that the touchdown occurs on the main wheels at landing speed with slight parachuting. In order to retain lift during the process of leveling off, the angle of attack must be increased to the landing angle of attack. During parachuting, the lift is less than the weight of the aircraft by 25-30%.

When an aircraft lands with airbrake retracted, the length of the leveling sector is increased, while if the airbrake is extended, due to the better braking the length of the landing sector is decreased by 50-100 m.

During the leveling sector, the speed of the aircraft is decreased from V_{gl} to V_{ldg}. The length of the leveling operation depends on the difference between these speeds. With a difference of 30 km/hr, it amounts to 350-400 m. The greater the landing angle of attack (8-10°), the longer the braking of the aircraft and the greater the length of the leveling sector. As a result, the landing distance increases, in spite of the fact that the length of the run is decreased slightly by landing at high angle of attack. As flying tests have shown, it is more suitable to "brake" on the ground (during the run) than in the air, when the aerodynamic quality is rather high (6-7). This leads us to the following conclusion: in order to avoid lengthening the holding sector unnecessarily, landing should be performed with $V_{ldg} = V_{gl} - 20$ km/hr.

The run. The speed at which the aircraft touches the ground is called the landing speed. It can be determined from the following formula:

$$V_{1dg}=\sqrt{\frac{2G}{\rho S c_{y\cdot 1dg}}},$$

where $c_{y\ 1dg}$ is the lifting coefficient at the moment the aircraft touches the ground.

The run begins from the moment the aircraft wheels touch the landing strip. The movement of the aircraft during this sector is straight and slow. At first the run is accomplished on the main wheels, then by moving the stick forward the pilot lowers the nose wheels. Most of the run occurs on three points with a low angle of attack. On the polar curve, this corresponds to the standing angle of attack 1-3° (Figure 65).

Immediately after grounding, when the aircraft is rolling on two points, /161
the spoilers are deflected and wheel braking begins. Whereas at the moment of landing coefficient c_y = 1.4-1.7, after the spoilers are extended, due to the flow separation on the wing, it is decreased to 0.08-0.12. The lift decreases sharply and complete loading of the landing gear wheels occurs.

It should be noted that at the moment the spoilers are extended a negative pitch moment is acting on the aircraft and the pilot must push the stick forward slightly to hold the aircraft at the landing angle of attack.

Extending the spoilers decreases the speed of the aircraft by 40-50 km/hr, which causes the aircraft to tend to drop its nose rapidly, to which the pilot must react by pulling the stick back to allow the nose wheel to drop smoothly.

Figure 104 shows an aircraft during the landing run with spoilers extended and braking parachute out. During the process of the run, the aircraft is decelerated by the drag of the aircraft and the friction of the wheels on the ground. The slight engine thrust decreases this decelerating force.

The diagram of forces acting on the aircraft during the landing run is the same as during the takeoff run (Figure 66). The only difference is that during the landing run the thrust P is considerably less than the sum of decelerating forces F_f and Q.

During the landing run, the summary braking force is defined as the difference between decelerating forces and the thrust of the engines: $R_{br} = Q + F_f - P$. As a result of the effects of the braking force, a negative acceleration (i.e., deceleration) appears

$$j_x=\frac{R_{br}}{m}=\frac{Q+F_f-P}{G}\cdot 9{,}81.$$

It follows from the formula that the greater the sum $Q + F_f$, the greater /162
will be j_x. The friction force F_f depends on the coefficient of friction of wheels with the surface of the earth f and the force of normal pressure of the aircraft on the earth N. It has been determined by testing that for aircraft with disk brakes and spoilers running on dry concrete f = 0.2-0.3 (considering braking).

Force N depends on the landing weight of the aircraft and the lift: N = G - Y. The force of friction can be expressed by the following formula:

$$F_f = fN = f(G - Y),$$

then

$$R_{br} = Q + f(G - Y) - P.$$

At the beginning of the landing run, when the lift is only slightly less than the weight, the force of friction will be low (low difference G - Y). For example, at 200-220 km/hr, the force of friction is 4000-5000 kg (for an aircraft with a landing weight of 35-40 t). At the end of the run, when the lift is slight, the force of friction increases.

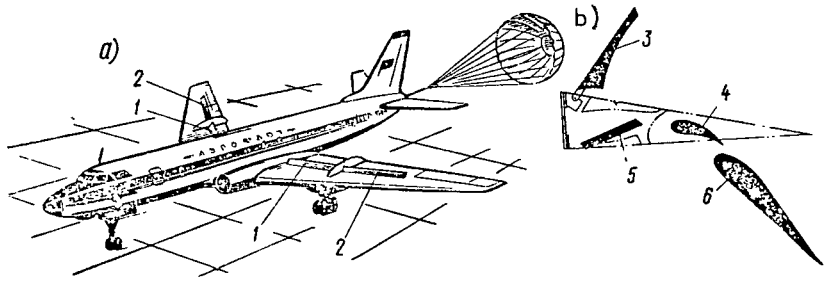

Figure 104. Aircraft During Run with Spoilers Extended and Braking Parachute Out (a) and Diagram of Opening of Spoiler (b): 1, Inner spoilers; 2, Outer spoilers; 3, Spoiler; 4, Front flap; 5, Door; 6, Flap

The force of aircraft drag at the beginning of the landing run (when the speed is near the landing speed, and angle of attack α = 9-10°) is rather great (Q = 5000-6000 kg for the same weights). This is facilitated by the lowered flaps and the airbrake.

The landing distance (Figure 103) is the summary length of the sectors of gliding, leveling and landing run. For aircraft with two engines in the tail portion of the fuselage, the landing distance is 1000-1200 m, and the required runway length (according to ICAO) is 1400-1700 m.

§4. Length of Post-landing Run and Methods of Shortening It

The kinetic energy of the aircraft at the moment of touchdown is dissipated and absorbed by the work of the braking forces: the aerodynamic drag, the friction of the wheels on the surface of the runway, the drag of braking parachutes, thrust reversal, etc. The dependences of these braking forces on the speed of the run are shown on Figure 105. The unit of braking force (drag force) used is the aerodynamic drag of the aircraft at touchdown. For example, for the TU-124, at the moment of touchdown with flaps at 30° and airbrake extended at 225 km/hr, c_x = 0.18, the aerodynamic drag Q = 4600 kg, the parachute drag is approximately 5500 kg and the braking force of the wheels is about 2500 kg. As the speed of the landing run decreases, the drag force of the parachute and the aerodynamic drag of the aircraft drop sharply, while the force of friction of the wheels increases. Thrust reversal of the engines is practically independent of the rate of movement of the aircraft. /163

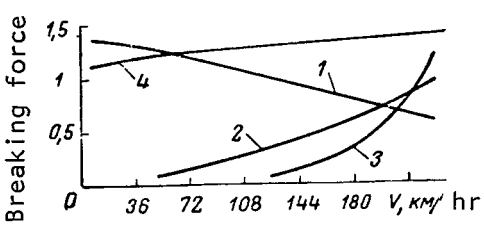

Figure 105. Nature of Change in Braking Forces During Post-landing Run of Aircraft (calculated): 1, Braking force; 2, Aerodynamic drag of aircraft; 3, Drag of braking parachute; 4, Thrust reversal

The length of the landing run of an aircraft can be determined using the formula

$$L_{l.r.} = \frac{V^2 l dg}{2 j_{x\,m.l.r.}} \text{ м},$$

where j_{xmlr} is the mean acceleration of braking (deceleration) of the aircraft during the landing run, m/sec^2.

As we can see from the formula, with fixed landing speed the length of the run can be decreased by increasing the mean braking acceleration.

During the first half of the landing run (Figure 105) the deceleration of aircraft movement is achieved under the influence of all these decelerating forces, after which the main role is played by the braking force of the wheels and thrust reversal (if there is a thrust reverser on the aircraft).

At the present time, braking wheels are equipped with special automatic braking devices, the principle of operation of which is based on the usage of the force of inertia of a flywheel rotating in parallel with the wheel.

If the wheel rotates without slipping, the flywheel in the automatic device rotates in synchronism with the landing wheel. If the wheel begins to slide, the flywheel introduces an acceleration and, working through a special device, interrupts the supply of pressure to the brake, as a result of which the braking force on the wheel is decreased. After the rotating speed of the wheel is increased once more and synchronism is established between rotation of wheel and flywheel, the pressure to the brakes is increased to the required level and the wheel is once more braked. In operation, this cycle is usually repeated quite rapidly and actually the pressure in the brakes never decreases completely. Thus, this device provides optimal braking, pumping at the boundary of sliding[1]. When this device is turned on, the pilot immediately provides full pressure in the brakes (depresses brake pedals completely).

Smoothly depressing the brakes, as is recommended for nonautomatic braking, in this case only increases the length of the landing run, since the maximum braking regime will not be used.

The usage of automatic brakes has allowed the length of the landing run /164
to be decreased by an additional 20-25%. The service life of the pneumatic system has also been increased. The mean acceleration of automatic braking is 1.7-1.8 m/sec^2 (disk brakes). In aircraft with spoilers opened at the moment of touchdown, the effectiveness of the brakes is even greater and j_{xmlr} = 2.25-2.5 m/sec^2. For example, in an aircraft with spoilers (j_m = 2.25 m/sec^2) with a landing speed of 216 km/hr (60 m/sec), L_{lr} = 800 m. For the TU-104 aircraft (no spoilers) with V_{ldg} = 240 km/hr (66.7 m/sec) with an average braking acceleration of 1.3 m/sec^2 (drum brake) the landing run length is 1700 m. For the TU-104 with disk brakes (with an average acceleration of 1.55 m/sec^2) the landing run length is 1430 m.

Even greater braking acceleration (drag) can be produced by releasing a braking parachute. For example, if the parachute is open at 225-215 km/hr, the drag is increased by 4600-4900 kg (TU-124 aircraft).

Figure 106a shows a diagram of the usage of a braking parachute. After touchdown, a button is pressed dropping the parachute from its container through hatch 1. After this, the pilot chute pulls the braking chute out, creating resistance to the movement of the aircraft. The parachute is connected to the aircraft by cable 3 through catch 2. At the end of the run, the braking parachutes are disconnected. Braking parachutes 4 are strip type, and the strength of the lines and canopy is sufficient for run /165
speeds of 260-230 km/hr. In a strip type parachute, the air partially passes through the canopy and therefore for this type of chute Δc_x = 0.25-0.55 (for an ordinary parachute Δc_x = 1.2-1.3). For example, one foreign braking parachute with a canopy diameter of 9.76 m and Δc_x = 0.55 creates a braking

[1] A. V. Chestnov, *Letnaya Ekspluatatsiya Samoleta* [Flying Operation of Aircraft], Voyenizdat. Press, 1962.

force of 17.25 t at 296 km/hr (military transport aircraft).

The length of the landing run on an ice covered runway can be reduced by 30-40% by using a braking parachute. Under these conditions, its effectiveness is particularly noticeable. However, the less the speed, the less the effectiveness of the parachute. For example, the braking parachutes on a TU-104 decrease the run length by 25-30% (wet or ice covered strip). Thus, under standard conditions for a landing weight of 58 t, the runlength is 1730 m, while the usage of the parachute reduces this figure to 1250-1350 m. The braking force is 10-14 t.

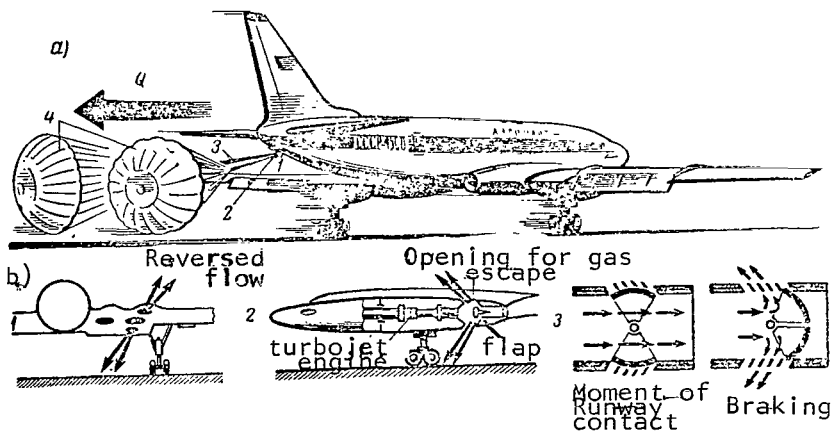

Figure 106. Usage of the Braking Parachute (a) and Diagram of Installation and Operation of Thrust Reversers (b) on Two External Aircraft Engines: 1, View from rear, reversed flow inclined by 20° from vertical; 2, Apertures for gas outlet directed at angle opposite to flight; 3, At moment of touchdown, reverse doors closed, during braking they direct gas in direction opposite movement. During taxiing, doors set in intermediate position.

One defect of this method of reducing the run length is the fact that with a side wind stronger than 6-8 m/sec at an angle of over 45° to the runway, the parachute will be deflected from the axis of the aircraft and will tend to turn the aircraft into the wind. As the side wind increases in speed, the probability of rotation also increases. However, even in this case it is recommended that the braking chute be used during the first half of the landing run, being extended immediately after touchdown (in practice with a delay of 5-7 sec). Another defect is the fact that the discarded parachute must be rapidly removed from the runway, transported, checked and packed. The service life of a braking parachute (with an average acceleration of 1.55 m/sec^2) is 40-50 landings. Calculation of the drag produced by the parachute is performed using the formula

$$Q_{par} = \Delta c_{x\,par} Sq,$$

where Δc_x is the drag of the parachute related to the wing area of the aircraft;

S is the wing area;

q is the impact pressure.

For example, for the braking parachute of a TU-124 with S_{can} = 40 m^2, $c_{x\ par}$ = 0.54 (S = 105.35 m^2):

$$\Delta c_{x\,par} = \frac{0{\cdot}54 S_{can}}{S} = \frac{0.54 \cdot 40}{105.35} = 0.205.$$

Ejection of the braking parachute at lower speed is less effective. At the end of the landing run, due to the decrease in speed and the angle of attack, which will be equal to the parked angle, force Q is practically equal to zero. It is considered that in the process of the entire landing run, an average braking force acts on the aircraft, creating a average negative acceleration

$$jx_{av} = 9.81 \frac{R_{br}}{G}.$$

The greatest value of negative acceleration is achieved after the braking parachute is extended and amounts to 4.4-4.2 m/sec^2. /166

Increasing the landing speed by 5% (from 210 to 220 km/hr) increases the length of the landing run by approximately 10%. Therefore, a decrease in landing speed is the most effective means of decreasing the run length. An increase in j_{xav} by the usage of spoilers and a braking parachute or thrust reversal of the engines can significantly shorten the landing run.

When the engine thrust is reversed, the reaction jet is directed forward and exits upward and downward at an angle to the horizontal. For example, in the two outboard engines of the English "Comet" turbojet aircraft, the reaction jet exits upward and downward at 45° to the horizontal.

The reverser (the device which deflects the flow) is rotated at 20° to the vertical, in order to direct the jet away from the fuselage and landing gear (Figure 106 b).

With sufficiently rapid movement of the aircraft, the jet will be deflected rearward and will not enter the air intakes, while at very low speeds or at rest of the aircraft the stream will move far forward.

The operating time of the reverser in a landing is generally not over 15 sec. The doors of the reversing device are operated pneumatically. The reverser is put in operation by moving a special lever forward. The throttles controlling the outboard engines must first be put in the idle position and lifted. The effectiveness of thrust reversal is decreased with decreasing aircraft speed.

However, when necessary thrust reversal can be used until the aircraft comes to a complete stop.

Thrust reversal should be applied the moment the aircraft touches the runway. The maximum reverse thrust theoretically is 70% of the forward thrust, but in practice only about 50% is realized.

The usage of thrust reversal makes it possible to decrease the landing run length by 20-25%. Also, in the "Comet-4B" aircraft the size of the flaps is increased and their angle of deflection is increased to 80°, greatly reducing the landing speed.

In aircraft with engines located in the wing and near the fuselage, the usage of thrust reversal is difficult due to the thermal effects of the reversed jets on the fuselage. It is easiest to use thrust reversers on engines mounted on pilons, as on the Boeing 707, DC-8, etc. If there are four engines mounted on the tail of the fuselage, the reversers are installed only in the outboard engines.

As was noted, in addition to braking parachutes, motor switch off during the landing run, and thrust reversal, spoilers and airbrakes are also used. The spoilers are plates which can be extended or deflected, mounted on the upper surface of the wings. One, two or three spoilers can be used on each wing. /167

The spoilers are extended after the aircraft wheels touch the runway. By separating the flow from the upper wing surface, the spoilers decrease the lifting force sharply and create considerable additional drag.

The graph on Figure 107 shows that with the spoilers closed the aerodynamic quality of the aircraft decreases from 6 to 4.4 upon transition from the landing position ($\alpha = 10°$) to the landing run position ($\alpha = 1°$); opening of the spoilers during the run decreases the aerodynamic quality by an additional factor of 4 (from 6 to 1.5).

Extending the spoilers has approximately the same influence on the dependence $c_y = f(\alpha)$.

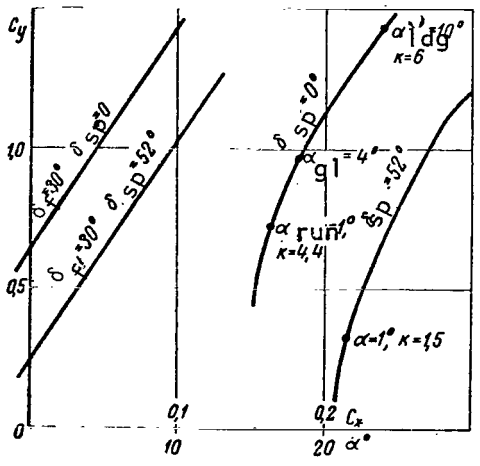

Figure 107. Coefficient c_y As a Function of Angle of Attack and Polar Curve of Aircraft During Landing (flaps down, Airbrake and Spoilers extended)

§5. Length of Landing Run As a Function of Various Operational Factors

The length of the landing run is essentially influenced by the aircraft weight, condition of the runway, direction and speed of wind, air temperature, etc. The length of the landing run also depends on the actions of the pilot in control of the aircraft.

The weight of the aircraft influences the length of the landing run primarily through the landing speed. As the weight of the aircraft is increased, the square of the landing speed is also increased and consequently the length of the landing run is increased to the same extent. For example, with landing weight of 30,000 kg, the length of the landing run under standard conditions is 930 m, whereas with a landing weight of 32,000 kg, i.e., increased by 1.065 times, the run length is increased by the same number of times and will be 930·1.065 = 990 m.

Thus, if the aircraft weight is increased by 6.5%, the run length will be increased by the same factor.

The temperature of the surrounding air influences the run length primarily through the density. As the temperature is increased with unchanged pressure, the density of the air is decreased.[2] If the temperature is increased by a certain factor, the value of V^2_{ldg} is increased by the same factor. Thus, if the temperature is increased by 5% over the standard temperature, V^2_{ldg} will be increased by approximately the same percent. /168

A decrease in density leads to a decrease in the drag Q during the run. Also, during the run the engines create a slight thrust and as the temperature is increased, this thrust is decreased, which helps to reduce the run length. If we ignore the influence of temperature on drag and thrust, we can approximately consider that an increase in temperature of 5% (for example from 15 to 30°C (from 288 to 303°K) will result in an increase in run length of approximately 5%.

It should be noted that under conditions other than the standard conditions, the landing speed indicated by the instrument (the broad

arrow) will be the same as at standard conditions, since with a change in air density the velocity indicator decreases the indicated speed due to methodic error. The fine needle of the indicator shows the true speed in this case.

The influence of head winds and tail winds on the length of the landing run is the same as this influence on the length of the takeoff run.

The braking effect is always greatest with the maximal speeds of utilization of spoilers and parachute. Therefore, a delay in using the spoilers of 1.5-2 sec increases the run length by 100-150 m, while ejection of the parachute at 180-140 km/hr decreases its braking effect by 35-50%. The wheel brakes should be applied immediately after the spoilers are extended, i.e., at 250-220 km/hr.

§6. Specific Features of Landing Runs on Dry, Ice or Snow Covered Runways

At the present time we still do not have sufficient data on methods of determining the effect of braking on wet or snow covered runways.

In spite of the variety of means of braking, the principal means remains the disk wheel brakes. It has been established that when landing on a dry concrete runway, about 70% of the energy of movement of the aircraft is absorbed by the brakes, and 30% by aerodynamic drag of the aircraft (usage of flaps and airbrakes). When landing on a wet runway, only about 50% of the kinetic energy is absorbed by the brakes, or if the tires are worn -- even less. The wheel brakes have an important role to play during a landing run if flight is terminated at speeds less than the separation speed by 15-20%, in which the spoilers and landing parachute are less effective. The pressure in the tires has a great influence on the effectiveness of braking: the less the pressure, the greater the contact area and the more reliably the brakes operate.

At the present time, the runway length required for aircraft operation is determined either on the basis of the condition of the provision of safety of interrupted or extended takeoff (see Figure 71), or from the conditions of the /169
conditions of the landing characteristics of the aircraft (see Figure 103). These characteristics are generally calculated for a dry runway surface. However, at most airports due to climatic conditions over one third of the year or perhaps even more the runway surfaces are moist, snow covered or frozen. Statistics show that on the world scale, one landing of twelve is performed on a wet runway[1].

[1] *Zarubezhnyy Aviatransport*, (Foreign Air Transport) No. 7, ONTI GOSNII GA [Technical Information Department, State Scientific Research Institute for Civil Aviation], 1965.

The experience of operation of domestic turbojet and turboprop aircraft, as well as data from foreign practice indicate that the presence of slush (wet snow, water) on runway surfaces has the following negative influence on the design of aircraft and landing operations: 1) additional drag appears as the slush strikes the aircraft, particularly in the case of aircraft with heavy landing gear; 2) the danger arises that liquid may enter the engine air intake; 3) controllability of the aircraft is reduced; and 4) the landing run length is significantly increased.

Pavements for runways include concrete, asphalt, etc. On a moist or wet runway, the wheel roll drag increases, but the coupling force between wheel and runway during braking decreases (in comparison to dry pavement). This results in an increase in the landing run length of the aircraft. This increase is so great that in many cases the length of the runway may be insufficient to complete the landing run.

A moist runway is understood to be the condition in which the pavement is moistened with water (after rain), while a wet runway means that there is a layer of water on the runway 2-3 mm thick. Tests performed in the USA showed that with a certain thickness of water on the runway and with certain parameters of the tires, the critical speed can be reached at which the tires are completely separated from the surface of the road by hydrodynamic forces created by the liquid between the tire and the surface of the runway (Figure 108 a). This speed is called the skidding speed or speed of hydroplaning.

The effect of aquaplaning significantly increases the landing run length on a wet runway. Investigations have shown that aquaplaning arises at speeds averaging over 160 km/hr. When this occurs, the contact between wheels and pavement is lost and a flim of water appears between them. This results in a loss of effectiveness of brakes and makes it difficult to maintain the direction of the landing run. The phenomenon of aquaplaning is explained by the fact that a hydrodynamic force acting on the surface of the pavement arises as the aircraft moves over the runway. When its vertical component becomes equal to or greater than the weight of the aircraft, contact of the wheels with the runway is lost. /170

The graph on Figure 108 b was produced theoretically and confirmed experimentally. Using this graph (with known pressure in the tires), we can establish the limiting speed, above which usage of the wheel brakes during a landing on wet surface is useless, or even dangerous in case of a strong side wind, so that only aerodynamic brakes should be used. As soon as the speed drops below the aquaplaning speed, the wheel brakes can be used.

At the moment the brakes are applied, a friction coupling force appears between aircraft wheels and runway. In some cases braking may result in wheel lockup (100% skid) i.e., a situation in which the movement of the aircraft with nonrotating wheels (skid) causes the force of friction to decrease, increasing the length of the landing run. The interaction of the braking wheel with the runway surface is generally evaluated by the coupling

coefficient or coefficient of friction, equal to the ratio of the tangential braking force to the normal loading on the wheel.

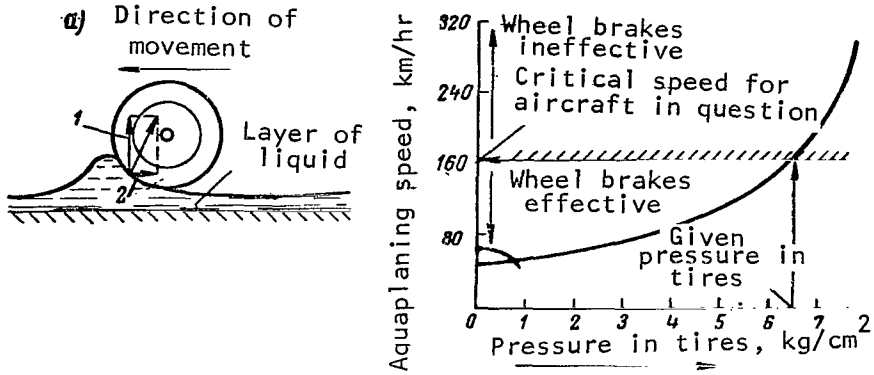

Figure 108. Formation of Hydrodynamic Lifting Force As Wheels Roll Along Wet Runway (a) and Aquaplaning Speed As a Function of Pressure and Tires (b): 1-2, Hydrodynamic lift and drag

On a clean, dry surface, the coupling coefficient of the tires is quite high and, if the rubber does not melt or burn due to the high temperature at the point of contact with the runway surface, this coefficient may vary between 0.7 and 0.8 depending on the tread profile (dry concrete). As the speed of the aircraft is increased, the coefficient decreases by 2-3 times.

Therefore, the mean value of coupling coefficient for a dry concrete runway is 0.15-0.25; for a moist runway this figure is 0.1-0.21 and for a wet runway, about 0.21[1]. For an asphalt runway (according to the data of the State Planning Institute and the Scientific Research Institute for Civil Aviation)[2], the coupling coefficient for all of the pavement conditions analyzed above is somewhat higher: from 0.33 to 0.23; for snow covered cement and asphalt pavements it is 0.3-0.25. Therefore the calculated landing run length of an aircraft on these pavements is 15-20% less. /171

When landing on an ice covered runway, the effectiveness of the brakes is sharply decreased, by an average of 25-30% in comparison with a landing on a dry, concrete runway. Due to this, it is generally recommended that a braking parachute be used, that one or two engines be shut down, etc. It is known that rapid dropping of the front wheel onto the runway after touchdown creates the best conditions for braking. However, as a rule, this method is most suitable for a dry runway pavement, since on wet pavement, frozen or

[1] Chestnov, A. V., *Letnaya Ekspluatatsiya Samoleta* [Flying Operation of the Aircraft], Voyenizdat. Press, 1962.
[2] GPI and NIIGA.

snow covered pavement, the braking effect of the wheels is reduced. Under these conditions, we must keep in mind the fact that running with the front wheel up creates additional aerodynamic drag, which is the main braking effect during this portion of the run. It is particularly difficult to perform a landing (or takeoff) on a runway covered with wet snow. Experience has shown that a layer of wet snow 25 mm thick increases the takeoff run length by 60%, and that a layer 75 mm thick makes a takeoff impossible.

The maximum permissible depth of a layer of liquid or water has been experimentally established as 12.7 mm. This depth will require an increase in takeoff run length of 20-30%.

§7. Landing with Side Wind

The side wind means the wind velocity component directed perpendicular to the runway.

At the present time, landings with side winds are made by the method of course lead, i.e., drift of the aircraft is compensated for by creating a certain lead angle ε in the course of the aircraft after exit from the fourth turn (Figure 109). If the course of the aircraft is changed by angle ε, determined from the relationship $\tan \varepsilon = W/V_g$, the ground speed V_g will be directed along the runway. Thus, if V_g = 250 km/hr, while W = 10 m/sec, the lead angle $\varepsilon = 8°$. However, during leveling off and holding the speed of the aircraft will decrease and the initial lead angle will become too low; the aircraft will begin to drift off of the runway. Therefore, at the moment of touchdown, the lead angle must be increased by approximately 1-1.5°.

The crew should have good visibility from the cockpit at lead angles of /172
10-15°, which are required with a side wind above 15 m/sec.

When drift is compensated for by a variation in landing course, the longitudinal axis of the aircraft does not correspond to the direction of movement, and flight is performed without slipping or bank. At the moment of touchdown, the control wheel should be turned in the direction of the drift, rotating the aircraft along the runway by lead angle ε. If when this maneuver is performed the longitudinal axis still makes a certain angle with the direction of the runway, side force Z will act against the wheels, tending to rotate the aircraft along the runway, since it is applied behind the center of gravity of the aircraft; however, this effect is not dangerous for the landing organs. As we can see from Figure 110, the nose wheel presents no moment, since it is oriented freely along the direction of movement while the side friction force on the main wheels creates stabilizing moment, tending to rotate the aircraft to line up with the runway. With a side wind, gliding should be performed at higher speeds (10 km/hr higher), and the landing speed should be 5-10 km/hr higher than the normal recommended speed. The pilot must control his aircraft on the approach to the landing strip carefully, being sure not to level off high or touchdown hard. The front leg must be lowered

immediately after landing in order to avoid zooming and to maintain the direction from the landing run using the control wheel. The control stick should be pushed forward to the stop in order to bring the nose wheel down to the pavement.

When landing with a side wind, the length of the landing run is increased by 10-15%. The maximum permissible value of side wind component (90° to runway axis) is 12-15 m/sec. In case of a large rotational moment, the down-wind engine may be switched off, the braking parachute can be released, thrust reversal and braking can be used. /173

§8. The "Minimum" Weather for Landings and Takeoffs

The takeoff-landing characteristics of an aircraft determine the limiting meteorological conditions ("minimum weather") for which operation of the aircraft (takeoff and landing) can be permitted.

The conditions include: a) minimum ceiling; b) minimum visibility at runway level; c) minimum lateral component of wind speed W_z.

The minimum ceiling determines the flying altitude to which the aircraft should come down out of the clouds and clear visibility of reference points on the ground or runway lights should be established. At this altitude, the crew can guide the aircraft down on the landing line visually. For turbojet aircraft landing at airfields equipped with ILS, with a glide path angle of 2° 40 min, the minimum cloud cover ceiling is 60-100 m.

The minimum visibility is considered the range at which the crew of an aircraft begins to see reference points on the ground and the beginning of the runway during the daytime, or landing lights and the illuminated runway surface at night. This range should be sufficient to make it possible to correct inaccuracies in aircraft course and separation from runway axis. The accuracy of guidance of the aircraft relative to the center line of the runway depends on the accuracy of output of course data by on-board and ground base apparatus and the precision of piloting according to the indicator on board the aircraft. Experiments performed by GOSNII GA[1] have established that for passenger jet aircraft the mean value of total deviation from the runway axis is ±60 m. Coming down out of the clouds with this amount of error, the pilot must correct the error with two sequential turns (Figure 111). During this time, the aircraft continues to descend on the glide path, generally between 2° 40 min and 4° (the higher value for airfields with difficult approaches). The time required to correct lateral deflection is influenced considerably by the inertia of the aircraft, its delay (4-5 sec) to movements

[1] S. M. Yeger, *Proyektirovaniye Passazhirskikh Reaktivnykh Samoletov* [Design of Jet Passenger Aircraft], Mashinostroyeniye Press, 1964.

of the control organs and the characteristics of lateral and transverse stability. Furthermore, an additional 2-3 sec is required for crew reaction from the time when the runway can first be seen. Therefore, it is required /174 that upon approach to the BMB or after flying over the BMB the crew of the aircraft must be able to see the beginning of the runway from the point of beginning of leveling off down to the touchdown (which in practice is 250-300 m from the beginning of the runway). Minimum visibility is then 800-1200 m, or 1500 m for night landings.

Thus, the transition to visual flight (exit from the cloud cover at 60-100 m for a glide path angle of 2° 40 min) occurs at 1250-1500 m from the beginning of the runway and during the subsequent 6-7 sec of flight (240-250 km/hr velocity) the crew must have a clear view of the runway, the point of beginning of leveling off and the point of touchdown. During this time, the pilot can perform course maneuvers if the aircraft is coming in at an angle, completing his maneuvers by the time he reaches an altitude of 40-50 m (at 600-800 m from the runway). Below an altitude of 50 m, it is forbidden for a jet aircraft to pull up for a second circle. This altitude corresponds approximately to flight over the BMB, and the crew should take all steps to assure a normal landing from this point.

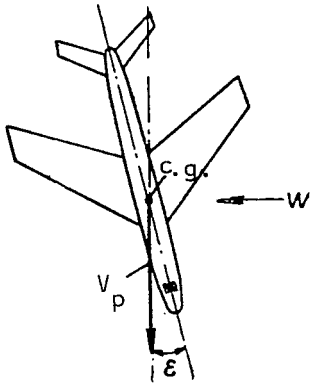

Figure 109. Elimination of Landing Drift by Course Lead Method (flight with leading course)

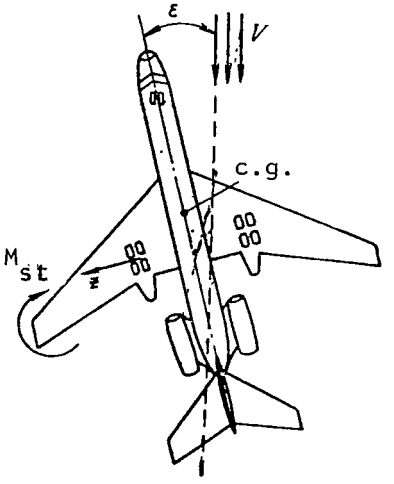

Figure 110. Diagram of Landing Run After Touchdown with Lead Angle ε

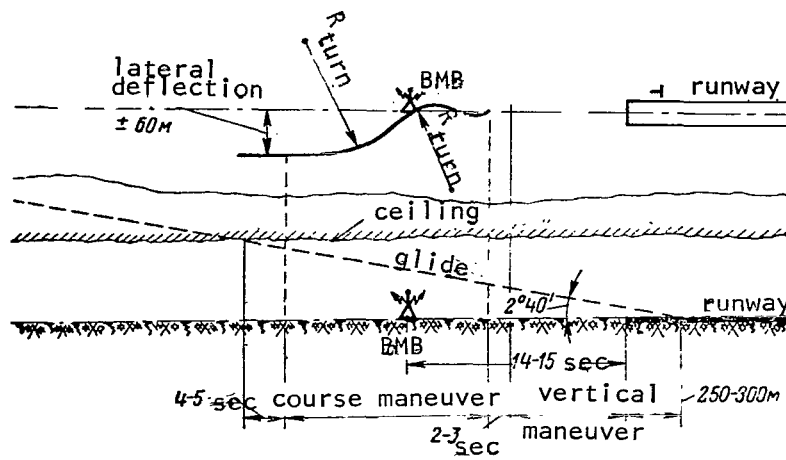

Figure 111. Determination of "Minimum Weather"

With lateral deviations of ±60 m and a gliding speed of 250-240 km/hr, the required ground length to bring the aircraft over to the landing line is 800-900 m. If the aircraft comes out of the clouds at 100 m altitude and 1800-1900 m range from the runway and the pilot, upon seeing the runway, decides to turn the aircraft, he can complete his maneuver at 600-700 m from the runway and bring the aircraft onto the landing course. With greater deviations (70-100 m) the required ground length is 1000-1200 m and the pilot will not be able to bring the aircraft onto the course line and perform his landing in the space available. Therefore, the radar controller guiding the /175
aircraft into a landing, upon determining this abnormal deviation of the aircraft from its course, should forbid the landing (before the aircraft gets down to 50 m altitude) and require the aircraft to go into a second circle.

The "minimum weather" is established not only from considerations of safety of landing of the aircraft under poor weather conditions, but also from considerations of takeoff safety. As was stated above, the height at which the aircraft flies over the BMB in case of extended takeoff with one non-operating motor is 20-25 m. If the height of obstacles in this flight sector is not over 11-14 m, there is no limit on the ceiling. Horizontal visibility should be at least 600-800 m. This quantity is determined as follows.

During a climb after takeoff, the pitch angle ϑ = 6-8° (depending on the angle of the climbing trajectory Θ). The angle of view downward from the crew's cabin for modern aircraft is 15-20°.

After takeoff at 60-70 m altitude (when the landing gear and flaps are raised) the crew should see the runway or orientation points on the surface such as approach lights (in order to maintain the takeoff course) at least 400-500 m in front of the aircraft. The additional visibility reserve due to

the slower reaction of the pilot is generally 2-3 sec, corresponding to an additional 200-300 m. Thus, the minimum visibility during a takeoff should be 600-800 m.

§9. Moving into a Second Circle

An aircraft may move into a second circle during any stage of the landing approach, including the leveling off. High power reserve makes it possible to move off into a second circle even with one motor out of operation (TU-104, TU-124, TU-134).

The decreased pickup of turbojet engines does influence the behavior of the aircraft at the moment the transition is made to the second circle. The problem is that the time required for the engine to shift from the idling regime (300-600 kg thrust) to the nominal thrust regime or higher is 15-18 sec, while in practice after 6-7 sec, i.e., after the throttle is placed in the "maximum thrust" position, the engine thrust reaches a value sufficient to provide not only horizontal flight, but some climb. On the basis of this, a unified method of piloting in case it becomes necessary to make a second circle has been developed (by Candidate of Technical Sciences M. V. Rozenblat).

After deciding to enter a second circle, the pilot sets the throttle to the maximum position. If the airbrake has been extended, its switch is shifted to the "retract" position. The aircraft is brought out of the descent and the speed is retained unchanged until the aircraft begins to climb. Six to eight sec after the throttles are pushed into the maximum position, the engines will develop thrust equal to 75-80% of the maximum (Figure 112, point 2), which will overcome the drag of the aircraft with some excess power available. When the available power exceeds the required power, the aircraft will begin to climb. /176

When necessary (for example with increased vertical descent rate) in order to decrease the rate of descent, immediately after the engines are shifted to the maximum regime the flight speed can be smoothly reduced by 10-15 km/hr, but never below the established gliding speed.

After the aircraft is shifted into a climb and the engines reach the maximum regime, the landing gear are brought up, causing the flying speed to increase sharply. When a safe speed is achieved and an altitude of 80-100 m is reached, the flaps are raised, and the engines are shifted to the nominal or cruising regime. The landing gear should not be raised until the engines reach a regime providing sufficient thrust for flight, since the drag of the aircraft is increased when the landing gear storage bay doors are opened causing the rate of descent to increase. The graph of Figure 112 shows that the aircraft continues to descend until the engines reach the required regime; when the vertical velocity component V_y = 3.5-4 m/sec, the additional descent will be 15-20 m. With V_y = 5-7 m/sec, the additional descent will be 30-40 m if the speed is retained the same, or 20-25 m if the flight speed is decreased

by 10-15 km/hr. Therefore, the lowest safe altitude for the decision to make a second circle with landing gear down, flaps in the landing position and airbrake on is usually 50 m. With the additional descent of up to 30 m, an altitude reserve is thus guaranteed.

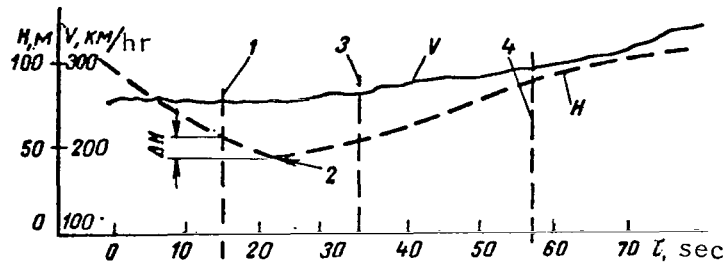

Figure 112. Change in Altitude and Flight Speed of TU-124 Aircraft upon Transition to Second Circle from Altitude of 75 m (average weight 33 t, $\delta_f = 30°$ and $\delta_{ab} = 40°$):

1, Moment of throttle shift and beginning of retraction of airbrake; 2, Moment of achievement of 75-80% maximum thrust by engines; 3, Moment of transition of engines to takeoff regime and beginning of raising of landing gear; 4, Beginning of raising of flaps

If the speed of the aircraft is decreased by 10-15 km/hr in the range of gliding speeds 240-260 km/hr, the additional climb resulting from kinetic energy is 18-25 m.

§1. Diagram of Forces Operating During Cornering

Of all of the curved trajectory maneuvers in the horizontal and vertical planes, the transport aircraft is permitted to perform only the cornering maneuver -- flight in a curved trajectory in the horizontal plane with a 360-degree turn. A portion of a cornering maneuver is called a turn. A stable cornering maneuver without slipping is considered proper.

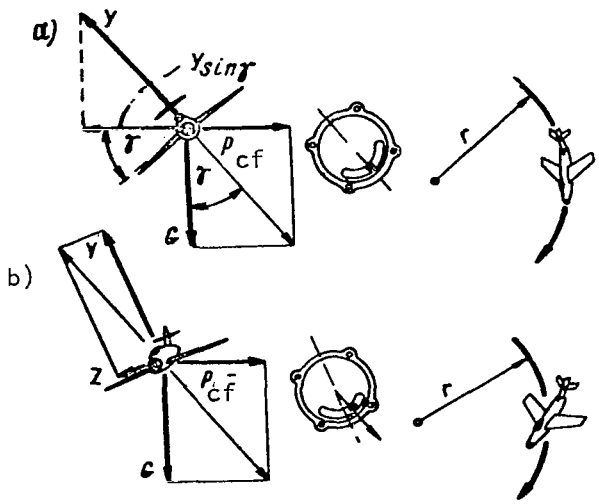

Figure 113. Forces Acting on Aircraft During Cornering: a, Proper cornering; b, Cornering with outward slip (nose of aircraft deflected toward interior of turn)

In order to perform cornering it is necessary that an unbalanced force act on the aircraft, curving the trajectory, and directed perpendicular to the trajectory (Figure 113). This force is a component of the lifting force Y sin γ (where γ is the bank angle), produced when the aircraft is banked. This force is called centripetal; it results in the appearance of a force equal and opposite to the centrifugal force:

$$P_{cf} = \frac{G}{g} \cdot \frac{V^2}{r} = m \frac{V^2}{r},$$

where m is the mass of the aircraft;

V is the speed in the turn;

r is the radius of the turn.

As the banking angle is increased in a proper turn, the lifting force must be increased so that its vertical component Y cos γ continues to balance the weight of the aircraft. /178

The forces acting on the aircraft during a horizontal turn should satisfy the following equalities

$$G=Y\cos\gamma;\ P=Q.$$

If Y is expressed through the overload n = Y/G, then

$$n_y=\frac{1}{\cos\gamma}.$$

This formula shows the relationship between overloading, which must be used to perform the horizontal turn and the banking angle γ (Figure 114). As we can see from the graph, in order to perform a horizontal turn at $\gamma = 60°$, we must create $n_y = 2$.

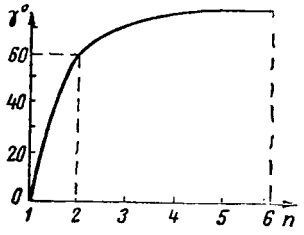

Figure 114. Overload As a Function of Banking Angle

In passenger aircraft, the bank angle is usually set at 20-30°, which affords the necessary maneuverability.

During an approach to landing under instrument flight rules, the bank cannot exceed 15°.

With most modern aircraft, horizontal turns are performed using the ailerons alone, almost without using the rudder, with the aircraft "itself" selecting an angular turning rate so that there will be no slippage. This has become possible due to the high degree of directional stability, which greatly facilitates maintenance of so-called "coordination," i.e., a combination of operations of the ailerons and rudder for which the velocity vector remains in the plane of symmetry of the aircraft and no slipping occurs[1].

§2. Cornering Parameters

Cornering parameters include the radius of the horizontal turn, time of the turn, angular velocity of the turn, etc.

The following formulas are known for the radius and time of a horizontal turn:

[1] M. L. Gallay, "Lateral and Directional Stability of the Aircraft," *Letchiku o Prakticheskoy Aerodinamike* [Practical Aerodynamics for the Pilot], Voyenizdat. Press, 1961.

$$r=\frac{V^2_{cor}}{g\cdot tg\,\gamma}=\frac{V^2_{cor}}{g\sqrt{n^2-1}};\ t_{cor}=0.64\frac{V_{cor}}{tg\,\gamma},$$

where V_{cor} is the speed during the cornering maneuver;
g is the acceleration of gravity; /179
n is the overload;
γ is the bank angle of the aircraft.

We can see from the formula that the radius of the turn depends strongly on the flight speed, increasing rapidly with increasing speed. The radius of the horizontal turn can be decreased by increasing the overloading, i.e., by increasing the bank angle of the aircraft.

During cornering, the aircraft has an angular velocity of

$$\omega=\frac{V_{cor}}{r}=\frac{g\sqrt{n^2-1}}{V_{cor}}.$$

Let us calculate the radius of turns performed during the landing approach around a large, rectangular course (γ = 15°, tan 15° = 0.268).

If the bank angles and the turns are greater than 15°, the maneuverability of the aircraft increases and the landing approach time decreases (the reserve of pilot's time increases).

For all aircraft, the first turn in the approach to landing begins according to the diagram at 2800 m altitude and 450 km/hr indicated speed. Let us define the radius of the first turn for a mean altitude of 2000 m, keeping in mind that the indicated speed of 450 km/hr corresponds to a mean air speed of 486 km/hr (135 m/sec):

$$r=\frac{V^2_{cor}}{g\,tg\,\gamma}=\frac{135^2}{9.81\cdot0.268}=\frac{18\,200}{9.81\cdot0.268}=6900\text{ m}$$

Where γ = 20° (tan 20° = 0.363), we produce r = 5100 m.

Let us determine the radius of the third turn when flying at V_{ind} = = 350 km/hr and γ = 15°:

Note: Tg = Tan

$$r=\frac{9480}{9.81\cdot 0.268}\approx 3600 \text{ m}$$

At angle γ = 20° and the same speed, the radius of the turn will be 2660 m.

On the fourth turn at V_{ind} = 320 km/hr and γ = 15° (landing gear down, flaps down 15°), r = 3000 m, and at 20° bank, r = 2200 m.

Let us determine the time for a turn with a bank angle of 15°. An increase in the radius of a turn also results in an increase in time required to perform the turn. The formula presented for t_{cor} is used to calculate the time for a complete cornering maneuver, i.e., a 360-degree turn. Usually, the aircraft performs turns of 180, 90 or fewer degrees.

The time required for a 180-degree turn (first and second turns performed together) is

$$t=0.64\cdot\frac{135}{0.268}\cdot 0.5=161.5 \text{ sec}=2 \text{ min } 41.5 \text{ sec}.$$

The time for the third turn is /180

$$t=0.64\cdot\frac{97.2}{0.268}\cdot 0.25=58 \text{ sec}.$$

The time for the fourth turn is

$$t=0.64\cdot\frac{89.0}{0.268}\cdot 0.25=53 \text{ sec}.$$

The angular velocity of rotation during the performance of the fourth turn is

$$\omega=\frac{V}{r}=\frac{89}{3000}=0.03 \text{ rad/sec}=1.7 \text{ deg/sec}.$$

CHAPTER XI

STABILITY AND CONTROLABILITY OF AIRCRAFT

§1. General Concepts on Aircraft Equilibrium

In studying the stability and controllability of an aircraft, it is represented as a body moving under the influence of external forces and rotating under the influence of the moments of these forces.

In any flight, equilibrium of forces and moments acting on the aircraft must be observed.

Equilibrium of the aircraft in flight is what we call the state in which the forces and moments acting on the aircraft cause no rotation, i.e., the given state is not disrupted.

In all flight modes, the aircraft should be balanced both in the longitudinal and lateral directions. Balancing means achievement of equilibribrium of moments using the control surfaces in any flight mode.

Equilibrium of forces and moments acting on the aircraft is analyzed relative to the three coordinate axes passing through its center of gravity. The coordinate axes used (Figure 115) are the longitudinal axis of the aircraft ox, the transverse axis oz and the vertical axis oy.

Figure 115 also shows the following moments: M_y is the yaw or track angle, rotating the aircraft about axis oy, and is considered positive if the aircraft rotates its bow to the left; M_x is the bank moment or the transverse moment, rotating aircraft around the ox axis, and is considered positive if the aircraft rotates toward the right wing; M_z is the pitch moment or the longitudinal moment, rotating the aircraft about the oz axis, and is called positive if the aircraft tends to lift its bow.

Equilibrium of the aircraft about these axes is divided into longitudinal equilibrium (about the axis oz), transverse equilibrium (about the axis ox) and track equilibrium (about the axis oy).

Three characteristic forms of body equilibrium are known: stable, unstable and neutral equilibrium. An example illustrating these forms of equilibrium might be the behavior of a ball on surfaces of various forms. The behavior of a ball on a concave curved surface characterizes stable equilibrium, on a convex surface -- unstable equilibrium and on a flat surface -- neutral equilibrium.

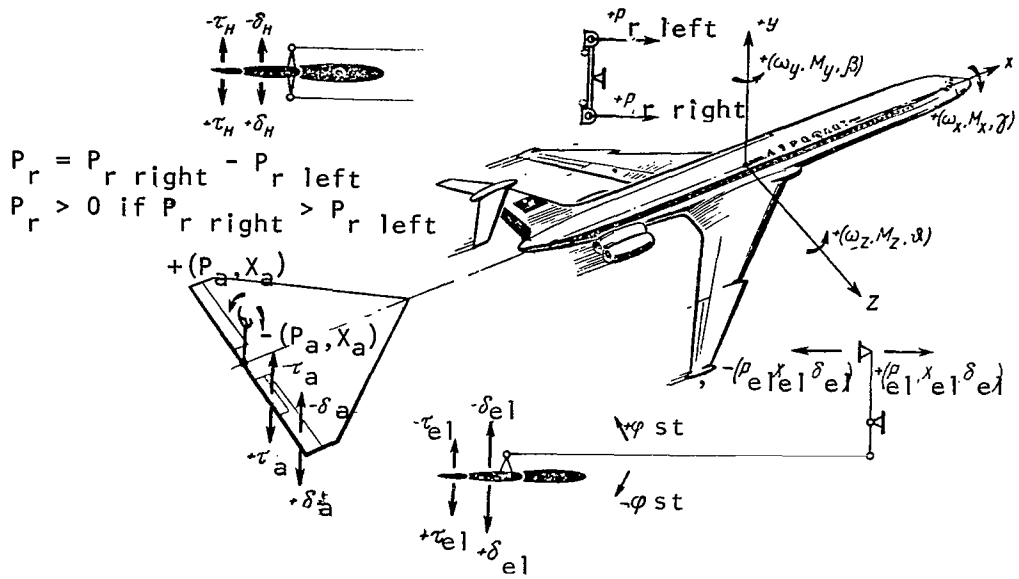

Figure 115. System of Aircraft Axes and Symbols Used for Moments of Angular Velocities, Deflection of Control Surfaces and Forces on Command Levers

Although aircraft equilibrium is a more complex phenomenon than the equilibrium of a ball, in flight an aircraft may be in the stable, unstable or neutral states. In correspondence with these forms of equilibrium, the aircraft is called stable, unstable or neutral. An unstable or neutral aircraft cannot satisfy the requirements of normal control in flight.

§2. Static and Dynamic Stability

The stability of an aircraft is its ability to retain its flight regime or return to its initial balanced regime in case of an arbitrary deviation resulting from external perturbations, without the aid of the pilot.

At the present time, books on aerodynamics frequently divide stability arbitrarily into static and dynamic stability, although in actuality an aircraft simply has stability, meaning the ability of the aircraft to return to movement at the initial kinematic parameters (velocity, angle of attack, etc.) after a perturbation is removed or, as they say, the ability of the aircraft to retain the initial flight regime.

Therefore, the stability of an aircraft consists of static stability and good damping properties, which determine and characterize the quality of the transient process when the equilibrium of the aircraft is disrupted. This is frequently called dynamic stability.

Let us analyze these properties of an aircraft individually in somewhat more detail.

In flight, an aircraft is subject to the effects of turbulence of the atmosphere, as well as short duration perturbations created by random deviations of the control surfaces by the pilot, etc. The perturbing moments disrupt the equilibrium of forces, causing the trajectory of the aircraft to curve and the velocity of the aircraft to change. The summary movement of the aircraft produced by adding the initial unperturbed and supplementary motions, is called the perturbed movement.

Static stability means the property of an aircraft causing it to create stabilizing moments when equilibrium is disrupted. For example, if a negative pitching moment arises and acts on the aircraft when the angle of attack is increased, this will be a stabilizing moment. Also, on the right wing causes a moment to arise tending to turn the aircraft to the right, it will also be a stabilizing moment.

Thus, if when equilibrium is disrupted, moments arise tending to restore the initial equilibrium position of the aircraft, the aircraft is called statically stable. The presence of static stability makes it possible for the pilot to control the aircraft normally, and to take proper control actions in emergency situations.

Dynamic stability means the tendency of an aircraft, after a perturbing force is removed, to restore the initial flight regime (velocity, altitude, overloading, flight direction) without interference from the pilot. Dynamic stability of the aircraft is characterized by: the period of damping of oscillations T, the time of damping of oscillations T_d (during which time the initial amplitude of oscillations is decreased by a factor of 20), the decrease in oscillating amplitude A in one period $m_d = A_1/A_3$ (Figure 116) and the relative oscillation damping coefficient ζ. Coefficient ζ determines the quality of the transient process or, in other words, the intensity of damping of oscillations from a perturbing movement.

In a dynamically stable aircraft, perturbed movement must be damped. The /183
movement may be either aperiodic (nonoscillating), in which a perturbed movement is rapidly damped, or periodic (oscillating), in which damping occurs with a certain amplitude and requires somewhat more time (Figure 117).

A neutral aircraft shows no tendency toward damping or increase in perturbations (Figure 117 b), while a dynamically unstable aircraft shows a tendency toward increased amplitude of perturbations with time (Figure 117 c).

Weak damping and oscillating periods which are too long are characteristics of poor aircraft stability. As the period is increased, the perturbed movement of the aircraft is "stretched out," i.e., extends over a longer period of time.

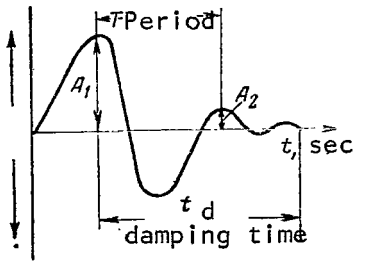

Figure 116. Determination of Characteristics of Short Period Damping Perturbed Movement (A_1, A_2 are amplitudes)

As we can see from Figure 118, the behavior of a dynamically unstable aircraft is characterized by an aperiodic increase in the pitch angle, that of a dynamically stable aircraft by damping oscillations.

If neither stabilizing nor destabilizing moments arise when the aircraft deviates from the equilibrium state, the aircraft is called statically neutral (Figure 118 c). /184

Static stability alone is insufficient to insure that the aircraft will have dynamic stability. This requires additional damping and inertial properties, as well as a proper relationship of characteristics of static stability relative to the various axes.

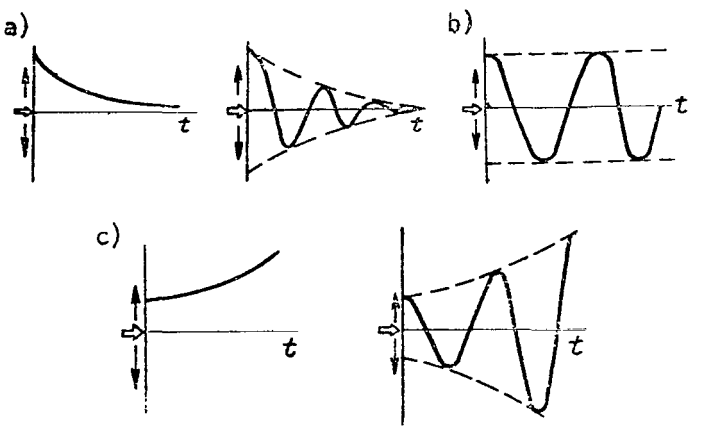

Figure 117. Characteristics of Perturbed Movement of Stable (a), Neutral (b) and Unstable (c) Aircraft (arrow shows initial equilibrium position)

The damping moments formed when the aircraft is rotated have a tremendous role to play in suppression of oscillations and provision of good controllability for example, longitudinal damping (pitch damping) is created primarily by the horizontal tail surfaces, while yaw damping (track damping) is produced by the vertical tail surfaces of the aircraft. When rotation about the ox axis occurs, the wings create a transverse damping moment.

With weak damping, aircraft oscillations will be attenuated slowly, particularly at altitudes of 10,000-11,000 m, and a great deal of time will be required for restoration of equilibrium. With too strong damping, the return to the equilibrium state is also delayed.

The inertial properties of an aircraft are characterized by its ability to retain the state of equilibrium or its previous angular rotational

velocity. The greater the moment of inertia, the more slowly the aircraft reacts to deflections of the stick and pedals. Jet aircraft have high moments of inertia relative to the y and z axes, since they have a relatively long fuselage, in which the main mass of the load is concentrated about the center of gravity. The moment of inertia relative to the x axis is less, since the wing span is less than the length of the fuselage.

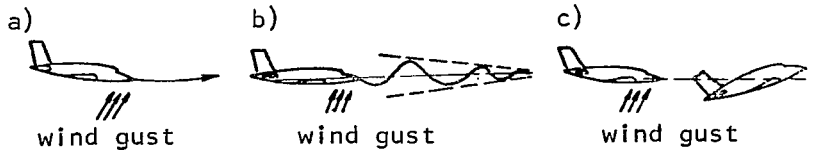

Figure 118. Behavior of Dynamically Unstable (a), Stable (b) and Neutral (c) Aircraft During Perturbed Motion

§3. Controllability of an Aircraft

The controllability of an aircraft is an important piloting characteristic, and means its capability to respond to the pilot's movements of the rudder and ailerons with corresponding movements in space or, as they say, the /185
ability of the aircraft to "follow the control surfaces." In controlling the aircraft, the pilot moves the stick and pedals and evaluates the behavior of the aircraft by the forces on the control surfaces. By moving the various surfaces, the pilot overcomes the inertial, damping and restoring moments acting on the aircraft.

If the forces are extremely high, the pilot will become fatigued during maneuvering. Such aircraft are described as being heavy to control. Unnecessarily light control should also be avoided, since it makes precise control of movements of control surfaces difficult and may cause the aircraft to shake.

The control surfaces should make it possible to balance the aircraft in all flight regimes used. This is evaluated using balancing curves, which characterize the change in balance angles of control surface deflection (and correspondingly the position of the control levers, as well as the forces on them) at various stable flight regimes as a function of a change in one of the parameters determining the regime (for example, flight speed, M number, angle of attack or slip angle, etc.).

The pilot also judges the controllability of an aircraft from the reaction of the aircraft to deflections of the control levers during maneuvering.

Controllability is divided into three forms: longitudinal, directional and transverse. The ability of the aircraft to rotate about the ox axis under the influence of the ailerons is called transverse controllability, about the oy axis under the influence of the rudder is called directional controllability

and about the oz axis under the influence of the elevator is called longitudinal controllability.

Characteristics of longitudinal controllability include the amount of elevator and stick travel required to change the aircraft velocity by a fixed amount, as well as the force applied to the stick by the pilot. One of the most important characteristics is the force gradient with respect to overloading $\Delta P_{el}/\Delta n_y$, showing the force which must be applied to the stick to change overloading by one unit.

The following parameters are used as characteristics of transverse controllability.

1) The force which must be applied to the stick to give the aircraft an angular rotation velocity about the ox axis of 1 rad/sec:

$$P_a^{\omega} = \frac{\Delta P_a}{\Delta \omega_x},$$

where ΔP_a is the force applied to the aileron control lever;

$\Delta \omega_x$ is the change in angular velocity of 1 rad/sec;

2) The force which must be applied to the control lever to balance the aircraft in straight line flight with a slip of one degree or a bank of one degree: /186

$$P_a^{\beta} = \frac{\Delta P_a}{\Delta \beta} \quad \text{or} \quad P_a^{\gamma} = \frac{\Delta P_a}{\Delta \gamma},$$

where $\Delta\beta$ is the change in slip angle of one degree;

$\Delta\gamma$ is the change in bank angle of one degree;

3) The change in angular velocity of a bank when the deflection of the ailerons is changed by one degree:

$$\omega_x^{\gamma} = \frac{\Delta \omega_x}{\Delta \delta_a},$$

where $\Delta\omega_x$ is the change in angular velocity of the bank;

$\Delta\delta_a$ is the change aileron angle of one degree.

The characteristics of directional controllability are the following parameters:

1) The force which must be applied to the pedals to impart an angular velocity of 1 rad/sec to the aircraft:

$$P_n^{\omega} = \frac{\Delta P_n}{\Delta \omega_y},$$

where ΔP_n is the force applied to the pedals;

$\Delta \omega_y$ is the change in angular velocity of 1 rad/sec;

2) the force which must be applied to the pedals to deflect the rudder when the aircraft is balanced in straight line flight with a slip of one degree or a bank of one degree;

$$P_n^{\beta} = \frac{\Delta P_n}{\Delta \beta} \text{ or } P_n^{\gamma} = \frac{\Delta P_n}{\Delta \gamma};$$

3) the change in angular velocity when the rudder is deflected by one degree, i.e., the bank reaction of the aircraft to deflection of the rudder:

$$\omega_x^n = \frac{\Delta \omega_x}{\Delta \delta_n},$$

where $\Delta \delta_n$ is the change in the rudder angle of one degree.

We can see from the definitions of aircraft stability and controllability that they characterize opposite properties of the aircraft: stability must be present to maintain the flight regime unchanged, while controllability must be present to allow it to be changed. However, there is a certain interrelationship between stability and controllability.

On a stable aircraft, the nature of the movements of the control levers and required deflections during piloting are simplified, and it is easier to determine the flight regime. It has been theoretically proven and confirmed by practice that the higher the stability of the aircraft, the less the delay and greater the accuracy with which it follows a deflection of the control surfaces. Therefore, stability and controllability provide for complete /187
utilization of the maneuvering capacity of the aircraft, assuring the required accuracy and simplicity of piloting and are an important condition for flight safety.

§4. Centering of the Aircraft and Mean Aerodynamic Chord

The position of the center of gravity of an aircraft relative to the wings is called the centering of the aircraft and is determined by the distance (in percent) from the origin of the mean aerodynamic cord (Figure 119):

$$\bar{x}_т = \frac{x_т}{b_{MAC}} \cdot 100\%; \quad \bar{y}_т = \frac{y_т}{b_{MAC}} \cdot 100\%,$$

where b_{mac} is the mean aerodynamic cord of the wing;

x_t is the horizontal distance from the lead point of the mac to the center of gravity;

y_t is the vertical distance from the mac to the c.g.

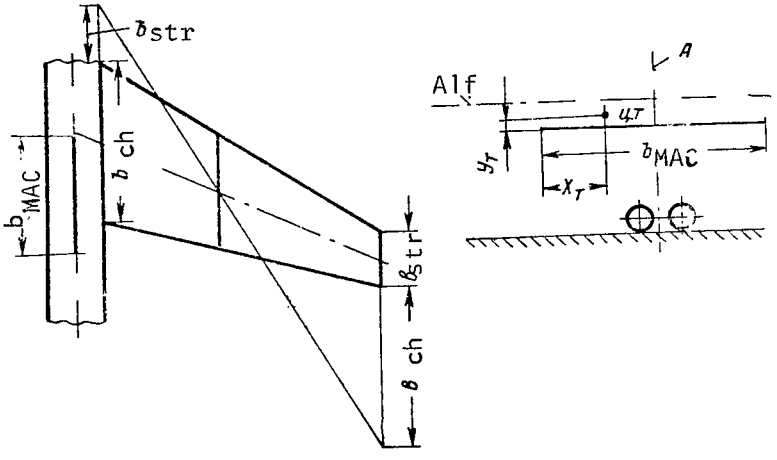

Figure 119. Diagram for Determining MAC of Trapezoidal Swept Wing (r.l.f.=reference line of aircraft; A, position of center of gravity corresponding to tipping of aircraft onto tail)

Since y_t is small in magnitude, x_t is of primary significance in an analysis of stability and controllability.

The center of gravity may be either above or below the reference line of the aircraft, depending on the actual weight of the aircraft (fuel load) and placement of motors.

In flight, the c.g. of the aircraft should be in strictly defined positions in reference to the mac, guaranteeing continued stability and controllability as the fuel is consumed. The fuel represents 25-45% of the

weight of the aircraft. In order to achieve the least displacement of the c.g. in flight, the fuel is consumed in a predetermined order, controlled by an automatic device (Figure 120).

As we can see from the graph, in order to remain within the required range of centerings ($\overline{x}_t$ = 21-30% MAC), the loaded aircraft without fuel must have $\overline{x}_t$ = 23.3-28.5% MAC (corresponding to sector AB on the figure). Then, with any fuel load centering of the aircraft will not go beyond these limits. For example, if a centering of 26% mac was produced for the loaded aircraft without fuel (landing gear down), when 8.5 t of fuel is taken on $\overline{x}_t$ = 26.7%, or with 10.5 t -- 24.3% MAC. After the landing gear are retracted, the centering moves aft one percent and will amount to 26.7 and 25.2% respectively. With a fuel remainder of 6.65 t, the centering will be furthest to the rear, and with a remainder of 3.15 t -- furthest to the front.

With centering $\overline{x}_t$ = 42-50% MAC, for aircraft with motors on the wings and 48-53% if the motor is located in the rear portion of the fuselage, the center of gravity is located in the plane of the main landing gear struts; with centering further to the rear, the aircraft may tip onto its tail (Figure 119).

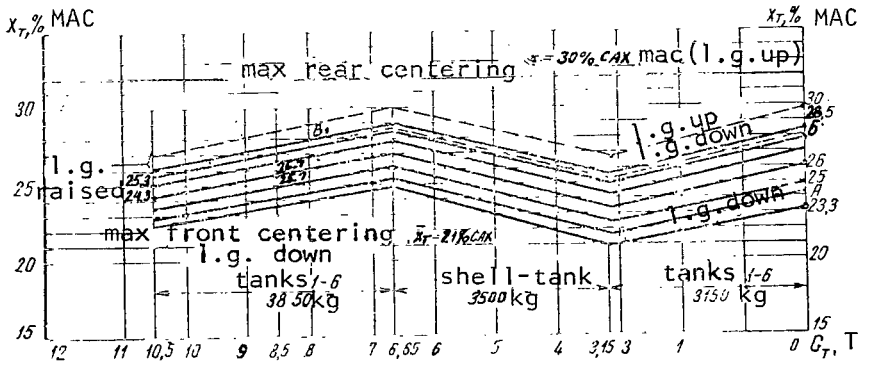

Figure 120. Change in Centering of Aircraft in Flight As a Function of Quantity of Fuel in Tanks (γ_t = 0.8 g/cm^3)

§5. Aerodynamic Center of Wing and Aircraft. Neutral Centering

We know that there is a point on the cord of the wing about which the moment of aerodynamic forces does not change when the angle of attack is changed. For example (Figure 121) with an angle of attack α_1, lifting force Y_1 creates a longitudinal moment M_z relative to a certain point F (Figure 121 a). As the angle of attack is changed to α_2, the lifting force /189 increases, but its arm length relative to point F is decreased as a result of displacement of the center of pressure (Figure 121 b). The new moment may be

greater than or less than the preceding moment. This depends on the way in which the relationship between the values of force and arm length change. It is possible to select a point F such that the value of the arm length changes in inverse proportion to the aerodynamic force. Then, the moment relative to this point will not change as the angle of attack is changed. This point is called the aerodynamic center of the wing. Thus, if $\alpha_3 > \alpha_2 > \alpha_1$ and $L_1 > l_2 > l_3$, then $Y_1 l_1 = Y_2 l_2 = Y_3 l_3$ is the constant moment of aerodynamic force relative to the aerodynamic center of the wing with various angles of attack. With wing shapes used, the aerodynamic center is located 23 to 25% of the distance along its cord.

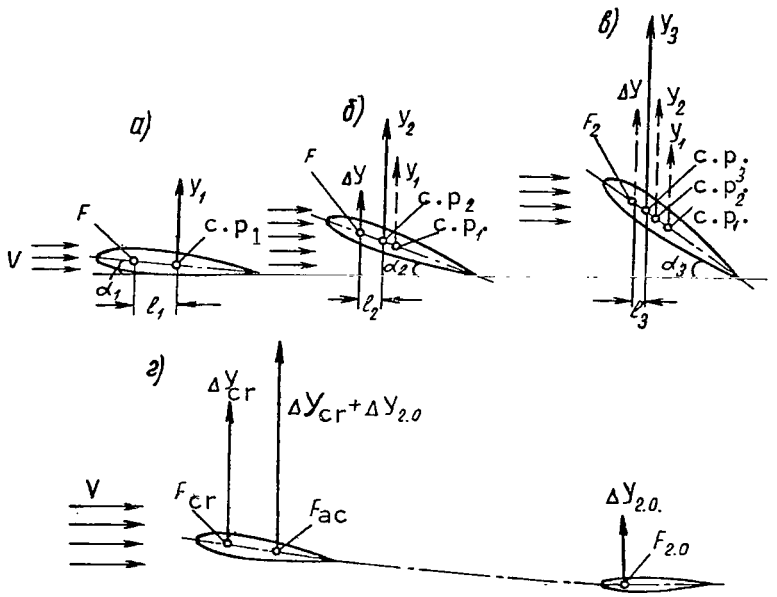

Figure 121. Explanation of Aerodynamic Center of Wing (a, b, c) and of Aircraft (d)

We can draw an important conclusion from the definition of the aerodynamic center: the increments of aerodynamic forces arising when the angle of attack is changed are applied to the aerodynamic center. Actually, force $Y_2 = Y_1 + \Delta Y$, applied at cp_2, can be divided into force Y_1 applied to cp_1 and force Y, applied at the aerodynamic center (Figure 121 b).

Since the moment of force ΔY relative to point F is equal to zero, the longitudinal moment of the wing at angle of attack α_2 will be the same as at angle of attack α_1.

The horizontal tail surfaces, like the wing, have their own aerodynamic center. /190

When the angle of attack is changed, additional lifting force arises on the wing, and ends on the horizontal tail surfaces, applied to the aerodynamic centers of the wing and horizontal tail surfaces (Figure 121 d). The resultant of parallel forces ΔY_w and ΔY_{ht} is applied at distances inversely proportional to the values of these forces. The point of application of this resultant is called the aerodynamic center of the aircraft. We must note here that for aircraft of known types, both the horizontal tail surface lifting force and its increment ΔY_{ht} are directed downward, no matter what the angle of attack of the wing.

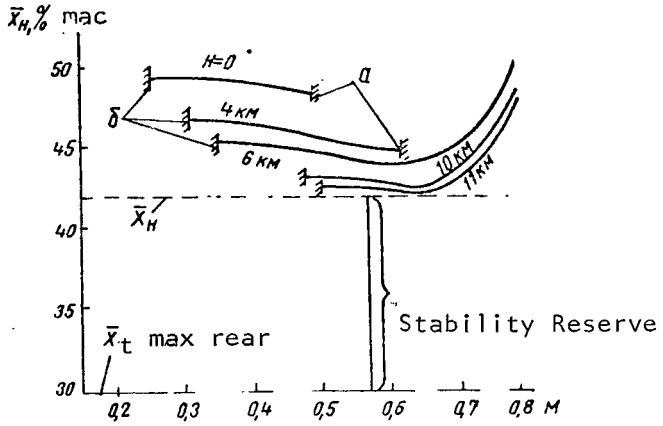

Figure 122. Neutral Centering of Aircraft with Respect to Overloads As a Function of M Number (example): a, Maximal indicated speed limitation; b, Minimum permissible indicated speed limitation

As we can see from the figure, the moment of supplementary forces relative to the aircraft aerodynamic center is zero; consequently, the longitudinal moment of the aircraft relative to this center does not change when the angle of attack is changed. Therefore, the position of the aircraft aerodynamic center does not change when the angle of attack is changed.

The aerodynamic center of the aircraft is shifted to the rear under the influence of aerodynamic force increments arising in the stabilizer, fuselage and engine cells. For example, if for the wing without the horizontal tail surface) $\bar{x}_F$ = 20-22% mac, for the aircraft $\bar{x}_F$ = 46-50% mac.

If the loads on the aircraft are so distributed that the center of gravity of the aircraft corresponds with its aerodynamic center, the aircraft becomes neutral in the longitudinal respect. In this case, the centering is called neutral. Since in this case the longitudinal moment of the aircraft will not change as a function of angle of attack, we must conclude that neutral centering is the aerodynamic center of the entire aircraft[1]. Neutral aircraft centerings are calculated for various altitudes and flight speeds (Figure 122).

[1] I. V. Ostoslavskiy, *Aerodinamika Samoleta* [Aerodynamics of the Aircraft], Oborongiz. Press, 1957.

As we can see from the figure, at Mach numbers M $\leq$ 0.6, neutral centering moves somewhat (by 1.1-1.7% mac) forward (relative to its initial values of 45-43% mac), while at altitudes over 6,000 m it shifts noticeably to the rear as a result of the effect of the compressibility of the air.

For H = 11,000 m, the change in neutral centering from 42 to 49% mac noted is explained by a displacement of the center of pressure of the wing to the rear at M numbers greater than the critical M number of the wing profile (approximately M > 0.7-0.72).

After determining the farthest forward position of the neutral centering, the limiting rearward centering for operation is defined 10-12% less than neutral centering. The distance between the neutral and limiting rear centering is called the reserve of stability for centering.

§6. Longitudinal Equilibrium

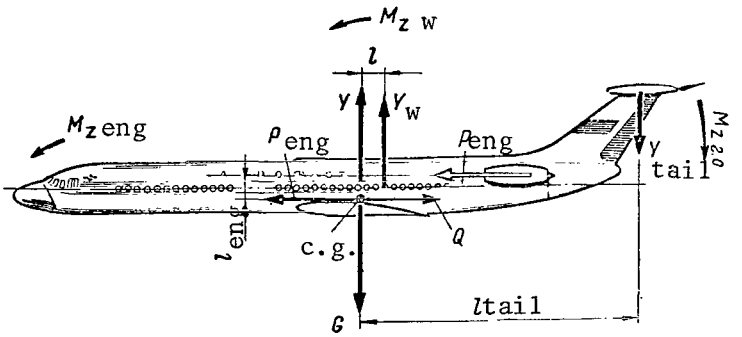

Figure 123. Diagram of Forces and Moments Acting on Aircraft About Transverse Axis

The pilot maintains longitudinal equilibrium or balancing by using the elevator and selecting the necessary motor thrust. Any stable flight regime is characterized by angle of attack α, flight speed V, altitude H and the angle of trajectory inclination Θ. In order to achieve longitudinal equilibrium of the aircraft, the forces acting in the directions of the ox and oy axes and the moments of these forces acting relative to the oz axis must be in equilibrium (Figure 123).

In horizontal flight, three conditions of equilibrium must be observed. /192

The first condition is: the lifting force of the aircraft Y must be equal to its weight.

We know that the lifting force of an aircraft is created by the wing, horizontal tail surface and partially by the engine nacelles. The lifting

force created by this fuselage is relatively slight, and is considered to be part of the lifting force of the wing. As we can see from the figure, these forces create moments about the transverse axis which decrease or increase the angle of attack. The lifting force of the wing in cruising flight creates negative pitch moment $M_{zw} = Y_w l$.

The lifting force of the horizontal tail surface is directed downward, and in all flight regimes used in practice creates the pitch moment

$$M_{ht} = Y_{ht} l_{ht}$$

In order for force Y_{ht} to be negative, the angle of attack of the horizontal tail surface α_{ht} must also be negative.

As we can see from Figure 124, $\alpha_{ht} < \alpha_w$ by the angle of downwash of the stream ε_{ht} (the downwash of the stream results from the action of the aircraft wing on the air stream). Also, α_{ht} is influenced by the angle of the stabilizer ϕ (generally zero to -4°). Thus, $\alpha_{ht} = \alpha_w + \phi - \varepsilon_{ht}$.

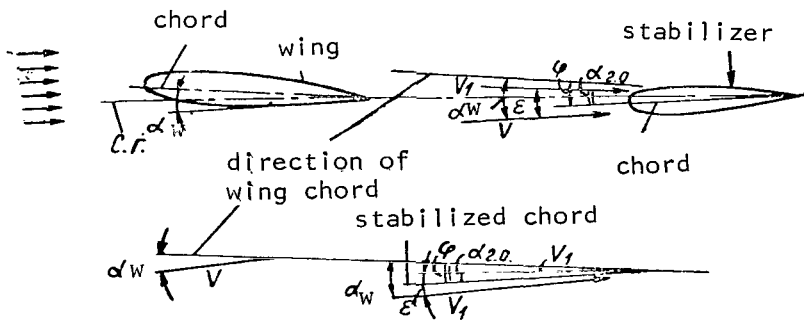

Figure 124. Determination of Angle of Attack of Horizontal Tail Surface (rl equals reference line of aircraft; V equals flight speed; V_1 equals velocity of diverted stream)

For ordinary aircraft with the stabilizer on the fuselage at a flight speed of M = 0.75-0.85 and c_y = 0.3-0.4, ε = 2-3°. For example, with α_w = 3°, ε = 2.68° and ϕ = -2°, angle α_{ht} = 3° - 2° - 2.68° = - 1.68°. The greater the angle of attack (greater the lifting capacity of the wing), the greater the downwash angle of the air stream.

In order to determine the summary longitudinal moment acting on the aircraft, we must add the longitudinal moment resulting from engine thrust /193

(M_{zen}) to the moments of the wings and horizontal tail surface.

The axis of an engine located in the rear portion of the fuselage is placed above the center of gravity of the aircraft; therefore, the thrust of the motors creates a diving moment $M_{zen} = P_{en} z_{en}$.

Thus, the summary longitudinal moment acting on the aircraft is determined by the sum of the longitudinal moments of the wing, horizontal tail surface and motor thrust.

Equality of the longitudinal moment to zero is the second condition of equilibrium.

The third condition for longitudinal equilibrium of an aircraft is equilibrium of the forces acting in the direction of the ox axis. In order for this condition to be fulfilled, the thrust of the engines must be equal to the drag of the aircraft: $P_{en} = Q$.

If this condition is not fulfilled, the movement of the aircraft will be accelerated or decelerated and, consequently, the lifting force will be changed and the flight trajectory will curve.

These three conditions for longitudinal balancing of the aircraft are fulfilled by varying the position of the elevator by the required angle and by adjusting engine thrust, depending on velocity, altitude, flying weight, centering, etc. We note that when equilibrium conditions are fulfilled, the resultant of the aerodynamic forces and the thrust of the engines can be considered to be applied to the center of gravity of the aircraft, and all forces are balanced, i.e., $P_{en} = Q$ and $Y = G$. Therefore, these forces will not be shown on figures in the following, only the additional forces and moments and their increments arising under the influence of perturbations being shown.

§7. Static Longitudinal Overload Stability

A disruption in longitudinal stability of an aircraft is accompanied by a change in the angle of attack at flight speed, the angle of attack changing at first more rapidly than velocity. Subsequently, on the other hand, the speed changes more rapidly. For example, by pulling the stick toward himself quickly, the pilot can increase the angle of attack by a factor of two or three times or more. However, in order for the aircraft to change its flight speed by 1.5 times, he must use not a fraction of a second, but dozens of seconds or even several minutes. This sharp difference in the nature of the change in angle of attack and velocity when longitudinal equilibrium is disrupted has made it necessary to distinguish between longitudinal angle of attack stability (overload stability) and velocity stability.

The stability of the aircraft in the first moment after equilibrium is disrupted is characterized by its angle of attack stability or overload

stability. This name is given to this form of stability since when the angle of attack is increased or decreased (at constant velocity) the lifting force is changed, so that the overload is also changed.

The value of the overload shows the extent to which the external load is greater than the weight of the aircraft. The overload is always related to the direction in which it is being analyzed. In flight, the external loads acting on the ox and oz axes are slight. Thus, the drag of the aircraft, which is 10-12 times less than the weight of the aircraft, acts along the ox axis; the loads arising only during slipping or as a result of side wind gusts act along the oz axis.

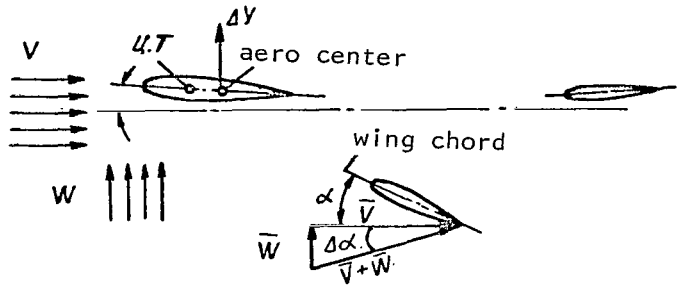

Figure 125. Forces Acting on Aircraft Entering a Vertical Wind Gust

Therefore, the main overload is that acting in the direction of the oy axis. In this case, the external load is the lift of the aircraft Y and

$$n_y = \frac{Y}{G}.$$

If constant c_y is maintained at the given aircraft speed, the lifting force will also be constant. The overload will also be unchanged, equal to zero.

An aircraft is called overload stable if it tends to retain the overload of the initial flight regime independently, without interference by the pilot.

If an aircraft is overload stable, when the angle of attack is changed the moments change so that the rotation of the aircraft which they cause results in disappearance of the additional overload. Let us assume that an aircraft in straight and level flight with an overload $n_y = 1$ and velocity V enters an ascending current with velocity W (Figure 125). This causes the direction of the resulting velocity to be changed, causing an increase in the angle of attack and an increase in lifting force ΔY (always at the aerodynamic

center) or an increase in overload $\Delta n_y = \Delta Y/G$. If force ΔY causes a diving rotation of the aircraft, the aircraft is stable. As we can see from the figure, this will result if the center of gravity of the aircraft is located in front of the aerodynamic center. Consequently, the appearance of a diving moment when the angle of attack is increased is a characteristic of overload stability of the aircraft. /195

If the external action led to a decrease in the angle of attack, a pitching moment would arise which would tend to increase the angle of attack, i.e., restore the initial overload regime.

With a certain position of the center of gravity (at the aerodynamic center), the aircraft will not react to disruption of equilibrium and will show no tendency either to return to initial overload or to further movement away from the initial value. This position of the center of gravity, as was discussed above, is called neutral centering. Movement of the center of gravity to the rear, behind neutral centering, results in the appearance of overload instability of the aircraft, since force ΔY will cause an increase in the pitch moment arising when equilibrium is disrupted.

Thus, overload stability of the aircraft will be characterized by the position of the center of gravity of the aircraft relative to the neutral centering or the aerodynamic center. Therefore, in addition to leading centering, which defines the capability of balancing of the aircraft in flight and during landing with maximum displacement of the elevator, we also determine permissible rear centering from the condition of provision of normal overload stability for the aircraft.

We can see from our analysis that a change in overload stability in flight may result from a change in the position of the center of gravity, as well as a change in neutral centering -- the aerodynamic center of the aircraft. The neutral centering of the aircraft may change in flight as the velocity or engine operating mode is changed, as well as when control is released. If overload stability increases with unchanged center of gravity, this indicates an increase in the distance between the center of gravity and neutral centering. On the other hand, if overload stability decreases, the distance between the center of gravity and neutral centering must be decreased.

As a rule, neutral centerings are determined for aircraft with fixed elevator; if the control is released, centering is moved forward by approximately 1-2% mac.

The operating mode of the engine influences the longitudinal stability of the aircraft to overloads. In jet aircraft, the downwash of the air stream in the area of the stabilizer changes not only under the influence of the wing, but also due to the effect of the exhaust gases of the jet engine on the surrounding medium. The stream leaving the engine at high velocity attracts a certain amount of the surrounding air along with it. This surrounding air changes the direction of the stream as it approaches it. Usually, the

horizontal tail surface is located above the stream (Figure 126), and the resultant of the air flow toward the stream decreases the angle of attack of the horizontal tail surface (makes the stream downwash more negative). /196

During a climb, the operating regime of the engines is nominal and the stream leaving the motor is at its highest power level. The downwash of this stream is then maximal and decreases the angle of attack of the horizontal tail surface significantly (makes the angle of attack α_{ht} considerably negative).

When the angle of attack of the wing is increased (aircraft enters a vertical wind gust) the angle of attack of the horizontal tail surface becomes more negative due to the increased downwash of the stream resulting from the change in lift of the wing and also from the stream of gases. The resultant of the increase in lifting force of the horizontal tail surface ΔY_{ht}, applied at its aerodynamic center and directed downward, will decrease the restoring moment of the horizontal tail surface and make the aircraft less effective in returning to its initial flight regime. This indicates the decrease in longitudinal stability reserve, i.e., the aerodynamic center of the aircraft is moved forward along the cord as a result of the engines operating at high thrust.

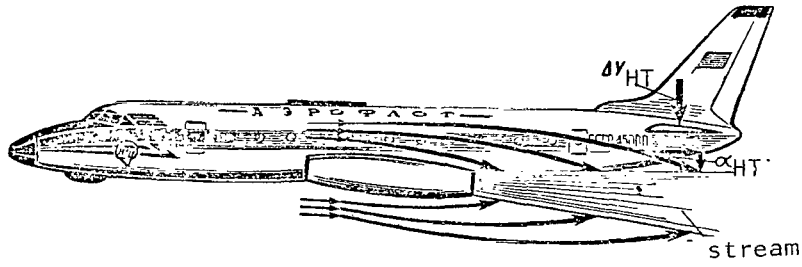

Figure 126. Pumping Effect of Jet Engine Exhaust Gas Stream on Surrounding Air Stream

When gliding at low engine setting, the influence of the stream from the engines can be ignored. In this case, the downwash of the stream on the stabilizer will be determined by the influence of the wing alone. The angle of attack of the horizontal tail surface increases (becomes less negative) and its effectiveness is increased. Longitudinal overload stability of the aircraft is increased. This increase in aircraft stability is equivalent to a displacement of the neutral centering of the aircraft (aerodynamic center) backward along the mac. This is why aircraft stability is slightly lower in a climb than in a glide.

Overload stability of the aircraft can be estimated by the overload force gradient $\Delta P_{el}/\Delta n_y$.

§8. Diagrams of Moments

/197

The degree of longitudinal stability of an aircraft is determined by wind tunnel testing. Models are tested with various deflections of the elevator, and the longitudinal moment M_z is measured using special scales. By determining moment M_z at several sequential angles of attack, we can construct graphs called moment diagrams $m_z = f(\alpha)$ for various M numbers (Figure 127).

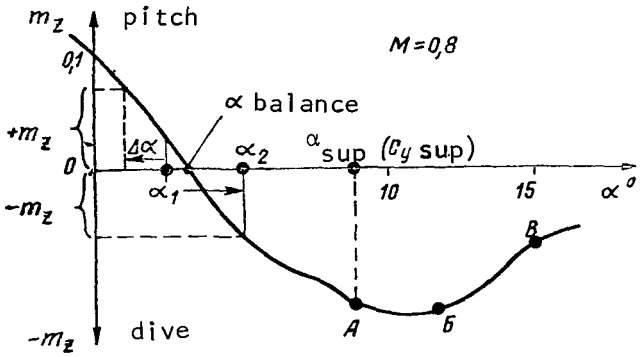

Figure 127. Coefficient of Longitudinal Moment m_z As a Function of Angle of Attack ($\delta_{el} = 0$)

The longitudinal moment coefficient (a dimensionless quantity such as c_x and c_y) can be determined using the following formula:

$$m_z = \frac{2M_z}{\rho V^2 S b_A} = \frac{2M_z}{qSb_A}.$$

The pitch moments may be either positive or negative.

Actually, in flight the elevator always has some balancing deflection. The angle of attack at which $m_z = 0 (M_z = 0)$ is called balanced, since at this angle α the aircraft is in the state of equilibrium. As we can see, as the angle of attack is increased to $\alpha_{sup} (C_{y\ sup})$ the aircraft acts stably, since the diving moment which arises causes it to return to its initial position.

A random decrease in the angle of attack by $-\Delta\alpha$ causes a positive pitch moment ($+m_z$) which returns the aircraft to its initial equilibrium position, corresponding to location of the center of gravity in front of the aerodynamic center.

Sector AB of curve $m_z = f(\alpha)$ corresponds to insensible equilibrium of the aircraft, since an increase in the angle of attack causes no change in the longitudinal moment. Sector BC of the moment diagram corresponds to (overload) unstable behavior of the aircraft: when the angle of attack changes, an additional positive pitch moment arises, tending to increase it still further.

/198

§9. Static Longitudinal Velocity Stability

A velocity stable aircraft is one which restores its assigned velocity without interference of the pilot after perturbation. For simplicity of discussion, we can consider that the angle of attack does not change when the velocity is changed. Let us assume that an aircraft flying horizontally at constant velocity V begins to descend for some reason (Figure 128 a). Due to the descent, it increases its velocity by ΔV.

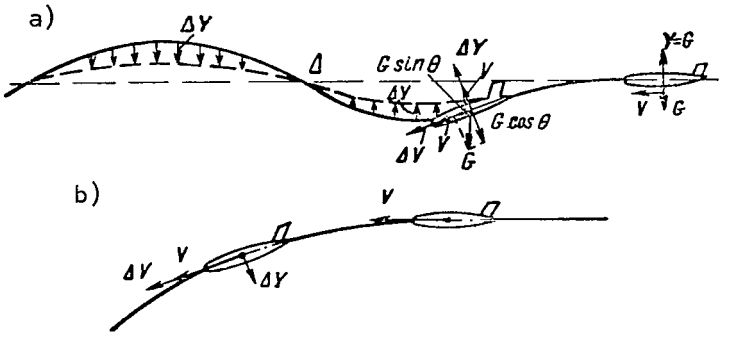

Figure 128. Behavior of Aircraft After Random Descent (a) and Flight Trajectory of Velocity Unstable Aircraft (b)

If angle of attack α or c_y remains unchanged, due to the increase in velocity, the lifting force also increases by ΔY. Due to this, the total lifting force becomes greater than the weight components and the aircraft trajectory begins to curve upward, the velocity begins to decrease, and ΔY also begins to decrease. After achieving its initial altitude (point c) the aircraft will have its initial velocity V, but its trajectory will be curved slightly upward. Therefore, the aircraft will continue to climb. Due to the increase in altitude, the velocity will begin to decrease, i.e., ΔV will become negative. This makes ΔY negative, and the trajectory begins to curve downward, etc. Thus, the aircraft will oscillate.

If the aircraft is velocity stable, these oscillations will be damped and the aircraft will come out of oscillations at its initial altitude and velocity. Oscillation damping occurs due to the fact that the forces involved in the oscillating process are always directed so as to even the trajectory. As we can see from the figure, when the trajectory is deflected downward and ΔV is positive, positive increments ΔY are also produced; when the trajectory deflects upward and ΔV is negative, negative ΔY results. Naturally, in practice the pilot will not wait until the oscillations damp out of their own accord. He takes control of the aircraft and immediately eliminates them.

However, it sometimes occurs that, in spite of an increase in velocity, the lifting force is not increased, but rather decreased, since the lifting force depends not only on velocity, but also on c_y. Due to the influence of compressibility in flight at large M numbers or due to elastic deformations, c_y may increase so sharply with increased velocity that the lifting force decreases rather than increases. In this case, the flight trajectory will curve ever more sharply downward (if the pilot does not take control of the aircraft quickly using the elevator), the speed will increase and the aircraft will go into a dive (Figure 128 b). No return to the initial position occurs.

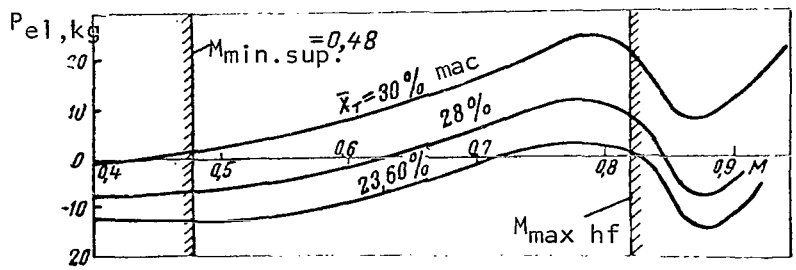

Figure 129. Dependence of Force on Elevator Control on M Number (nominal mode, horizontal flight, H = 10,000 m, tremor deflected by $\tau = 2.3°$)

It is easiest for the pilot to judge velocity stability from the nature of the change in forces on the control stick when the aircraft velocity or M number changes. As we know, balancing of an aircraft at various speeds of horizontal flight requires varying force on the stick.

Figure 129 shows the forces required to balance the aircraft at various M numbers (see §10 of this chapter). Thus, where $\bar{x}_t$ = 28% mac and M = 0.62, the force on the stick is equal to zero, since the aircraft is balanced by the trimmer and, consequently, the stick can be released in this position. This is the balanced regime. As the aircraft accelerates to large M numbers, pressure forces will arise on the stick (if the trimmer is left in its initial position), indicating that the aircraft is velocity stable. Actually, suppose the M number increases to 0.74. We can see from the graph that in order to hold this new speed (M = 0.74), the pilot must apply a pressure of /200
P = +10 kg to the stick, i.e., create a diving moment with the elevator in order to balance the positive pitch which has arisen.

We can conclude from the above that if at M = 0.62 with the stick released, a random increase in M number to 0.74 occurs, a positive pitch moment should act on the aircraft, increasing the angle of attack, and the aircraft will return without interference from the pilot to its initial velocity (M = 0.62). Consequently, this aircraft is velocity stable. A similar picture will occur if the velocity is decreased.

At Mach numbers M > 0.8, the compressibility of air begins to have a significant influence, and the pressure force resultant (center of pressure) is displaced rearward; an additional negative pitch moment begins to act on the aircraft. Therefore, whereas at M = 0.74, a force of 10 kg must be applied to the stick, at M = 0.82 the force will only be 8 kg, i.e., the pressure force on the stick is decreased, and some velocity instability appears. However, since the aircraft wing is swept, the phenomenon of pulling into a dive (during acceleration), a property of velocity instability, is not observed.

A decrease in pushing force is observed in a narrow range of M numbers, then beginning at M = 0.88-0.9, the force required increases once more, indicating the appearance of a considerable positive pitch moment, increasing with increasing M number.

§10. Longitudinal Controllability

Longitudinal overload stability determines the characteristics of longitudinal controllability of an aircraft, related to rotation of the aircraft about the oz axis and creation of overloads.

If the performance of a maneuver requires that the overload be changed, the pilot should do this by deflecting the elevator, disrupting the equilibrium and overcoming the moments attempting to return the aircraft to its initial overload.

The primary moments preventing rotation of the aircraft about the oz axis are: the aircraft overload stability moment, the damping moment and the moment of inertia.

The greater these moments preventing rotation of the aircraft, the greater the angle to which the elevator must be deflected and the greater the force required at the control stick in order to change the overload. Since the pilot feels the value of force applied to the stick and the overload resulting from it, longitudinal controllability of the aircraft can best be evaluated by the gradient of overload force $\Delta P_{el}/\Delta n_y$ and the elevator travel used $\Delta\delta_{el}/\Delta n_y$.

The overload force gradient is numerically equal to the ratio of additional force ΔP_{el} on the stick to the increase in overload Δn_y produced as a result of this force. /201

Let us assume that the aircraft is performing horizontal flight and $n_y = 1$ (Figure 130). Then, in order to produce $n_y = 2$, the pilot must pull the stick toward himself with a force of 40-70 kg (for small M numbers, 40 kg and for M = 0.7-0.8, 50-70 kg). Since overload stability characterizes the ability of the aircraft to retain the initial overload regime, obviously the higher the stability the greater the force required at the control stick to

change the overload.

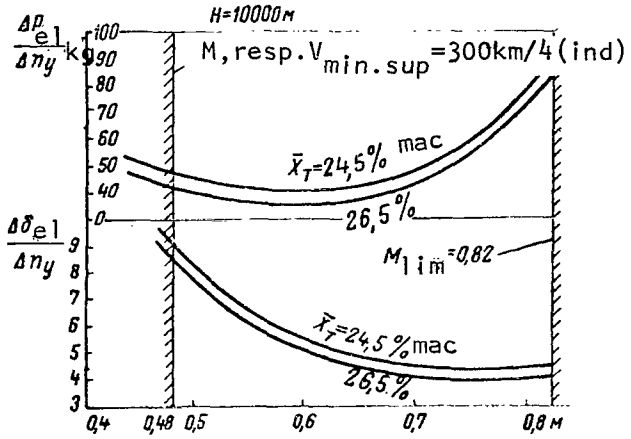

Figure 120. Overload Force Gradient $\Delta P_{el}/\Delta n_y$ and Elevator Travel $\Delta\delta_{el}/\Delta n_y$ As a Function of M Number (H = 10,000 m)

We can also see on Figure 130 that if the centering moves further forward, the force required to change n_y increases. This is explained by an increase in the distance between the center of gravity of the aircraft and its aerodynamic center. Thus, the further forward the centering of the aircraft, the heavier it is to control.

The limit in forward centering is selected from the condition of aircraft balancing during takeoff and landing.

In order to exclude (during takeoff) stream separation from the horizontal tail surface, the elevator can be deflected 20-25° upward. During landing, the pilot should increase c_y to $c_{y\,ldg}$. By pulling the stick toward himself, he increases the angle of attack, creating positive pitch moments. When the angle of attack is increased, an increase in lift Δy occurs, applied to the aerodynamic center and creating a negative pitch moment opposing the pilot. The greater the distance between the aerodynamic center and the center of gravity, the greater this hindering moment will be. Since the movement of the elevator is considerable at low velocities, it may be found that the limitng deflection of the elevator is insufficient to tilt the aircraft to its landing angle. Therefore, the maximum rearward position of the center of gravity is fixed so that the permissible deflection of the elevator is sufficient to allow the pilot to land.

The usage of an adjustable stabilizer makes it possible to fly in aircraft with more forward centering, since in this case the effectiveness of the elevator is increased.

Usually, some reserve in elevator deflection (3-4°, but no less than 10% of the complete deflection of the elevator) is installed.

Let us now analyze the deflection of the elevator $\Delta\delta_{el}/\Delta n_y$ necessary to create an additional unit of overload. As we can see from Figure 130, as the velocity increases, the effectiveness of the elevators also increases sharply.

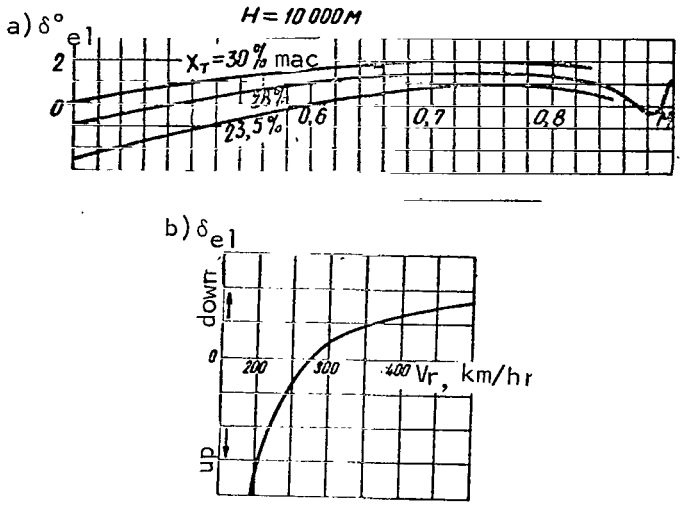

Figure 131. Balancing Curves of Elevator Deflection (produced as a result of flying tests): a, In straight flight at nominal engine operating mode; b, Coming in for a landing

For example, whereas at M = 0.5, the elevator must be deflected by 8° in order to cause a double overload, at M = 0.78 the required deflection is only 4°.

The balancing curves, showing the dependence of elevator deflection on M number, are also used to characterize longitudinal controllability (Figure 131).

According to these curves, for example with rear centerings ($\bar{x}_t$ = = 28% mac), maintenance of longitudinal equilibrium at M = 0.62 requires that the elevator be deflected from its neutral position by 1.2° downward; at M = 0.74, 1.5° downward; at M = 0.82, the balancing downward deflection of the elevator is decreased slightly, becoming once again +1.2. /203

Thus, as the aircraft accelerates from M = 0.62 to M = 0.74, longitudinal balancing requires that the elevator deflection be moved downward by 0.3°, while further acceleration to M = 0.82 requires that it be decreased by the same amount.

Beginning at M = 0.88-0.9, the positive pitch moment increases sharply, and the elevator must be deflected considerably downward.

§11. Construction of Balancing Curve for Deflection of Elevator

Using the moment diagrams for various deflections of the elevator, we can determine for these deflections coefficients c_y with $m_z = 0 (c_{y_1}, c_{y_2}, \ldots, c_{y_n})$ and construct the balancing diagram for deflection of elevator as a function of c_y (Figure 132). The left branch of the graph (left of c_{y_5}) can be produced by wind tunnel testing of a model, while the right branch can only be produced in test flights testing the stability and controllability of the aircraft at high angles of attack; in these tests, the deflection of the elevator as a function of c_y is determined for each M number. For this, the

aircraft is placed in the regime $c_y > c_{y\ sup}$ and held in this regime until the beginning of "pickup," allowing us to determine the degree of stability of the aircraft and sufficiency of the elevators to bring the aircraft out of this regime. The aircraft is also braked in order to determine the minimum velocity and nature of its behavior at this velocity.

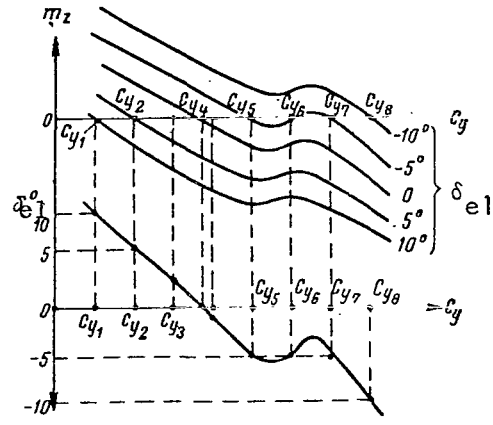

Figure 132. Construction of Elevator Deflection Balancing Diagram

The balancing curves on Figure 133 give us an idea of the nature of the dependence of elevator deflection δ_{el} for aircraft equilibration with respect to longitudinal moments at stable flight regimes on coefficient c_y. As we see, these curves are similar in form to the moment diagram, for which proportionality of the deflection of elevator to the coefficient of longitudinal moment m_z is also characteristic.

In order to record the deflections of the elevator during flight tests, the aircraft is accelerated to M = 0.65-0.85, and then at constant M number, the elevator is "fed" toward the pilot in order to cause the aircraft to climb. This "feeding" of the elevator is performed with $c_{y\ sup}$ with constant increase in overload n_y to 2-3. /204

Let us analyze the movement of the aircraft upon transition to large angles of attack ($c_y > c_{y\ sup}$), when the pilot is controlling the aircraft.

Let us assume that as a result of the influence of a powerful ascending air current (or as a result of creation of an overload in a test flight) the aircraft arrives at $c_{y_1} > c_{ypu}$ (Figure 133). It was noted in chapter II that if $c_{y\ sup}$ is exceeded, longitudinal stability of the aircraft may be disrupted, since as a result of redistribution of pressure on the wing, so-called "capture" -- involuntary progressive increase in the angle of attack -- occurs.

The angle of attack near which "capture" occurs is called the "capture" angle of attack (the coefficient c_y and overload above which "capture" begins are named similarly).

If at the moment of capture the pilot moves the elevator downward by $\Delta\delta_{el_1}$, by the time the angle of attack $\alpha_1(c_{y1})$ is achieved for which δ_{el_1} is

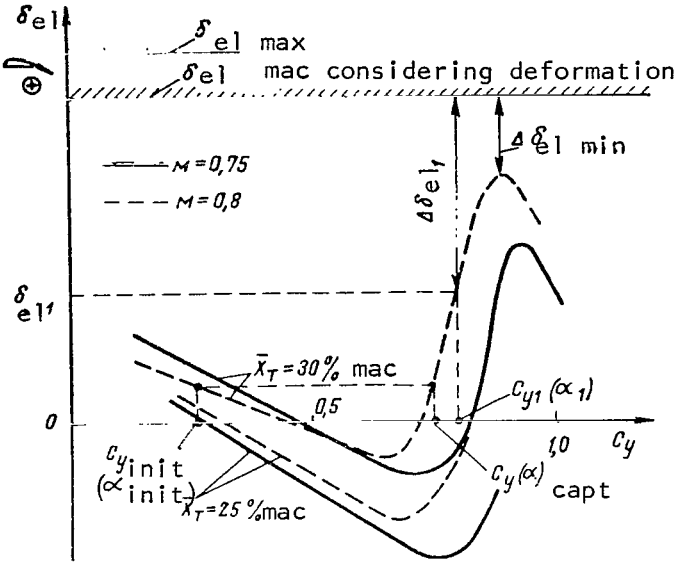

Figure 133. Required Elevator Deflection As a Function of c_y

the balancing deflection, further increase in the angle of attack does not occur and the aircraft is balanced at angle of attack α_1 and will retain this angle[2]. /205

The behavior of an aircraft in this curved flight with $n_y > 1$ will be characterized by a tendency to increase the pitch angle without increasing the angle of attack.

In order to return the aircraft to its initial flight regime, the pilot still has the elevator reserve $\Delta\delta_{el_1}$ separating the balancing elevator deflection from the maximal deflection, corresponding to complete deflection downward (to the stop). The further the pilot moves the elevator downward from this balancing position, the greater the angular velocity with which the aircraft will begin to decrease the angle of attack, i.e., the more rapidly the overload will be decreased to unity.

A position should not arise in which the required downward elevator deflection to restore balancing is greater than that available, including consideration of deformation of force transmitting hardware. Otherwise, it will be impossible to balance the aircraft, and the pilot will not be able to return it to the initial flight regime.

Figure 133 shows that with more forward centering (25% mac) the elevator reserve is greater, and the controllability is better. This results from the fact that with forward centering in the initial balancing regime the elevator control stick must be held closer to the pilot than with rearward centering and, consequently, the elevator reserve to maximum deflection is increased.

It has been noted in the process of flight tests that after an aircraft is put in a high overload position, soaring requires that a positive pitch moment be created by applying a force of 80-100 kg to the stick. This force, which equalizes the aerodynamic load acting on the deflected elevator, deforms the force transmitting elements, shortening them. As a result, full forward deflection of the stick did not result in full deflection of the elevator. With maximum deflections of the elevator (29-31°) the actual angle of position

[2] M. V. Rozenblat, *Piloter o Peregrazke* [To the Pilot Concerning Overloading], Aeroflot Redizdat Press, 1964.

was only 24-25°, due to deformation (Figure 134).

The only method of creating a reserve of elevator movement for aircraft control in this case is unloading of the control cable by using the elevator trimmer.

When the trimmer of the elevator is deflected, the hinge moments decrease, and the deflection of the elevator is increased as a result of unloading of the control cables.

During the process of flight tests of an aircraft at high angles of attack, the following peculiarity was discovered. We know that when a back-swept wing moves at high angles of attack, flow separation begins where the ailerons are located. This leads to a change in the aileron hinge moment such that both ailerons tend to move upward by approximately 2-4°. This phenomenon /206
has come to be called "floating" of the ailerons. In its effect, it is equivalent to an additional deflection of the elevator upward, since it causes an additional loss in lift at the terminal portion of the wing where the lift properties are worsened by the separation. "Floating" of ailerons worsens longitudinal instability of the aircraft with swept wings at high angles of attack and makes capture of the aircraft even sharper. The design-aerodynamic measures analyzed in §3 of Chapter III improve the overload stability characteristics of a swept wing aircraft at high angles of attack.

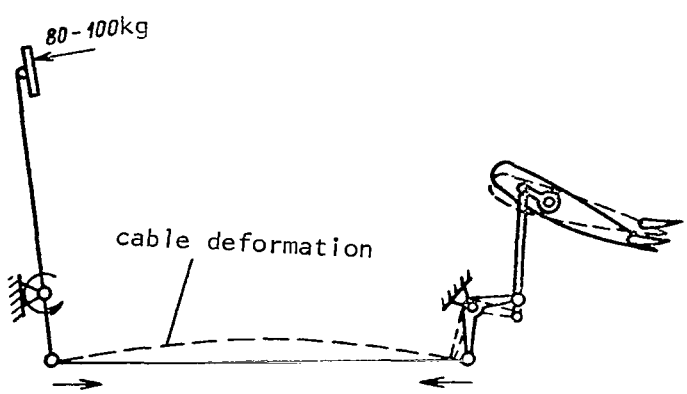

Figure 134. Diagram of Deformation of Control Cable As Vertical Gust Is Being Overcome

"Floating" of the ailerons can be reduced by fastening the external portion of the ailerons using special mechanical devices or by decreasing the size of the ailerons. The transition to hydraulic amplifiers (booster control) installed in the immediate area of the ailerons can eliminate elastic deformation of the control cable, which facilitates floating of the ailerons.

A pilot flying a passenger aircraft with a swept wing should avoid areas with strong turbulence, in which the characteristics of longitudinal overload stability appear so unfavorably.

§12. Vertical Gusts. Permissible M Number in Cruising Flight

During flight through atmospheric turbulence, in tensive and frequent vertical gusts of air result in large longitudinal and lateral oscillations of the aircraft. The accelerations arising in this case lead to the appearance of inertial forces characterized by overloads on the aircraft. A vertical /207
gust is a vertical air movement resulting in an increase in overload in not over 2 sec.

The horizontal components of wind gusts have no essential significance for the movement of the aircraft. For example, horizontal wind gusts up to 6-15 m/sec cause slight velocity pulsations in modern aircraft flying between 200 and 250 m/sec, and create slight overloads, whereas vertical wind gusts at these speeds cause 10-15 times more overloading [3].

Longitudinal overloading (or more accurately an increment in overloading) acting in the horizontal plane can be determined according to the following formula:

$$\Delta n_x = \frac{\Delta V}{g \Delta t},$$

where ΔV is the change in velocity resulting from an oncoming gust;
Δt is the time of action of the gust.
Thus, if a horizontal wind gust causes a velocity variation of 11 m/sec in two seconds, the increment to the longitudinal overload will be $\Delta n_x = 11/2 \cdot 9.81 \approx 0.56$; with a time of action of three seconds, $\Delta n_x = 0.37$. The sign of the overload will depend on whether the gust is a headwind or tailwind. In the case of a headwind gust, the sign will be plus (the crew and passengers will be pressed against the backs of their seats), and with a tailwind gust the sign will be minus (the crew and passengers will be pulled away from the backs of their seats).

What must the velocity of a vertical gust be in order for the aircraft to be brought to $c_{y\ sup}$ or to the mode of involuntary increase in overload ("capture")? As we can see from Figure 135, at M = 0.8 when a gust of $W_{i\ sup}$, an aircraft with an initial value of c_{yhf} will reach $c_{y\ sup}$, while the effects of a gust at $W_{i\ capt}$ will cause it to reach $c_{y\ capt}$. In this case, the balancing position of the elevator will be insufficient to return the aircraft to its initial parameters.

In order to estimate the effects of a vertical air stream on the wings of /208
an aircraft, we must use the so-called velocity of the effective gust. The indicator effective gust W_{ief} differs from the real indicator gust (measured under concrete conditions), since there are no sharply differentiated vertical

[3] Kulik, M. M., *Obosnovaniye rekomendatsky po Pilotirovaniyu Samoletov pri Poletakh v Zonakh Atmospernoy Turbulentnosti* [Basis for Recommendations for Piloting Aircraft on Flights in Zones of Atmospheric Turbulence] GosNII GA Press, 1963.

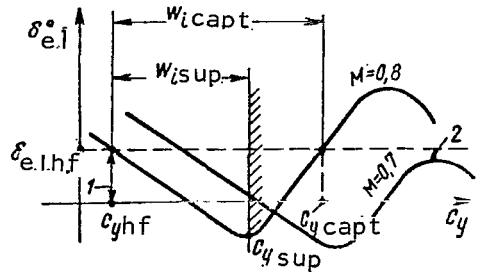

Figure 135. Determination of Effective Indicator Vertical Gust Bringing Aircraft to $c_{y\ sup}$ and $c_{y\ capt}$: 1, Initial balancing regime; 2, Effective diving moment

movements in the atmosphere, as a result of the influence of viscosity of the air. There is always a transition zone, in which the rate of the vertical component varies from zero to some value W_{ief}. Various aircraft with their inherent specific features of aerodynamics react differently to the same gust. For example, it has been established that for aircraft with swept wings, $W_{ief} = 1.11\ W_i$.

Calculation of the velocity of an effective vertical gust is performed using the formula

$$W_{ief} = \frac{W_i}{0.9} = 1.11 V_i \Delta\alpha,$$

where $\Delta\alpha$ is the increase in angle of attack calculated from α_{hf};

V_i is the indicator velocity of the aircraft.

Let us assume that the pilot does not interfere in control and that the elevator is "clamped" in the initial balanced position. Let us calculate the gust speed W_{ief} required to bring the aircraft to $c_{y\ sup}$. The flight is performed at $c_{yhf} = 0.35$ and $\alpha = 3°$ at M = 0.75 and H = 10,000 m. In this case $c_{y\ sup} = 0.715$ and $\alpha_{sup} = 7.2°$. Let us determine: the increment of angle of attack $\Delta\alpha = 4.2°$ or 0.073 rad, the indicator velocity V_i = 475 km/hr = = 132.0 m/sec, so $W_{ief} = 1.11\ V_i\Delta\alpha = 1.11 \cdot 132 \cdot 0.073 = 10.7$ m/sec.

The effective indicator vertical gust corresponding to the beginning of involuntary increase in overload -- "capture" with fixed control -- is calculated using the same formula, except that the increase in angle of attack is selected from α_{hf} to the beginning of "capture." Thus, for the same conditions $\Delta\alpha = 7°$, and $W_{ief} = 1.11 \cdot 132 \cdot 0.157 = 23$ m/sec.

When a vertical gust at 10.7 m/sec acts upon the aircraft, it goes to $c_{y\ sup}$, while where $W_{ief} = 23$ m/sec, the "capture" regime is begun, and a self-sustaining increase in overload and vibration of the entire aircraft occur.

As we can see from Figure 136, at M = 0.75, the reserve for a vertical gust for the weight and flight altitudes here analyzed is maximal. At /209

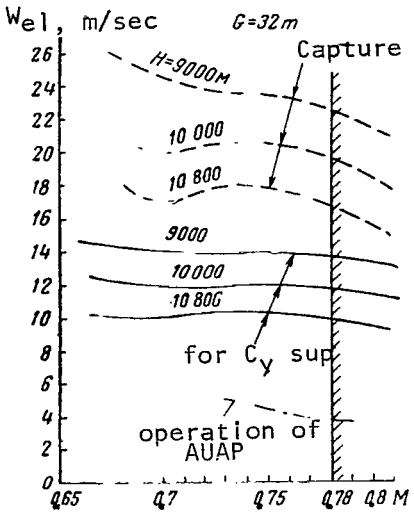

Figure 136. Permissible Effective Indicator Vertical Gust As a Function of M Number of Flight (TU-124 aircraft)

M = 0.75-0.78, a slight reduction is observed, and at M > 0.78 this reserve is somewhat greater. Therefore, for this aircraft, the maximum permissible M number in horizontal flight is 0.78, in order to retain a sufficiently high reserve of vertical gust stability.

§13. Permissible Overloads During a Vertical Maneuver

In addition to vertical air gusts, an aircraft may be subjected to the action of extended ascending or descending air currents, which cause considerable vertical displacement of the aircraft, independent of pilot action.

In stable horizontal flight, the sum of vertical forces acting on the aircraft is equal to zero and the overload

$$n=\frac{Y}{G}=1.$$

When the aircraft crosses a vertical gust, the angle of attack increases rapidly and consequently the lifting force increases as well. All of this causes vertical and angular displacement of the aircraft, which in turn once more influences the angle of attack. In this case, the overload

$$n_W=\frac{Y_W}{G}=\frac{Y+\Delta Y}{G}=1+\Delta n.$$

The increment of overload Δn occurs as a result of the summary increment of angle of attack resulting from the influence of the vertical gust and angular displacement of the aircraft caused by the gust. The overload acting on the aircraft can be represented in this case by the following expression:

$$n_W=1+\Delta n=1\pm\frac{1}{2}\rho c_y^{\alpha}\frac{V_i W_i}{\frac{G}{S}}K$$

(the "plus" sign relates to an ascending gust, the "minus" sign to a descending gust),

where c_y^{α} is the tangent of the angle of inclination of curve $c_y = f(\alpha)$, i.e., the gradient of the change in coefficient c_y as a function of angle of attack α;

V_i is the indicator velocity of the aircraft;

W_i is the indicator velocity of the vertical gust;

K is a coefficient characterizing the increase in the vertical gust (K = 0.85-0.95).

As we can see from the formula, the overload acting on the aircraft depends on the flight speed and force of the vertical gust. Flights of high-speed aircraft at high altitudes have shown that when the aircraft enters a vertical gust with a certain velocity W_i, the overload n_W (related to the moment of action of the gust) is much less than $n^a_{y\ max}$, but even in this case separation of the flow over the wing occurs, which may lead to rolling of the aircraft. Usually, rolling is preceded by the appearance of a considerable positive pitch moment, under the influence of which the aircraft climbs and loses speed. /210

Therefore, limitations on overloads move along two lines: along the line of aerodynamics, i.e., with respect to $c_{y\ sup}$, and along the line of strength of the aircraft, i.e., with respect to the maximum coefficient of operational overload $n^a_{y\ max}$.

In order to avoid exceeding $c_{y\ sup}$ and prevent the aircraft from going into a roll, permissible flight altitudes are established as a function of flying weight (see Chapter VII, §8).

§14. Behavior of Aircraft at Large Angles of Attack

At the present time, the separation characteristics, rolling and termination of rolling of aircraft with low stabilizers and engines installed on the wings have been studied rather well.

However, there is still very little material available on the behavior of aircraft with T-shaped tails and motors located in the rear portion of the fuselage during flow separation at high angles of attack. The balancing characteristic analyzed in §11 related completely to an aircraft with load stabilizer.

Let us analyze some features of the behavior of an aircraft moving into large angles of attack. The flight speed of the aircraft corresponding to $c_{y\ max}$ is called the minimum speed or the separation speed. The problem is

that when $c_{y\ max}$ is achieved in flight, the flow separates, causing a sharp decrease in the lift and a considerable increase in the drag. (The separation speed for a smooth wing is represented as V_s, for the takeoff position of the wing mechanism as V_{s_1}, for the landing position -- V_{s_0}.)

Due to the asymmetrical development of separation on the wings of the aircraft, a banking moment arises and the aircraft rolls. By roll, we mean a movement of the aircraft about the longitudinal axis such that the angular velocity of rotation $\omega_x > 0.1$ rad/sec, i.e., greater than 6° per second.

In order to determine the minimum velocity corresponding to $c_{y\ max}$, the aircraft is decelerated at unit overload. Since the lifting force of the wing depends on $c_y V^2$, as the speed is reduced gradually, the value of c_y should increase, which does occur, while the pilot, gradually pulling the stick toward himself, shifts the aircraft into high angles of attack. The speed at which sharp flow separation occurs is accompanied by rapid rolling of the aircraft, and this is the minimum speed or the speed of separation V_s. A case has been observed in which an aircraft developed such a high angular velocity /211 ω_x that it rotated by 180° in a few seconds.

With flaps down, the movement of the stick may not be sufficient to achieve V_{s_0} or V_{s_1}. Then, the flight speed corresponding to maximum rearward position of the stick is taken as the minimum speed.

As we can see from processing of strip chart recorders (Figure 137) when an aircraft with a low stabilizer is decelerated at an altitude of 12,000 m (flaps and landing gear up) after an indicated speed of 200 km/hr is achieved, the aircraft maintains almost constant $c_y = 1.45$ and overload $n_y = 1$ for several seconds. The deflection of the elevator "upward" varies from 3 to 3.8°. At $c_y = 1.5$, a slight vibration of the ailerons and stick begins. Rolling occurred at $c_y = 1.58$ toward the right wing. In this case, the angular banking velocity ω_x reached 0.19 rad/sec (approximately 11 deg/sec), and the nose dropped at 4 deg/sec. During the roll, the ailerons were observed to move upward by 2-2.5° (negative deflection).

After 0.3-0.5 sec of roll, the pilot moved the stick away from himself ($\delta_{el} = +2°$) and transferred the aircraft to lower values of c_y. In 3-4 sec, the vibrations stopped. After the ailerons were moved to stop the bank, the aircraft rapidly stopped rolling, the effectiveness of the ailerons being sufficient. By pulling the stick toward himself (deflecting the elevator "upward" by 2-3.5°), the pilot brought the aircraft back to horizontal flight at 320-340 km/hr.

In order to determine permissible values of $c_{y\ sup}$, the elevator is "fed" at various values of M number (Figure 138). In order to improve safety, this maneuver is performed at high altitude (about 12,000 m). When the stick is moved energetically backward, the aircraft is transferred to angles of attack (high α_{sup}) at which "capture" or involuntary positive pitch occurs.

As we can see from the strip chart recordings, the aircraft first accelerated, then when M = 0.66 was reached, the pilot began to increase the overload by pulling the stick sharply back. The angular rate of rotation about the transverse axis reached 12° per second (ω_z = 0.2 rad/sec). At this point, the pilot slowed the rate at which he was pulling back the stick, and the deflection was left constant at 3° "upward." The overload increased sharply, reaching a maximum value of 2.8, and "capture" began at $n_y = 2(c_y = 0.85)$ (sector ab). As the overload increased to 2.05-2.2 ($c_y \approx 1$), the aircraft started vibrating and the ailerons began to "float" (deflection of both ailerons upward due to elastic deformation of the control cable). The aircraft did not roll, but a bank did occur at 4-4.3 deg/sec. The maximum "floating" of ailerons was 4.5-5°. /213

When the elevator was shifted at M = 0.7, vibration was noted at c_y = 0.85, while at M = 0.8 -- at c_y = 0.65. When the stick was moved forward, the maximum balancing deflection of the elevator (M = 0.8 and c_y = 0.9) was 5.3°, and the maximum balancing force required to bring the aircraft back to the initial regime was 60 kg.

It was noted in the process of testing that the warning vibration which arises as the minimum flight speed is approached is insufficiently intense to be noticed by the pilot. A stronger vibration occurred at the moment of "capture" or at the moment the aircraft started to roll. /214

In most aircraft as the separation regime is approached, the vibration of the tail surfaces is noted due to interference between the tail and streams from the wings of the aircraft. In those cases when vibration was not observed, devices have been installed to cause artificial vibration of the stick, warning the pilot that he was approaching the separation regime. From the point of view of formation of vibration and rolling of the aircraft, it is dangerous to perform a takeoff in which during the first stage of takeoff the air speed is 20% higher than the separation speed V_{s_1}, as well as landing during which the flight speed of the aircraft exceeds the separation speed V_{s_0} by 30%.

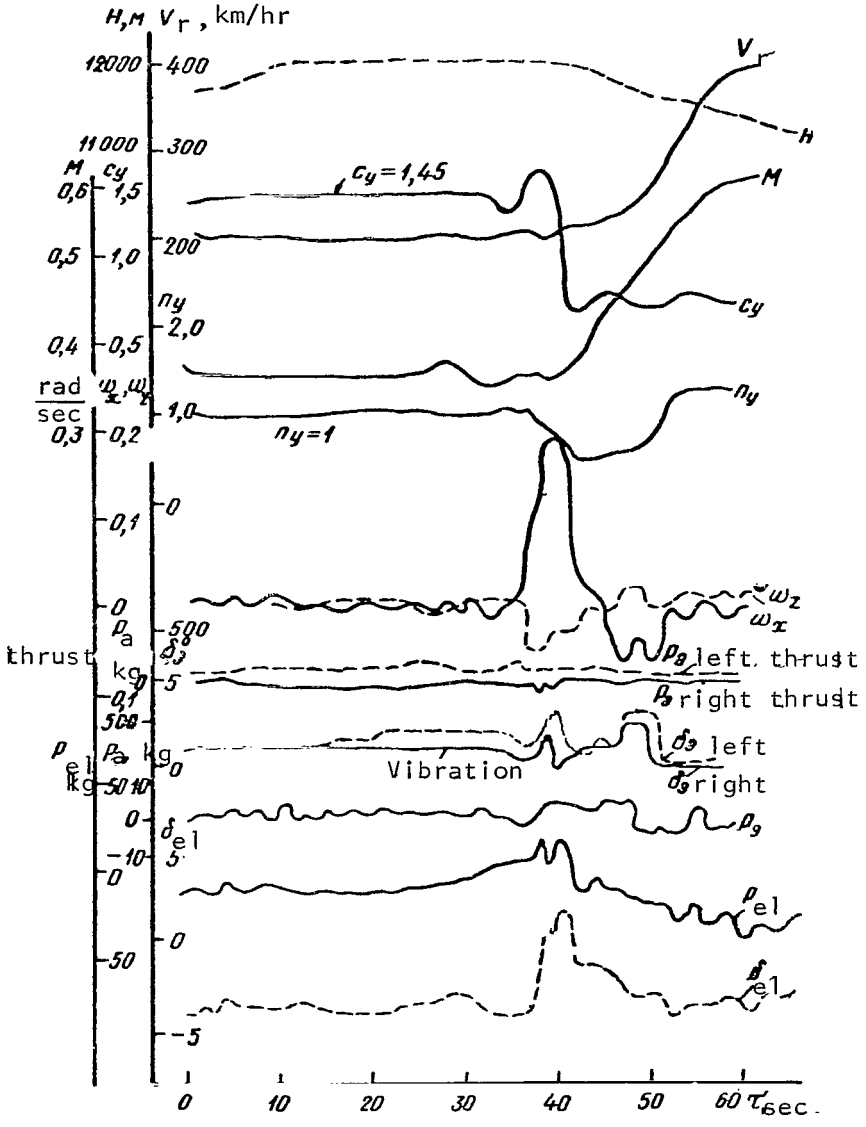

Figure 137. Recording of Strip Chart Recorders During Deceleration of Aircraft

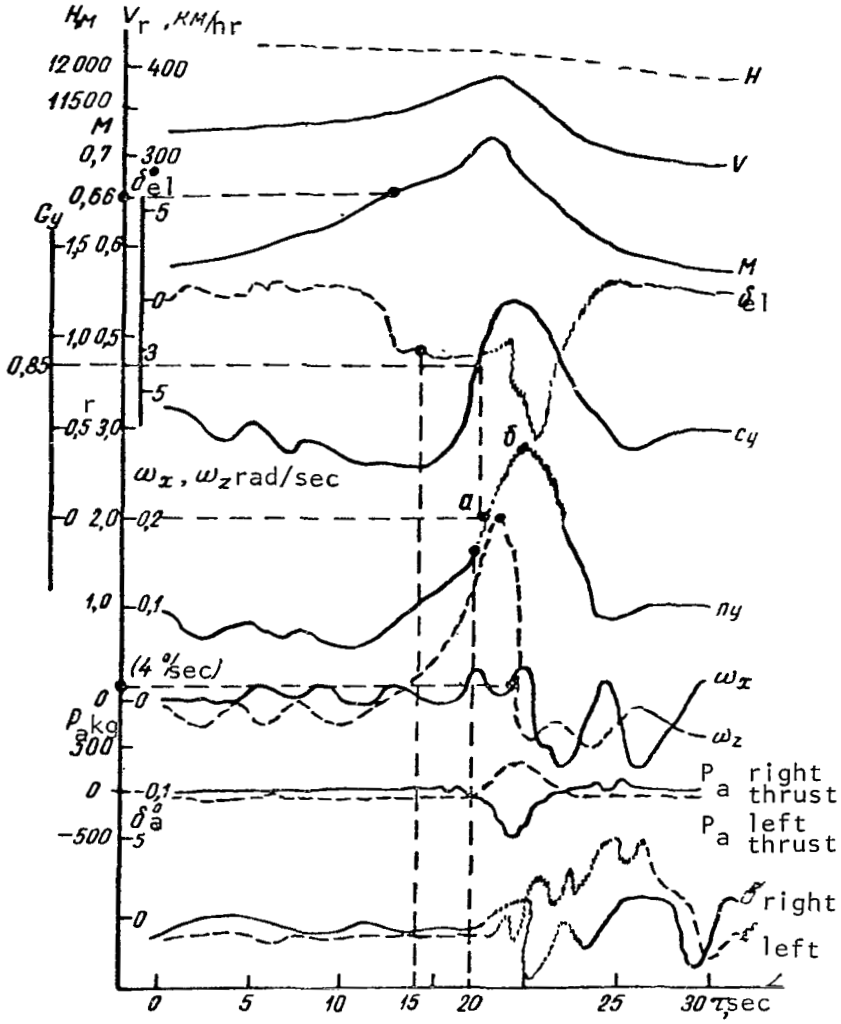

Figure 138. Recording of Strip Chart Recorders As Aircraft Is Transferred to $n_y > 1$

In horizontal flight (flaps up) at high altitudes when a zone of strong turbulence is entered, separation may occur. In this case, if the aircraft has satisfactory characteristics (a diving moment appears) and the pilot takes control, the aircraft will eliminate the disruption of equilibrium.

The problem is somewhat worse as concerns the separation characteristics of an aircraft with a high horizontal tail surface and motors in the tail portion of the fuselage.

If in aircraft with low stabilizer, high slip angles ε are created immediately before separation, and the slipping of the stream disappears

immediately after separation, causing an increase in the angle of attack and lifting force of the stabilizer ($\alpha_{ht} \approx \alpha_{cr}$), i.e., an increase in the diving moment, in aircraft with T-shaped tail surfaces (high stabilizer) after the stream separates from the wing, vortexes from the fuselage, and the stream from the wing, engine nacelles and mounting struts strike the stabilizer, causing a positive pitch moment (Figure 139). This decreases the negative significance of the longitudinal moment coefficient, and the aircraft has no tendency to tip over on its nose. When the stabilizer is below the separated stream zone, which occurs with very high angles of attack, the horizontal tail surface creates considerable drag and a diving moment appears. In connection with this, after separation, a positive pitch moment may arise, making the situation worse; after separation begins, the elevator should be fully deflected "downward." Therefore, in some aircraft with T-shaped tails, a diving moment is created artificially using a "pusher" ("recoil" system)[4].

This device, working from an angle of attack transducer located on the fuselage, creates forces acting on the stick in the direction of a dive at an angle of attack near α_m. This force should be high enough to overcome the force applied by the pilot and should continue acting until the angle of attack is decreased. /215

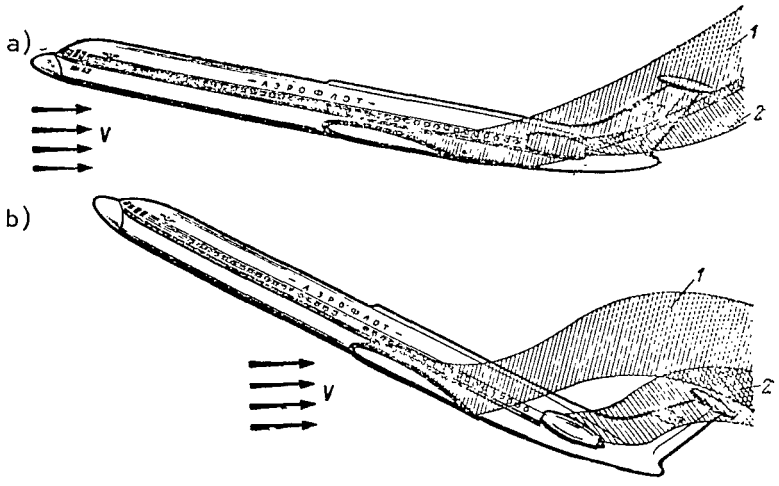

Figure 139. Flow Spectra Around Aircraft with T-shaped Tail Surface After Flow Separation: a, Angle of attack 3° greater than separation angle; b, Angle of attack 18° greater than separation angle; 1, Air stream from wing; 2, Air stream from nacelles and struts of engines

In order to prevent elimination of overload by separation, the "pusher" is equipped with a special device with a gyroscope which limits the increase in angle of attack as a function of the angular velocity of the beginning of separation.

The "pusher" can also eliminate the stable rolling mode "long term positive pitching moment), in which the aircraft leaves the roll only after a considerable decrease in velocity and altitude.

[4] *Zarubezhnyy Aviatransport*, No. 12, GosNII GA Press, 1965.

§15. Automatic Angle of Attack and Overload Device

The automatic angle of attack and overload device (AUAP) is used to warn the pilot that the aircraft is flying at large angles of attack as the minimum velocity is approached and during flights in bumpy air.

During flights using this device, the instantaneous angle of attack at which the aircraft is flying and the vertical overload are determined. Also, at each moment in time the value of the critical angle of attack is determined /216
as a function of the M number of flight.

The device consists of a number of aggregates. The main units are: 1) the angle of attack measuring device, which measures the local angles of attack in conjunction with the wind vane on the fuselage; 2) the critical angle measuring device which outputs the required voltage as a function of the M number of the flight; 3) the overload transducer, installed in the area of the center of gravity of the aircraft; 4) an indicator device on the instrument panel in front of the pilot. Using this device, the pilot can observe the current angles of attack at which he is flying, the critical angle of attack (more precisely, the angle of attack at which the automatic device operates under the given conditions) and the vertical overload.

When the aircraft enters a critical regime (the operating regime, which is somewhat less than the permissible) the lower sector of the movable critical angle of attack sector on this instrument corresponds with the arrow indicating the instantaneous angle of attack (Figure 140). At this moment, a /217
lamp with the inscription "α_{cr}" lights up in front of the copilot. Also, if the aircraft undergoes overloads greater than those permissible, the arrow indicating instantaneous overload approaches the sector of dangerous overloads and the lamp with the inscription "$n_{y\ sup}$" lights up.

When either of these lamps lights up, the "attention" lamp on the display begins to flash.

Adjustment of this device is performed individually for operation in flight with all flaps and gear up and for flight with flaps down for takeoff and for landing. For example, in the ordinary flying mode (flaps up), the α_{cr} warning lights up when angles of attack of 1.4-2° less than the permissible angles are reached. These parameters are shown for one aircraft equipped with the AUAP device in Table 13.

We can see from Figure 140 that the angle of attack reserve up to the moment of operation is 1.8-3.2° (M = 0.7-0.82). For example, for M = 0.8, the reserve from α_{hf} = 3° to α_{op} = 5.2° is 2.2°, and the reserve to $c_{y\ sup}$ is 4°. In order to achieve $c_{y\ sup}$ = 0.7 in flight at M = 0.8, we must create an overload n_y = 0.7/0.275 = 2.52. However, at α_{op} = 5.2° (c_y = 0.53), i.e., at overload n_y = 0.53/0.275 = 1.93, the "$n_{y\ sup}$" light comes on. The pilot's

action in controlling the longitudinal attitude of the aircraft prevents the aircraft from entering the dangerous rolling regime.

TABLE 13

M Number	0,6	0,65	0,7	0,75	0,8	0,82
a°_{sup}	10,6	9,8	8,8	8	7	6,6
$a^\circ_{oper.cr}$	9,2	8,4	7,4	6,3	5,2	4,6
a°_{hf} for H=10km	5,7	5	4,2	3,5	3	2,8
$C_{y\ sup}$	0,96	0,91	0,84	0,78	0,7	0,66
$C_{y\ oper}$	—	—	0,715	0,62	0,53	—
$C_{y\ hf}$	—	—	0,355	0,315	0,275	0,26
$n_{y\ oper}$	—	—	2,0	1,96	1,93	—

Note: Commas represent decimal points.

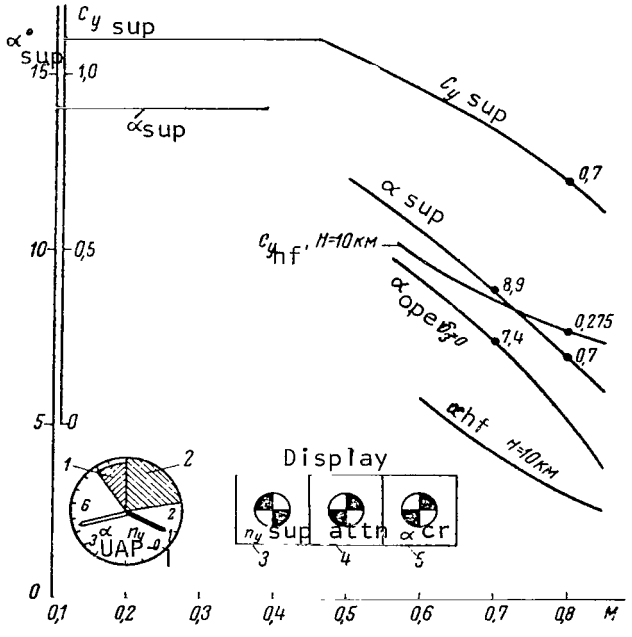

Figure 140. Operating Characteristics of AUAP As a Function of M Number: 1, Movable sector of critical angles α_{cr}; 2, Sector of dangerous overloads; 3, Nonflashing lamp warning of dangerous n_y; 4, Flashing lamp; 5, Nonflashing lamp signalling critical angles α

The speed reserve from the moment when the light signalling the dangerous regime lights up until the minimum permissible speed is reached is usually 25-40 km/hr and the reserve before rolling is 80-100 km/hr indicated speed.

With flaps down, the automatic device also warns the pilot in advance of any deviation from the normal regime. For example, where α_{op} = 9-10° (near the angles of attack used in landing and takeoff), transfer of the aircraft into the nonpermissible regime is signalled by lighting of the "α_{cr}" lamp.

§16. Lateral Stability /218

Lateral equilibrium of the aircraft can be disrupted by two factors which are interrelated: slipping and banking. Thus, if the cause of a disruption of lateral equilibrium is banking, as a result of the force of

gravity an unbalanced lateral force will appear, applied at the center of gravity, which will distort the trajectory of movement. The aircraft begins to slip. In the same way, if the disruption of lateral equilibrium occurs as a result of slipping of the aircraft, an increase in lateral force ΔZ occurs, applied at the lateral aerodynamic center, the trajectory is curved and as a result an unbalance transverse moment ΔM_x appears. The aircraft begins to bank. Thus, when lateral equilibrium is disrupted, the aircraft begins to rotate about the axes of ox and oy simultaneously.

The term lateral stability means the ability of an aircraft to return to its initial position after any small perturbation independently, without pilot action, except for unavoidable course deviation.

For a better understanding of lateral stability, it is methodologically expedient to analyze first stability of the aircraft relative to the ox axis, then separately relative to the oy axis. The former is called transverse stability, the latter -- directional stability.

Simultaneous directional and transverse stability represent lateral stability of the aircraft.

§17. Transverse Static Stability

Transverse stability is the ability of an aircraft to eliminate a bank automatically, or, in other words, to bank in the direction opposite to slippage. For example, if the aircraft slips to the right, the aircraft should bank to the left.

In order for an aircraft to eliminate bank independently, it is necessary that a transverse moment arise on the lower wing during slipping such as to cause rotation toward the higher wing. The banking of the aircraft itself has no direct influence on the magnitude of transverse moments. Its influence is felt through slipping. The bank angle determines the slip angle which is the direct cause of transverse moments.

The degree of transverse stability is evaluated according to the value of transverse moment Δm_x restored per one degree of slip angle β, i.e., according to the value of m_x^β, called the coefficient of transverse static stability:

$$m_x^\beta = \frac{\Delta m_x}{\Delta \beta}.$$

In a transversely stable aircraft, when slipping occurs to the right wing (positive slipping), a negative transverse moment appears on the left wing, and coefficient m_x^β is negative. The value of this coefficient is determined /219

primarily by the form of the wing and the height of the vertical control surface. For swept wings with no transverse V, the transverse stability coefficient is usually quite high, and must be decreased by giving the wing a negative transverse V = -(1-3°). This decreases the moment of the bank striving to bring the aircraft out of the slipping state.

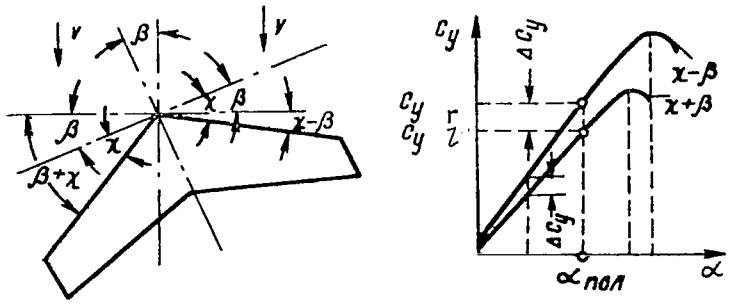

Figure 141. Change in Sweep Angle of Wing During Slipping and Influence of Slipping on Dependence of c_y on Angle of Attack

Transverse static stability depends both on the angle of attack and on the flight speed. Mechanization of the wing is also quite important. The increase in transverse static stability with increasing coefficient c_y is explained as follows. When a swept wing slips, the sweep angle of the wing is changed (Figure 141). Where the sweep angle is decreased (right wing), the load bearing qualities increase. The curve of the function $c_y = f(\alpha)$ for this wing is higher than for the wing for which the sweep angle increases during the slip. We see from the graph that at high angles of attack (more precisely at high values of c_y) the difference in the values for the wings increases. Therefore, the higher the angles of attack at which flight is performed, the greater the banking moment created during slipping.

As a result, transverse stability of a swept wing is higher, the higher the angle of attack. Whereas during climbing, horizontal flight and descent (angles of attack 2.5-3.3°) the transverse static stability is within the limits of normal values, during the landing regime it increases.

The increase in lateral static stability at high angles of attack has a negative influence on the prelanding regime and may worsen the flying qualities of an aircraft, causing it to rock and giving it poor damping characteristics. Therefore, when the flaps are lowered (high values of c_y), when flight is being performed at low speeds, the transverse static stability is high. /220

An increase in transverse stability of an aircraft at low angles of attack is aided by aerodynamic deflection of the wings.

Aerodynamic baffles also extend the beginning of development of terminal separation and help to increase the transverse stability of an aircraft at high angles of attack.

§18. Directional Static Stability

Directional stability is the ability of an aircraft to eliminate slipping automatically. During flight with slipping, as a result of lateral air current against the fuselage, aerodynamic force Z arises, the moment of which relative to the center of gravity creates a rotating moment M_y about vertical axis oy. Normally, the point of application of the lateral force is behind the center of gravity of the aircraft, as a result of which force Z tends to rotate the aircraft (like a weather vane) toward the wing onto which the aircraft is slipping. Quantitatively, the degree of directional stability is determined by the value of stability coefficient m_y^β. Physically, coefficient m_y^β defines the amount of increase in rotational moment M_y^β when the slipping angle β changes by one degree, i.e.,

$$m_y^\beta = \frac{\Delta m_y}{\Delta \beta}.$$

The greater m_y^β, the greater the directional stability of the aircraft and the more intensively it eliminates slipping.

Modern aircraft have sufficient directional stability, coefficient m_y^β is negative, i.e., when the aircraft slips over onto the right wing (positive β) a directional moment appears to rotate the aircraft to the left.

Directional stability of aircraft is provided primarily by the vertical tail surface.

§19. Lateral Dynamic Stability

Let us assume that an aircraft is banked onto the right wing under the influence of external perturbation. This results in right slippage, and the trajectory of the aircraft is bent to the right. Further movement of the aircraft depends on the ratio between transverse and directional stability. Let us assume that the transverse stability is greater than the directional stability, i.e., m_x^β is greater than m_y^β. In this case the bank is rapidly eliminated, the aircraft moves from right bank to left bank and begins to slip on the left wing. However, since the slipping is not completely eliminated, once more a banking moment onto the right wing appears. The aircraft goes into a right bank once more. Thus, a rocking of the aircraft occurs, called lateral oscillating instability.

On the other hand, if m_x^β is less than m_y^β, i.e., the directional moment is greater than the transverse moment, after the aircraft is banked, the bank is retained, but the slipping is rapidly eliminated. The remaining bank curves

the trajectory, i.e., the aircraft descends in a spiral to the right. This is known as lateral spiral instability.

The dynamics of the lateral movement of the aircraft under the influence of external conditions and its behavior under the influence of the pilot's actions are determined in these examples not only by the sign and magnitude of coefficients m_y^β and m_x^β, but also by the presence of certain relationships between them. Therefore, the magnitude of κ, which is directly dependent on the ratio m_x^β/m_y^β and numerically equal to the ratio of angular velocities of bank and yawing, is very important in lateral dynamic stability as well as the controllability of the aircraft.

$$\varkappa = \frac{\omega_x}{\omega_y}.$$

This parameter characterizes the lateral movement of the aircraft.

Figure 142 shows a recording from a strip chart recorder when the rudder is moved with (a) and without (b) the yaw damper. Recording of characteristics ω_x and ω_y at low flight speeds was performed with flaps fully down. After the rudder impulse was transmitted, the direction of the aircraft began to slip with a bank.

As we can see from the recordings, after 8.8 sec κ = 2, after 12.1 sec, 1.94 and further, as the oscillations were damped, the value decreased. Attenuation of oscillations shows the dynamic lateral stability of the aircraft. The value of κ should lie between zero and one. We can see on Figure 143 that this condition is observed at various altitudes only within a definite range of M numbers, for example for H = 10,000 m at M > 0.75. At smaller M numbers, $\kappa > 1$. When the value of κ is extremely high, so that the ratio m_x^β/m_y^β is high, the aircraft will be judged unsatisfactory by its pilots. This is explained by the fact that with high transverse stability, the reaction of the aircraft to slipping becomes quite sharp. In this case, even small slip angles cause the aircraft to bank sharply, and banking and yawing movements with comparatively short repetition periods occur, and are not always damped. This "rocking" of the aircraft is usually evaluated by pilots /223
as lateral instability, although actually it is an excess of lateral stability, causing the aircraft to respond eagerly to the slightest random slipping. In landing modes, the values of κ produced are rather high (on the order of of 1.5-2), leading to yawing and rocking of the aircraft (Figure 144). Piloting of the aircraft is more difficult, and the pilot must frequently operate the controls. Flight in bumpy air becomes particularly unpleasant.

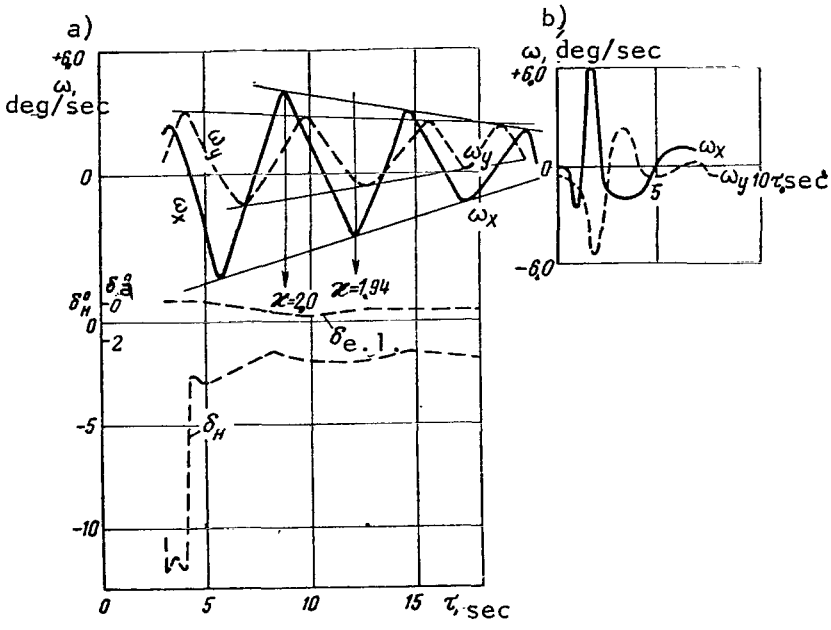

Figure 142. Determination of Value of χ(V_r = 220 km/hr, δ_n is the angle of deviation of the rudder, H = 2000 m, landing gear and flaps down)

The dependence of the parameters T, κ and m_{b1}, characterizing the lateral dynamic stability of the aircraft, on flight speed are shown on Figure 144.

§20. Yaw Damper

We know that an arrow-shaped aircraft will have satisfactory lateral stability if, in addition to transverse and directional stability and the optimal combination of these two, it also has good damping properties, providing intensive damping of lateral oscillations.

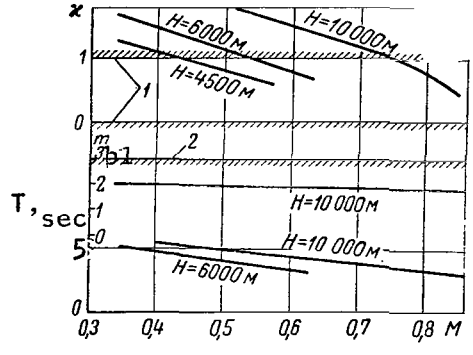

Figure 143. Characteristics of Lateral Dynamic Stability As a Function of M Number (angle χ = = 35°, landing gear and Flaps Up); 1, 2, Normalized values of parameters

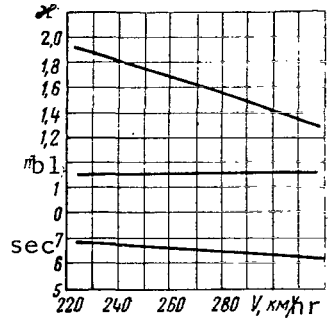

Figure 144. Characteristics of Lateral Dynamic Stability As Functions of Flight Speed (l.g. down, flaps down, H = = 2100 m)

The installation of dampers has allowed improvement in the damping characteristics in the event of perturbations to be achieved, particularly during takeoff and landing. At the same time, the effectiveness of the ailerons has been increased.

Thus, the stability of an aircraft is increased and the work of the pilot is greatly eased, especially in transient modes. For example, the yaw damper provides automatic damping of aircraft course and bank oscillations by artificially increasing the damping coefficient by automatically shifting the rudder to an angle proportional to the angular velocity. As the yaw damper operates, the intensity of damping of lateral oscillations is increased; this means that the number of oscillations to complete damping and the total time of damping are decreased. The amplitude of oscillations A (Figure 116) during one period is decreased so greatly that the value $m_{b1} = A_1/A_2$ is decreased by several times. Figure 142 b shows a diagram of the decrease in angular velocities when the yaw damper is turned on after a pulse is fed to the rudder. The period of oscillation is decreased to 5-7 sec, $m_{b1} = 5\text{-}8$ and the sense and significance of parameter κ are lost.

The actuating mechanism of the damper (Figure 145) is a telescopic arm. Control of the rudder during operation of the damper is performed using a hydraulic amplifier which transmits the force to the rudder.

The angular velocity transducers, which measure ω_x and ω_y, are gyroscopes with two degrees of freedom, reacting to the angular velocity of rotation of /224
the aircraft about the oy and ox axes. As the aircraft oscillates about these axes, periodic changes in angular velocities of yaw ω_y and bank ω_x occur. Electrical signals are produced which are proportional at each moment to the values of these velocities, then are amplified and sent to the telescoping arms. The telescoping arms are installed in the arms of the rigid control system from the pedals in front of the pilot. The hydraulic amplifier deflects the rudder depending on the linear displacement of the shaft of the telescoping arm according to an established control law. For example, with the landing gear down and flaps down, deflection of the rudder occurs on the basis of signals from the ω_y and ω_x transducers. The control law can be represented by the following formula:

$$\Delta\delta_r = A\omega_y + B\omega_x,$$

where $\Delta\delta_r$ is the deflection of the rudder;

A, B are the coefficients of proportionality corresponding to the adjustment of the damper.

With the landing gear and flaps up, the signal from the ω_x transducer is disconnected and the operation of the damper follows the law $\Delta\delta_r = A\omega_y$.

The operation of the telescopic arms has no influence on the movement of the pedals, although the rudder is deflected by an angle proportional to the angular velocity of rotation of the aircraft. When the aircraft rotates to the right, the rudder is deflected to the left and vice versa.

Let us use the following examples to analyze when and how the rudder is deflected by the damper:

1. Let us assume that in flight with landing gear and flaps down, the pilot turns to the right. To do this, he deflects the stick to the right, banking the aircraft to the right by angle γ (Figure 146 a). Due to the difference in lifting forces on the wings, transverse bank moment $+M_{xa}$ appears from the ailerons, under the influence of which the aircraft begins to rotate to the right at angular velocity $+\omega_x$. As it banks to the right, /225
the aircraft will slip at angle $+\beta$ to the right (lower) wing (Figure 146 b), and lateral moments M_x and M_y appear.

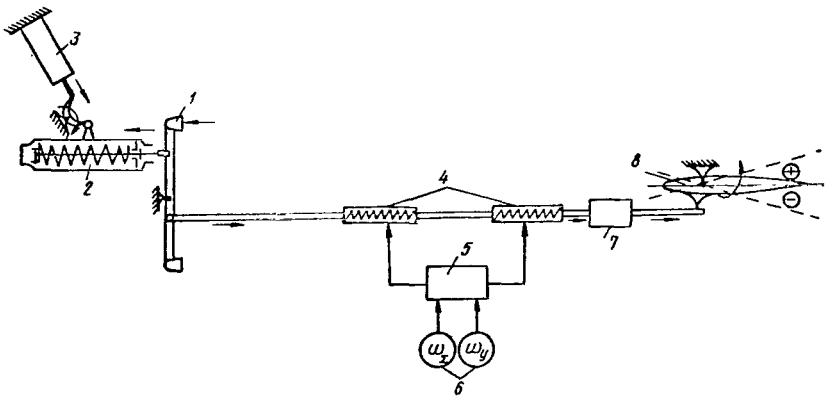

Figure 145. Diagram of Operation of Yaw Damper in Rudder System: 1, Pedal; 2, Spring load; 3, Trimming mechanism; 4, Telescopic arm; 5, Amplifying unit; 6, Angular velocity transducer; 7, Hydraulic amplifier; 8, Rudder

In a laterally stable aircraft, as slipping begins, transverse moment M_{xs1} arises, acting to eliminate the bank, i.e., acting to lift the wing (Figure 146 c). This moment, proportional to the coefficient of transverse stability m_x^β and slip angle β is: $-M_{xs1} = -m_x^\beta \beta C$ (where $C = qS\ell$, q is the velocity pressure, S is the area of the wing, ℓ is the wing span) and acts against the deflected ailerons, as a result of which the effectiveness of transverse control is worsened. The greater the transverse static stability of the aircraft (bank stability), which is a property of all swept wing aircraft at low flight speeds (V = 240-280 km/hr), the more sharply the

aircraft will react with reverse bank to the lifting (lagging) wing during slipping, so that a position arises in which the ailerons are ineffective. Due to the directional stability, as the aircraft slips to the right a moment appears proportional to the coefficient of directional stability $-M_{ysl} = -m_y^{\beta}\beta C$, rotating the aircraft to the right at angular velocity $-\omega_y$ /226 (Figure 146 d) in attempting to eliminate the slip, slightly reducing the loss of effectiveness of the ailerons. Therefore, the less slipping at the moment when the aircraft is banked, the less will be the bank in the direction of the rising wing.

Thus, in order to increase the effectiveness of the ailerons, it is necessary when the aircraft is banked to reinforce rotating moment M_{ysl}, adding a moment from the rudder resulting from its deflection by angle $+\Delta\delta_{r3}$. This deflection is created by the yaw damper.

With flaps and landing gear down, the deflection of the rudder from the yaw damper is determined from the formula:

$$\Delta\delta_r = A\omega_y + B\omega_x.$$

The signal ω_x deflects the rudder by angle $\Delta\delta_{r1} = B\omega_x$. However, due to the appearance of the angular rotation velocity $-\omega_y$ (rotation of the right due to shifting of the rudder) the rudder will also be automatically deflected by the damper in the opposite direction by angle $-\Delta\delta_{r2} = -A\omega_y$. The summary deflection of the rudder $+\Delta\delta_{r3}$ will be less than from the signal $+\omega_x$ alone (Figure 146 d) so that the effectiveness of operation of the damper will be slightly reduced. However, the controllability of the aircraft (more precisely, the effectiveness of the ailerons) is increased significantly in comparison to the controllability without this damper.

2. If the disruption of equilibrium of the aircraft occurs due to a gust from the left (Figure 146 e) forming a right bank (we will consider that the pilot has not yet had time to move the controls), slipping onto the right wing occurs at angle $+\beta$. As in the preceding case, lateral moments occur. Transverse moment $-M_x$ will bring the aircraft out of the bank, and rotating moment $-M_y$ will act to reduce the slip angle. Thus, as a result of the gust we have $+\omega_x$ and as a result of the slipping, $-\omega_y$. The rudder is deflected by $\Delta\delta_{r1} = B\omega_x$ in addition to $\Delta\delta_{r2} = -A\omega_y$.

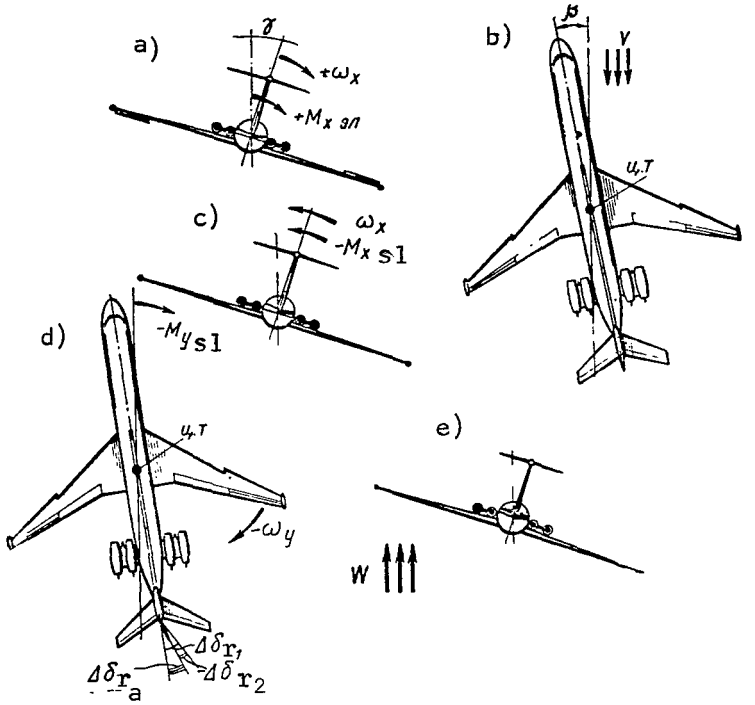

Figure 146. Explanation of Operation of Automatic Rudder Control by Damper

Actually, the operation of the yaw damper is more complex than what we have just analyzed. In particular, after equilibrium is disrupted, transverse moment $-M_x$ results in angular velocity $-\omega_x$ (rotation to the left) and the rudder is shifted to the left. However, the action of angular velocity $-\omega_x$ is much less than $+\omega_x$ created by action of the pilot or a vertical gust, since the initial deflection of the rudder rapidly eliminates the slipping. The summary deflection of the rudder may be so great that the aircraft reduces slipping onto the right wing energetically, even perhaps beginning to slip onto the left.

In this case, a bank onto the right wing will appear again, and the aircraft as a result will yaw back and forth several times, rocking from wing to wing. The damper causes the oscillations to die out quickly, and the pilot feels no sensible rocking. /227

Also in flight (flaps up, ω_x signal disconnected) with momentary application of a side wind gust, the aircraft will first energetically rotate, and slipping occurs at angle β. Due to the ω_y signal, the rudder is deflected by the damper to eliminate the slipping, and due to the action of the damper, in addition to the damping properties of the aircraft, rotation under the influence of the side wind will be retarded (for simplicity we will not analyze the banking moment). When, due to the directional stability and deflection of the rudder to reduce slippage, the aircraft tries to return to its initial position, ω_y of opposite sign appears and the initial deflection of the rudder is decreased. The effect of the directional stability of the aircraft is slightly reduced. The movement of the aircraft will be directed to eliminate the slipping, and it returns to its initial position, eliminating

the initial slipping, and may even begin slipping on the other wing. However, these oscillations of the aircraft about the oy axis are rapidly damped and rocking is eliminated.

The pilot may get the impression that the directional stability of the aircraft with the yaw damper is worse, and that the aircraft is less stable, although in actuality, the yaw damper causes perturbations which arise to be quickly attenuated. Thus, each angular velocity of rotation of the aircraft about the oy and ox axes corresponds to a definite deflection of the rudder. If angular velocity ω_y is 1 deg/sec, deflection of the rudder will be $A\omega_y$ degrees, while if ω_x = 1 deg/sec -- $\delta_r = B\omega_x$ degrees (A and B are equal to about 1.5-2).

In order to increase reliability of damper operation, usually two series connected telescoping arms are installed, operating simultaneously. Their control action is added. The stroke of each arm is 6-8 mm, and the maximum deflection of the rudder by the damper is 5-6°.

When the rudder is turned off or when there is no angular velocity of rotation of the aircraft, the telescoping arm automatically takes up a neutral position.

The hydraulic amplifiers of the yaw dampers operate without reverse. This means that the aerodynamic load arising in flight on the rudder is not transmitted to the pedals, and the entire hinge moment from the rudder is absorbed by the amplifier piston. The pilot need only expend the force required to move its valve. Since this force does not give the pilot any "control" feeling," the desired magnitude and nature of force change must be created by inclusion of a special spring loading device in the control system. When the pedals are moved (by the pilot) the load springs are compressed, /228
imitating the aerodynamic load from the rudder. The force from the pedal can be removed (during long flight with deflected rudder) by an electromechanical trimming mechanism which shifts the body of the spring loader to a position in which the load is reduced to zero. In all cases of failure of the yaw damper, control of the rudder is performed by the pilot with the pedals, requiring him to overcome the hinge moment from aerodynamic loads.

§21. Transverse Controllability

Transverse control of the aircraft is performed by the ailerons, and in certain aircraft by the ailerons together with interceptors. Deflection of the interceptors (aiding the ailerons) is performed after the ailerons are deflected by 8-10°. This type of control is characteristic for aircraft with large wing areas. The effectiveness of transverse control of the aircraft is greatly augmented.

Also, the ailerons are frequently made in sections, in order to reduce "floating" in case of flow separation on the wing. The ailerons are usually

deflected by ±20° (up and down), and the angle of rotation of the control wheel is 120-180°. The angle of aileron deflection by the autopilot averages ±2.5-3.5°. In the portion of the wing where the ailerons are placed the relative thickness of the wing profile is slight, 10-12%, the relative curvature 0.8-1.5%. The comparatively small relative thickness and slight curvature allows the ailerons to be deflected by the same angle up and down. The rotating moment thus produced (as a result of difference in the drag of the wings with ailerons up and down) is slight, even at large angles of attack and has almost no influence on the behavior of the aircraft (rotation about vertical axis).

A swept wing shape has an unfavorable influence on transverse controllability, particularly at large angles of attack. The tendency of swept wing aircraft to react sharply by banking to slipping and to eliminate aircraft banking (by operation of the ailerons) significantly decreases the effectiveness of the ailerons. Their effectiveness is decreased by side flow of the boundary layer along the length of the wing, increasing the intensity of flow separation at its ends. Aerodynamic baffles prevent early development of flow separation in the terminal cross sections and thereby increase the effectiveness of aileron operation.

Let us look upon the force applied to the control wheel for ailerons in order to create an angular banking velocity of 1 rad/sec, $\Delta P_a/\Delta\omega_x$ as a characteristic of transverse controllability, as well as the change in angular banking velocity ω_x resulting from a change in aileron deflection of one degree, $\Delta\omega_x/\Delta\delta_a$. /229

During transverse rotation, a damping moment arises which should be equalized by the banking moment from the ailerons.

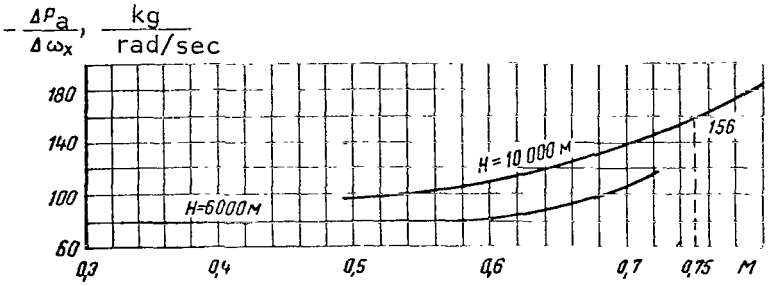

Figure 147. Force on Control Wheel As a Function of M Number

As we can see from Figure 147, at M = 0.7-0.75, the force is 105-156 kg. This means that if we must create an angular ω_x = 3 deg/sec, a force of 5.5-7 kg must be applied to the wheel. The higher ω_x, the greater must be the force on the wheel. As ω_x is doubled, the force also doubles. As the flight altitude is increased with constant M number, the force on the wheel increases, since, due to the decrease in velocity pressure, the aileron deflection angles increase. We can see from the figure that at 10,000 m, the forces are greater than at H = 6000 m.

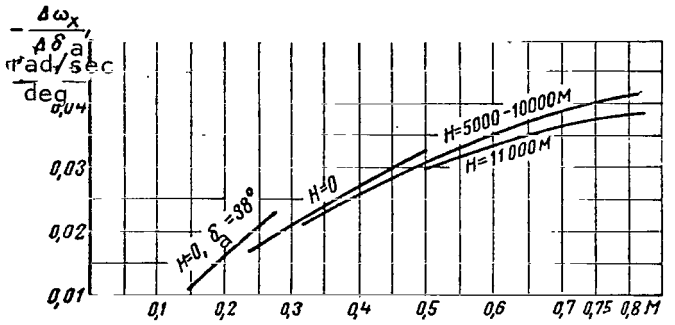

Figure 148. Aileron Effectiveness As a Function of M Number

The aileron effectiveness can be estimated as a function of M numbers and altitudes using the graph on Figure 148. The higher the absolute value of $\Delta\omega_x/\Delta\delta_a$, the more effective are the ailerons. At speeds near the maximum the effectiveness of the ailerons should allow the development of an angular velocity of ω_x = 12 deg/sec, with forces not over 35 kg on the wheel (according to the technical conditions). For example, at H = 10,000 m and M = 0.75, the creation of ω_x = 1 rad/sec (57.3°) requires a force of P_a = 156 kg at the wheel. If a force of 35 kg is applied, we produce an angular velocity ω_x = 12.8 deg/sec. The aileron deflection used is

/230

$$\delta_a = \frac{\omega_x}{\frac{\Delta\omega_x}{\Delta\delta_a}} = \frac{12,8}{2,29} = 5,6°.$$

The quantity 2.29 $\frac{\text{deg/sec}}{\text{deg}}$ (0.04 $\frac{\text{rad}\cdot\text{sec}}{\text{deg}}$) is taken from the graph of Figure 148.

The aileron effectiveness in a landing maneuver (M = 0.2, V_r = 250 km/hr) can also be estimated using the graph of Figure 148. As we can see, with an aileron deflection of one degree we produce ω_x = 9.45 deg/sec ($\Delta\omega_x/\Delta\delta_a$ = = 0.0165).

With a force on the wheel of 90 kg at these speeds ω_x = 1 rad/sec, and the production of an angular rotation velocity of 9.45 deg/sec requires a force of 14.8 kg.

§22. Directional Controllability. Reverse Reaction for Banking

The rudder is deflected to the right and to the left by the pedals by 20-25°, by the auto pilot by an average of ±4-5°. Axial compensation of the rudder is generally 28-29% of its area (in order to produce acceptable forces). On most aircraft, it has been noted that, due to increased area of axial compensation at angles of deflection of 10-12° or more (about one third of the pedal travel) the tip of the rudder moves out into the stream and forces on the pedal begin to decrease. A phenomenon of overcompensation

arises. In order to eliminate this phenomenon, the rudder control system includes spring loaders. They compensate for the decrease in force on the pedals at large deflection angles or during slipping.

Also, interceptors may be used. They have an angular profile and are fastened to the front of the rudder in front of its rotation axis (Figure 149).

The action of an interceptor can be reduced to the following. When the rudder is deflected by 10-12°, the interceptor on the left side enters the stream and creates separation (and therefore a change in pressure distribution) in the portion of the rudder behind the axis of rotation. The interceptor on the right side is covered by the vertical tail surface and does not interfere with the flow. Due to the rarefaction formed on the left side, the rudder attempts to move to the left (move with the stream), which creates an additional load on the right pedal as the rudder is held in its deflected position. As we can see from the graph, the force on the pedal increases with increasing angle of deflection of the rudder, while where there is no interceptor the force begins to decrease at deflection angles 10-11° (overcompensation effect). /231

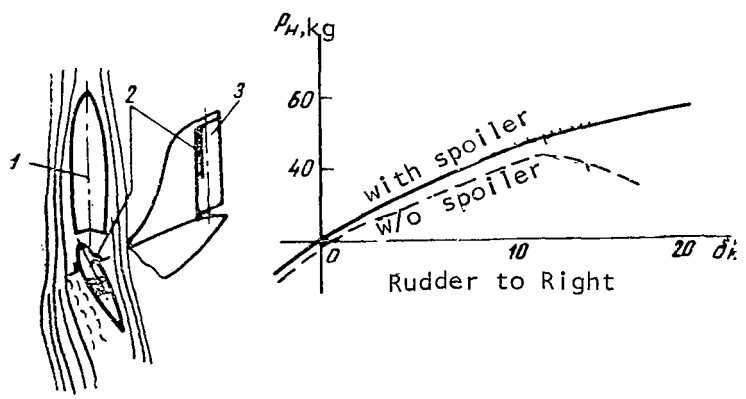

Figure 149. Force on Pedals As a Function of Deflection of Rudder During Straight Line Flight with One Motor Off (V_r = 300 km/hr, landing gear down, δ_3 = 20°, H = 1500-2000 m): 1, Vertical tail surface; 2, Interceptor; 3, Rudder

Thus, installation of the interceptor causes an increase of the hinge moment and produces a direct force on the pedals, this force being greater, the greater the angle of inclination of the rudder.

Let us look upon the banking reaction of the aircraft to a deflection of the rudder defined by $\Delta\omega_x/\Delta\delta_r$ as a characteristic of directional controllability, where $\Delta\omega_x$ is the change in angular bank velocity; $\Delta\delta_r$ is a change in rudder deflection of one degree.

As we can see from Figure 150, up to M = 0.84-0.85, $\Delta\omega_x/\Delta\delta_r$ is positive, i.e., the bank follows the control. At high M numbers, the sign becomes negative, i.e., the bank is opposite. This means that a reverse bank reaction occurs when pedal is fed. Let us analyze this feature of aircraft with swept /232

wings in more detail.

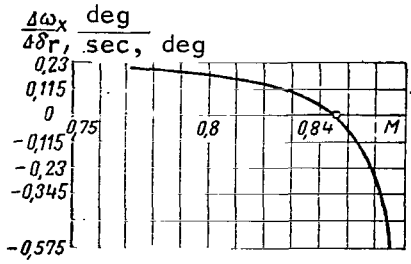

Figure 150. Dependence of $\Delta\omega_x/\Delta\delta_r$ on M Number (H = = 10,000 m; at M = 0.84, reverse banking reaction of the aircraft to deflection of rudder begins)

In a transversely stable aircraft when left pedal is applied a slip to the right occurs and, as a result, a moment arises tilting the aircraft onto the left wing; conversely, when right pedal is fed, a bank to the right occurs. This reaction of the aircraft to deflection of the rudder is called normal or direct.

However, when an aircraft with swept wings flies at high M number, this regularity may be disrupted (for example, when right pedal is fed, the aircraft banks to the left rather than the right).

The appearance of a reverse bank reaction when the rudder is deflected results from the influence of compressibility of the air on the aerodynamic characteristics of the wing. At subcritical speeds, the sweep of the wing helps to increase the transverse stability of the aircraft and, consequently, reinforce the direct bank reaction to deflection of the rudder. The picture is different at supercritical flight speeds.

During slipping, the effective sweep angles of the right and left wings change, so that their critical M numbers also change (Figure 151). The wing which is moved forward shows a decrease in M_{cr} as a result of the decrease in effective sweep angle, while the lagging wing, on the other hand, shows an increase in M_{cr} as a result of the increased sweep angle. This change in M_{cr} means that in slipping the wave crisis develops at different times on each wing -- first on the wing on which the effective sweep angle is less. This time differential in development of the wave crisis on the left and right wings and, consequently, the asymmetry in the change of their lift, causes the appearance of a reverse bank reaction when pedal is fed. /223

Figure 152 shows the regularity of deflection of ailerons during acceleration with slipping in an aircraft with reverse bank reaction to slipping. It is easy to determine the M number at which the degree of normal reaction of the aircraft to slipping begins to decrease (point 1) and when the normal reaction is transferred to a reverse reaction (point 2). At this same point 2, where the curve passes through zero, there is neither a direct nor a reverse bank reaction to slipping. In other words, when flying with M number corresponding to point 2 the aircraft does not have any bank reaction to slipping; the manifestation of this is that when the pedals are deflected a pure yaw motion occurs without any tendency to bank.

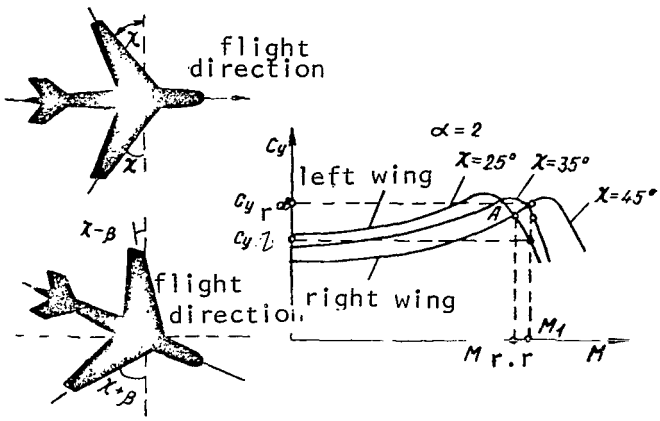

Figure 151. Change in Effective Sweep Angle and Coefficient c_y As a Function of M Number with Constant Angle $\alpha = 2°$ for Wings Differing in Sweep Angle

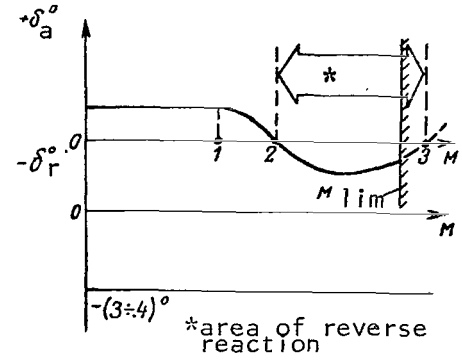

Figure 152. Deflection of Ailerons During Acceleration with Slipping on an Aircraft with Reverse Bank Reaction to Slipping

Between points 2 and 3 we find the area of reverse bank reaction to slipping. To the right of point 3, direct reaction is restored once again. Frequently, this point is unattainable, since the corresponding M number is beyond the limiting permissible number for the aircraft (as is the case on Figure 152).

The beginning of the reverse reaction can be found by accelerating and deflecting the rudder.

If an aircraft with a swept wing ($\chi = 35°$) flies at a speed corresponding to M_1 (Figure 151) at which the reverse reaction occurs ($M_1 > M_{rr}$), when right pedal is fed during left slip, for example with an angle $\beta = 10°$, the effective sweep angles of the wings change: the angle of the left wing is 25°, of the right wing -- 45°. As a result of this, the development of the wave crisis on the left wing is reinforced, while it is retarded on the right wing. As a result, coefficient c_y on the left wing is sharply decreased, while it is slightly increased on the right wing, leading to high transverse moments, tending to bank the aircraft in the direction of the slip.

The greater the sweep of the wing and the thinner the wing profile, the weaker the reverse bank reaction will be, since the change in c_y with M number will be smoother. The M number corresponding to the point of intersection of curves $c_y = f(M)$ for sweep angles 25 and 45° is represented by M_{rr}. The pilot should know the M number of the reverse reaction of his aircraft and recall /234

the factors which might lead to improper piloting if he is forced to fly at $M > M_{rr}$.

We note in conclusion that in modern aircraft the rudder is practically never used in flight. Control of lateral aircraft movement (curves, turns, spirals and other evolutions) are actually performed by the ailerons alone. Exceptions include takeoff and landing, during which gusts of wind (particularly side gusts) are sometimes countered using deflections of the rudder.

§ 23. Involuntary Banking ("Valezhka")

In high-speed aircraft with swept wings, so-called involuntary banking may occur, which has come to be called "valezhka." This phenomenon occurs both at low altitudes at high indicated speeds, and at high altitudes at high M numbers.

Valezhka may occur for two reasons: a) as a result of the appearance of a banking moment under the influence of a difference in lifting force on the left and right wings and b) due to a drop in aileron effectiveness.

The difference in lifting force on the wings is created due to geometric or rigidity asymmetry of the aircraft. Geometric asymmetry is characterized by a difference in effective angles of attack of portions of the right and left wings. If the wings have different structural rigidity and therefore different deformations, a difference in angle of attack may occur. All of this leads to large banking moments at high flight speeds.

However, this banking moment sometimes cannot be countered by deflecting the ailerons, since under certain conditions their effectiveness is decreased. Suppose, for example, a banking moment on the right wing appears. In order to counter this moment, the pilot deflects the right aileron downward, the left aileron upward. However, when the ailerons are deflected at high indicated speed (when the velocity pressure is great) moments appear which twist the wing. Due to the elasticity of the wing, the angle of attack of the right wing is decreased, that of the left wing increased. This diminishes the effect of aileron deflection. The forces on the control wheel increase sharply. This phenomenon is called aileron reverse.

At high altitudes, the aileron effectiveness drops due to the presence of supersonic zones and compression drops on the wing.

In all cases where valezhka occurs, the pilot should take measures to prevent banking of the aircraft, and the bank should be corrected with the ailerons. Countering of valezhka at high M numbers by feeding pedal against the bank may result, in some aircraft with swept wings (as a result of the reverse bank reaction) to an increase in the bank. /235

§24. Influence of Compressibility of Air on Control Surface Effectiveness

The controllability of an aircraft, dependent on the operation of the horizontal control surfaces, may change essentially at high M numbers. Let us analyze the operation of the control surfaces at various M numbers. As we know, when the surfaces are deflected at subcritical speeds, a change in the flow spectrum and pressure distribution occurs throughout the entire profile of the control surface, as a result of which aerodynamic force R_{ht} arises (Figure 153 a). The change in pressure distribution is explained by the fact that deflection of the control surface creates small perturbations, propagating in all directions at the speed of sound, including against the direction of flow, which is subsonic. These small perturbations cause changes in pressure along the profile of the air foil.

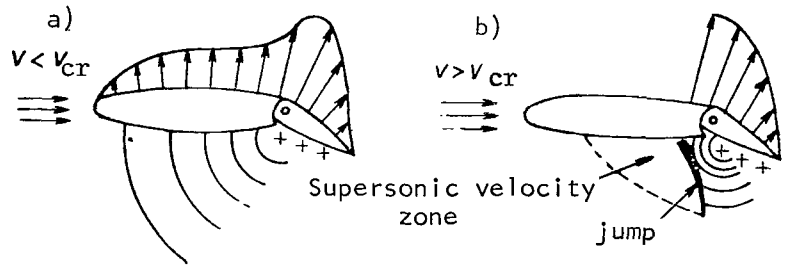

Figure 153. Explanation of the Influence of Air Compressibility on Control Surface Effectiveness

If flight is performed at supercritical M numbers, at which the wave crisis is developed on the control surface, the effectiveness of the articulated surfaces is decreased considerably. This occurs for the following reasons.

After supersonic velocities arise on the tail surfaces, when the pressure jump ends, the deflection of the control surface can no longer change the nature of the flow around the entire tail surface, nor can it change the pressure distribution over the surface (Figure 153 b). In this case, the perturbations caused by deflection of the articulated control surface section, propagating at the speed of sound, cannot extend to the portion of the tail surface where the flow rate is higher than the speed of sound. Therefore, the nature of the flow changes only over that section of the tail surface which is located behind the compression jump. Thus, the creation of additional aerodynamic force by deflection of the articulated surface includes only a portion of the tail surface, so that the magnitude of the force is decreased.

In order to improve the effectiveness of the surfaces at high speeds, M_{cr} for the tail surfaces can be increased by using high-speed profiles and

giving the tail surface an arrow-like form in cross section. In order to prevent early loss of tail surface effectiveness, M_{cr} should always be greater for the tail surface than M_{cr} for the wing. Also, the horizontal tail surface should be removed (upward or downward) from the vortex flow zone behind the wing, in order to avoid decreases in its effectiveness.

§25. Methods of Decreasing Forces on Aircraft Control Levers

In order to control the aircraft, the pilot deflects the control surfaces by applying certain forces to the command levers. The forces on the levers depend on the hinge moments arising as the articulated surfaces are deflected. If these forces are great and the flight requires a good deal of maneuvering, operation of the control organs becomes fatiguing. At high speeds, significant hinge moments are characteristic, so that great forces must be expended to control the aircraft.

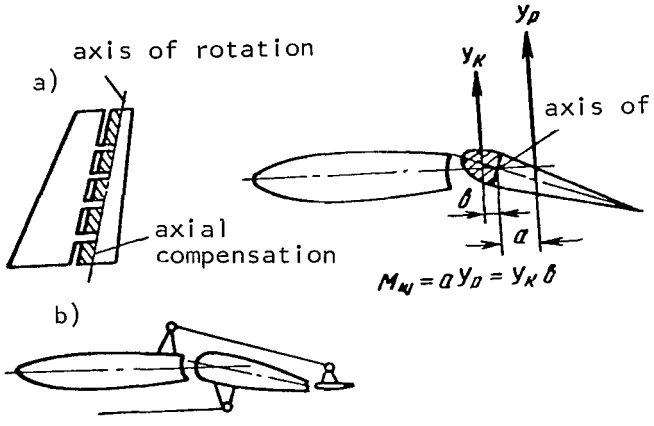

Figure 154. Explanation of Hinge Moment and Operation of Axial Compensation (a), and Diagram of Operation of Servo-compensator (b)

The hinge moment is the moment created by the aerodynamic force arising on the articulated surface as it is deflected relative to its axis of rotation. This moment acts against deflection of the surface and is perceived by the pilot as a force on the control stick or pedals (Figure 154). The hinge moment increases with increasing angle of deflection of the surface (from its equilibrium position), with the area and cord of the surface and with velocity pressure.

In order to decrease the force on the stick, axial or internal compensation, servo-compensators and trimmers are used. Axial compensation is achieved by displacing the point of rotation of the surface (hinge) backward, thus decreasing the hinge moment (Figure 154). Axial compensation of the elevator covers about 30% of its area, of the rudder -- about 28-29% of its area, of the ailerons -- 28-31%. Greater values of axial compensation may lead to overcompensation. Its essence is as follows. The hinge moment can be decreased to zero, or if the hinge is moved

even further rearward a hinge moment of the "reverse" sign may appear. In this case, the hinge moment appearing when the surface is deflected will tend to increase the angle of deflection. This is an unfortunate phenomenon, and is called overcompensation.

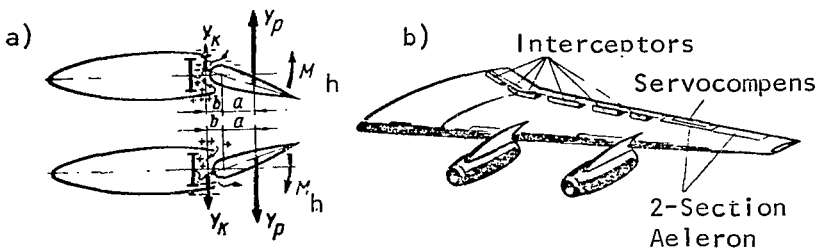

Figure 155. Internal Aerodynamic Compensation (a) and Interceptors for Transverse Control on Wings of DC-8 Aircraft (b)

On the TU-104 aircraft, in order to decrease loads on the ailerons, internal aerodynamic compensation is used (Figure 155), which is similar to axial compensation but differs in that when the control surface is deflected, compensation does not extend beyond the wing profile. Internal aerodynamic compensation is achieved by a plate fastened to the front of the aileron. On one end of this plate there is a sealing strip, the other end of which is fastened to the rear wall of the nonmoving wing. This strip is a barrier, separating the internal cavity of the rear portion of the wing into two nonconnected cavities. When, for example, the aileron is deflected downward, the flow rate over the wing increases, and the pressure correspondingly decreases. Due to the decrease in pressure, air is pumped out of the upper cavity of the chamber and the pressure in this cavity decreases. The pressure beneath the wing and in the lower cavity increase. As a result of the pressure difference in the upper and lower cavities, aerodynamic force Y_k acts on the strip and plate. This force creates a moment about the axis of rotation of the aileron which decreases the hinge moment. The compensation works similarly when the aileron is deflected upward. The advantage of internal aerodynamic compensation is /238 that it produces a very slight increase in drag of the wing, since there are no protruding parts of the aileron before its axis of rotation. However, it does have certain defects as well. The aileron plates within the wing limit the angle of deflection of the ailerons. For the elevator and rudder, which have considerable deflection, the usage of this compensation is difficult due to the thin tail surface profiles. The flexible strip must be carefully maintained during operation. If the strip is damaged, the compensation fails.

The servo-compensator (or Flettner) is a small supplementary control surface located at the rear end of the main articulated surface and hinge connected to the nonmoving portion of the tail surface (vertical tail surface for the rudder or wing for the ailerons) by a tension member (Figure 154 b). Deflection of the control surface automatically causes the servo-compensator to move in the opposite direction. The aerodynamic force arising on the servo-compensator is opposite in its sign to the aerodynamic force on the control surface. As a result of this, the hinge moment of the surface is

decreased. Servo-compensators are installed on the ailerons and rudder, less frequently on the elevators. Servo-compensators are deflected by ±3-14°. This reduces the force required to acceptable levels.

Trimmers allow loads operating over long periods of time and corresponding to deflection of the rudder or aileron to be completely or almost completely removed; they cannot be used to decrease the forces arising during brief deflections of these surfaces (for example when moving into a new flight regime or when countering external perturbation).

The area of the elevator trimmer of a modern aircraft is 7-10% of the area of the elevator, the area of the rudder trimmer is 8-10% the area of the rudder, while the area of the aileron trimmer is 6-8% of the area of the ailerons.

The angles of deflection of the trimmers are so selected that in case of accidental operation of the electrical control mechanisms for the trimmers, resulting in movement of the control surfaces, the pilot will be physically able to hold the control surface in the required positions. For example, if the trimmer of the rudder is deflected by ±3-4° and the rate of movement is 0.5 deg/sec, accidental operation of the trimmer will cause it to deflect fully (in 6-7 sec) and at speeds of 300-350 km/hr, creates forces on the pedals of 25-30 kg; at 500-600 km/hr at H = 1000 m, the force created is 70-80 kg. This force can be overcome by the pilot and copilot and represents no emergency situation.

The angle of deflection of the aileron trimmers is also ±3-4°, and the rate of movement is about 0.4 deg/sec. With the maximum deflection of the trimmer, force on the control lever of 12-36 kg respectively is required for speeds of 300-500 km/hr. The angle of deflection of the elevator trimmers is 6-8° upward, 8-10° downward, and the rate of movement is 1 deg/sec. Accidental connection of the elevator trimmer electric drive and deflection of the trimmer by 3-4° creates a load of 22-27 kg on the stick at 300 km/hr, 60-70 kg at 520 km/hr. Consequently, this also creates no emergency situation. /239

§26. Balancing of the Aircraft During Takeoff and Landing

Let us analyze how the aircraft is balanced during takeoff at 200-300 km/hr (Figure 156). At the moment when the front landing gear lifts (V = 200 km/hr, takeoff with preliminary lift of front gear), the angle of deflection of the elevator $\delta_{el} = -16.7°$, and the force on the stick is 37.5 kg. As the speed increases, the effectiveness of the elevator increases and the pilot decreases its deflection, while the force increases. At the moment of liftoff of the aircraft (V = 240 km/hr), the angle of deflection of the elevator is -14° and the force on the stick is 45 kg. After liftoff as the flight speed increases, the elevator feed is decreased, and the force on the stick also decreases.

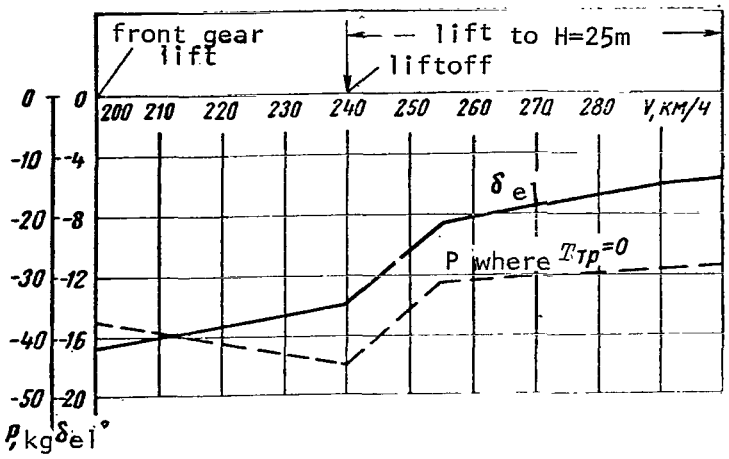

Figure 156. Deflection of Elevator and Force on Stick As a Function of Velocity During Takeoff

Usage of the trimmer reduces the force. For example, at 200 km/hr, a deflection of the trimmer by one degree decreases the force by 3 kg, at 240 km/hr -- by 4.35 kg, at 300 km/hr -- by 7 kg. As we can see from the graph, at 300 km/hr, in order to remove the force, the elevator trimmer must be deflected by approximately 4°. Before takeoff, the elevator trimmer is preset at 1.5-2° (the wheel is turned toward the pilot). Further trimmer adjustment is performed in flight after the landing gear and flaps have been raised. /240

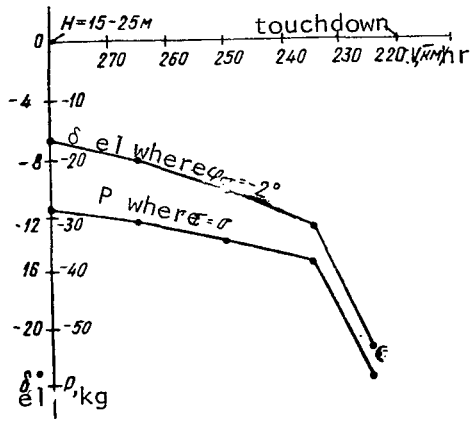

Figure 157. Deflection of Elevator and Force on Control Stick As a Function of Velocity During Landing

Balancing of the aircraft during landing consists of the following. As the velocity is decreased in the glide, the deflection of the elevator upward and force on the stick increase. As we can see from Figure 157, if the elevator is deflected upward by 7° at 275 km/hr, and the force is 28 kg (trimmer neutral), at 230 km/hr these quantities are 13° and 38 kg respectively. At the moment of touchdown at 220 km/hr, the angle of deflection of the elevator is approximately 22° and the force on the stick is about 60 kg. Actually, the trimmer is used to decrease the force to 15-18 kg until the moment of touchdown. Let us analyze how this occurs. After the flaps are dropped to the landing position (landing gear down), the elevator trimmer is deflected by 7-10° to remove the force on the

stick. At 280-300 km/hr, the force on the stick is near zero. As the velocity is decreased during the glide and the elevator deflection is increased to 15-17°, the pulling forces on the stick increase, amounting to 10-15 kg at the moment of touchdown. An adjustable stabilizer allows the loads on the elevator to be decreased significantly if it is deflected by -2 to -5°.

Chapter XII. Influence of Icing on Flying Characteristics

§1. General Statements

In jet aircraft, icing generally occurs on the front edges of the wings, vertical tail surface and stabilizer, the windshields of the pilot and navigator, the temperature receptor and navigational instrument tubes projecting outward from the fuselage and also the edges of the air intakes, engine support pilons, blades of the intake directing apparatus and first compressor stage. In modern turbojet aircraft with high power reserve, icing of the fuselage, wings and horizontal tail surfaces changes the flying data (flight speed, vertical velocity component, etc.) only slightly; the main danger to flight under icing conditions does not result from an increase in aircraft weight due to deposition of ice, but rather from the deterioration in characteristics of stability and controllability of the aircraft. /241

The ice films which are formed (if the anti-icing system is not used) may significantly change the wing profile and the profile of the horizontal tail surface, creating increased turbulence and flow separation, which is particularly dangerous for low speed flight during the approach to landing. Although icing of the wings and fuselage change the flying characteristics but little, icing of the stabilizer, even when the ice is rather thin, may have an essential influence on the stability and controllability of the aircraft. Flow separation on the horizontal tail surface depends primarily on the form of the ice deposited and to a considerably lesser extent on its thickness.

Deposition of ice on the air intake, followed by separation of the ice and entry of ice particles to the compressor blades may cause damage to the compressor and to the engine. Therefore, icing of the intake channels and first stage of the compressor cannot be permitted, not due to the decrease in thrust which results, but rather due to the possibility of complete disruption of compressor operation. Icing of the aircraft occurs primarily in clouds (usually at temperatures below freezing), consisting of supercooled water droplets which freeze when they strike the surface of the flying aircraft and form ice deposits on various aircraft parts. The quantity of ice deposited depends on the time which the aircraft spends under icing conditions. For example, in flights of a TU-104 aircraft, icing was observed between 3000 and 8000 m at surrounding air temperatures from -8 to -34° in cirrus, alto altocumulus and altostratus clouds. Icing has not been observed at high altitudes outside the clouds.

The maximum time of continuous aircraft operation under intensive icing conditions was 12-15 min, and the maximum ice thickness (according to the indicator) was 46-50 mm. The brief time which the jet aircraft spends under icing conditions results from the high flight speeds (650-850 km/hr). Climbs to 8000-11,000 m occur in 15-28 min, and the aircraft climbs through the main layer of clouds near the earth (2000-4000 m) at high vertical speeds

(12-16 m/sec) in 3-5 min. The same thing occurs during the descent. The greatest possibility of icing occurs during circling flight in the area of an airfield, at which time the aircraft flies at 350-380 km/hr, spending 10-12 min in the approach to landing.

When flying at very high speeds, the surface of the aircraft is heated, /242
which prevents icing to some extent. The surface of the wing is particularly heated, since heat is liberated due to internal friction in the boundary layer and the temperature of the leading edge of the wing is increased. There is a point along the profile of the wing where the flow is completely decelerated, which is accompanied by an increase in temperature ΔT of the air in relation to the temperature of the surrounding air. This temperature increase depends on the flight speed and can be calculated using the formula

$$\Delta T = \frac{V^2}{2000},$$

where speed V is taken in m/sec.

The values of temperature increase for various flight speeds are shown in Table 14.

TABLE 14

V, km/hr	520	600	650	700	750	800	850	900
ΔT°C	10.4	13.8	16.2	18.7	21.6	24.6	28	31

However, during icing of an aircraft the actual increase is 30-50% less. This results from the fact that the water droplets which deposit on the surface of the aircraft will be partially or completely evaporated and therefore will decrease the temperature of the surface. Also, heat exchange occurs in the boundary surface, also reducing the temperature.

§2. Types and Forms of Ice Deposition. Intensity of Icing

The forms of aircraft icing are various and depend primarily on the extent of supercooling of the droplets in the clouds. The following types of ice are differentiated[1]:

[1] O. K. Trunov, *Obledeneniye Samoletov i Sredstva Bor'by s Nimi* [Icing of Aircraft and Methods of Its Control], Mashinostroyeniye Press, 1965.

a) Transparent ice (glaze) -- deposited on aircraft flying in medium with large, supercooled droplets forming even, dense and transparent layer (Figure 152 a). Ice formation temperature 0 to -5°. This form of icing is particularly dangerous, since it attaches itself firmly to the surface of the aircraft. If there is a heating element on the front edge, barrier ice is formed (Figure 158 e);

b) Translucent mixed ice -- encountered more frequently (Figure 158 b), formed at -5 to -10°, sharply worsening aerodynamic quality of aircraft;

c) Hoar frost -- a white, large-grained crystalline ice, formation temperature about -10° (Figure 158 c), uneven deposition form with ragged projecting edges, making flight dangerous (early flow separation possible);

d) Rime -- a white, fine crystalline deposit formed by water vapor frozen upon contact with the cooled surface of the aircraft, representing no danger for jet aircraft;

e) Barrier ice -- deposited on the leading edge at temperatures above 0°, on remaining portions at lower temperatures (the effect of the heating element appears), the moisture which precipitates does not freeze, but is blown away by the air and freezes to the surface of the wing (stabilizer) on both sides of the leading edge, forming an ice deposit in a grooved shape along the leading edge (Figure 158 e). When deposited on the leading edge of the stabilizer, may result in complete flow separation.

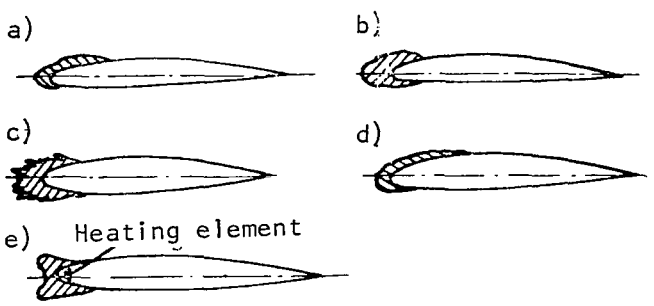

Figure 158. Characteristic Forms of Ice Deposits on Wings

Since the testing of an aircraft for stability and controllability with icing of the wings and stabilizers represents a certain difficulty, particularly during the warm season of the year, in recent times tests have been made using models in wind tunnels with icing imitators fastened to the wings and stabilizer. Flying tests of aircraft with ice imitators glued onto the front edge of the stabilizer are also performed.

As wind tunnel tests of model aircraft have shown, icing imitators placed on the leading edge of the stabilizer cause slight changes in the characteristics of stability and controllability. The forms of the imitators (Figure 159) are similar to the natural forms of ice deposition. For example, imitator form 1 represents the ice deposit produced during intensive icing

with poor operation of edge heater (the ice takes on the form of a groove); 2 represents barrier ice with the heating element operating; 3 represents the deposition of ice at temperatures of -3 to -8° with the heating system not operating.

The influence of icing of the stabilizer on characteristics of longitudinal stability and controllability will be described below. /244

In order to estimate the degree of danger of icing of an aircraft, the concept of the intensity of icing has been introduced, characterizing the quantity of ice deposited (in mm) per min. The following scale has been evolved: a) low intensity -- ice deposited at 1 mm/min; b) moderate -- from 1 to 2 mm/min and c) high -- from 2 mm/min up.

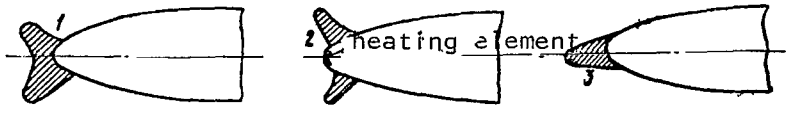

Figure 159. Forms of Imitators of Icing of Leading Edge of Stabilizer

§3. Influence of Icing on Stability and Controlability of Aircraft in Prelanding Guide Regime

In order to estimate the influence of icing of the leading edge of wing and stabilizer on the flying characteristics of an aircraft, as well as the stability and controllability, special flying tests are performed under conditions of moderate or slight icing at temperatures of the surrounding air between -3 and -17°C between 1000 and 2000 m altitude with indicated speeds of 400-420 km/hr (speeds near those used in the landing approach).

Piloting of an iced aircraft with an ice thickness of 30-40 mm on the control surface profile (anti-icing system switched off) in horizontal flight and during a climb with landing gear and flaps up without the creation of any maneuvering loads does not differ essentially from piloting under normal conditions, i.e., with no icing. No noticeable changes in stability or controllability of the aircraft were observed. The forces on the control levers remain practically unchanged; no seizing or wedging of the elevator or ailerons was noted. As the ice continued to increase in thickness, the motor operating regime had to be increased by 4-5% in order to maintain steady speed.

The data produced during wind tunnel testing of an aircraft model with icing imitators on the leading edge of the stabilizer indicated that icing of the leading edge of the stabilizer should not result in disruption of stability or loss of control during sharp deflections of the elevator. This allowed flying tests to be performed safely.

Sharp inputs of elevator control ("feed") during the approach to landing at 260-290 km/hr (without icing) with landing gear, flaps and airbrake down showed that the aircraft was stable in the longitudinal direction with overload decreased down to 0.2. As we know, the pilot senses his control of the aircraft from the resistance which he feels at the control stick during the process of performance of various maneuvers. In order to create a considerable overload, large forces must be applied to the stick. /245

When the stick is "fed" forward, the pilot should feel a force on the stick, greater the less the overload created. In those cases when the pilot ceases to feel the control of the aircraft, longitudinal overload stability of the aircraft is disrupted.

A reduction in the force on the control stick during icing conditions results from a change in the hinge moments due to redistribution of pressures on the horizontal tail surface. This is explained by the appearance of local air flow separation over the lower surface of the stabilizer.

We can see from the graph on Figure 160 that at 290-260 km/hr as the overloads decrease, the force on the control stick increases, as does the angle of deflection of the elevator. The amount of elevator feed which must be applied per unit of overload at 290 km/hr is less than at 250 km/hr. The forces on the stick change as follows. For example, in order to create an overload n_y = 0.4 at V = 260 km/hr, a force of 22 kg is required, while at V = 290 km/hr -- 37 kg is required. With sharp deflections of the elevator, the overload (particularly, 0.2) was retained for 3-4 sec and no drop in force on the stick was observed.

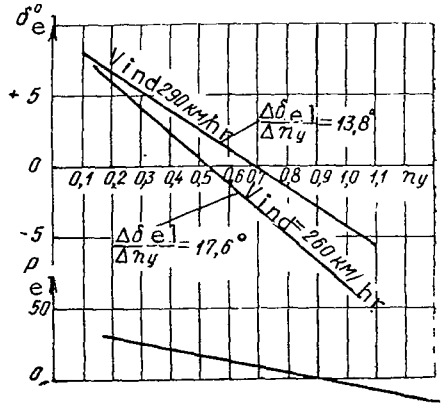

Figure 160. Deflection of Elevator and Force on Control Stick As a Function of Overloads (produced in flying tests)

The model tests performed in the wind tunnel using the horizontal tail surface and negative angles of attack (-10 to -18°) showed that when the leading edge of the stabilizer is iced (the failure of anti-icing system), no disruption of longitudinal static stability or change in hinge moments of the elevator was observed. A change in static stability or hinge moment of the elevator is observed only at angles of attack corresponding to negative overloads. For zero overload values, the graph $m_z = f(\alpha)$ in the case of an iced leading edge of the stabilizer, changes its inclination very slightly with the three forms of imitators used, i.e., the longitudinal static stability remained practically unchanged.

The flow angles were measured with flaps down, and for wing angles of attack of 2-4°, the flow angles were 5-6° (with /246

$\phi = -2°$).

As was stated above, when gliding in for a landing, the wing has $\alpha = 3°$; therefore, with a flow angle of about 5°, we produce a negative value of angle of attack of the horizontal tail surface: $\alpha_{ht} = \alpha_{cr} = \phi - \varepsilon = 3° - 2° - 5° = -4°$.

With the same angle of attack, flow separation on a swept stabilizer does not occur, since its critical angle of attack during icing changes from 16-17° by only 3-4°[1]. Even with large flow angles (in the case of icing of the leading edge of the stabilizer by barrier ice of considerable thickness), the angle of attack of the horizontal surface does not change its critical value.

We analyzed the case in which tha anti-icing system did not work or was not connected, and investigated what might occur if an aircraft began icing as it descended for a landing. In practice, failure of the anti-icing system on turbojet aircraft at V_{ind} = 400-450 km/hr, the temperature drops along the leading edge of the wings (hot air heating system turned on) decrease only slightly, while the electrical stabilizer and vertical fin heating system operate normally with one engine out, being independent of the number of engines in operation on the aircraft. Greater difficulties can be created by untimely switching on of the system heating wings, vertical tail surface and stabilizer than by failure of one engine, with the resulting reduction in hot air uptake. It has been noted that when the anti-icing system on the wing is turned on after ice has grown to 24 mm thickness on a controlled surface the ice was shed from the heated leading edge in one minute, while when the anti-icing system of the stabilizer was turned on, ice was shed from both halves of the stabilizer in 1-2 cycles (2-4 min). In order to be safe during a landing approach with the anti-icing system not operating, the pilot should bring his aircraft down smoothly, not creating overloads less than 1.

[1] All related to a swept stablizer with χ = 40-45°.

NATIONAL AERONAUTICS AND SPACE ADMINISTRATION
WASHINGTON, D.C. 20546

OFFICIAL BUSINESS

FIRST CLASS MAIL

POSTAGE AND FEES PA
NATIONAL AERONAUTICS
SPACE ADMINISTRATIO

04L 001 26 51 3DS 69255 00903
AIR FORCE WEAPONS LABORATORY/WLIL/
KIRTLAND AIR FORCE BASE, NEW MEXICO 8711

ATT E. LOU BOWMAN, CHIEF,TECH. LIBRARY

POSTMASTER: If Undeliverable (Section
Postal Manual) Do Not R

"The aeronautical and space activities of the United States shall be conducted so as to contribute . . . to the expansion of human knowledge of phenomena in the atmosphere and space. The Administration shall provide for the widest practicable and appropriate dissemination of information concerning its activities and the results thereof."

—NATIONAL AERONAUTICS AND SPACE ACT OF 1958

NASA SCIENTIFIC AND TECHNICAL PUBLICATIONS

TECHNICAL REPORTS: Scientific and technical information considered important, complete, and a lasting contribution to existing knowledge.

TECHNICAL NOTES: Information less broad in scope but nevertheless of importance as a contribution to existing knowledge.

TECHNICAL MEMORANDUMS: Information receiving limited distribution because of preliminary data, security classification, or other reasons.

CONTRACTOR REPORTS: Scientific and technical information generated under a NASA contract or grant and considered an important contribution to existing knowledge.

TECHNICAL TRANSLATIONS: Information published in a foreign language considered to merit NASA distribution in English.

SPECIAL PUBLICATIONS: Information derived from or of value to NASA activities. Publications include conference proceedings, monographs, data compilations, handbooks, sourcebooks, and special bibliographies.

TECHNOLOGY UTILIZATION PUBLICATIONS: Information on technology used by NASA that may be of particular interest in commercial and other non-aerospace applications. Publications include Tech Briefs, Technology Utilization Reports and Notes, and Technology Surveys.

Details on the availability of these publications may be obtained from:

SCIENTIFIC AND TECHNICAL INFORMATION DIVISION

NATIONAL AERONAUTICS AND SPACE ADMINISTRATION

Washington, D.C. 20546